Evaluation of process parameters and membranes for SO_2 electrolysis

AJ Krüger

13061631

Thesis submitted for the degree *Philosophiae Doctor* in Chemistry at the Potchefstroom Campus of the North-West University

Promoter: Prof H Krieg

Co-promoter: Dr D Bessarabov

April 2015

DECLARATION

I, Andries J. Krüger, declare that the thesis entitled: "*Evaluation of process parameters and membranes for SO_2 electrolysis*", submitted in fulfilment of the requirements for the degree *Philosophiae Doctor* in Chemistry, is my own work, except where acknowledged in the text, and has not been submitted in whole or in part to any other tertiary institution.

Signed at North-West University (Potchefstroom Campus)

22 April 2015

Andries J Kruger Date

ACKNOWLEDGEMENTS

To my Heavenly Farther *all* honour must be awarded for giving me the ability to express myself both personally and within the scientific community. May this work be acceptable for an Entity which loves and nurtures all we know and are.

For the loving and consistent support from my wife, *Annike Krüger*, words are not enough. Thank you for always understanding when, after a days' work in the laboratories, I reeked of sulphur.

To my parents, *Hennie and Marianne Kruger*, thank you for supporting me during this period of frustration, happiness and above all academic growth. Your love and patience showed me that anything is possible when faced with difficult times.

To Professor Henning Krieg, the frequent talks about life and the path not chosen have enriched my student years. Your meticulousness regarding research has indeed, to some extent, crept into my own method of madness when doing research. I should also acknowledge your patience and resolve when reviewing my work which always contained all the information, but in no logical order.

The greatest appreciation must without a doubt be extended to Dr. Dmitri Bessarabov for his part in shaping me as a scientist. Your 'never say die' approach to solve and handle difficult issues has shown me that nothing is impossible how improbable it may seem. I must also thank you for the multiple opportunities you gave me for international travel and extending my general knowledge regarding hydrogen.

To Dr. Jochen Kerres and his research group, thank you cannot justify the appreciation I have for the PBI based blend membranes, as well as the interesting conversations when I visited your group. I am honoured to know a researcher with such a vision for research.

To Jan Kroeze, Adrian Brock and Ted Paarlberg for always being available to answer any and all questions regarding my setup and general system questions, thank you. The occasional coffee and braais made the difficult times easier to bear.

ABSTRACT

The environmentally unsafe by-products (CO_2, H_2S, NO_x and SO_2 for example) of using carbon-based fuels for energy generation have paved the way for research on cleaner, renewable and possibly cheaper alternative energy production methods. Hydrogen gas, which is considered as an energy carrier, can be applied in a fuel cell setup for the production of electrical energy. Although various methods of hydrogen production are available, sulphur-based thermochemical processes (such as the Hybrid Sulfur Process (HyS)) are favoured as alternative options for large scale application. The SO_2 electrolyser is applied in producing H_2 gas and H_2SO_4 by electrochemically converting SO_2 gas and water. This study focused firstly on the evaluation of the performance of the SO_2 electrolyser for the production of hydrogen and sulphuric acid, using commercially available PFSA (perfluorosulfonic acid) (Nafion®) as benchmark by evaluating i) various operating parameters (such as cell temperature and membrane thickness), ii) the influence of MEA (membrane electrode assembly) manufacturing parameters (hot pressing time and pressure) and iii) the effect of H_2S as a contaminant. Subsequently, the suitability of novel PBI polyaromatic blend membranes was evaluated for application in an SO_2 electrolyser.

The parametric study revealed that, depending on the desired operating voltage and acid concentration, the optimisation of the operating conditions was critical. An increased cell temperature promoted both cell voltage and acid concentration while the use of thin membranes resulted in a reduced voltage and acid concentration. While an increased catalyst loading resulted in increased cell efficiency, such increase would result in an increase in manufacturing costs. Using electrochemical impedance spectroscopy at the optimised operating conditions, the MEA

manufacturing process was optimised with respect to hot press pressure and time, while the effect of selected operating conditions was used to evaluate the charge transfer resistance, ohmic resistance and mass transport limitations. Results showed that the optimal hot pressing conditions were 125 $kg.cm^{-2}$ and 50 $kg.cm^{-2}$ for 5 minutes when using 25 and 10 cm^2 active areas, respectively. The charge transfer resistance and mass transport were mostly influenced by the hot pressing procedure, while the ohmic resistance varied most with temperature.

Applying the SO_2 electrolyser in an alternative environment to the HyS thermochemical cycle, the effect of H_2S on the SO_2 electrolyser anode was investigated for the possible use of SO_2 electrolysis to remove SO_2 from mining off-gas which could contain H_2S. Polarisation curves, EIS and CO stripping were used to evaluate the transient voltage response of various H_2S levels (ppm) on cell efficiency. EIS confirmed that the charge transfer resistance increased as the H_2S competed with the SO_2 for active catalyst sites. Mass transport limitations were observed at high H_2S levels (80 ppm) while the ECSA (electrochemical surface area obtained by CO stripping) showed a significant reduction of active catalyst sites due to the presence of H_2S. Pure SO_2 reduced the effective active area by 89% (which is desired in this case) while the presence of 80 ppm H_2S reduced the active catalyst area to 85%.

The suitability of PBI-based blend membranes in the SO_2 electrolyser was evaluated by using chemical stability tests and electrochemical MEA characterisation. F_6PBI was used as the PBI-containing base excess polymer which was blended with either partially fluorinated aromatic polyether (sFS001), poly(2,6-dimethylbromide-1,4-phenylene oxide (PPOBr) or poly(tetrafluorostyrene-4-phosphonic acid) (PWN) in

various ratios. Some of the blend membranes also contained a cross-linking agent which was specifically added in an attempt to reduce swelling and promote cross-linking within the polymer matrix. The chemical stability of the blended membranes was confirmed by using weight and swelling changes, TGA-FTIR and TGA-MS. All membranes tested showed low to no chemical degradation when exposed to 80 wt% H_2SO_4 at 80°C for 120 h. Once the MEA doping procedure had been optimised, electrochemical characterisation of the PBI MEAs, including polarisation curves, voltage stepping and long term operation (> 24 h) was used to evaluate the MEAs. Although performance degradation was observed for the PBI membranes during voltage stepping, it was shown that this characterisation technique could be applied with relative ease, producing valuable insights into MEA stability. Since it is expected that the SO_2 electrolyser will be operated under static conditions (cell temperature, pressure and current density) in an industrial setting (HyS cycle or for SO_2 removal), a long term study was included. Operating the SO_2 electrolyser under constant current density of 0.1 A cm^{-2} confirmed that PBI-based polyaromatic membranes were suitable, if not preferred, for the SO_2 environment, showing stable performance for 170 hours.

This work evaluated the performance of commercial materials while further adding insights into both characterisation techniques for chemical stability of polymer materials and electrochemical methods for MEA evaluation to current published literature. In addition to the characterisation techniques this study also provides ample support for the use of PBI-based materials in the SO_2 electrolyser.

Keywords: Hybrid Sulfur Process, SO_2 electrolyser, Hydrogen production, electrochemical impedance spectroscopy, PBI blend membranes, H_2S deactivation, electrochemical surface area, CO stripping

OPSOMMING

Die negatiewe invloed op die natuur van die byprodukte (soos byvoorbeeld CO_2, H_2S, NO_x en SO_2) wat geproduseer word deur die aanwending van koolstof-gebaseerde energieproduksie, het die weg gebaan vir navorsing oor skoon, hernubare en heel moontlik goedkoper alternatiewe metodes van energie-opwekking. Waterstofgas, wat tans as 'n energiedraer beskou word, kan as brandstof in brandstofselle aangewend word om elektriese energie te genereer. Afgesien van bestaande metodes vir waterstofproduksie, word die Hibried Swael Proses (HyS) as die beste moontlike opsie vir grootskaalse produksie beskou. Die SO_2 elektroliseerder word gebruik om H_2 asook H_2SO_4 te produseer deur die elektrochemiese reaksie tussen SO_2 en water. Hierdie studie het eerstens gefokus op die evaluering van die SO_2-elektroliseerder vir die produksie van waterstofgas en swaelsuur deur gebruik te maak van 'n kommersieel beskikbare PFSA-(perfluoro-sulfoonsuur) membraan deur i) verskeie bedryfsparameters (wat seltemperatuur en membraandikte insluit) te evalueer, ii) die invloed van vervaardigingsparameters van die membraan-elektrodesamestelling (MES) te ondersoek (soos byvoorbeeld die warmsaamperstyd en -druk) en iii) die invloed van die teenwoordigheid van H_2S-gas as kontaminant te evalueer. Vervolgens is die toepasbaarheid van nuwe PBI-poli-aromatiese gemengde membrane getoets vir gebruik in die SO_2-elektroliseerder.

Die parametriese ondersoek het aangedui dat, afhangend van die spanning en suurkonsentrasie benodig, die kondisies vir die elektroliseerder baie noukeurig gekies moet word. 'n Verhoogde seltemperatuur het beide die selspanning en suurkonsentrasie bevoordeel, terwyl die gebruik van dun membrane die spanning en suurkonsentrasie verlaag het. Terwyl 'n hoër katalislading die seleffektiwiteit verhoog het, sou dit die kostes ook dienooreenkomstig verhoog. Deur die gebruik

van elektrochemiese impedansie-spektroskopie (EIS) by die voorafbepaalde geoptimiseerde bedryfstoestande kon die MES-vervaardigingsparameters van die warmsaampersdruk en -tyd geoptimiseer word. Geselekteerde bedryfskondisies is gebruik om die ladingoordrag-weerstand, ohmiese weerstand en die massa-oordragbeperkings te evalueer. Resultate het getoon dat die beste warmsaampers-parameters 125 kg cm^{-2} en 50 kg cm^{-2} vir 5 minute vir 25 en 10 cm^2 aktiewe oppervlaktes onderskeidelik was. Die ladingoordrag-weerstand en massa-oordragbeperking is hoofsaaklik deur die warmsaampers-prosedure beïnvloed terwyl, die ohmiese weerstand die meeste deur seltemperatuur beïnvloed is.

Die gebruik van die SO_2 elektroliseerder in alternatiewe omgewings anders as in die HyS-proses, is ondersoek deur die effek van H_2S op die SO_2 elektroliseerder te evalueer om sodoende die toepaslikheid van die SO_2 elektroliseerder te bepaal om SO_2-gas te verwyder uit die by-produkgasse van die mynbou-industrie. Polarisasiekrommes, EIS asook CO-adsorpsie/desorpsietegnieke is aangewend om die invloed van verskeie vlakke van H_2S (dpm) op die spanning, as 'n funksie van tyd, en sel-effektiwiteit te bepaal. EIS het n toename in die ladingoordrag-weerstand bevestig wat aan die H_2S-adsopsie toegeskryf is wat die aantal aktiewe posisies vir SO_2-adsopsie beperk. Massa-oordragbeperkings was teenwoordig by hoë vlakke van H_2S (80 dpm) terwyl die elektrochemiese oppervlak-area (ECOA, bepaal deur die CO-adsorpsie/desorpsietegniek) 'n merkwaardige verlaging in aktiewe gekataliseerde posisies as gevolg van die teenwoordigheid van H_2S gas getoon het. Suiwer SO_2-gas het die effektiewe aktiewe area tot soveel as 89 % verlaag, wat in dié geval verlang word, terwyl die teenwoordigheid van soveel as 80 dpm H_2S slegs 85 % van die aktiewe gekataliseerde posisies kon bedek.

Die toepaslikheid van PBI-gebaseerde gemengde membrane is getoets vir die gebruik in die SO_2-elektroliseerder deur gebruik te maak van chemiese stabiliteitstoetse, asook elektrochemiese MES-karakterisering. F_6PBI is deurgaans gebruik as die PBI-bevattende basis-oormaat-komponent wat gemeng is met of gedeeltelike gefluorineerde aromatiese poli-eter (sFS001) of poli-(2,6-dimetielbromied-1,4-fenieleenoksied) (PPOBr) of poli-(tetrafluorostireen-4-fosfoonsuur) (PWN) in verskeie verhoudings. Die gebruik van 'n kruisverbindingsagent, wat 'n poging was om die swelling te verlaag en om die kruisbinding in die polimeer self te bevorder, is vir spesifieke gemengde polimere ingesluit. Die chemiese stabiliteit van die gemengde membrane is deur gewig- en swelverandering, TGA-FTIR- en TGA-MS-tegnieke bevestig. Alle membrane wat getoets is, het minimaal tot geen chemiese verval getoon nie nadat hulle blootgestel is aan 80 massa% H_2SO_4 by 80°C vir 120 uur. Na afloop van die optimisering van die PBI-gebaseerde MES inenting-prosedure is elektrochemiese karakteriseringstegnieke soos polarisasiekrommes, spanningstappe asook langtermynbedryf (24 uur) gebruik om die MES te evalueer. Afgesien van 'n verlaagde effektiwiteit na die spanningstap-karakteriseringstegniek wanneer die PBI-gebaseerde polimere gebruik is, is die toepaslikiheid van die spesifieke tegniek vir MES-stabiliteitskarakterisering wel bevestig. Aangesien die SO_2-elektroliseerder heelwaarskynlik onder statiese toestande (seltemperatuur, druk en stroomdigtheid) in 'n industriële opset bedryf sal word (soos in die HyS proses, of vir SO_2-verwydering), is dit goedgedink om 'n langtermynstudie in te sluit. Deur die SO_2-elektroliseerder by 'n konstante stroomdigtheid van 0.1 A cm^{-2} te bedryf, is die geskiktheid van die PIB-gebaseerde poli-aromatiese membrane bevestig, of selfs verkies, in die SO_2 omgewing deur stabiele gedrag vir 170 uur te toon.

Hierdie studie het die bedryf van kommersiële materiaal (polimere) geëvalueer terwyl beide karakteriseringstegnieke vir chemiese stabiliteit van polimere en elektrochemiese evalueringsmetodes vir MES'e tot die bestaande literatuur toegevoeg is. Afgesien van die karakteriseringstegnieke, verskaf hierdie studie ook oortuigende data vir die gebruik van PBI-gebaseerde polimeermaterial in die SO_2 elektroliseerder.

Sleutelwoorde: Hibried Swael Proses, SO_2 elektroliseerder, Waterstofproduksie, electrochemiese impedansie-spektroskopie, PBI-gemengde membrane, H_2S-de-aktivering, elektrochemiese oppervlak-area, CO adsorpsie/desorpsie.

TABLE OF CONTENTS

LIST OF TABLES

LIST OF FIGURES

List Of Journal Publications Related To This Study

Krüger AJ, Krieg HM, van der Merwe J, Bessarabov D. Evaluation of MEA manufacturing parameters using EIS for SO_2 electrolysis. Int J Hydrogen Energy 2014;39:18173–81. doi:10.1016/j.ijhydene.2014.09.012.

Krüger AJ, Cichon P, Kerres J, Bessarabov D, Krieg HM. Characterisation of a polaromatic PBI blend embrane for SO_2 electrolysis. Int J Hydrogen Energy 2015:1–12. doi:http://dx.doi.org/10.1016/j.ijhydene.2014.12.081.

Krüger AJ, Krieg HM, Bessarabov D. Effect of H2S on SO2-depolarised water electrolysis. Int J Hydrogen Energy 2015;40:4442–50. doi:10.1016/j.ijhydene.2015.02.036.

Krüger, A.J., Krieg, H. M., Grigoriev, S. A. and Bessarabov, D. (2015), Various operating methods and parameters for SO2 electrolysis. Energy Science & Engineering. Doi 10.1002/ese3.80

Krüger AJ, Kerres J, Bessarabov D, Krieg HM. Evaluation of covalently and ionically cross-linked PBI-excess blends for application in SO2 electrolysis. Int J Hydrogen Energy 2015;40:8788-96. Doi:10.1016/j.ijhydene.2015.05.063.

Conference Oral Papers Accepted:

Andries J. Krüger, Jochen Kerres, Dmitri Bessarabov, Henning M. Krieg. Application of novel PBI based PEM for SO_2-depolarised water electrolysis. CARSIMA 2014 Conference, 1 – 3 December 2014, Cape Town, South Africa.

Andries Krüger, Henning Krieg, Jochen Kerres, Dmitri Bessarabov. Various operating methods for SO_2 electrolysis for H_2 and H_2SO_4 production. 5th World Hydrogen Conference and Convention, 25 – 29th September, Everbright Convention Centre, Shangai, China.

J.Kerres, V. Atanasov, I. Hajdok, A. Chromik, A. Katzfuβ, C. Seyb, K. Aniol, A. Carlsson, **A. Krüger**, H. Krieg, V. Gogel, U. Storr, L. Jörissen, Nonfluorinated and Highly Fluorinated (Co)Polyers and their Application in Both Low-T and Intermediate-

T Fuel Cell and in Electrolysis Membranes. Advances in Polymer Electrolyte Membrane Fuel Cell Systems 2013" conference at Asilomar Conference Grounds, Pacific Grove, California USA.

CONFERENCE POSTER PAPERS ACCEPTED:

Andries Krüger, Henning Krieg, Dmitri Bessarabov. Electrochemical characterization of the effect of H_2S on platinum during SO_2 electrolysis. Catalysis society of South Africa 25th Annual Conference, 10 – 13 November 2014, University of Witswaterand.

A. Krüger, H. Krieg, D. Bessarabov. Electro-catalyst oxidation of SO_2 as a function of catalyst loading. Catalysis society of South Africa 24th Annual Conference, 17 – 20 November 2013, Wild Coast Sun, Port Edward, South Africa.

Andries Krüger, Henning Krieg, Jochen Kerres, Dmitri Bessarabov, Evaluation of novel PBI based membranes for H_2 production through SO_2 electrolysis, 13th Topical Meeting of the International Society of Electrochemistry Workshop, Pretoria, 2013.

Andries Krüger, Henning Krieg, Jochen Kerres, Dmitri Bessarabov, Evaluation of various MEA's for SO_2 depolarised electrolysis, Poster No.: 22, WHEC2012.

CHAPTER 1: INTRODUCTION

1.1 BACKGROUND

With the increasing demand for electricity, the balancing of production capacity and sustainability for the production of energy becomes more important. Presently, the high energy production using traditional sources such as natural gas (NG), coal and fossil fuels, can meet current demand, but with increased legislation imposed on environmental and sustainability issues, the focus is shifting towards energy production that is clean and renewable. Some of the more promising alternative methods for the production of energy (electricity) include wind [1,2], solar [3,4] and hydro-electricity [5–7]. In some cases these methods can be combined, for example wind and hydro [8,9], wind, solar and hydro [10–12] or solar and hydro [13].

Of some of the alternative energy production methods, hydrogen gas has been identified as a possible energy carrier, for example when coupled with proton exchange membrane fuel cells (PEMFC). Hydrogen gas can be produced from several sources including more traditional carbon-based fuels, such as NG, or from renewable sources such as biomass [14] or water. In the latter case, water electrolysis can be used to produce pure hydrogen and oxygen from water [15–17]. The central components of a water electrolyser usually consist of flow fields (wherein the reactants are transported), gas diffusion layers (GDLs) and a membrane electrode assembly (MEA) consisting of a proton exchange membrane (PEM) coated with a catalyst on both sides of the PEM. Figure 1.1 shows a schematic diagram of the general cell design of a water electrolyser.

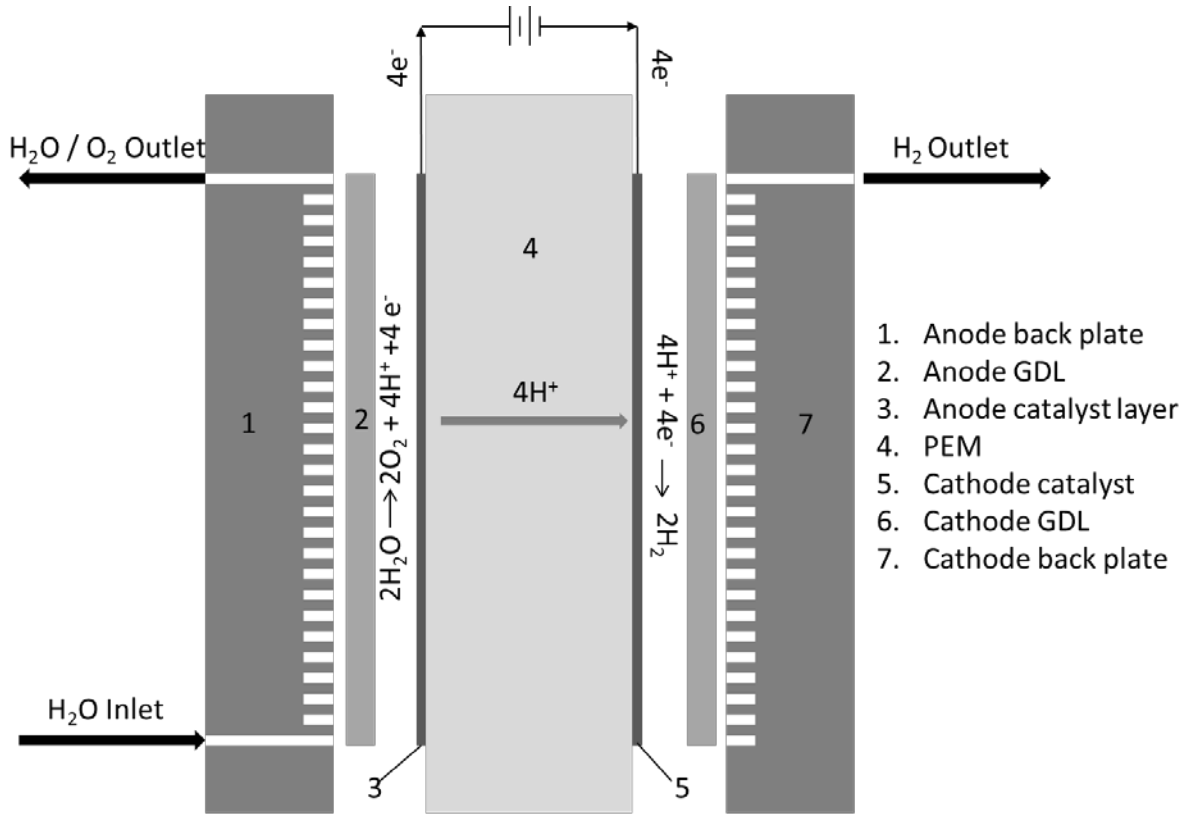

Figure 1.1: Schematic representation of the general components and mechanism of a water electrolyser.

At the anode catalyst, which usually consists of iridium oxide, water is oxidised to produce oxygen gas, protons and electrons [18]. The PEM membrane, usually made from perfluorosulfonic acid (Nafion®), facilitates the transport of protons to the cathode where it is recombined with the electrons from the anode via an external electrical circuit to produce hydrogen gas. Figure 1.2 shows the chemical structure of Nafion®, which is most often used in both the fuel cell and water electrolyser environment. While normal water electrolysis produces clean hydrogen from a non-carbon-based source, a theoretical voltage of 1.23 V is needed with a practical operating voltage of around 1.5 – 2 V [15,18,19]. This operating voltage would have to be reduced to compete with current industrial operations for large scale hydrogen production.

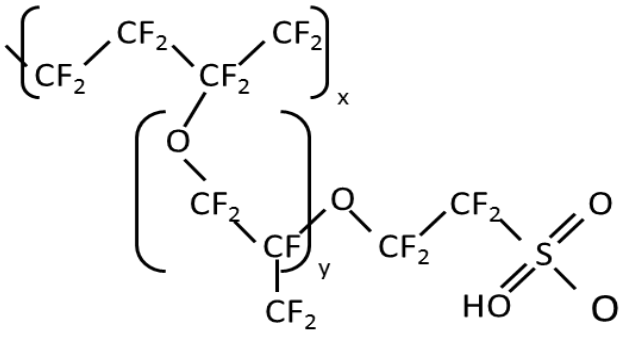

Figure 1.2: Typical chemical structure of a PFSA-based membrane (Nafion®).

Numerous alternative methods for the large-scale production of hydrogen from renewable sources have been suggested, of which the thermochemical cycles have shown significant advantages [20–23]. Two of these thermochemical cycles, the Sulfur Iodine (SI) and Hybrid Sulfur (HyS) processes, have received considerable attention in the last decade [21,24]. In both cycles H_2SO_4 is thermally decomposed to water, oxygen and sulfur dioxide as shown in equation 1.1 [20,25–27].

$$2\mathrm{H}_2SO_4 \rightarrow 2H_2O + 2SO_2 + O_2 \qquad (1.1)$$

While the oxygen separation from sulfur dioxide forms part of both cycles, the conversion of the sulfur dioxide to hydrogen differs significantly [24,28,29]. In the sulfur iodine cycle, SO_2 is reacted with water in the presence of I_2 at 120°C (known as the Bunsen reaction), producing sulphuric acid and hydroiodic acid (equation 1.2).

$$\mathrm{SO}_2 + I_2 + 2H_2O \rightarrow H_2SO_4 + 2HI \qquad (1.2)$$

$$2HI \rightarrow H_2 + I_2 \qquad (1.3)$$

The separation of the two acids is achieved spontaneously in the presence of excess iodine. The sulphuric acid is recirculated to the sulphuric acid decomposition step – equation (1.1), while the hydroiodic acid is decomposed at 350 – 450°C to form H_2 and I_2 (which is also recycled within the cycle – equation (1.3)) [25,24,30]. Thus the SI cycle produces both hydrogen and oxygen from water using I_2 and sulfur in a closed loop.

As mentioned before, the sulphuric acid decomposition and oxygen step is similar for both the SI and HyS cycle. The application of the SO_2 within the cycles is however different; where the SI cycle converts the SO_2 and water in the presence of I_2 to H_2SO_4 and HI, the HyS cycle directly produces H_2SO_4 and H_2 by reacting SO_2 and water electrochemically, as shown in equation (1.4).

$$SO_2 + 2H_2O \rightarrow H_2SO_4 + H_2 \qquad E° = 0.158 \text{ V vs SHE} \qquad (1.4)$$

The advantage of this thermochemical cycle is the electrolysis of SO_2 over the water electrolysis described earlier is the theoretical voltage needed for the reaction. While water electrolysis needs 1.23 V, with a practical voltage of 1.5 - 2 V, the SO_2 electrolyser's theoretical voltage is only 0.158 V [20,22], with a practical voltage below 1 V [31]. Figure 1.3 shows a schematic of the SO_2 electrolyser and its operation. During SO_2 electrolysis, water is oxidised in the presence of SO_2 at the anode, which is either dissolved in H_2SO_4 or in pure gas form, to produce sulphuric acid, protons and electrons. The protons are transported through a separator/membrane before being recombined with the electrons at the cathode, supplied by an external electrical circuit to produce hydrogen according to equation (1.5).

$$2H^+ + 2e^- \rightarrow H_2 \qquad E° = 0 \text{ V vs. SHE} \qquad (1.5)$$

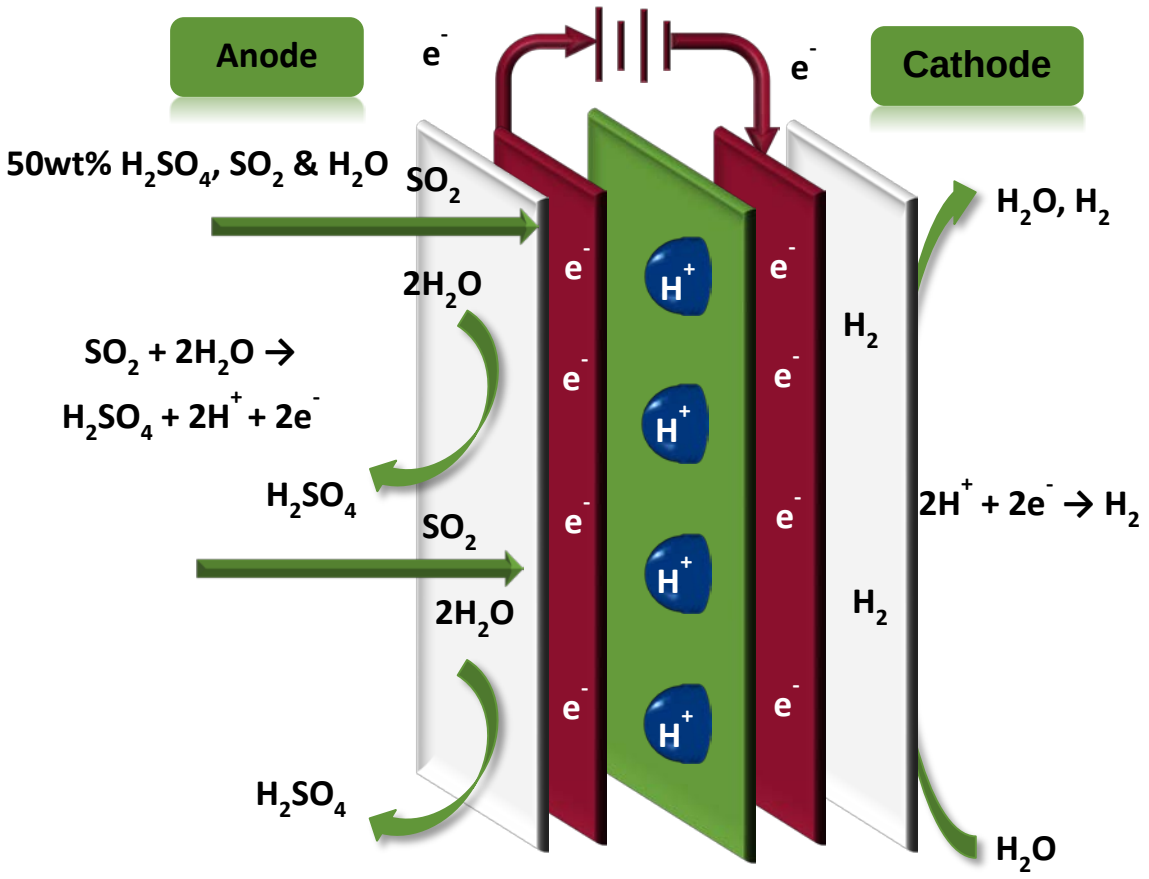

Figure 1.3: Schematic of the SO_2 electrolyser (Prepared by the author).

Before discussing the various modes of operation, some consideration should be given to the membrane electrode assembly (MEA - consisting of a PEM coated on both sides with a catalyst layer), which is at the heart of the electrolyser. Generally the catalyst, for both anode and cathode of an SO_2 electrolyser consists of a platinum group based metal (PGM) [32,33]. A suitable catalyst should show fast kinetics towards SO_2 oxidation (equation 1.4) while having excellent stability in the highly corrosive environment. Either pure platinum (also known as platinum black, PtB) or platinum supported on carbon (Pt/C) is used as catalyst, similar to what is currently being used in the fuel cell environment. The catalyst stability is usually determined by cyclic voltammetry (CV), while linear sweep voltammetry is employed to evaluate the catalyst activity [34,35]. While various other metals (including gold) have been investigated for the SO_2 electrolyser, platinum is still the best performing catalyst in terms of activity and stability [34].

To be suitable for SO_2 electrolysis, the PEM should show chemical stability in the highly acidic (H_2SO_4) environment with high proton and low SO_2 transport. A variety of membrane materials are stable in such acidic environments. The most common membrane currently used both in a fuel cell and water electrolyser environment, is made from perfluorosulfonic acid (for example PFSA shown in Figure 1.2) [18,36]. Alternative proton exchange membranes that have shown promising results are made from sulfonated polyetheretherketone (sPEEK) [37], sulfonated Diels-Alder polyphenylenes (SDAPP), stretched recast PFSA, PFSA/fluorinated ethylene propylene (FEP) blends and perfluorocyclobutane-biphenyl vinyl ether (BPVE)-based membranes [38]. However, all these materials are most suitable for low temperature (<100°C) applications. In view of the high temperature for the operation of the SO_2 electrolyser (120°C, [39]), materials capable of higher operating temperatures, which are often based on or blended with polybenzimidazole (PBI) materials, are being investigated [40]. Examples of these include pure PBI, partially fluorinated poly(arylene ether) (sFS) blended with PBI, non-fluorinated poly(arylene etherethersulfone) (sPSU) with or without PBI [41] and ionically and ionically-covalently cross-linked PBI blended membranes [40,42]. Apart from pure PBI, recent studies have also focussed on PBIOO and F_6PBI-based membranes [40]. Figure 1.4 shows the structure of F_6PBI which has been shown to have superior stability in acidic environments [40,42].

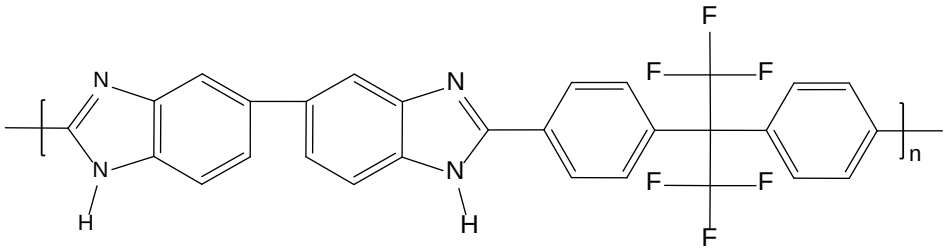

Figure 1.4 : Structure of F_6PBI [40,42]**.**

To characterise a membrane's performance in terms of SO_2 electrolysis various techniques are available. Similar to the Fenton's test used in fuel cell research, the chemical stability of membranes used in the SO_2 electrolyser can be characterised by exposing the membranes to 80 wt% sulphuric acid at 80°C for 120 h [41,40]. TGA-MS analysis has been used to determine the chemical stability of the materials by determining changes in the structures of the membrane material after acid

exposure [40,42]. In addition, electrochemical impedance spectroscopy (EIS), which is also widely used in the fuel cell environment [43,44], has been applied to evaluate the performance of various MEAs in an SO_2 electrolyser by separating the charge resistance (kinetic), ohmic resistance (membrane resistance) and the mass transport limitations [45].

According to literature there are currently three possible methods of operating an SO_2 electrolyser: i) supplying SO_2 dissolved in H_2SO_4 as the anode reactant and clean H_2SO_4 as the cathode reactant, ii) using pure SO_2 gas as anode and liquid water as cathode (for temperatures lower than 100°C) and iii) humidifying the anode SO_2 supply while running a dry cathode (for temperatures above 100°C) [39].

The first method of operation (H_2SO_4 containing dissolved SO_2) was suggested by the Westinghouse Corporation in the 1970s [46]. Although the low solubility of sulfur dioxide in concentrated sulphuric acid (50 wt%) [47] resulted in a limited current and significant mass transport limitations, it did demonstrate the operation of the SO_2 electrolyser.

Sivasubramanian *et al.* [23] showed that the electrolyser could be operated using SO_2 gas as anode and liquid water as cathode (method 2) using a proton exchange membrane (PEM). The water needed for the reaction is supplied by the diffusion of water from the cathode to the anode. Although a maximum current density of 0.4 A cm^{-2} could be reached, the diffusion of water from the cathode to the anode was offset by the electro-osmotic drag (water drawn from the anode to cathode due to proton transport). Staser *et al.* [48] showed that the operating current density could be increased to 1 A cm^{-2} using a membrane with a thickness of 25 µm (NR-211) by increasing the differential pressure across the membrane. Although this increased current density significantly improved the hydrogen production capacity, the sulphuric acid produced is diluted due to the permeation of water from the cathode to the anode.

The third method entails a relatively new concept reported in only one published journal article in which the anode SO_2 supply is humidified [39]. In their study, they showed that the operation of a humidified SO_2 electrolyser, using sulfonated polybenzimidazole (PBI)-based membranes, could be used to produce hydrogen. They further showed that the PBI-based membrane, despite being thicker than the NR212 membrane, yielded a better performance than the N212-based membrane at an operating temperature of 80°C.

Apart from its suitability for the production of H_2, the SO_2 electrolyser (using either method 2 or 3 depending on the membrane type), could also be used in the mining environment. It is well-known that SO_2 is a major component of the off-gas stream produced in many mining industries [49–54]. Although no literature is available on this topic, it would be interesting to investigate whether the SO_2 electrolyser could be used to convert the significant amount of SO_2 vented annually [53] to H_2 gas and sulphuric acid while simultaneously reducing the amount of vented SO_2. Unfortunately however, the composition of the flue gas produced by the mining industry consists not only of SO_2 but also contains CO, CO_2, NH_3, NO, NO_2 and H_2S. The presence of these gaseous components could influence the effectiveness of the SO_2 electrolyser catalyst significantly. The effect of these components on other systems, that also incorporate MEA technology like fuel cells, has been investigated intensively and shows that performance is reduced significantly, especially for sulfur (SO_2, H_2S) compounds and CO [55,56]. Similar studies have however not been conducted for the SO_2 electrolyser.

1.2 PROBLEM STATEMENT

Although literature does provide a number of papers on specific aspects of SO_2 electrolysis, a detailed investigation of the operating parameters is not available when operating the electrolyser under ambient pressures (i.e. no pressure differential across the PEM). This is for example required when specific cell performance or acid concentrations are needed.

Apart from the optimisation of the operating parameters, a more specific analysis of factors contributing to the overall cell voltage is necessary. This can be achieved by analysing effects that are known to influence MEA performance such as kinetics, membrane resistance and mass transport. As MEA manufacturing is a key process in the overall SO_2 electrolysis system a detailed MEA manufacturing study would contribute to the improvement of the cell performance.

As discussed above, the application of the SO_2 electrolyser within the mining industry could be a possibility. For this reason the effect of contaminant gases such as H_2S should be evaluated to determine their effect on the SO_2 electrolyser anode.

In order to further increase the electrolyser performances by increasing the electrolyser temperature is an easy and hence obvious choice. To facilitate temperatures above 100°C, membranes other than PFSA-based have to be identified and evaluated. PBI-based membranes have the ability to conduct protons at temperatures as high as 180°C within the HT-PEMFC environment [57]. However, before doing SO_2 electrolysis at these elevated temperatures, various issues must first be overcome, including chemical and temperature stability, MEA doping methods, activation procedures and optimisation of polymer blend ratios.

1.3 AIM AND OBJECTIVES OF STUDY

In view of the above mentioned, the aim of the study was i) to determine the influence of specific variables (operating conditions, MEA manufacturing and H_2S contamination) on the performance of the SO_2 electrolyser using Nafion® as benchmark and ii) to investigate the suitability of PBI-based membranes for SO_2 electrolysis.

To achieve the above mentioned aim the following objectives were identified:

i) Automation of a SO_2 electrolyser system to facilitate the operation of an SO_2 electrolyser whilst also increasing the operational safety[1].

ii) Characterise and optimise specific operating parameters such as cell temperature, catalyst loading and membrane thickness.

iii) Evaluate the influence of the MEA manufacturing process on cell performance.

iv) Investigate the effect of H_2S contamination on the performance of an SO_2 electrolyser.

v) Determine the suitability of PBI-based membranes for the SO_2 electrolyser and optimise the doping of PBI-based MEAs.

vi) Investigate the performance of PBI blends containing poly(2,6-dimethylbromide-1,4-phenylene) oxide (PPOBr) and poly(tetrafluorostyrene-4-phophonic) acid (PWN).

[1] Forming the backdrop and pre-requirement for the study, this objective is not discussed in the individual experimental chapters but in Appendix A.

1.4 OUTLINE OF THESIS

A brief discussion is given in ***Chapter 1*** on energy supply, focussing on the use of H_2 as an energy carrier and its manufacture using electrolysis. The characterisation techniques of the catalyst and membrane used in the SO_2 electrolytic cell are briefly described before presenting the aim, objectives and the outline of the thesis.

In ***Chapter 2*** the influence of various parameters including hot pressing pressure, cell temperature, catalyst loading, membrane thickness, membrane type and SO_2 concentration supplied to the anode on the performance of the SO_2 electrolyser is presented. The use of dissolved SO_2 in H_2SO_4 as anolyte and de-aerated H_2SO_4 as catholyte is also briefly analysed by varying the cell temperature, membrane thickness and acid concentration used.

Using the optimised parameters from Chapter 2, the influence of the MEA manufacturing process is evaluated in ***Chapter 3***. Polarisation curves and electrochemical spectroscopy analysis (EIS) were employed to both determine the cell performance and to differentiate the membrane and the charge transfer resistance, as well as the mass transport limitations.

In ***Chapter 4***, using the optimal conditions determined in Chapter 2 and 3, the influence of H_2S as a contaminant on the cell performance was evaluated. The effect of H_2S was established by using EIS while the electrochemical surface area (ECSA) was determined by CO stripping.

In ***Chapter 5*** the MEA acid doping procedure when using PBI-based membranes (PBI membranes must be doped with acid for proton conductivity) was optimised. The influence of the process parameters discussed in Chapter 2 and 3, were subsequently determined when using PBI-based membranes. Chemical stability as well as electrochemical analysis is also provided to further elucidate the applicability of these membranes.

Applying the optimised MEA doping procedure determined in Chapter 5, the suitability of novel covalently and ionically cross-linked PBI-excess blends for SO_2 operation is evaluated in ***Chapter 6***. The H_2SO_4 stability was determined, while

polarisation curves and voltage stepping was used to evaluate the performance within the SO_2 electrolyser.

In ***Chapter 7*** the results from Chapters 2-6 are recapitulated from which the overall conclusions of the thesis are summarised. Finally, recommendations are presented for possible future work that might i) further increase electrolyser efficiency and ii) broaden the set of characterisation techniques for MEA evaluation.

In ***Appendix A*** the automation of the SO_2 electrolyser system used to generate the data shown in this study is presented.

In ***Appendix B*** the front pages of the published articles from this study are presented.

1.5 REFERENCES

[1] Dai K, Bergot A, Liang C, Xiang W-N, Huang Z. Environmental issues associated with wind energy – A review. Renew Energy 2015;75:911–21. doi:10.1016/j.renene.2014.10.074.

[2] Harvey LDD. The potential of wind energy to largely displace existing Canadian fossil fuel and nuclear electricity generation. Energy 2013;50:93–102. doi:10.1016/j.energy.2012.12.008.

[3] Bahadori A, Nwaoha C. A review on solar energy utilisation in Australia. Renew Sustain Energy Rev 2013;18:1–5. doi:10.1016/j.rser.2012.10.003.

[4] Sarver T, Al-Qaraghuli A, Kazmerski LL. A comprehensive review of the impact of dust on the use of solar energy: History, investigations, results, literature, and mitigation approaches. Renew Sustain Energy Rev 2013;22:698–733. doi:10.1016/j.rser.2012.12.065.

[5] Kaldellis JK. The contribution of small hydro power stations to the electricity generation in Greece: Technical and economic considerations. Energy Policy 2007;35:2187–96. doi:10.1016/j.enpol.2006.06.021.

[6] Philpott A, Guan Z, Khazaei J, Zakeri G. Production inefficiency of electricity markets with hydro generation. Util Policy 2010;18:174–85. doi:10.1016/j.jup.2010.09.001.

[7] Rehman S, Al-Hadhrami LM, Alam MM. Pumped hydro energy storage system: A technological review. Renew Sustain Energy Rev 2015;44:586–98. doi:10.1016/j.rser.2014.12.040.

[8] Angarita JL, Usaola J, Martínez-Crespo J. Combined hydro-wind generation bids in a pool-based electricity market. Electr Power Syst Res 2009;79:1038–46. doi:10.1016/j.epsr.2009.01.002.

[9] Suomalainen K, Pritchard G, Sharp B, Yuan Z, Zakeri G. Correlation analysis on wind and hydro resources with electricity demand and prices in New Zealand. Appl Energy 2015;137:445–62. doi:10.1016/j.apenergy.2014.10.015.

[10] Santos-Alamillos FJ, Pozo-Vázquez D, Ruiz-Arias JA, Von Bremen L, Tovar-Pescador J. Combining wind farms with concentrating solar plants to provide stable renewable power. Renew Energy 2015;76:539–50. doi:10.1016/j.renene.2014.11.055.

[11] Ahmed NA, Miyatake M, Al-Othman AK. Power fluctuations suppression of stand-alone hybrid generation combining solar photovoltaic/wind turbine and fuel cell systems. Energy Convers Manag 2008;49:2711–9. doi:10.1016/j.enconman.2008.04.005.

[12] Vick BD, Moss TA. Adding concentrated solar power plants to wind farms to achieve a good utility electrical load match. Sol Energy 2013;92:298–312. doi:10.1016/j.solener.2013.03.007.

[13] Ehnberg SGJ, Bollen MHJ. Reliability of a small power system using solar power and hydro. Electr Power Syst Res 2005;74:119–27. doi:10.1016/j.epsr.2004.09.009.

[14] Ma S, Wang H, Wang Y, Bu H, Bai J. Bio-hydrogen production from cornstalk wastes by orthogonal design method. Renew Energy 2011;36:709–13. doi:10.1016/j.renene.2010.08.019.

[15] Su H, Linkov V, Bladergroen BJ. Membrane electrode assemblies with low noble metal loadings for hydrogen production from solid polymer electrolyte water electrolysis. Int J Hydrogen Energy 2013;38:9601–8.

[16] Dedigama I, Angeli P, Ayers K, Robinson JB, Shearing PR, Tsaoulidis D, et al. In situ diagnostic techniques for characterisation of polymer electrolyte membrane water electrolysers – Flow visualisation and electrochemical impedance spectroscopy. Int J Hydrogen Energy 2014;39:4468–82. doi:10.1016/j.ijhydene.2014.01.026.

[17] Wei G, Wang Y, Huang C, Gao Q, Wang Z, Xu L. The stability of MEA in SPE water electrolysis for hydrogen production. Int J Hydrogen Energy 2010;35:3951–7. doi:http://dx.doi.org/10.1016/j.ijhydene.2010.01.153.

[18] Carmo M, Fritz DL, Mergel JJ, Stolten D. A Comprehensive review on PEM electrolysis. Int J Hydrogen Energy 2013;38:4901–34. doi:10.1016/j.ijhydene.2013.01.151.

[19] Millet P, Ngameni R, Grigoriev SA, Mbemba N, Brisset F, Ranjbari A, et al. PEM water electrolyzers: From electrocatalysis to stack development. Int J Hydrogen Energy 2010;35:5043–52. doi:10.1016/j.ijhydene.2009.09.015.

[20] Gorensek MB, Summers WA. Hybrid Sulfur flowsheets using PEM electrolysis and a bayonet decomposition reactor. Int J Hydrogen Energy 2008;34:1–18.

[21] Gorensek MB. Hybrid Sulfur cycle flowsheets for hydrogen production using high-temperature gas-cooled reactors. Int J Hydrogen Energy 2011;36:12725–41.

[22] Gorensek MB, Staser JA, Stanford TG, Weidner JW. A thermodynamic analysis of the SO2/H2SO4 system in SO2-depolarized electrolysis. Int J Hydrogen Energy 2009;34:6089–95.

[23] Sivasubramanian P, Ramasamy RP, Freire FJ, Holland CE, Weidner JW. Electrochemical hydrogen production from thermochemical cycles using proton exchange membrane electrolyzer. Int J Hydrogen Energy 2007;32:463–8.

[24] Orme CJ, Klaehn JR, Stewart FF. Membrane separation processes for the benefit of the sulfur–iodine and hybrid sulfur thermochemical cycles. Int J Hydrogen Energy 2009;34:4088–96. doi:http://dx.doi.org/10.1016/j.ijhydene.2008.06.046.

[25] Zhang P, Chen SZ, Wang LJ, Yao TY, Xu JM. Study on a lab-scale hydrogen production by closed cycle thermo-chemical iodine-sulfur process. Int J Hydrogen Energy 2010;35:10166–72.

[26] Staser J, Ramasamy RP, Sivasubramanian P, Weidner JW. Effect of Water on the Electrochemical Oxidation of Gas-Phase SO2 in a PEM Electrolyzer for H2 Production . Electrochem Solid-State Lett 2007;10:E17–9.

[27] George Karagiannakis Alexandra Zygogianni, Chrysoula Pagkoura, Athanasios G. Konstandopoulos CCA. Hydrogen production via sulfur-based thermochemical cycles: Part 1: Synthesis and evaluation of metal oxide-based candidate catalyst powders for the sulfuric acid decomposition step. Int J Hydrogen Energy 2011;36:2831–44.

[28] Atkin I, Elder RH, Priestman GH, Sinclair DC, Allen RWK. High temperature oxygen separation for the sulphur family of thermochemical cycles - part I: Membrane selection and flux testing. Int J Hydrogen Energy 2011;36:10614–25. doi:http://dx.doi.org/10.1016/j.ijhydene.2011.05.113.

[29] He G, Elder RH, Sinclair DC, Allen RWK. High temperature oxygen separation for the sulphur family of thermochemical cycles – Part II: Sulphur poisoning and membrane performance recovery. Int J Hydrogen Energy 2013;38:785–94. doi:10.1016/j.ijhydene.2012.10.088.

[30] Raffaele Liberatore Giampaolo Caputo, Claudio Felici, Alberto Giaconia, Salvatore Sau, Pietro Tarquini ML. Hydrogen production by flue gas through

sulfur-iodine thermochemical process: Economic and energy evaluation. Int J Hydrogen Energy 2012;37:8939–53.

[31] Staser JA, Gorensek MB, Weidner JW. Quantifying Individual Potential Contributions of the Hybrid Sulfur Electrolyzer. J Electrochem Soc 2010;157:B952–8.

[32] Xue L, Zhang P, Chen S, Wang L. Pt-based bimetallic catalysts for SO2-depolarized electrolysis reaction in the hybrid sulfur process. Int J Hydrogen Energy n.d. doi:http://dx.doi.org/10.1016/j.ijhydene.2014.02.128.

[33] Sophie Charton Patrick Rivalier, Eric Chainet, Jean-Pierre Caire JJ. Hybrid sulfur cycle for H2 production: A sensitivity study of the electrolysis step in a filter-press cell. Int J Hydrogen Energy 2010;35:1537–47.

[34] Hector R. Colon-Mercado DTH. Catalyst evaluation for sulfur dioxide-depolarized electrolyzer. Electrochem Commun 2007;9:2649–53.

[35] O'Brien JA, Hinkley JT, Donne SW, Lindquist SE. The electrochemical oxidation of aqueous sulfur dioxide: A critical review of work with respect to the hybrid sulfur cycle. Electrochim Acta 2010;55:573–91. doi:http://dx.doi.org/10.1016/j.electacta.2009.09.067.

[36] Rubio MA, Urquia A, Dormido S. Diagnosis of performance degradation phenomena in PEM fuel cells. Int J Hydrogen Energy 2010;35:2586–90. doi:10.1016/j.ijhydene.2009.03.054.

[37] Mark Elvington David Hobbs HC-M. Membrane Characterization for a Sulfur-Dioxide Depolarized Electrolyzer (SDE). Savannah River National Laboratory; 2009.

[38] Elvington MC, Colon-Mercado H, McCatty S, Stone SG, Hobbs DT. Evaluation of proton-conducting membranes for use in a sulfur dioxide depolarized electrolyzer. J Power Sources 2010;195:2823–9.

[39] Jayakumar JV, Gulledge A, Staser JA, Kim C-H, Brian C B, Weidner JW. Polybenzimidazole Membranes for hydrogen and sulfuric acid production in the Hybrid Sulfur Electrolyzer. ECS Electrochem Lett 2012;1:F44–8.

[40] Peach R, Krieg HM, Krüger AJ, van der Westhuizen D, Bessarabov D, Kerres J. Comparison of ionically and ionical-covalently cross-linked polyaromatic membranes for SO2 electrolysis. Int J Hydrogen Energy 2014;39:28–40.

[41] Schoeman H, Krieg HM, Kruger AJ, Chromik A, Krajinovic K, Kerres J. H2SO4 stability of PBI-blend membranes for SO2 electrolysis. Int J Hydrogen Energy 2012;37:603–14.

[42] Kruger AJ, Cichon P, Kerres J, Bessarabov D, Krieg HM. Characterisation of a polaromatic PBI blend membrane for SO2 electrolysis. Int J Hydrogen Energy 2015;40:3122–33. doi:http://dx.doi.org/10.1016/j.ijhydene.2014.12.081.

[43] Reid O, Saleh FS, Easton EB. Determining electrochemically active surface area in PEM fuel cell electrodes with electrochemical impedance spectroscopy and its application to catalyst durability. Electrochim Acta 2013;114:278–84. doi:10.1016/j.electacta.2013.10.050.

[44] Tsampas MN, Brosda S, Vayenas CG. Electrochemical impedance spectroscopy of fully hydrated Nafion membranes at high and low hydrogen partial pressures. Electrochim Acta 2011;56:10582–92. doi:10.1016/j.electacta.2011.05.110.

[45] Krüger AJ, Krieg HM, van der Merwe J, Bessarabov D. Evaluation of MEA manufacturing parameters using EIS for SO2 electrolysis. Int J Hydrogen Energy 2014;39:18173–81. doi:10.1016/j.ijhydene.2014.09.012.

[46] Brecher LE, Spewock S, Warde CJ. The Westinghouse Sulfur Cycle for the thermochemical decomposition of water. Int J Hydrogen Energy 1977;2:7–15. doi:http://dx.doi.org/10.1016/0360-3199(77)90061-1.

[47] Kruger AJ, Krieg HM, Neomagus HWJP. SO2 Solubility in 50 wt % H2SO4 at Elevated Temperatures and Pressures. J Chem Eng Data 2014;59:1–7. doi:dx.doi.org/10.1021/je4002366.

[48] Staser JA, Weidner JW. Effect of Water Transport on the Production of Hydrogen and Sulfuric Acid in a PEM Electrolyzer. J Electrochem Soc 2009;156:B16–21.

[49] Kriek RJ, Ravenswaay JP van, Potgieter M, Calitz A, Lates V, Bjorketun ME, et al. SO2 - an indirect source of energy. J South African Inst Min Metall 2013;113:593–604.

[50] Frins E, Bobrowski N, Osorio M, Casaballe N, Belsterli G, Wagner T, et al. Scanning and mobile multi-axis DOAS measurements of SO2 and NO2 emissions from an electric power plant in Montevideo, Uruguay. Atmos Environ 2014;98:347–56. doi:10.1016/j.atmosenv.2014.03.069.

[51] Lupiáñez C, Guedea I, Bolea I, Díez LI, Romeo LM. Experimental study of SO2 and NOx emissions in fluidized bed oxy-fuel combustion. Fuel Process Technol 2013;106:587–94. doi:10.1016/j.fuproc.2012.09.030.

[52] Mandi RP, Yaragatti UR. Control of CO2 emission through enhancing energy efficiency of auxiliary power equipment in thermal power plant. Int J Electr Power Energy Syst 2014;62:744–52. doi:10.1016/j.ijepes.2014.05.039.

[53] Bessarabov D, van Niekerk F, van der Merwe F, Vosloo M, North B, Mathe M. Hydrogen Infrastructure within HySA National Program in South Africa: Road Map and Specific Needs. Energy Procedia 2012;29:42–52. doi:10.1016/j.egypro.2012.09.007.

[54] Krüger AJ, Krieg HM, Bessarabov D. Effect of H2S on SO2-depolarised water electrolysis. Int J Hydrogen Energy 2015;40:4442–50. doi:10.1016/j.ijhydene.2015.02.036.

[55] Zhai Y, Bender G, Bethune K, Rocheleau R. Influence of cell temperature on sulfur dioxide contamination in proton exchange membrane fuel cells. J Power Sources2 2014;247:40–8.

[56] Cheng X, Shi Z, Glass N, Zhang L, Zhang J, Song D, et al. A review of PEM hydrogen fuel cell contamination: Impacts, mechanisms, and mitigation. J Power Sources 2007;165:739–56.

[57] Su H, Jao T-C, Barron O, Pollet BG, Pasupathi S. Low platinum loading for high temperature proton exchange membrane fuel cell developed by ultrasonic spray coating technique. J Power Sources 2014;267:155–9. doi:10.1016/j.jpowsour.2014.05.086.

CHAPTER 2: VARIOUS OPERATING METHODS AND PARAMETERS FOR SO_2 ELECTROLYSIS*

Chapter Overview

The application of PFSA-based proton exchange membranes (PEM) was investigated for the production of hydrogen and sulphuric acid using a SO_2-depolarized electrolyser system (using a 25 cm^2 active area). Parameters investigated included hot pressing pressure for the MEA manufacturing, cell temperature, membrane thickness, catalyst loading, membrane type and SO_2 anode feed concentration. The effects of cell temperature, membrane thickness and acid concentrations were also investigated when using a second method where clean sulphuric acid as cathode and SO_2 saturated sulphuric acid as anode were used. Electrochemical impedance spectroscopy showed that the pressure exerted in the MEA manufacturing step had a significant influence, with 125 kg cm^{-2} yielding the highest current density. High temperatures (> 80°C) and thin membranes (≈120 µm) showed the best performance while thicker membranes produced higher acid concentration when using the first system. The SO_2 concentration in the anode had a significant influence with the overpotential increasing with decreasing SO_2 concentration. When using the second method, it was found that the SO_2 solubility in sulphuric acid was important as the mass transport of the SO_2 limits the overall reaction rate. From the two systems tested, the first method *i.e.* dry SO_2 anode and liquid water cathode showed the best operational effectiveness reaching a maximum of 0.32 A cm^{-2} at 80°C using N115 coated with 1 mgPt cm^{-2} while the second system under the same conditions achieved a current density of 0.18 A cm^{-2} when using N117.

* Krüger, A.J., Krieg, H. M., Grigoriev, S. A. and Bessarabov, D. (2015), Various operating methods and parameters for SO_2 electrolysis. Energy Science & Engineering. Doi 10.1002/ese3.80

2.1 INTRODUCTION

It is well known that the electrolysis of water is regarded as an alternative to the conventional methods for the production of hydrogen [1]. With the development of proton exchange membranes (PEM), the interest in the electrochemical production of oxygen and hydrogen from water has significantly increased as PEM-based water electrolysis is an efficient and environmental friendly method that can be used for the production of hydrogen when zero-carbon power sources such as renewable or nuclear are used [1]. It is well known that the theoretical energy input for water electrolysis is 1.229 V with the practical operating voltage in the 1.7 – 2 V range. Attempts to increase the overall electrolysis efficiency have been made, for example in the development of high temperature steam electrolysis [2]. More intricate systems have also been nominated as possible improvements on normal electrolysis including thermochemical cycles. Almost 100 thermochemical cycles have been identified by the department of energy (DOE-USA) of which the sulfur-based cycles, specifically the Sulfur Iodine (SI) and the Hybrid Sulfur (HyS) cycles [3] seem most favourable. The HyS cycle, which is the focus of this study, requires a high temperature step (also present in the SI cycle), which has conventionally been assumed to be supplied by nuclear reactors, where sulphuric acid (H_2SO_4) is decomposed to SO_2, H_2O and O_2. Subsequently, the oxygen is removed as a product, while the SO_2 and H_2O are fed to a PGM (Platinum Group Metal) catalysed SO_2 electrolyser where the SO_2 and water are converted to H_2 and H_2SO_4 by means of a PEM (proton exchange membrane) electrode assembly (MEA) [4]. The overall reaction for the electrolysis step is shown in Equation 2.1.

$$2H_2O + SO_2 \rightarrow H_2SO_4 + H_2 \qquad (2.1)$$

The produced H_2SO_4 is recycled to the decomposer to complete the cycle [5]. By making certain assumptions for the decomposer and separation step, Gorensek *et al.* [3] showed that when operating the electrolyser at 0.6 V and 0.5 A cm^{-2}, the entire HyS cycle can achieve a thermal to electrical efficiency of 47% [3]. The advantage of the SO_2 depolarised electrolysis is that the theoretical potential needed to drive the electrolysis step is only 0.158 V [4] with practical potentials of 0.5 – 0.9 V, which is considerably lower than that of water electrolysis. However, for the electrolyser to

be economically feasible, the hydrogen produced must be of high purity as its purity is essential when used in the fuel cell market where it has been clearly shown that impurities, such as SO_2, reduce the operation efficiency of a fuel cell dramatically [6]. On the other hand, a high concentration of sulphuric acid (in the range of 65 wt% [7]) is needed to ensure that the subsequent HyS decomposition step is efficient enough to make the entire HyS cycle competitive compared to other hydrogen production methods currently being explored [8].

When the Westinghouse Corporation initially developed the SO_2 electrolyser in the 70s, it was run using a diaphragm as separator, where clean sulphuric acid was fed to the cathode and sulphuric acid saturated with SO_2 gas fed to the anode [5]. Although initial results were poor due to the high ohmic resistance of the separator and the limited mass transport of the SO_2 gas in the acid, it did show the potential of SO_2 depolarized electrolysis. Sivasubramanian *et al.* [4] showed that the performance of the SO_2 electrolyser can be increased by exchanging the diaphragm with PFSA-based proton exchange membranes, such as Nafion® and supplying the cathode with liquid water and the anode with dry SO_2 gas. More recently Staser *et al*. [9] showed that the cell voltage can be decreased further by increasing the cathode water pressure, whereby the authors almost reached the desired electrolyser operating conditions initially proposed by Gorensek *et al*. [3], reaching 0.760 V at 0.5 A cm^{-2}. The acid concentration produced was however not sufficient for re-circulation to the decomposer. Other aspects that need further attention include the SO_2 crossover from the anode to the cathode leading not only to the removal of unreacted SO_2, but also to an increased cell voltage due to catalyst poisoning on the cathode while simultaneously producing unwanted and potentially toxic gases such as H_2S in the H_2 product stream. Although the high cathode pressure used by Staser *et al*. [10] significantly reduced the SO_2 crossover, further work is required to increase the produced acid concentration.

In this chapter a preliminary evaluation of commercial PFSA-based proton exchange membranes for use in SO_2 electrolysis is reported. The various parameters include hot pressing pressure used in the MEA manufacturing step, operating cell temperature, catalyst loading, membrane thickness, membrane type and SO_2 concentration in the anode. Furthermore, the effect of using clean sulphuric acid as

the cathode feed and SO_2 saturated sulphuric acid as the anode feed (as was used initially in the HyS cycle) was evaluated by varying the cell temperature, membrane thickness and acid concentration used.

2.2 EXPERIMENTAL

2.2.1 GENERAL OPERATING PROCEDURE

All membrane samples, including both the Nafion® (Ion Power) and the modified PFSA membranes (FZP-50, Fumatech) were pre-treated in 1M H_2SO_4 at 80°C for 90 min [4], unless stated otherwise. Membrane electrode assemblies were manufactured by hot-pressing (model# 3912, Carver USA) the membranes between two gas diffusion electrodes (FuelCellEtc, USA), consisting of carbon cloth and a micro-porous layer onto which the catalyst had been deposited. A pressure of 125 kg cm^{-2}, unless stated otherwise, at a temperature of 120°C for 5 min was used. The hot-pressed MEAs were stored in a plastic bag in DI water until use. Before SO_2 electrolysis, all MEAs were hydrated at the intended operating temperature for at least 2 h within the electrolyser. Electrolysis was achieved by supplying dry SO_2 gas (150 ml min^{-1}) to the anode using a thermal mass flow controller while DI water was circulated through the cathode compartment as previously described [11]. The acid produced was collected in a glass separation vessel at the anode side. Figure 2.1 shows the experimental system, where a 25 cm^2 electrolyser (Fuel Cell Technologies) was used.

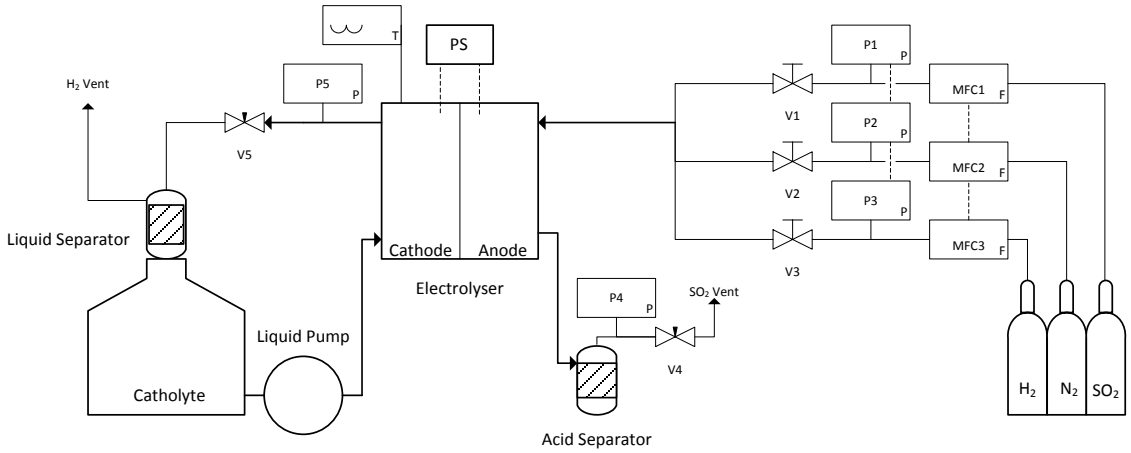

Figure 2.1: Schematic of the experimental SO_2 electrolysis setup with a liquid cathode and a dry SO_2 anode feed with (1) – SO_2 flow meter, (2) – SO_2 electrolyser, (3) – Cathode, (4) – Anode and (5) – Glass acid separator.

All membranes were pre-conditioned by running the electrolyser at 0.1 A cm^{-2} for 20 min before the polarisation curve was started. The polarisation curves were obtained by increasing the current density incrementally every 90 s while recording the voltage. The system used was controlled by a Labview® program.

Electrochemical impedance spectroscopy (EIS) analysis was applied using a Gamry REF300 potentiostat equipped with a frequency response analyser (FRA). The impedance of the electrolyser was measured galvanostatically with a perturbation signal of 10% (2% at current densities higher than 0.25 A cm^{-2} to avoid voltages above 1.1 V) with a frequency range of 10 kHz to 10 mHz. The anode was used as the working electrode while the cathode served as both the counter and reference electrode. An electrical circuit was fitted to the data to determine the membrane resistance, charge resistance and mass transport effect as described in [2].

2.2.2 VARIABLES TESTED

The effects of various parameters were investigated in this study to determine their influence on SO_2 electrolysis. These parameters include hot pressing pressure, temperature, catalyst loading, membrane thickness, membrane type and the SO_2 concentration supplied to the anode. Finally, a second system was used to evaluate the effect of using SO_2 saturated sulphuric acid as the anode and clean sulphuric acid as the cathode where the effect of cell temperature, membrane thickness and acid concentration on cell performance was determined.

The effect of the applied pressure during MEA hot-pressing was evaluated in a pressure range of 50 – 140 kg cm^{-2}. Both the pressing temperature and time were kept constant at 120°C and 5 min respectively while both polarisation curves and EIS were used for characterisation.

To determine the influence of temperature on electrolysis [13], the system was operated at temperatures ranging from 50 – 90°C (each with a new MEA) using N117 and a catalyst loading of 1 mgPt cm^{-2}. Since reaction kinetics are generally increased using a higher catalyst loading [13], three catalyst loadings were tested including 0.3, 0.5 and 1 mgPt cm^{-2}. It should be noted that the 1 mgPt cm^{-2} catalyst loading contained platinum black (with no supporting material) while both the 0.5 and 0.3 mgPt/C cm^{-2} contained platinum on a carbon support. The notation of Pt/C will be used to indicate the platinum supported on carbon catalyst.

As it has been shown previously that the water transport through the membrane influenced the SO_2 electrolysis even when a water pressure gradient was used [14], the effect of membrane thickness was investigated by additionally measuring the sulphuric acid concentration and the specific resistance. The acid concentration was determined by titration with 0.1M NaOH and phenolphthalein as indicator, while the area specific resistance (Ω cm^2) was measured using a high frequency milliohm meter (HP 4328A).

It has been shown for fuel cell applications that the type and configuration of PFSA-based materials, such as different side chains on the PTFE type backbone [15], different equivalent weights being used [15] and alterations to the membrane

configuration to promote proton conductivity [16] influence performance. It was shown that by including zirconium particles within the membrane matrix, the membranes' water content increased at higher temperatures [16]. To determine this influence on SO_2 electrolysis, such a zirconium-containing membrane (FZP-50, Fumatech) was evaluated using 1 mgPt cm^{-2} at 80^oC and compared to a commercial Nafion®-based N115.

While previous studies reported in the literature refer to the use of pure SO_2 gas [4] as the anode this is not always possible when the electrolyser is connected to an industrial process, such as a coal-fired plant [17], where the concentration of SO_2 is depleted after the scrubbing methods to reduce SO_2 emissions. Hence, to determine the influence of the SO_2 concentration, the electrolyser performance was determined using a SO_2 feed concentration range of 10 – 100% (v/v) where N_2 gas was used to dilute the SO_2.

To determine the influence of dry SO_2 gas vs. SO_2 dissolved in diluted H_2SO_4 feed, clean sulphuric acid was supplied to the cathode and SO_2 saturated sulphuric acid to the anode, as schematically illustrated in Figure 2.2. Two double walled glass containers, each with a volume of 250 ml (± 5 ml) were used as the anode and cathode feed compartments, respectively. Batch solutions (2 000 ml) of 30 and 65 wt% sulphuric acid were prepared by diluting 98 wt% H_2SO_4 in DI water (18 MΩ cm). Each glass container was filled with 50 ml of acid. The temperature of the acid solutions was controlled by circulating pre-heated water through the outer compartments using a FED-12ED Julabo water bath. Prior to the application of current, SO_2 gas was bubbled through the anode compartment for at least 2 hours at 50 ml min^{-1} to ensure saturation, while the cathode solution was purged with N_2 gas. No pressure was used to increase the SO_2 content in the anode compartment due the glass construction of the vessels.

Notation	*Description*
⌐	Acid Line
⌐	Commucincation
T1	Water Bath Temp
T2	Electrolyser Temp
PS	Power Supply
PC	Programmable Computer
PP	Peristaltic Pump

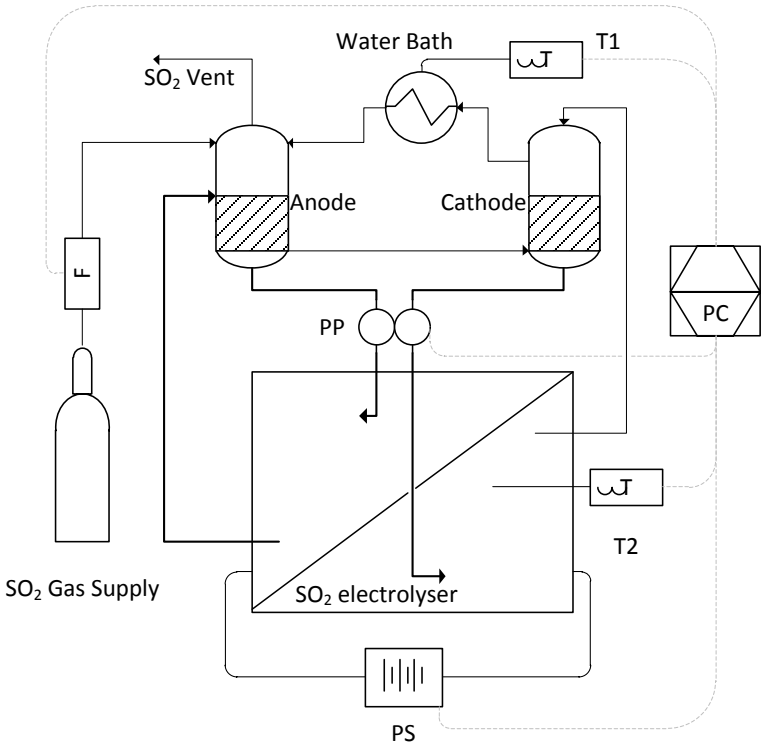

Figure 2.2: Schematic representation of the SO_2 electrolyser system used with an acid cathode and a SO_2-saturated anode feed.

Both anode and cathode solutions were circulated through the electrolyser cell back to the glass containers using a peristaltic pump (WMB, Du520). The same DC power supply was used as for the liquid cathode/dry SO_2 anode system (Figure 2.1). Polarisation curves were obtained by increasing the applied current incrementally every 90 seconds. For this investigation Scanning Electron Microscope (FEI Quanta 250 FEG with ESEM capabilities) images were made of the membrane electrode assemblies for characterisation purposes.

2.3 RESULTS AND DISCUSSION

2.3.1 INFLUENCE OF HOT PRESSING PRESSURE

The pressure exerted in the hot-pressing step was varied from 50 to 140 kg cm^{-2} where both polarisation curves and electrochemical impedance spectroscopy were used to evaluate the effect of the pressure used on the performance. Figure 2.3 shows the polarisation curves for N117 at 80°C with a catalyst loading of 1 mgPt cm^{-2}. From Figure 2.3 it is interesting to notice that the 50 and 140 kg cm^{-2} are comparable at low current densities (< 0.03 A cm^{-2}) while the 50 kg cm^{-2} pressure has better performance up to 0.14 A cm^{-2}. With increased current density (> 0.15 A cm^{-2}) the 140 kg cm^{-2} pressure shows both better performance and a reaches higher current density than the 50 kg cm^{-2}. The 125 kg cm^{-2} pressure shows the best performance irrespective of the current density used. It should also be noticed that the 125 kg cm^{-2} reaches almost 0.3 A cm^{-2} (0.1 A cm^{-2} more than the 140 kg cm^{-2}). It has been shown that the pressure applied in the MEA manufacturing step for fuel cell application also influences performance [12]. A change in the gas diffusion electrode (similar to the one used in this study) gas permeability was observed for gases. Thus the permeability of the reactant SO_2 to the anode, as well as the produced H_2SO_4 permeability from the anode to the flow field, should also be influenced significantly.

To determine why the pressure influences the overall performance of the electrolyser electrochemical impedance spectroscopy (EIS) was done at 0.15 A cm^{-2}. The current density was selected as the 50 kg cm^{-2} could only reach 0.17 A cm^{-2}, i.e. the perturbation current signal of 0.1 amperes would cause the voltage to increase above the 1 volt corrosion limit set by the use of graphite flow field plates.

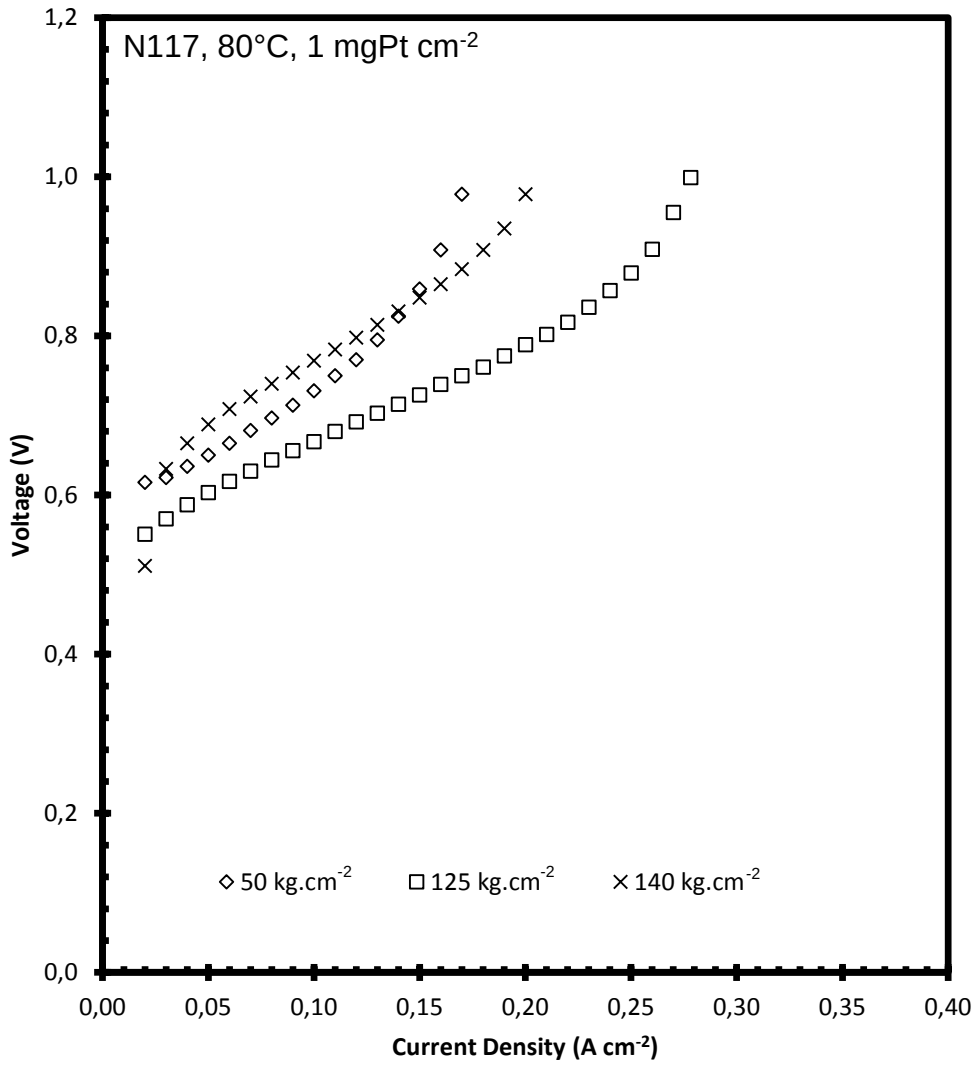

Figure 2.3: Polarisation curves as a function of hot pressing pressure for N117, 1 mgPt cm^{-2} at 80°C.

Figure 2.4 illustrates the EIS data attained for the various hot pressing pressures. It is apparent that the membrane resistance (interception with the x-axis) was not significantly influenced by the hot pressing pressure as has been previously reported in literature [18]. By visual inspection Figure 2.4 confirms the improved polarisation curve attained for the 125 kg cm^{-2} compared to the 50 kg cm^{-2} hot-pressed MEA due to the improved charge transfer characteristics as shown by the width of the semi-circle.

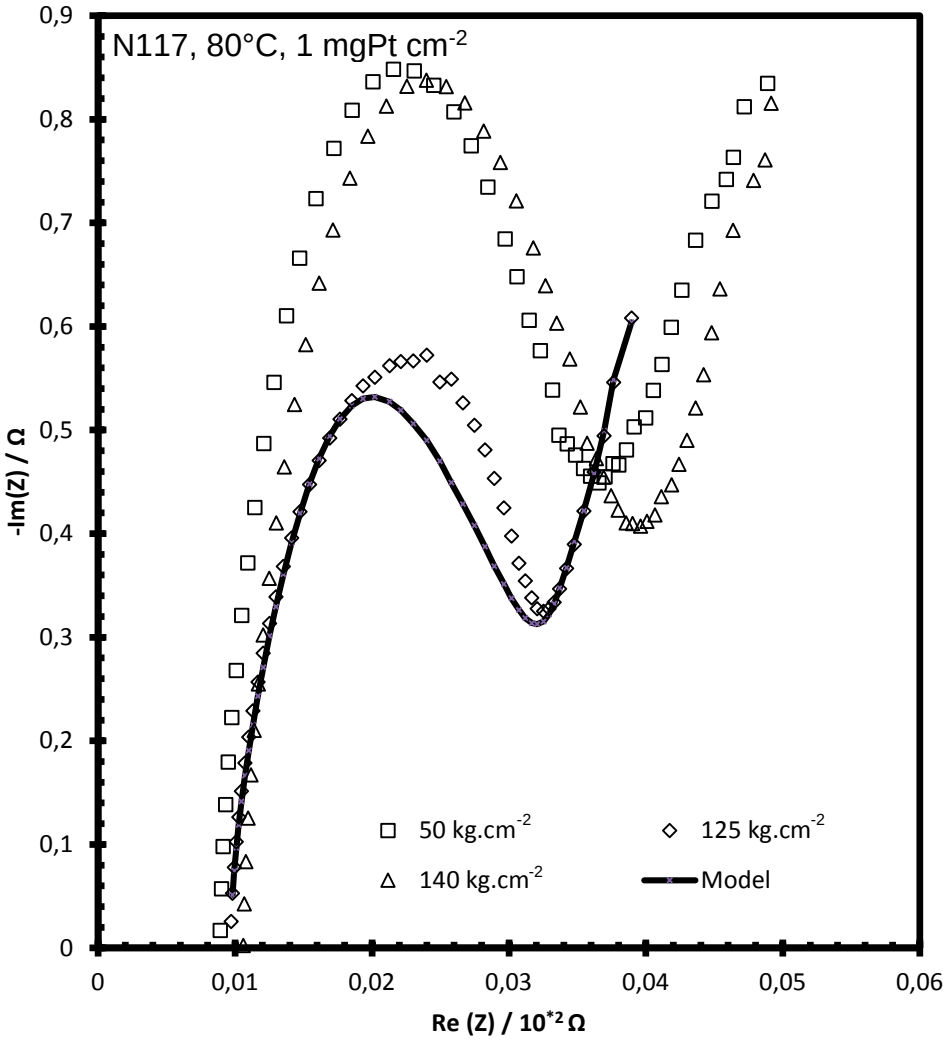

Figure 2.4: Nyquist plots for SO_2 electrolysis as a function of MEA hot pressing pressure. The EIS shown were performed at 0.15 A cm^{-2}.

Mass transport effects can be identified by the straight line in the low frequency range in Figure 2.4 (far right of the x-axis) and is present at all pressures used [12]. Using the electrical circuit as previously described [2] a model fitment could be made to separate the membrane resistance, charge resistance and mass transport limitations. The data obtained from the model supports the assumption made regarding the membrane resistance and was confirmed with the membrane resistance increasing slightly from 8.30 to 10.20 mΩ when the pressure was increased from 50 – 140 kg cm^{-2}, respectively. The charge resistance was comparable between 125 and 140 kg cm^{-2} (20.98 vs. 28.50 mΩ respectively) while the 50 kg cm^{-2} had the highest resistance of 56.90 mΩ. The mass transport

limitations increased as the applied hot pressing pressure increased. It is clear that the most influential factor for performance, at 0.15 A cm^{-2}, appears to be the charge resistance as this is the only parameter in which the 125 kg cm^{-2} is better than the 50 and 140 kg cm^{-2}.

2.3.2 INFLUENCE OF TEMPERATURE

The effect of temperature on the cell performance for the 25 cm^{-2} active area acid electrolyser is shown in Figure 2.5 for N117 (183 µm) using a 1 mgPt cm^{-2} catalyst loading. Experiments were repeated at 50 and 80°C showing an error of 5% on the operating voltage. Sivasubramanianet *et al*. [4] showed that at low current densities, and no cathode water pressure, the water diffusion from the cathode to the anode provided sufficient water for the reaction. This is however not true at current densities above 0.4 A cm^{-2}, where the water drawn to the cathode due to electro-osmotic drag offsets the natural diffusion of water through the membrane. This was confirmed in this study showing the clear limit on the current density attainable due to the water mass transport limitations. It is well known that the uptake of water by PFSA-based membranes is temperature dependent, i.e. increasing the proton conductivity of the membrane, with an electro-osmotic drag coefficient of 2 at 20°C compared to the 3.3 at 90°C at a constant current [19]. The significant increased performance for the SO_2 electrolyser with increased temperature can be attributed to the higher proton conductivity (due to higher water uptake). However, Staser *et al*. [10] showed that the solubility coefficient (cm^2 s^{-1}) during the crossover of SO_2 from the anode to the cathode increased with increasing temperature, which could reduce the hydrogen evolution efficiency dramatically.

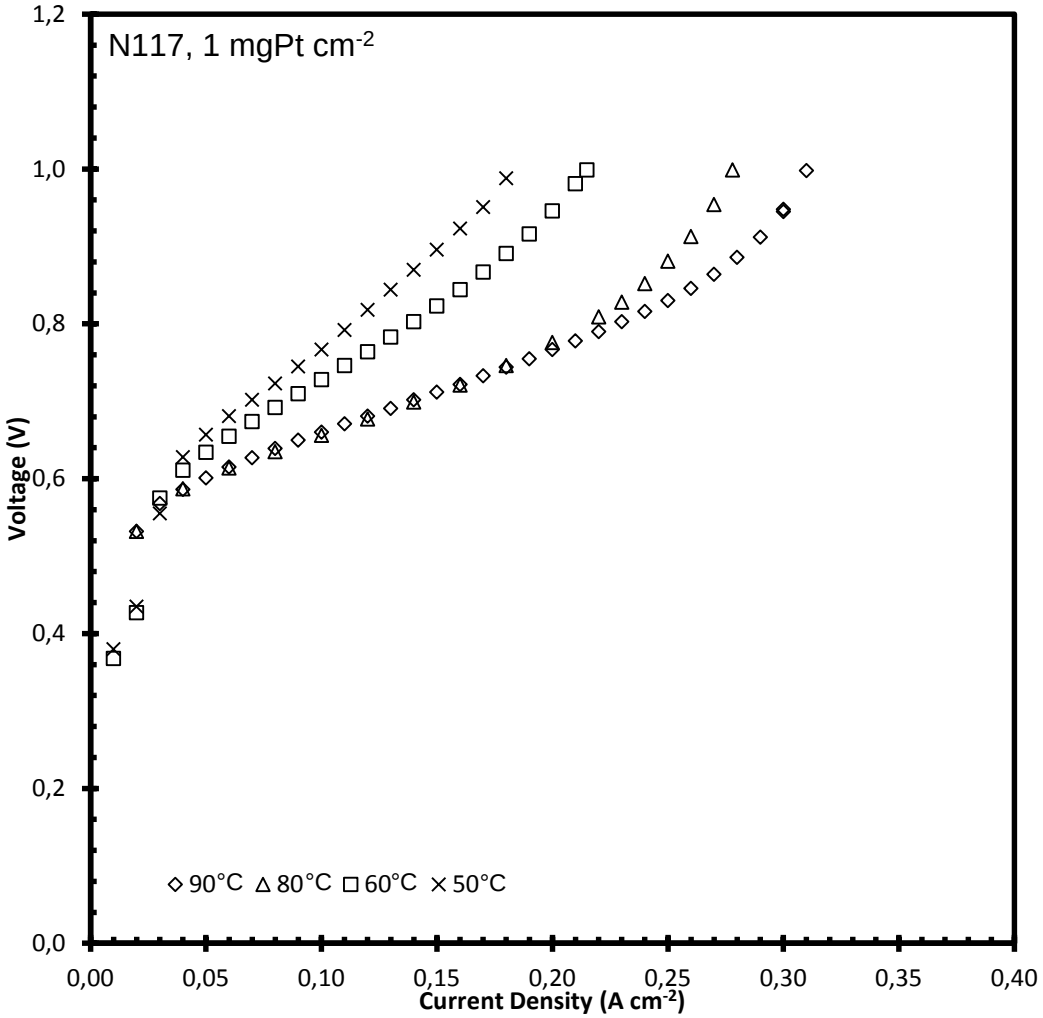

Figure 2.5: Temperature effect on SO_2 electrolysis using N117 and 1 mgPt cm^{-2}.

Table 2.1 shows both the acid concentration and the high frequency values (area specific resistivity, Ω cm^2) as a function of temperature and current density for N117. It can be seen that the cell temperature did not have a significant influence on the area specific resistance at any current density. However, the resistance did increase as a function of the current density. This was also illustrated by Staser *et al*. [20] who obtained an increase in the resistance as a function of the acid concentration produced, i.e. current density.

Table 2.1: Acid concentration produced and area specific resistance of N117 as a function of current density at various temperatures.

	50°C		60°C		80°C		90°C	
Current density (A cm^{-2})	$[H_2SO_4]$ (mol L^{-1})	R_{AC} (Ω m^2)	$[H_2SO_4]$ (mol L^{-1})	R_{AC} (Ω cm^2)	$[H_2SO_4]$ (mol L^{-1})	R_{AC} (Ω cm^2)	$[H_2SO_4]$ (mol L^{-1})	R_{AC} (Ω cm^2)
0.05	4.75	0.12	4.38	0.125	4.5	0.125	4.44	0.10
0.1	6.88	0.11	6.63	0.125	4.53	0.125	5.81	0.11
0.15	6.72	0.11	8.28	0.15	7.1	0.138	6.56	0.12
0.18	7.5	0.125	-	-	-	-	-	-
0.2	-	-	9.81	0.163	6.88	0.138	6.94	0.11
0.25	-	-	-	-	7.44	0.138	-	-
0.28	-	-	-	-	-	-	12.69	0.125

When considering the acid concentration, it is clear from Table 2.1 that at 50°C the acid produced is slightly more concentrated than at 60°C for current densities below 0.15 A cm^{-2}. However, when the current density was increased above 0.15 A cm^{-2} the acid concentration increased from 50°C to 60°C. While this tendency did not hold when increasing to 80°C, it is noticeable that an acid concentration of 12.69 mol L^{-1} ± 0.2 mol L^{-1} (corresponding to 55 wt%) was reached at 90°C at 0.28 A cm^{-2}. While this product acid was the most concentrated H_2SO_4 attained under these conditions, the concentration was below the optimum concentration for the HyS cycle, which should be in the region of 65 wt% [7]. It is clear from the results presented that to increase the concentration of the acid, the cell would have to run at higher current densities while maintaining a reasonable operating voltage. Staser *etal.* [20] showed that the specific-area resistance increased significantly with increased acid concentration produced, although a water pressure was used on the cathode.

2.3.3 INFLUENCE OF CATALYST LOADING

Figure 2.6 shows the data obtained for the different catalyst loadings tested. It is clear that at low current densities the cell performances are almost identical. This is probably due to the low reaction rate of SO_2 at the anode allowing the water enough time to diffuse through the MEA. A slight difference (37 mV when comparing 0.5 and 0.3 loadings) can however be observed when the current densities are above 0.18 A cm^{-2}, where the 1 mgPt cm^{-2} achieved a higher current density when compared to the 0.5 mgPt/C cm^{-2} or 0.3 mgPt/C cm^{-2}. This effect has been seen when a differential pressure was applied where it was shown that the catalyst loading of 1.5 mgPt cm^{-2} vs. 0.5 mgPt/C cm^{-2} had little to no effect on cell performance [9] using catalyst coated membranes. It must be noted that the particle size and catalyst wt% in the ink used to manufacture the GDEs also influenced the overall catalyst utilisation [21] making a direct comparison more difficult as the supplier of the GDEs had confirmed that the PtB catalyst particle size was 9 µm while the Pt/C (60 wt%) catalyst was 4.0 – 5.5 nm. However, the aim in this specific study was to compare the two different commercial catalysts which unfortunately were not available with the same catalyst particle size.

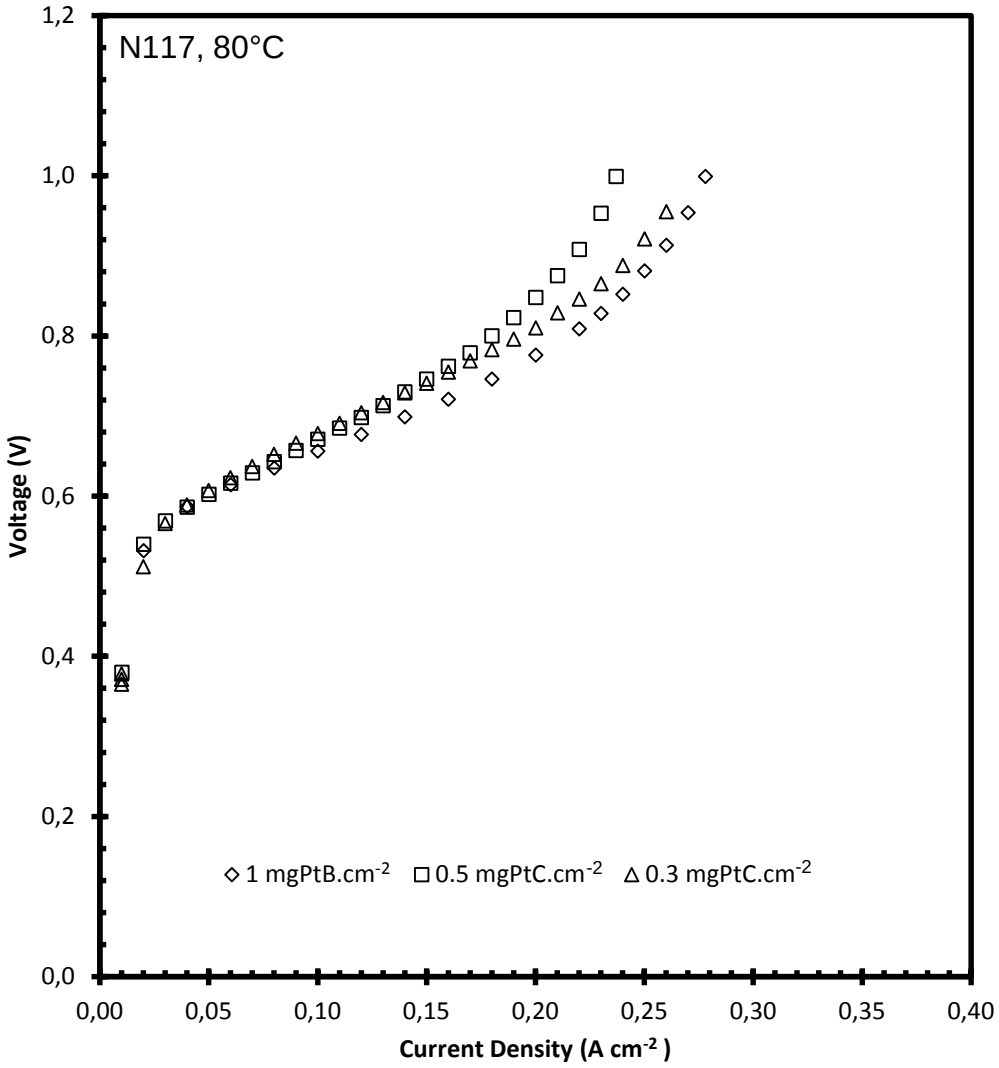

Figure 2.6: Effect of catalyst loading on cell voltage at 80°C.

In a recent study Lee *et al*. [22] investigated the effect of catalyst loading on SO_2 oxidation using a three electrode system. They were able to show that the Pt utilization was influenced significantly by the electrochemical surface area showing an decrease in utilisation with increasing Pt loading [22]. In spite of this inverse proportionality, they were able to show that the exchange current density increased from 9.0 x 10^{-9} to 2.7 x 10^{-5} A cm^{-2} when the Pt loading was increased from 0.4 to 4.02 mgPt cm^{-2}. The area specific resistance was also measured for each catalyst loading and no considerable difference could be established with the resistivity being in the 0.14 – 0.15 Ω cm^2 region.

2.3.4 INFLUENCE OF MEMBRANE THICKNESS

Although literature does provide information on the effect of membrane thickness on the cell performance when operating under a differential pressure, it does not supply data on its affect at ambient anode and cathode pressures [14]. This is illustrated in Figure 2.7 showing the effect of membrane thickness for 3 different Nafion membranes on SO_2 electrolysis. All MEAs were produced using 0.5 mgPt/C cm^{-2} GDEs.

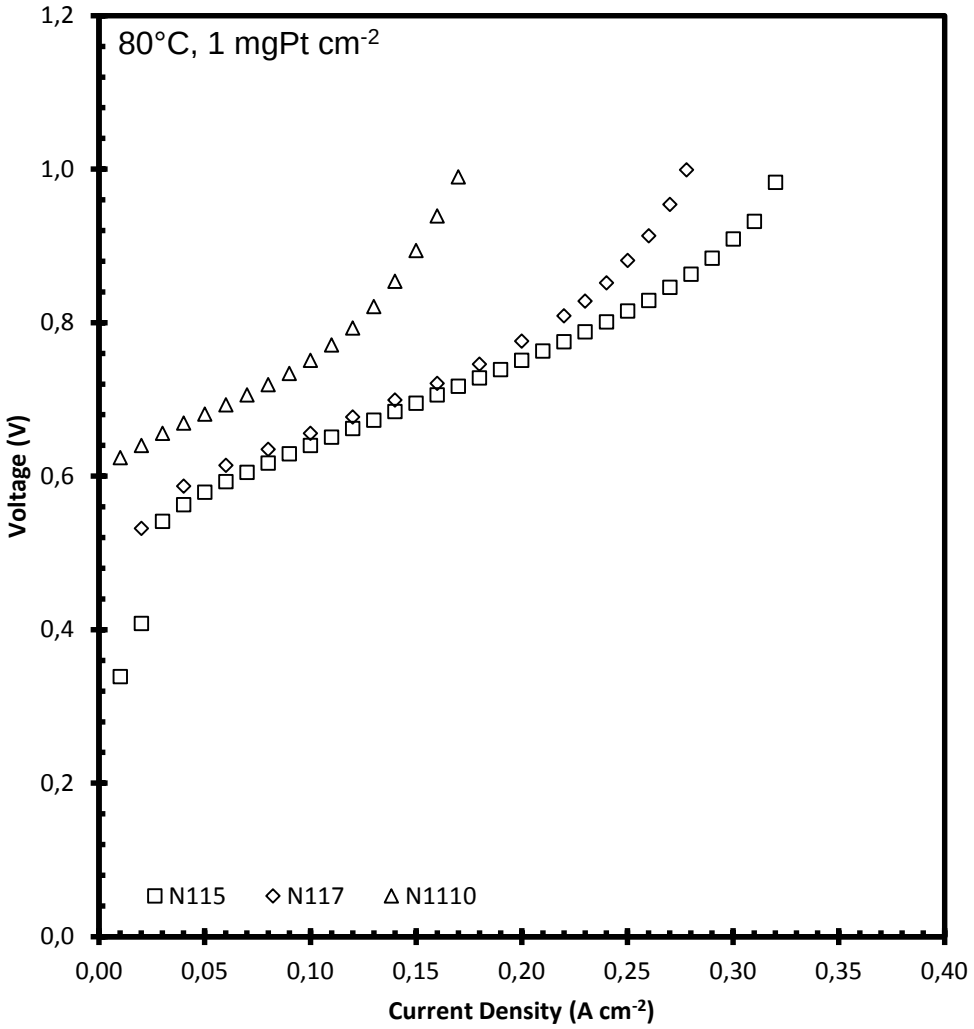

Figure 2.7: Effect of membrane thickness on SO_2 electrolysis performance at 80°C.

When considering the membrane thicknesses of these membranes (N115 = 122 µm; N117 = 183 µm; and N1110 = 245 µm) it is evident that the membrane thickness has a significant influence on the cell performance in terms of current density with N115 reaching 0.32 A cm^{-2} compared to 0.17 A cm^{-2} achieved by N1110. It is well-known

that the water permeation of Nafion® membranes is dependent on membrane thickness with thicker membranes having a lower diffusion coefficient [23] due to a larger diffusion path. Thus, at a constant current density and temperature the total water flux to the anode will increase for thinner membranes. This effect will then, in turn, decrease the acid concentration of thinner membranes while thicker membranes will produce more concentrated sulphuric acid. This was confirmed when considering Table 2.2 where the acid and area specific resistance as a function of membrane thickness at a constant temperature of 80°C is shown.

Table 2.2: Acid concentration produced and area specific resistance as a function of membrane thickness.

	N115		N117		N1110	
Current density ($A\ cm^{-2}$)	$[H_2SO_4]$ ($mol\ L^{-1}$)	R_{AC} ($\Omega\ cm^2$)	$[H_2SO_4]$ ($mol\ L^{-1}$)	R_{AC} ($\Omega\ cm^2$)	$[H_2SO_4]$ ($mol\ L^{-1}$)	R_{AC} ($\Omega\ cm^2$)
0.05	2.53	0.10	5.063	0.14	7.01	0.15
0.1	4.53	0.11	7.25	0.14	7.38	0.18
0.15	6.88	-	-	0.13	8.94	0.19
0.2	7.4	0.11	7.75	0.15	-	-
0.25	7.44	0.12	8.69	0.15	-	-
0.32	8.84	0.14	-	-	-	-

Although cell temperature does influence the operating voltage it was shown that the acid concentration influences the reaction kinetics of SO_2 reduction, as well as the average membrane conductivity even when using a differential pressure [20]. As in Table 2.1, the area specific resistance seemed to increase with increasing current. In addition, the resistance also showed an increase with increasing membrane thickness, where the resistance of N1110 (at 0.1 A cm^{-2}) was nearly twice that of N115. The increasing resistance with increasing current density could be attributed to the produced acid concentration. As N1110 had lower water diffusing to the anode, the acid would be more concentrated compared to N115 and N117. This increase of acid concentration with membrane thickness was also reported by Staser *et al*. [20] when using a pressure differential. Although the acid concentrations were lower due to the permeating water (pressure driven effect) the effect of membrane

thickness on acid concentration was still present. It is also interesting to note that the acid concentration increased more rapidly for N115 (increased by 6.34 mol L^{-1} from 0.05 to 0.32 A cm^{-2}) than for N117 (increased by 3.63 mol L^{-1} over the same current density range).

2.3.5 COMPARISON OF N115 AND FZP – 50

While Nafion® is the commercial standard membrane used for water electrolysis and therefore, often referred to for SO_2 electrolysis, there are other PFSA-based proton exchange membranes of interest. One example is a novel FZP-50 PFSA-based proton exchange membrane from Fumatech, which was evaluated using ambient pressure at 80°C with a 0.5 mgPt/C cm^{-2} catalyst loading. Figure 2.8 shows the comparative performance of N115 and FZP-50 during SO_2 electrolysis. It is clear that the FZP-50 yielded lower voltages at current densities above 0.2 A cm^{-2} than N115. Although the membrane thickness of the FZP-50 is almost 40 µm thinner than the N115 it does show that alternative PFSA membranes are suitable for SO_2 electrolysis.

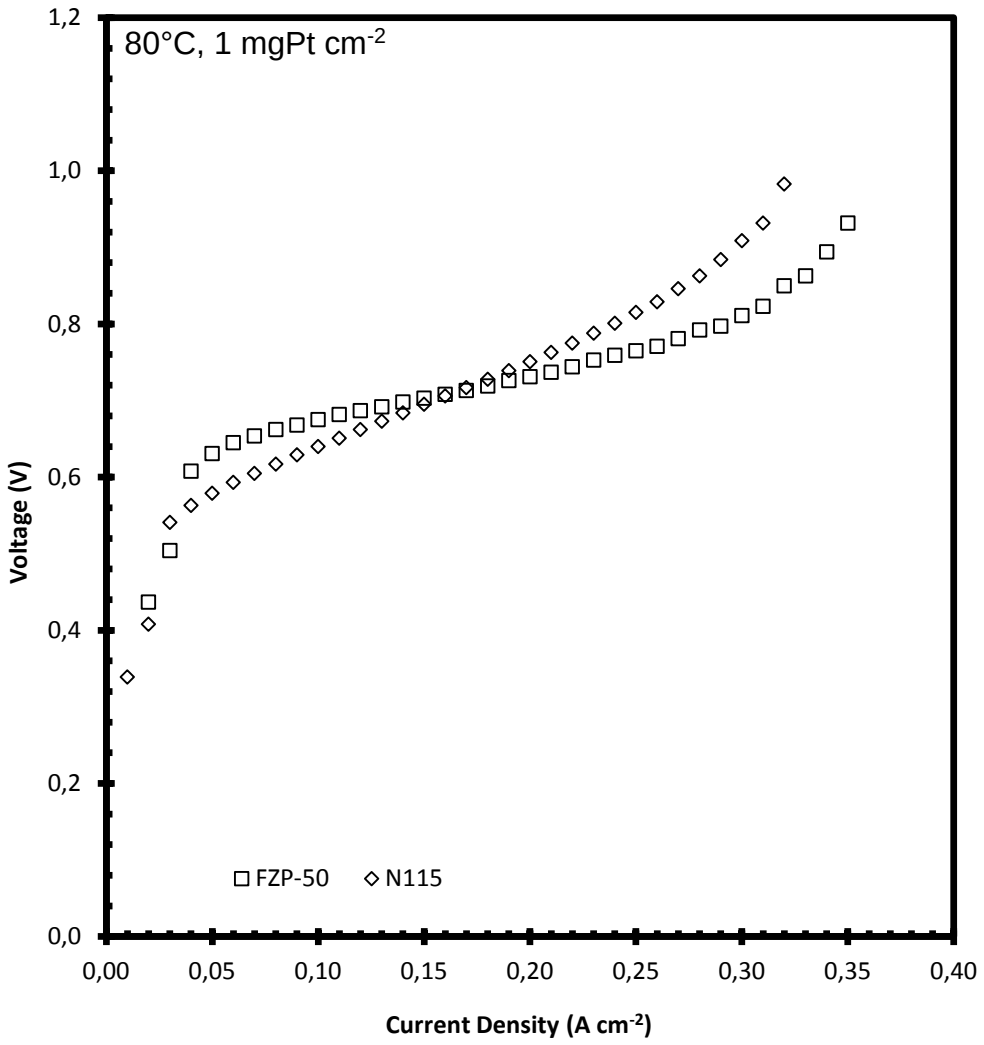

Figure 2.8: Comparison between N115 and FZP-50 PFSA membranes at 80°C and 1 mgPt cm^{-2}.

The FZP-50 PFSA membrane contains zirconium oxide within the polymeric membrane to facilitate water sorption which was initially manufactured for operation of PEM Fuel Cells at temperatures close or higher than 100°C where PFSA membranes have the drawback of losing conductivity (and in turn its water content). It is clear that this improved ability to retain water within the PFSA membrane is advantageous in the SO_2 electrolyser especially at higher current densities, as can be seen from Figure 2.8. According to the measurements, the ohmic resistance of FZP-50 remained near constant, increasing only 0.01 Ω cm^2 over the entire operating current density, while the N115 increased from 0.1 to 0.14 Ω cm^2 showing that the FZP-50 membrane is more stable (better proton conductivity at high acid concentration) in an acid environment than the N115. The acid concentration

produced was similar for the two membranes with N115 producing a slightly higher acid concentration (8.84 vs. 7.2 mol L^{-1} at 0.32 A cm^{-2}). Although the N115 produced slightly higher acid concentrations, the FZP-50 operated under lower potentials, ultimately reducing the energy input needed.

2.3.6 INFLUENCE OF SO_2 FEED CONCENTRATION

To determine this influence the performance of the SO_2 electrolyser fed with a reduced concentration of SO_2 was investigated. In Figure 2.9 the results obtained when feeding the anode concentrations of 100%, 90%, 50% and 10% (v/v) SO_2 gas using 1 mgPt cm^{-2} and N115 at 80°C are presented.

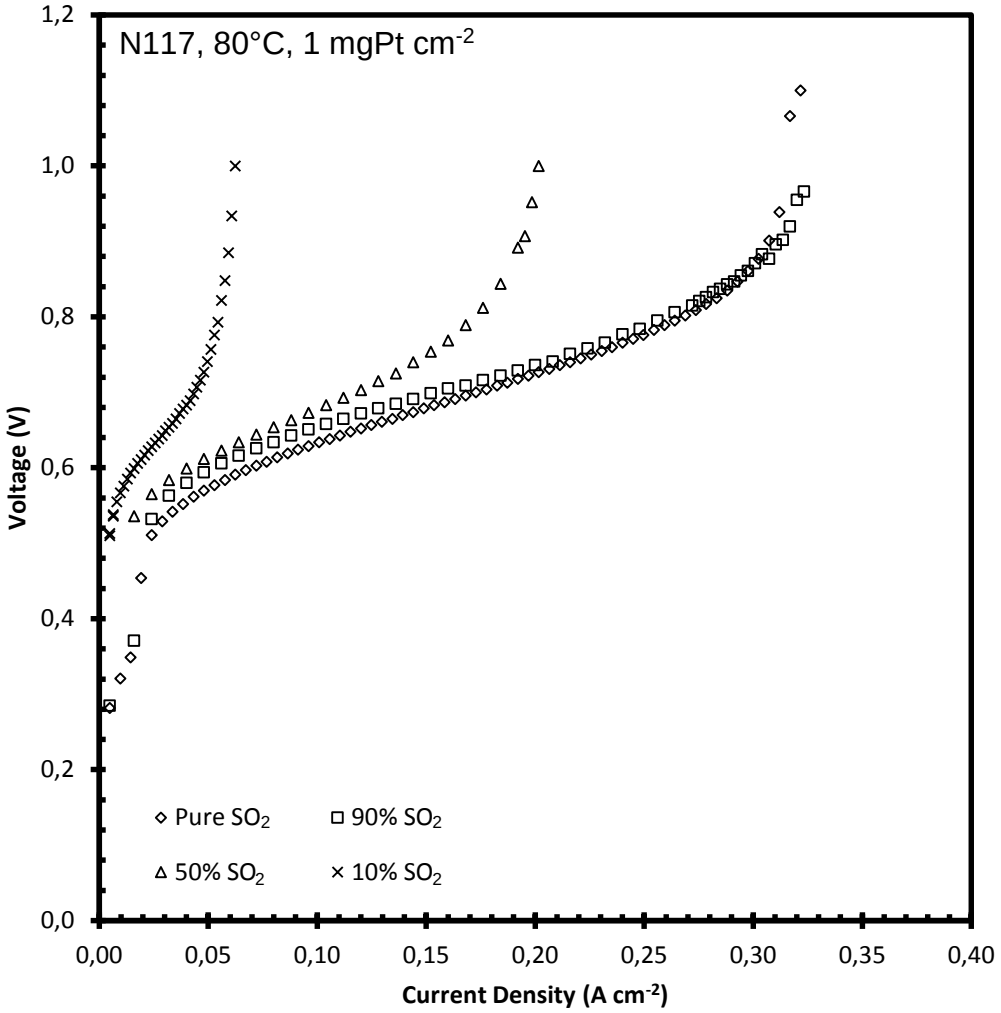

Figure 2.9: Effect of reduced SO_2 concentration on SO_2 electrolysis.

The significant increase in the potential with decreasing SO_2 concentration at constant current density was to be expected in view of the starvation of the anode reactant. This effect was also shown by Seong *et al*. [25] who did however show that better performances could be attained at higher temperatures (reaching 0.2 A cm^{-2} for 20% SO_2), although it was not clear if a pressure difference was used. The overall voltage increase could be linked both to the decreased amount of SO_2 available and to the increased diffusion paths of the SO_2 through the N_2. The voltage penalty caused by reducing the SO_2 concentration from 100% to 50% is 225 mV at 0.2 A cm^{-2}. A possible mitigation step apart from the increased temperatures suggested by Seong *et al*. [25], could be to increase the anode pressure, which would reduce the operating potential at lower SO_2 concentrations.

2.3.7 INFLUENCE OF FEED STREAM CONFIGURATION

Operating the SO_2 electrolyser using alternative configurations is possible, for example by using clean sulphuric acid as the cathode feed and SO_2 saturated sulphuric acid as the anode reactant feed. This configuration was investigated by varying the operating temperature, the membrane thickness and the acid concentration. For this configuration either N115 or N117 was used.

2.3.7.1 INFLUENCE OF TEMPERATURE

Figure 2.10 illustrates the effect of temperature on the performance of SO_2 electrolysis using a 30 wt% sulphuric acid solution. N117 was used with a catalyst loading of 1 mgPt cm^{-2} and an electrolyser with a 25 cm^2 active area. It was expected that the overall performance would increase with increasing temperature (as had been observed by the SO_2 dry anode fed results presented in Figure 2.5). This was however not the case when the SO_2 was dissolved in H_2SO_4, which could probably be ascribed to the solubility of SO_2 in H_2SO_4. It has been shown [26], [27] that the solubility of SO_2 gas in 30 wt% sulphuric acid solution decreases with increasing temperature at constant pressure, thereby reducing the amount of SO_2 gas available for the reaction, resulting in an increased operating voltage.

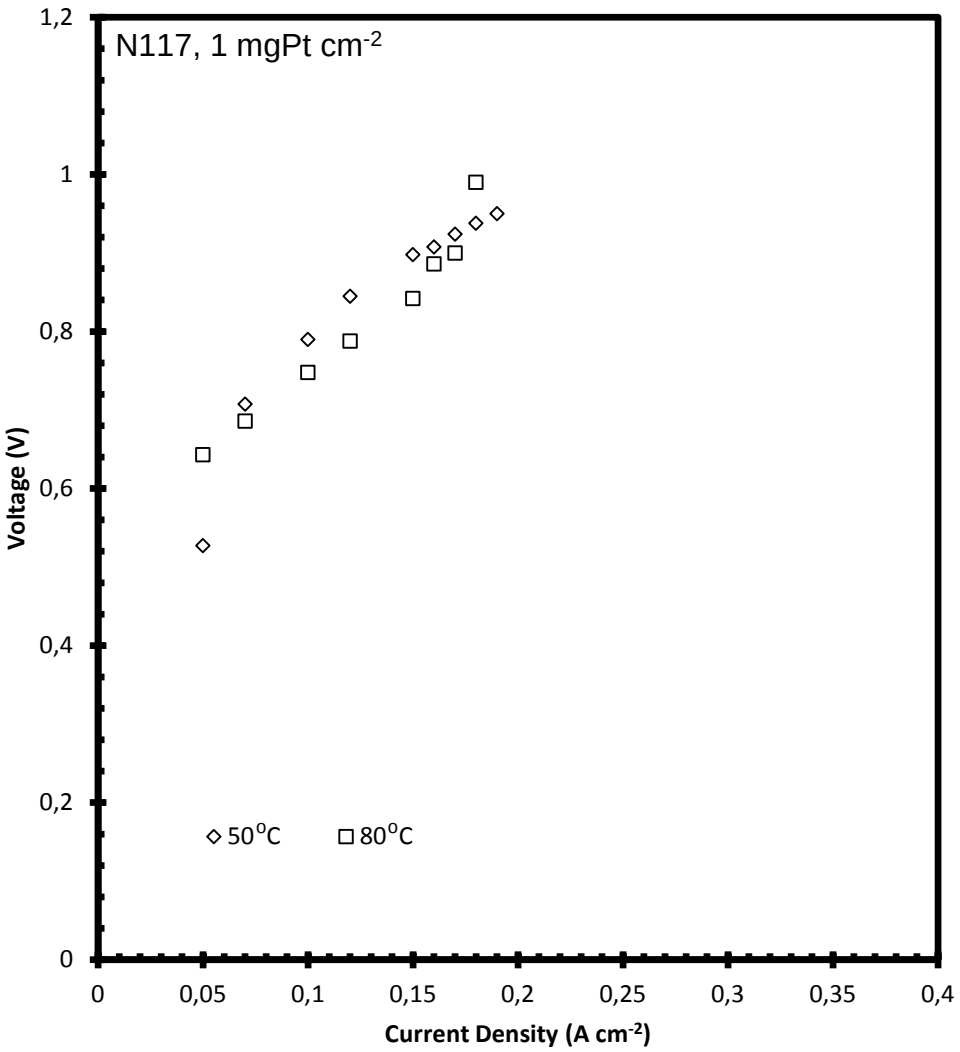

Figure 2.10: Effect of cell temperature on cell performance using acid/acid feed and N117.

The presence of the relatively high overpotential (compared to using SO_2 anode feed – See Figure 2.5) is also due to the fact that the dissolved SO_2 gas has a significantly lower diffusivity in the liquid H_2SO_4 than it would have in a gas. The lower SO_2 concentration combined with the mass transport limitation resulted in a maximum operational current density of 0.2 A cm^{-2}. It should be reported that the system had fairly poor voltage stability at 50°C with an increase of 100 mV per hour, which could have been caused by the poor reaction kinetics. However, at 80°C there was no significant increase in voltage.

Figure 2.11 shows surface SEM images taken after electrolysis from the cathode for both the 50 and 80°C MEA's. According to Figure 2.11a it is clear that some sulfur

deposition (determined with EDX analysis and visible as the light grey area between the carbon fibres) has occurred on the GDE used at 50°C. This deposition of sulphur was due to SO_2 diffusion from the anode to the cathode where possible parasitic reactions could occur [10], [28] producing elemental sulphur or H_2S gas, although no odour was apparent during operation. The cathode acid turned slightly milky, indicating that H_2S and SO_2 dissolved in the liquid. The darker area in Figure 2.11(a) is the land area of the flow field showing that the sulphur produced is only present within the flow field area.

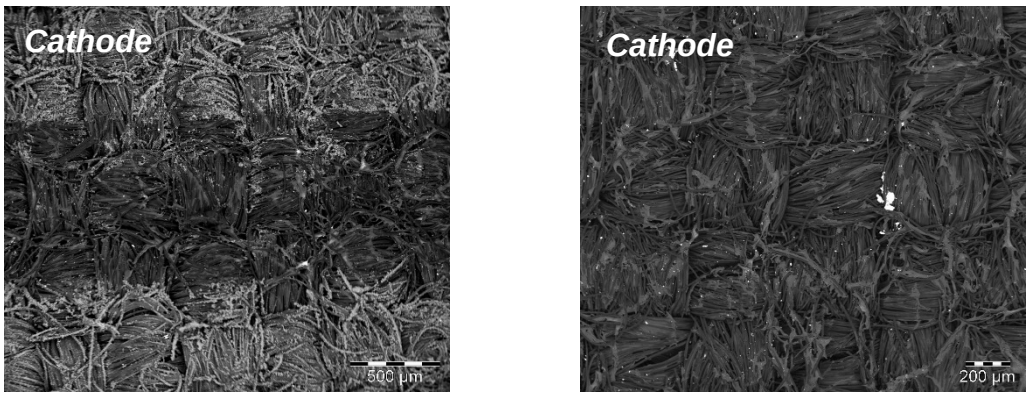

(a) (b)

Figure 2.11: SEM images of the cathode GDE surface after SO_2 electrolysis at 50°C (a) & 80°C (b).

Figure 2.11(b) shows the cathode surface after electrolysis at 80°C. Although there is less (determined by visual inspection) sulphur deposited on the surface, its presence confirms that even with a reduced amount of SO_2 dissolved (due to increased solution temperature) some SO_2 did diffuse through the membrane.

2.3.7.2 INFLUENCE OF MEMBRANE THICKNESS

The effect of membrane thickness (N117 vs. N115) was also investigated for this system using 1 mgPt cm^{-2} GDEs at 80°C. The results are shown in Figure 2.12. In view of the data obtained from the liquid cathode and dry SO_2 anode experiments (Figure 2.7), it was expected that the thinner membrane would perform better. However, for this configuration the thicker N117 membrane showed a slightly better performance. This effect can be explained in terms of the SO_2 transport across the membrane. As the SO_2 flux across the membrane is dependent on the membrane

thickness [10], it could be expected that N115 allowed more SO_2 to the cathode than N117. The presence of SO_2 at the cathode was shown to reduce cell performance by increasing the cell potentials [28].

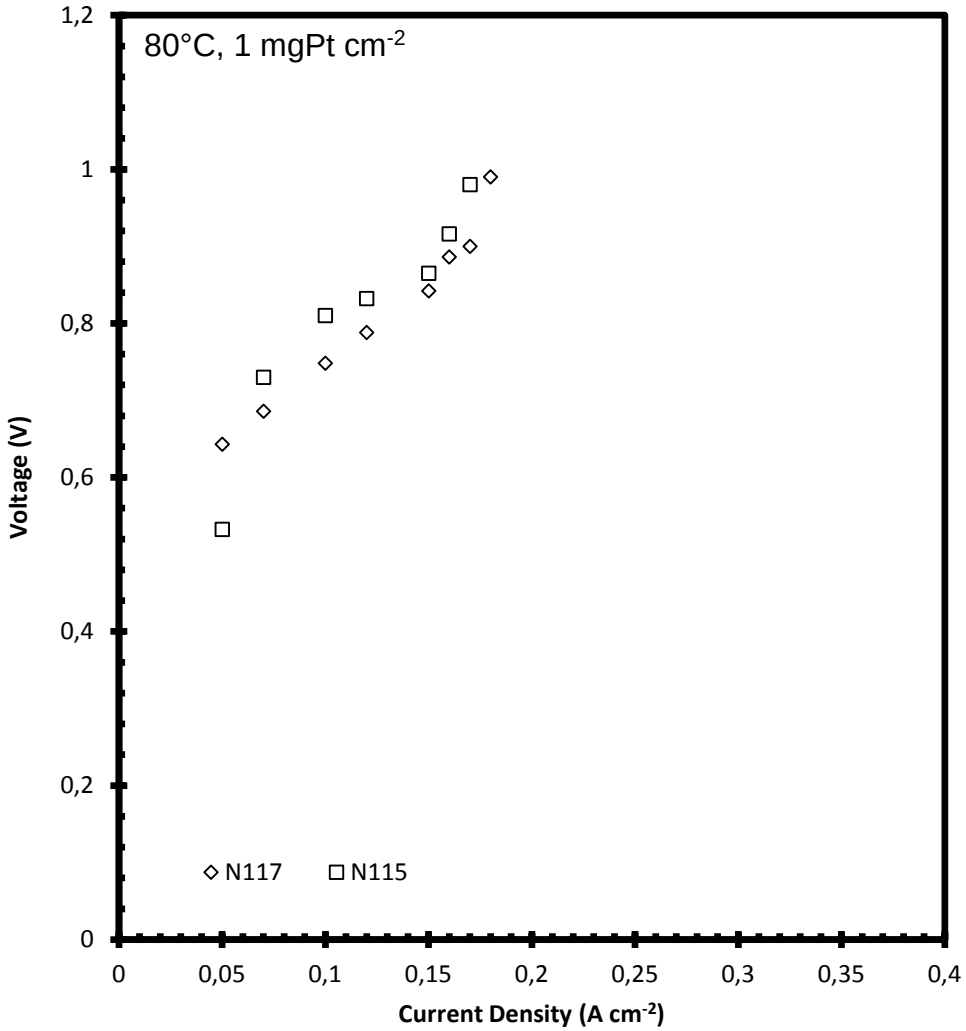

Figure 2.12: Effect on membrane thickness on cell performance when using acid/SO_2-acid reactants.

In order to show this effect more clearly SEM images were taken of the cross-section of each membrane electrode assembly after electrolysis (Figure 2.13). From the SEM images one can clearly see the membrane thickness difference between the N117 and N115. When considering the S deposition observable from the cross section of the N117 MEA (Figure 2.13(a)), it is clear that only small amounts of S had been deposited on the cathode side of the MEA, confirming the observations made

earlier for N117 (Figure 2.11(b)). From Figure 2.13(b) it is clear that significantly more S had been deposited on the cathode explaining its worse performance.

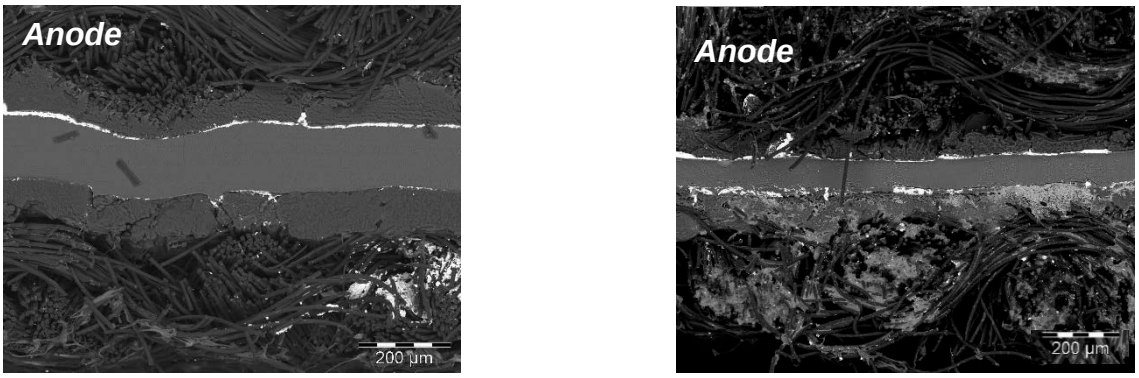

(a) (b)

Figure 2.13: Cross sectional view of N117(a) & N115(b) MEAs after SO_2 electrolysis.

2.3.7.3 INFLUENCE OF H_2SO_4 CONCENTRATION

To determine the effect of acid concentration the performance was determined using a 30 wt% and a 65 wt% H_2SO_4 feed solution. It is clear from the V-*i* curve (Figure 2.14) that a higher overpotential was present when using the more concentrated 65 wt%. This can be attributed to the low solubility characteristics of SO_2 gas in more concentrated acid solutions. Gorensek *et al*. [26] showed that the SO_2 solubility decreased from 0.748 to 0.665 g SO_2 per 100 g H_2SO_4 when the acid concentration was increased from 30 to 65 wt% at constant pressure and temperature. In addition, the diffusion of the SO_2 from the solution to the anode catalyst will decrease with increasing sulphuric acid concentration as the viscosity of the acid increases from 1 centipoise (39.92 wt% H_2SO_4) to 2.8 centipoise (65.13 wt% H_2SO_4) at 80°C [29]. The OCV (open circuit voltage) determined for both acid concentrations was 0.183 V (30 wt%) and 0.265 V (65 wt%), respectively. These values can be compared (although slightly lower) to the values obtained theoretically (from the Nernst equation using an OLI MSE model-generated species activities) by Gorensek *et al*. [26] who reported a theoretical reversible potential of 0.206 V (30 wt%) and 0.347 V (60 wt%) at 80°C for an SO_2 electrolyser operated with a liquid cathode and a dry SO_2 anode under 6 bar differential pressure. The higher reversible potential as a function of acid concentration might be due to the adsorption of sulphur species to the anode before any current is available.

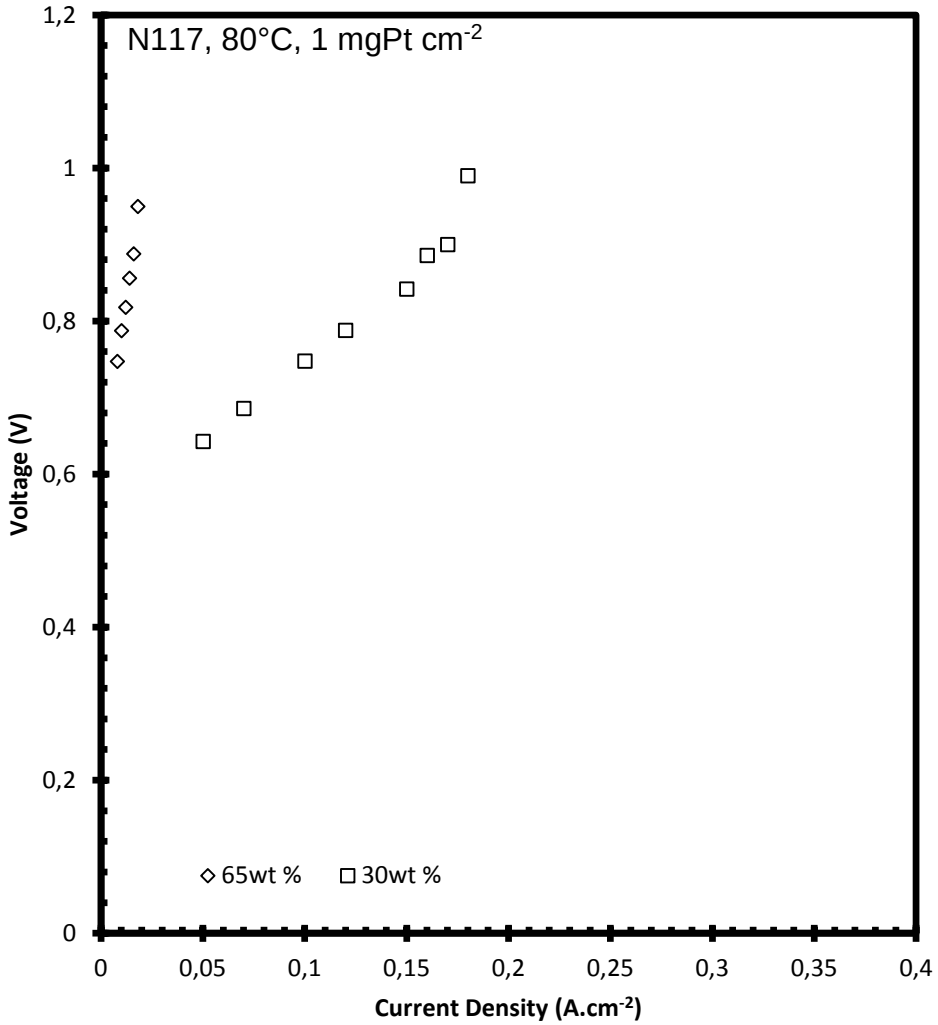

Figure 2.14: Effect of H_2SO_4 concentration used for the acid/SO_2-acid system at 80°C when using N117.

2.4 CONCLUSION

Various parameters influencing SO_2 electrolysis were investigated, including a liquid cathode and dry SO_2 anode fed system where the influence of hot pressing pressure, cell temperature, catalyst loading, membrane thickness, membrane type and SO_2 concentration were investigated. Subsequently the reactant configuration was changed to a clean sulphuric acid cathode feed and a SO_2 saturated H_2SO_4 feed setup, where the influence of cell temperature, membrane thickness and acid concentration used was determined. The significant investigation of these various parameters have not been investigated in such detail. Using the dry SO_2-fed setup,

it was found that performance was influenced by the hot pressing pressure during MEA manufacture, while higher cell temperature, thinner membranes and operating at low current densities improved performance. The highest acid concentration of 12.69 mol $L^{-}1$ was attained using a N117 at 90°C and 0.28 A cm^{-2}. The effect of catalyst loading showed little influence at low current densities (<0.2 A cm^{-2}), although the 1 mgPt cm^{-2} loading showed slightly better performance at higher current densities. The overall cell voltage was a strong function of SO_2 concentration supplied to the anode, showing an increase in voltage as the SO_2 concentration was decreased. It was shown that the SO_2 solubility in sulphuric acid was crucial when the cathode was supplied with clean sulphuric acid and the anode with SO_2 saturated sulphuric acid. Increasing the cell temperature from 50°C to 80°C showed a decrease in performance (due to a decrease in SO_2 solubility in sulphuric acid as temperature is increased). Decreasing membrane thickness also resulted in high overpotential which is probably due to increased SO_2 crossover from the anode to the cathode.

2.5 REFERENCES

[1] M. Carmo, D.L. Fritz, J. Mergel, D. Stolten, A Comprehensive review on PEM electrolysis, International Journal of Hydrogen Energy, 38 (2013) 4901 - 4934.

[2] H. Zhang, S. Su, X. Chen, G. Lin, J. Chen, Configuration design and performance optimim analysis of solar-driven high temperature steam electrolysis system for hydrogen production, International Journal of Hydrogen Energy, 38 (2013) 4298 - 4307.

[3] M.B. Gorensek, W.A. Summers, Hybrid Sulfur flowsheets using PEM electrolysis and a bayonet decomposition reactor, International Journal of Hydrogen Energy, 34 (2008) 1 - 18.

[4] P. Sivasubramanian, R.P. Ramasamy, F.J. Freire, C.E. Holland, J.W. Weidner, Electrochemical hydrogen production from thermochemical cycles using proton exchange membrane electrolyzer, International Journal of Hydrogen Energy, 32 (2007) 463 - 468.

[5] L.E. Brecher, S. Spewock, C.J. Warde, The Westinghouse Sulfur Cycle for the thermochemical decomposition of water, International Journal of Hydrogen Energy, 2 (1977) 7-15.

[6] X. Cheng, Z. Shi, N. Glass, L. Zhang, J. Zhang, D. Song, Z.-S. Liu, H. Wang, J. Shen, A review of PEM hydrogen fuel cell contamination: Impacts, mechanisms, and mitigation, Journal of Power Sources, 165 (2007) 739 - 756.

[7] M.B. Gorensek, Hybrid Sulfur cycle flowsheets for hydrogen production using high-temperature gas-cooled reactors, International Journal of Hydrogen Energy, 36 (2011) 12725 - 12741.

[8] P. Zhang, S.Z. Chen, L.J. Wang, T.Y. Yao, J.M. Xu, Study on a lab-scale hydrogen production by closed cycle thermo-chemical iodine-sulfur process, International Journal of Hydrogen Energy, 35 (2010) 10166 - 10172.

[9] J. Staser, R.P. Ramasamy, P. Sivasubramanian, J.W. Weidner, Effect of Water on the Electrochemical Oxidation of Gas-Phase SO2 in a PEM Electrolyzer for H2 Production. Electrochemical and Solid-State Letters, 10 (2007) E17 - E19.

[10] J.A. Staser, J.W. Weidner, Sulfur Dioxide Crossover during the production of Hydrogen and Sulfuric Acid in a PEM Electrolyzer, Journal of The Electrochemical Society, 156 (2009) B836 - B841.

[11] R. Peach, H.M. Krieg, A.J. Kruger, A. Chromik, K. Krajinovic, J. Kerres, Comparison of ionically and ionical-covelently cross-linked polyaromatic membranes for SO_2 electrolysis, International Journal of Hydrogen Energy, 39 (2014) 28 - 40.

[12] F.-P. Ting, J.-C. Lin, C.-M. Lai, S.-D. Chyou, K.-L. Hsueh, Electrochemical Impedance Spectroscopy to Evaluate the Effect of Pressure Exerted in the Hot-Pressing Stage on the Performance of PEMFC, International Journal of Electrochemical Science, 7 (2012) 7165 - 7178.

[13] D.K. Z. Williamson, Sae-Keun Chun, Tonghun Lee, Cody Squibb, Experiemental evaluation of cell temperature effects on miniature, air-breathing PEM fuel cells, Applied Thermal Engineering, 31 (2011) 3761 - 3767.

[14] J.A. Staser, J.W. Weidner, Effect of Water Transport on the Production of Hydrogen and Sulfuric Acid in a PEM Electrolyzer, Journal of The Electrochemical Society, 156 (2009) B16 - B21.

[15] C. Lei, D. Bessarabov, S. Ye, Z. Xie, S. Holdcroft, T. Navessin, Low equivalent weight short-side-chain perfluorosulfonic acid ionomers in fuel cell cathode catalyst layers, Journal of Power Sources, 196 (2011) 6168-6176.

[16] H. Zhang, C. Ma, J. Wang, X. Wang, H. Bai, J. Liu, Enhancement of proton conductivity of polymer electrolyte membrane enabled by sulfonated nanotubes, International Journal of Hydrogen Energy, 39 (2014) 974-986.

[17] A. Lokkiluoto, P.A. Taskinen, M. Gasik, A.V. Kojo, H. Peltola, M.H. Barker, K.-H. Kleifges, Novel process concept for the production of H_2 and H_2SO_4 by SO_2-depolarized electrolysis, Environment, Development and Sustainability, 15 (2012) 529 - 540

[18] H. Su, V. Linkov, B.J. Bladergroen, Membrane electrode assemblies with low noble metal loadings for hydrogen production from solid polymer electrolyte water electrolysis, International Journal of Hydrogen Energy, 38 (2013) 9601 - 9608.

[19] Z. Luo, Z. Chang, Y. Zhang, Z. Liu, J. Li, Electro-osmotic drag coefficient and proton conductivity in Nafion membrane for PEMFC, International Journal of Hydrogen Energy, 35 (2010) 3120 - 3124.

[20] J.A. Staser, M.B. Gorensek, J.W. Weidner, Quantifying Individual Potential Contributions of the Hybrid Sulfur Electrolyzer, Journal of The Electrochemical Society, 157 (2010) B952 - B958.

[21] K. Wikander, H. Ekstrom, A.E.C. Palmqvist, G. Lindebergh, On the influence of Pt particle size on the PEMFC cathode performance, Electrochemica Acta, 52 (2007) 6848 - 6855.

[22] S.-K. Lee, C.-H. Kim, W.-C. Cho, K.-S. Kang, C.-S. Park, K.-K. Bae, The effect of Pt loading amount on SO_2 oxidation reaction in an SO_2-depolarized electrolyzer used in the hybrid sulfur (HyS) process, International Journal of Hydrogen Energy, 34 (2009) 4701 - 4707.

[23] P.W. Majsztrik, M.B. Satterfield, A.B. Bocarsly, J.B. Benziger, Water sorption, desorption and transport in Nafion membranes, Journal of Membrane Science, 301 (2007) 93-106.

[24] Y.M. Feng, A. Su, A three-dimensional full-cell CFD model used to investigate the effects of different flow channel design on PEMFC performance, International Journal of Hydrogen Energy, 32 (2007) 4466 - 4476.

[25] S.U. Jeong, W.C. Cho, K.S. Kang, K.K. Bae, C.S. Park, C.H. Kim, Effect of sulfur dioxide concentration on cell performance and sulfur dioxide crossover, 224th ECS Meeting, The Electrochemical Society, 2013.

[26] M.B. Gorensek, J.A. Staser, T.G. Stanford, J.W. Weidner, A thermodynamic analysis of the SO_2/H_2SO_4 system in SO_2-depolarized electrolysis, International Journal of Hydrogen Energy, 34 (2009) 6089 - 6095.

[27] A.J. Kruger, H.M. Krieg, H.W.J.P. Neomagus, SO_2 Solubility in 50 wt % H_2SO_4 at Elevated Temperatures and Pressures, Journal of chemical and engineering data, (2014).

[28] M.C. Elvington, H. Colon-Mercado, S. McCatty, S.G. Stone, D.T. Hobbs, Evaluation of proton-conducting membranes for use in a sulfur dioxide depolarized electrolyzer, Journal of Power Sources, 195 (2010) 2823 - 2829.

[29] O.T. Fasullo, Sulfuric Acid: Use and Handeling, New York: McGraw-Hill Book Company1965.

CHAPTER 3: EVALUATION OF MEA MANUFACTURING PARAMETERS USING EIS FOR SO_2 ELECTROLYSIS*

Chapter Overview

As shown in Chapter 2 the MEA manufacturing parameters influence the performance of a 25 cm^2 active area cell. Following this a detailed study follows on the membrane electrode assembly (MEA) manufacturing parameters such as hot pressing pressure and pressing time were investigated for the use in a SO_2 electrolyser on a 10 cm^2 active area cell is presented. The SO_2 electrolysis was optimised in terms of cell temperature, membrane thickness and catalyst loading. The electrolysis efficiency was evaluated using polarisation curves while electrochemical impedance spectroscopy (EIS) was used to determine the membrane resistance, activation energy and mass transport limitations. An electrical circuit, which included inductance, ohmic resistance, charge transfer, constant phase and Warburg elements, was used to fit the experimental data. The optimum hot pressing conditions were 50 kg cm^{-2} for 5 min at 120°C. Increased cell temperature (80°C) resulted in a reduction of mass transport, while thicker membranes resulted in an increased mass transport resistance due to lower water transport through the membrane. Increased catalyst loading (from 0.3 to 1 gPtC cm^{-2}) improved the cell performance due to improved kinetics confirmed by the EIS data.

* Krüger AJ, Krieg HM, van der Merwe J, Bessarabov D. Evaluation of MEA manufacturing parameters using EIS for SO_2 electrolysis. Int J Hydrogen Energy 2014;39:18173–81. doi:10.1016/j.ijhydene.2014.09.012.

3.1 INTRODUCTION

The production of hydrogen as an energy carrier in the energy sector has received increased interest in both the research and commercial community [1,2]. Since many current methods of hydrogen production, for example from coal result in the production of pollutants, it is necessary to evaluate alternative methods. The Westinghouse Corporation in the 70's proposed such an alternative method known as the Hybrid Sulfur (HyS) cycle which forms part of the so-called thermo-chemical cycles [3]. The HyS process aims at producing high quantities of hydrogen and sulphuric acid from both water and SO_2 gas in an electrolysis step which is incorporated into the three step HyS cycle [4]. Although it was initially suggested to couple this process with a nuclear heat source, recent papers have shown that other heat sources could also be used, for example, the coupling of the SO_2 electrolysis step with a pyrometallurgical plant of nickel and copper concentrate [5]. According to Lokkiluoto *et al.*, this process would not be closed as had been initially proposed for the HyS cycle, but would use the SO_2, which is a by-product produced from current industrial processes like flash smelting of metal sulfides, for the production of H_2 and H_2SO_4. Commercially H_2SO_4 is generally produced by a contact process whereby sulphur solids are oxidised in the presence of oxygen to produce SO_2 gas. The SO_2 is then further converted to SO_3 over a V_2O_5 catalyst in the presence of water which is used to increase the acidity to 98% H_2SO_4 [6].

An SO_2 electrolyser can be operated using three modes of operation, the first using SO_2 saturated sulphuric acid as the anolyte and clean sulphuric acid as the catholyte as first proposed by Westinghouse in the HyS cycle [4]. The second method of operation, proposed by Sivasubramanian *et al.* [7], entails supplying the anode with dry SO_2 gas while the cathode receives liquid water. The water diffusion across the membrane was shown to be sufficient for the reaction up to a current density of 0.4 A cm^{-2}. Staser *et al.* [8] improved the performance of this operating method by applying a pressure on the cathode. The characterisation of the MEA performance can be achieved by either focusing on the membrane or catalyst characteristics. Methods that have been used to evaluate the membrane include polarisation curves, long term operation, SEM, TEM, TGA-MS and FTIR [9,10]. Variables investigated when evaluating catalysts for SO_2 electrolysis, include catalyst loading, catalyst composition and catalyst stability [11–13]. Techniques that can be used for such

catalyst evaluation include catalyst utilisation, polarisation curves, cyclic voltammetry and linear voltammetry [11,12,14]. Determining the operating performance of both the membrane and catalyst simultaneously can also be achieved within the electrolyser cell using electrochemical impedance spectroscopy (EIS), which can be used to determine the ohmic resistance, activation energy and mass transport effects in an MEA [15]. In addition the technique can be applied in-situ. Thirdly, the anode can be supplied with humidified SO_2 gas while operating a dry cathode. Although this technique is new, one paper (at the time of writing this thesis) is available showed increased performance although thicker membranes are used [16].

This chapter will focus on both the influence of the membrane electrode (MEA) manufacturing method (pressure and time), as well as other MEA related properties (membrane thickness, catalyst loading and active area) on SO_2 electrolysis. While electrochemical impedance spectroscopy has not yet been used extensively to evaluate SO_2 electrolysis, the suitability of this method [17] i) to evaluate membrane, catalyst and charge transfer resistances and ii) to determine the mass transport during SO_2 electrolysis will be evaluated.

3.2 EXPERIMENTAL

For this study Nafion® 117 (Ion Power, USA) membranes (N1110 for membrane thickness evaluation) were pre-treated by boiling the membrane samples in 1 M H_2SO_4 solution at 80°C for 90 min to remove any impurities [10]. After the acid treatment step, the membranes were rinsed in water until neutral and stored. All MEA's were made by hot-pressing (Carver Hot Press, Model #3912) two gas diffusion electrodes (FuelCellEtc, USA) using 1 mgPtB cm^{-2}, unless stated otherwise, on both sides of the PEM using a pressure of 50 kg cm^{-2} for 5 min at a temperature of 120°C unless stated otherwise.

The same experimental system used previously [9], was used to evaluate the MEA's. All MEA's tested were hydrated at the desired operating temperature for 2 h by circulating pre-heated water through the electrolyser cell (10 cm^2, Fuel Cell Technologies). An activation step was performed by running the electrolyser at a constant current of 0.1 A cm^{-2} for 20 min. Polarisation curves were then recorded by increasing the current density by 0.025 A cm^{-2} every 90 seconds [9].

For this study galvanostatic electrochemical impedance spectroscopy (EIS) [15] was used by applying an AC current of 10% of the applied DC current over a frequency range of 0.1 to 100 kHz using a Gamry REF300 potentiostat [18,19].

To model EIS data, an equivalent circuit model can be developed, based on literature [15], that presents processes or components in the SO_2 electrolyser. If a suitable fit is attained, the equivalent circuit model can be used to determine the membrane resistance (ohmic), activation energy (charge transfer) and mass transport limitations (Warburg) [15]. For this study the best fit was attained using the equivalent circuit model shown in Figure 3.1.

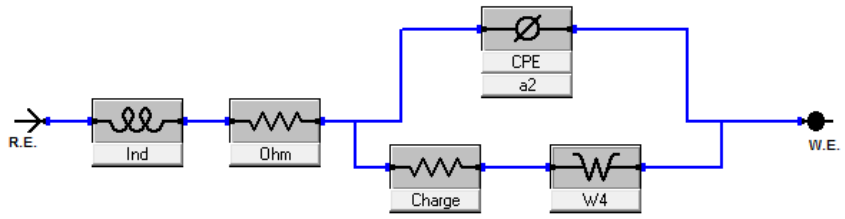

Figure 3.1: Equivalent circuit model used to fit the experimental data. Ind – Inductance, Ohm – Ohmic resistance, Charge – Charge transfer resistance, CPE – constant phase element, W – Warburg impedance.

Although the contribution of the inductance (*Ind*) of the electrical cables is small, it is measured by the equipment and was therefore included in the model. While the ohmic resistance (*Ohm*) describes the ohmic losses of the whole cell, which includes the resistance of the membrane, GDE, catalyst and contact resistances (between the membrane and GDE), the contribution of the membrane resistance is significantly higher than the resistance of the GDE and contact [15] and therefore be referred to as the membrane resistance unless stated otherwise. For this reason the contact and GDE resistances were neglected. The activation energy of the reaction can be described by both the charge transfer resistance (*Charge*) related to the reaction and the constant phase element (*CPE)* related to the non-ideal capacitance, which is present in the semi-circle region of the experimental data. The Warburg term (*W4)*, was used to describe the mass transport effects in the cell [20]. For this study the

ohmic (*Ohm*), activation energy (*Charge*) and mass transport (*W4*) parameters will be used to evaluate the overall MEA performance.

3.3 RESULTS AND DISCUSSION

3.3.1 HOT PRESS PRESSURE

To optimise the hot pressing three pressures were investigated. In Figure 3.2 the voltage response of a N117 membrane, which had been hot-pressed at 80°C at various pressures, in a SO_2 electrolyser is presented. It is clear that the pressure used for the MEA manufacturing process does have an influence on the overall performance of the electrolyser as has been previously demonstrated for single cell PEM fuel cells [15]. According to Figure 3.2, the 50 kg cm^{-2} hot pressing pressure resulted in the best V*i* curve for SO_2 electrolysis. Increasing (100 kg cm^{-2}) or decreasing (25 kg cm^{-2}) the applied pressure to the MEA had a similar negative effect on the overall operating voltage. An increase in voltage can usually be ascribed to an increase in the resistance of the anode, cathode or membrane [21]. The cathode resistance is usually neglected due to the low voltage needed for H_2 evolution, while the anode resistance is assumed to be the majority of the catalyst resistance with the membrane resistance (ohmic) being a function of the hydration and type of membrane.

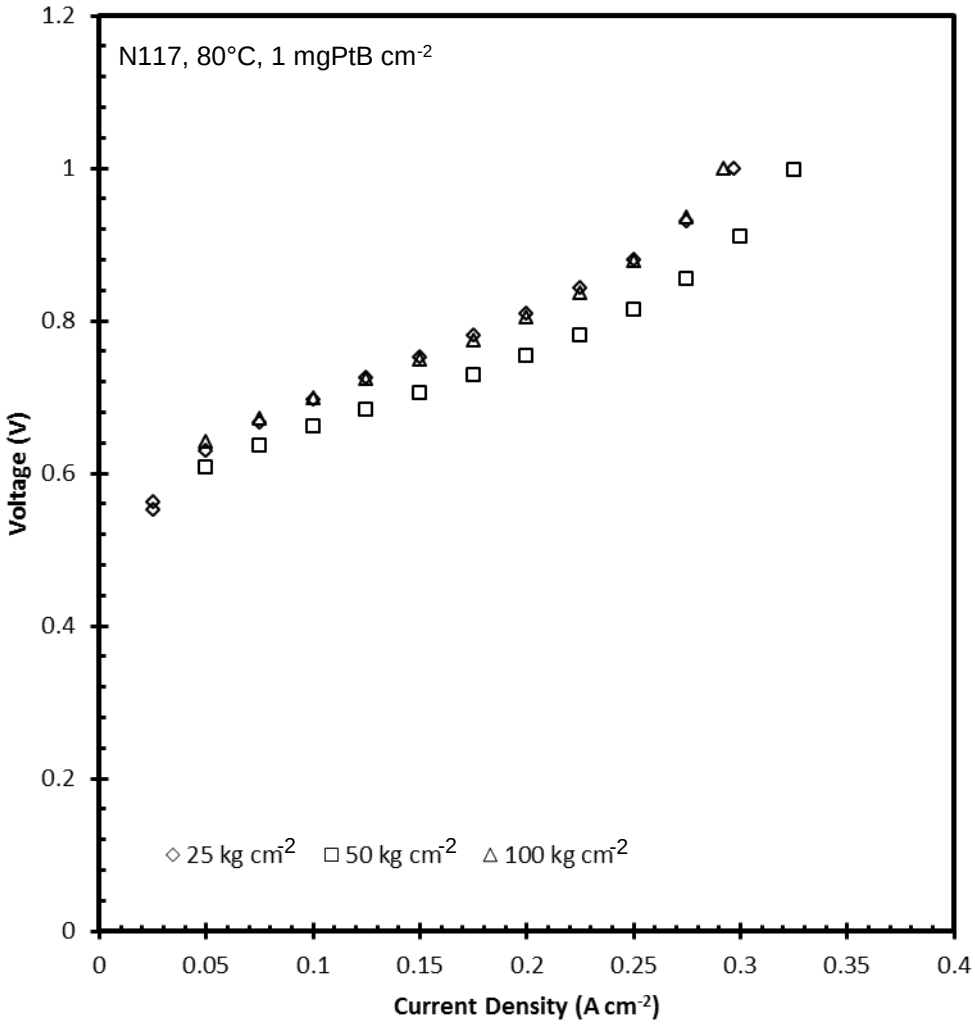

Figure 3.2: Effect of hot pressing pressure on SO_2 performance using N117, 80°C and 1 mg PtB cm^{-2}.

EIS can be performed in two different modes: potensiostatic and galvanostatic EIS. Potensiostatic EIS applies fixed DC potential while small AC potential perturbation is applied. When galvanosatic EIS is used a fixed DC current and small AC perturbation current is used [15]. Since the polarisation curves were produced at fixed current densities only galvanostatic EIS was used in this study. The EIS data for the effect of hot pressing pressure as a function of various current densities is shown in Figure 3.3.

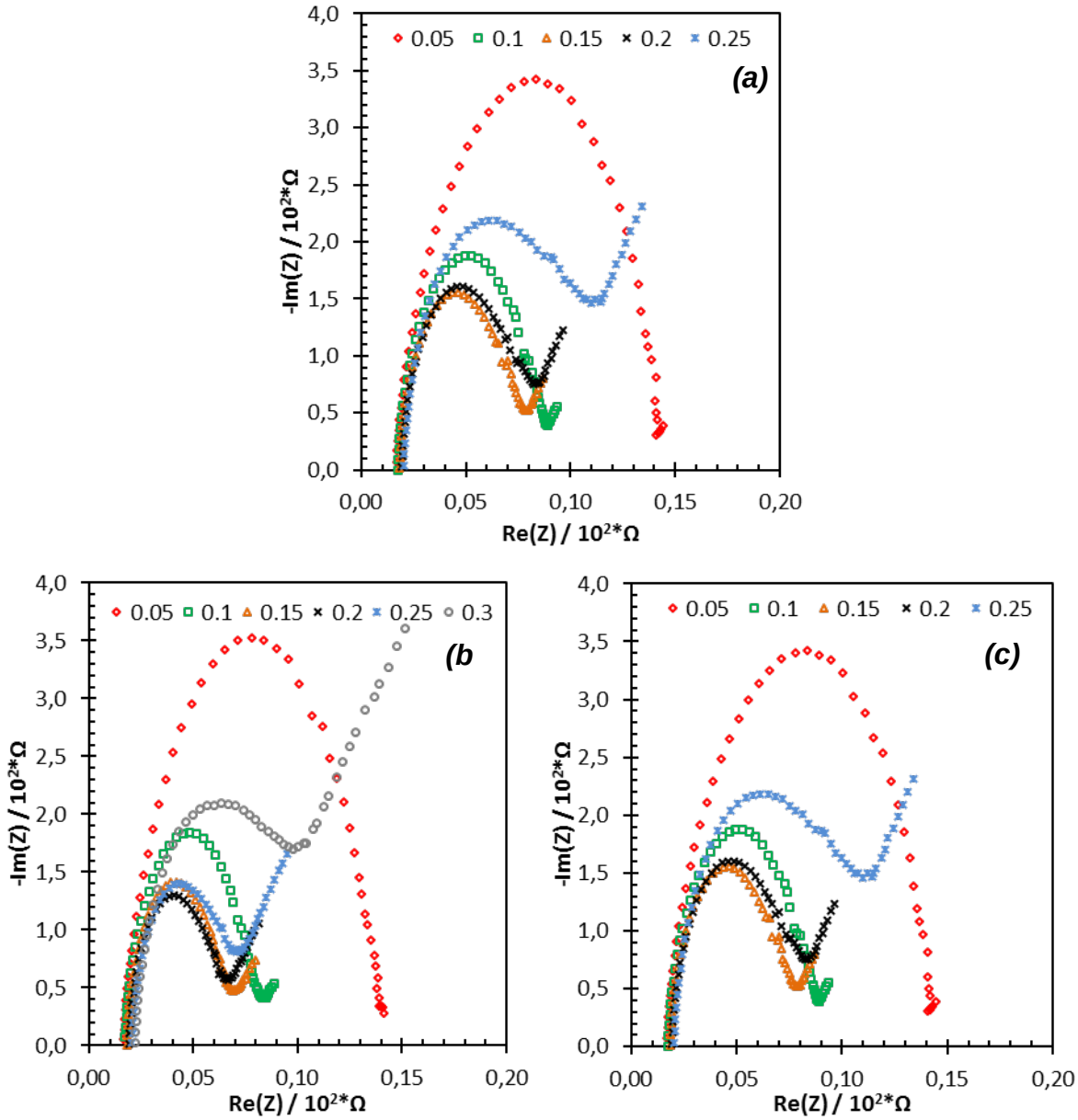

Figure 3.3: EIS analysis for N117 hot pressed at (a) 25, (b) 50 and (c) 100 kg cm^{-2} at various current densities (A cm^{-2}).

According to literature [18] the through-plane membrane resistances can be obtained from where the impedance data crosses the real (x) axis, while the activation resistance is related to the diameter of the semi-circle of the impedance data and the mass transport can be obtained from the 45 degree line (usually present at high current densities) [22].

From Figure 3.3 it is clear that the membrane resistance (*ohmic*) increases with increasing current density for all three hot pressing pressures. The small increase in

membrane resistance is however negligible compared to the effect of the activation resistance and mass transport. As was observed in Figure 3.2, the 50 kg cm^{-2} reached a higher current density (0.3 A cm^{-2}) compared to 25 and 100 kg cm^{-2} where only 0.25 A cm^{-2} was reached.

When considering the activation resistance (*charge*) of the 50 kg cm^{-2} (Figure 3.3b), it is clear that the activation resistance decreased (as seen by the decrease in the semi-circle) when the current density was increased from 0.05 to 0.15 A cm^{-2}. However, at higher current densities (above 0.15 A cm^{-2}) the resistance increased which can be ascribed to mass transport dominating the impedance data. For the mass transport a general increase in resistances was observed with increasing current densities as can be expected due to the limited water transport at higher current densities [8]. Since higher current densities produce more concentrated sulphuric acid at the anode, the observed increase in the open circuit potential was expected [23]. The higher acid concentration also reduces the water reactant needed for the reaction.

It is clear from Figure 3.3, that it is difficult to compare impedance data as a function of both current densities and operating parameters. To simplify the comparison of each operating parameter, the impedance data at the highest current density was considered. Figure 3.4 illustrates the correlation between the different hot pressing pressures at 0.25 A cm^{-2}. The insert in Figure 3.4 shows the model fitted to the 50 kg cm^{-2} experimental data. Although a slight deviation is present at lower frequencies (associated with the mass transport), the simplified model used to simulate the data gives an accurate fitting when compared to similar models presented in literature [24]. Since the model gave a similar good fit for all EIS data presented in this paper, the modelled data was only included for the data presented in Figure 3.4.

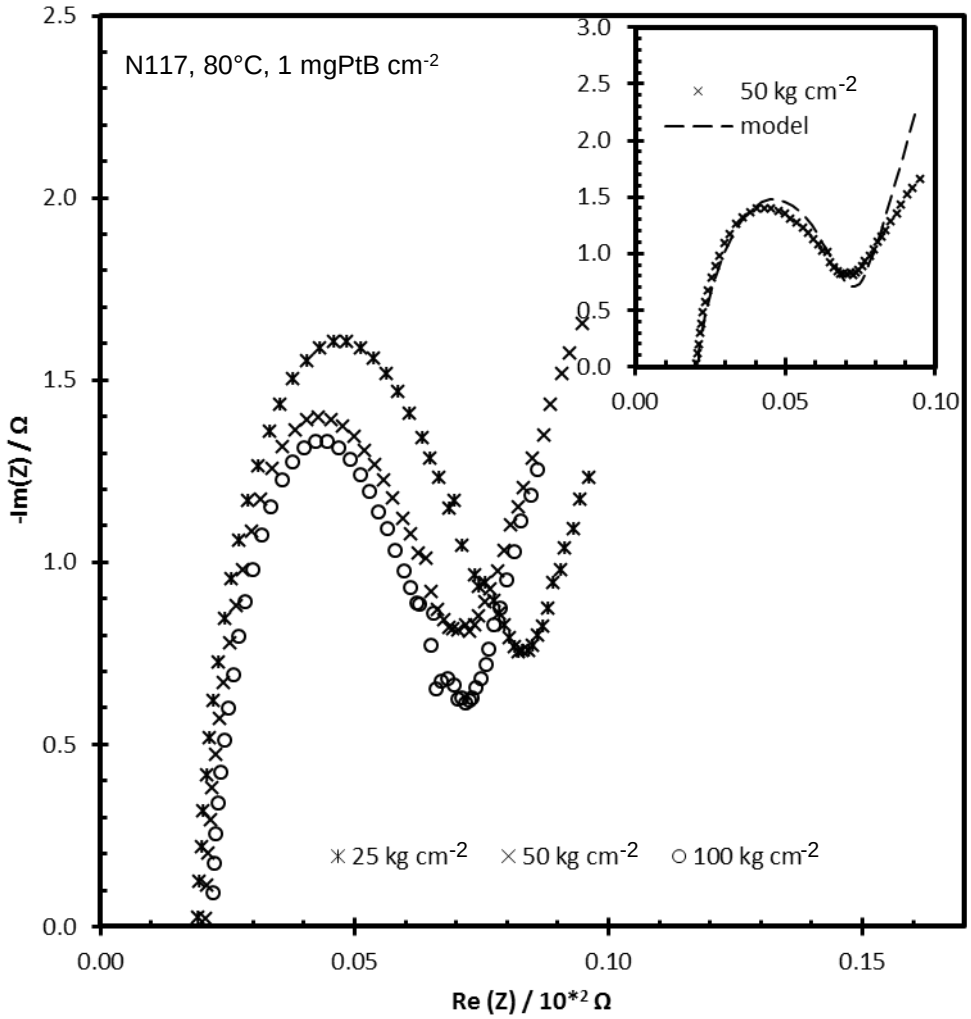

Figure 3.4: EIS data at 0.25 A cm^{-2} as a function of hot-pressing pressure. Insert shows the model fitted to the 50 kg cm^{-2} data.

Using the model, values could be obtained for the ohmic, activation and mass transport resistances as shown in Figure 3.5.

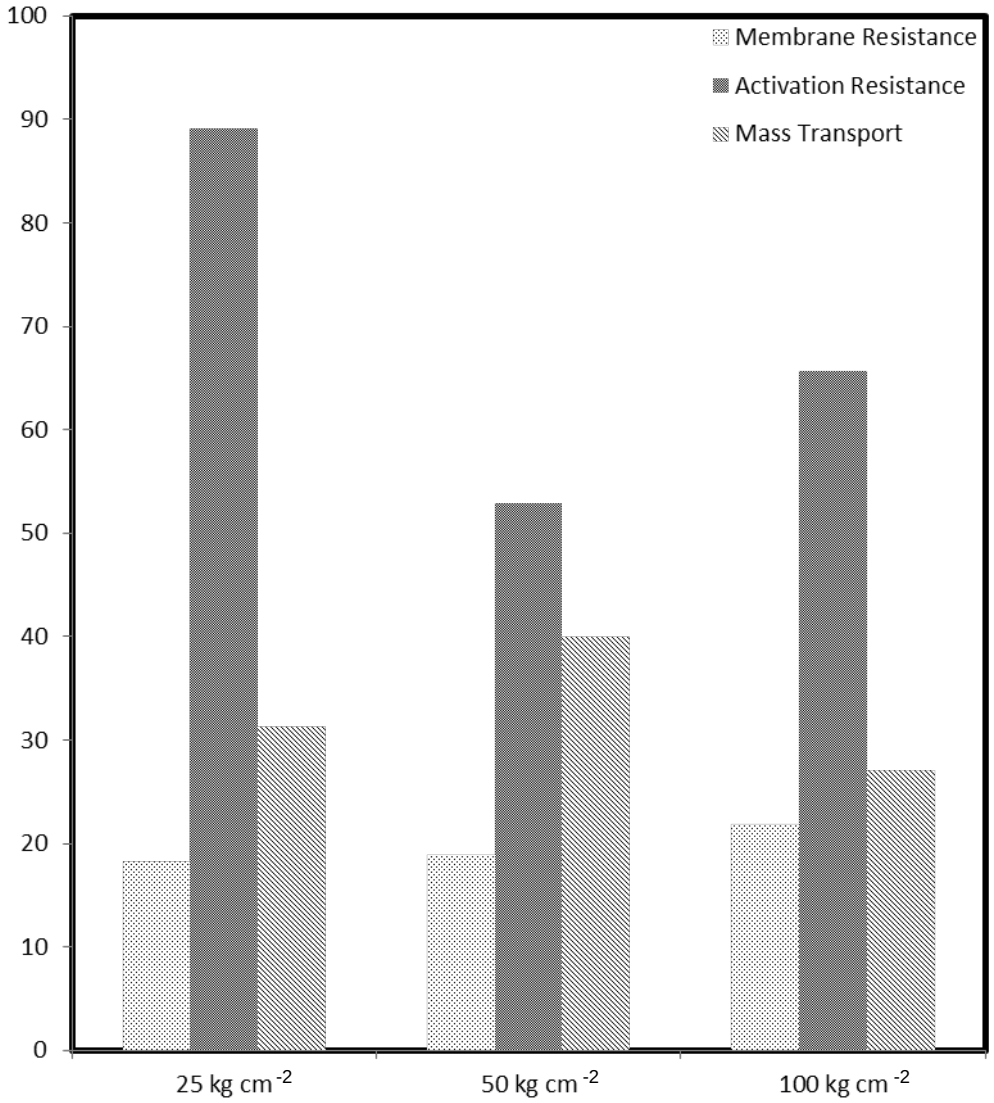

Figure 3.5: Model Values (mΩ) for different hot pressing pressures

By increasing the hot pressing pressure by a factor of four, the membrane resistance increased by 3 mΩ according to Figure 3.5. However, the increasing membrane resistance is not linear which shows that increasing the pressure further could affect the membrane resistance significantly. Unlike the membrane resistance, the highest activation resistance was observed at 25 kg cm^{-2}, which can be attributed to inadequate contact between the membrane and the catalyst. Increasing the pressure improved the contact between the membrane and catalyst as seen by the membrane resistance when 50 kg cm^{-2} was used. However, when increasing the pressure to 100 kg cm^{-2} an improved contact between the membrane and the catalyst is expected. This is not observed for this case as the mass transport contribution became the limiting factor. A decrease (increase) in Warburg value is

associated with higher (lower) mass transport effect. This effect can be attributed to a change in the GDE porosity as shown for fuel cells using the same GDE materials, where an increase in hot-pressing pressure resulted decreased GDE porosity which would increase the mass transport effect [18]. Based on these results it seems that hot pressing had no significant influence on the membrane resistance. The activation resistance and mass transport were influenced as a function of the pressure applied.

3.3.2 HOT PRESS TIME

Figure 3.6 shows the voltage response for various time periods of hot-pressing. The pressure applied was 50 kg cm^{-2} at 120°C. A clear difference is observed as a function of the time used. For this experiment the highest current obtained was of importance as this can be related to the mass transport limitations.

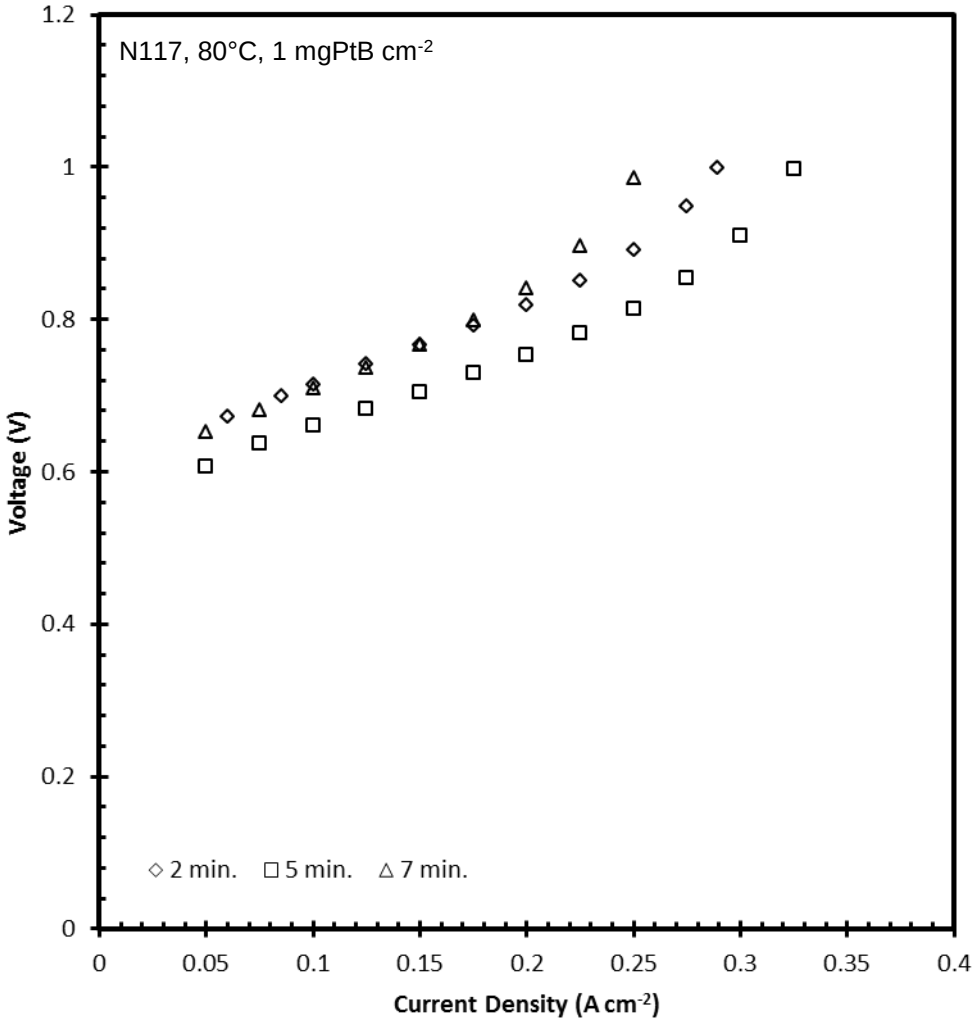

Figure 3.6: Polarisation curves for different hot pressing times using N117, 80°C and 1 mgPtB cm^{-2}.

Similar to the hot-pressing pressure results, the intermittent hot pressing time (5 min) gave the highest obtainable current densities. When hot pressing for 2 and 7 min almost identical VI curves were obtained at current densities below 0.2 A cm^{-2} however at higher current densities an increased performance for the 7 min hot pressed MEA was observed.

Figure 3.7 shows the impedance data as a function of hot pressing times showing that both mass transport and overall cell resistance directly influence the operating voltage.

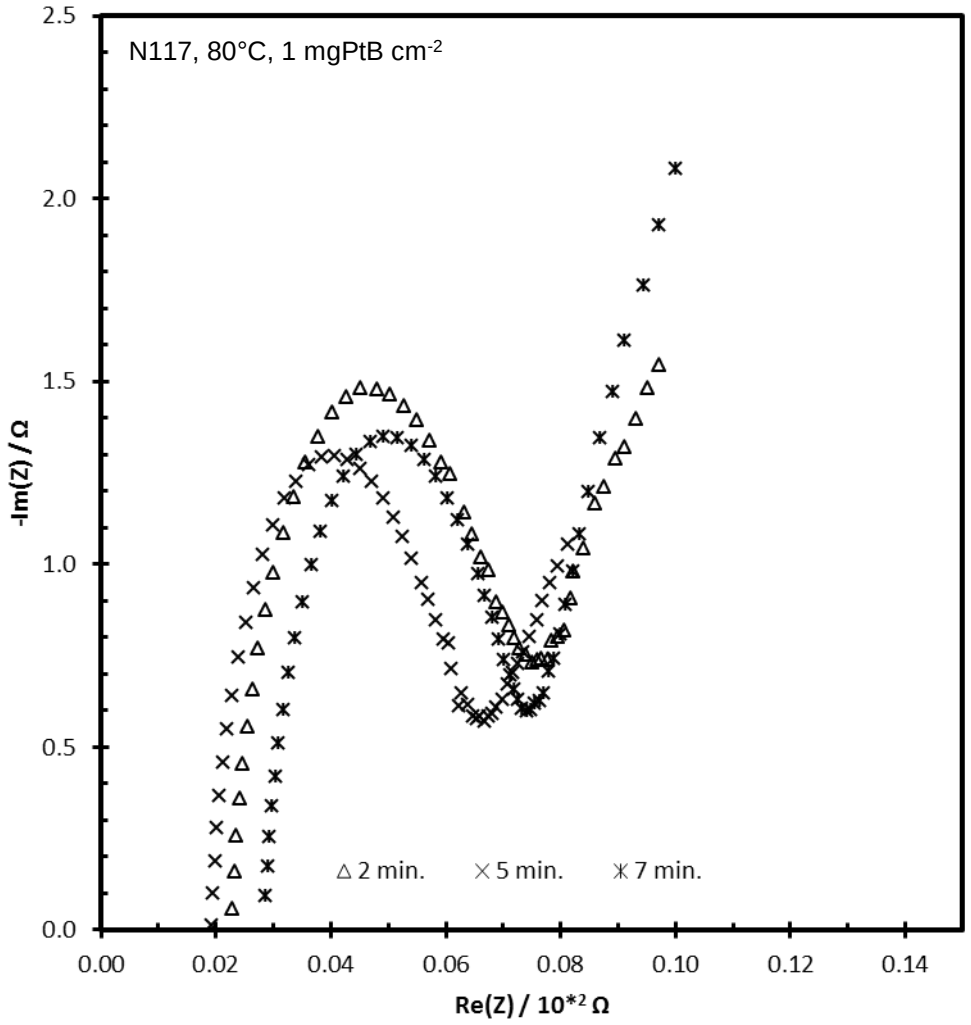

Figure 3.7: EIS data as a function of hot pressing time for 0.2 A cm^{-2}.

The data from Figure 3.7 confirms the results presented in Figure 3.6, i.e. that the best performance was obtained when using the 5 min hot pressed MEA. Using the modelled data, values were again obtained for the ohmic, activation and mass transport effect and is presented in Figure 3.8. According to the impedance data for the 2 min hot-pressing time, the activation resistance is the largest, which can be ascribed to the weak contact between the membrane and the GDE. The 7 min hot pressing resulted in the lowest activation resistance which can be ascribed to the improved contact between the membrane and the GDE. Although the activation resistance was low, the mass transport was limiting the performance as can also be seen by the low current density achieved in the polarisation curve (Figure 3.6).

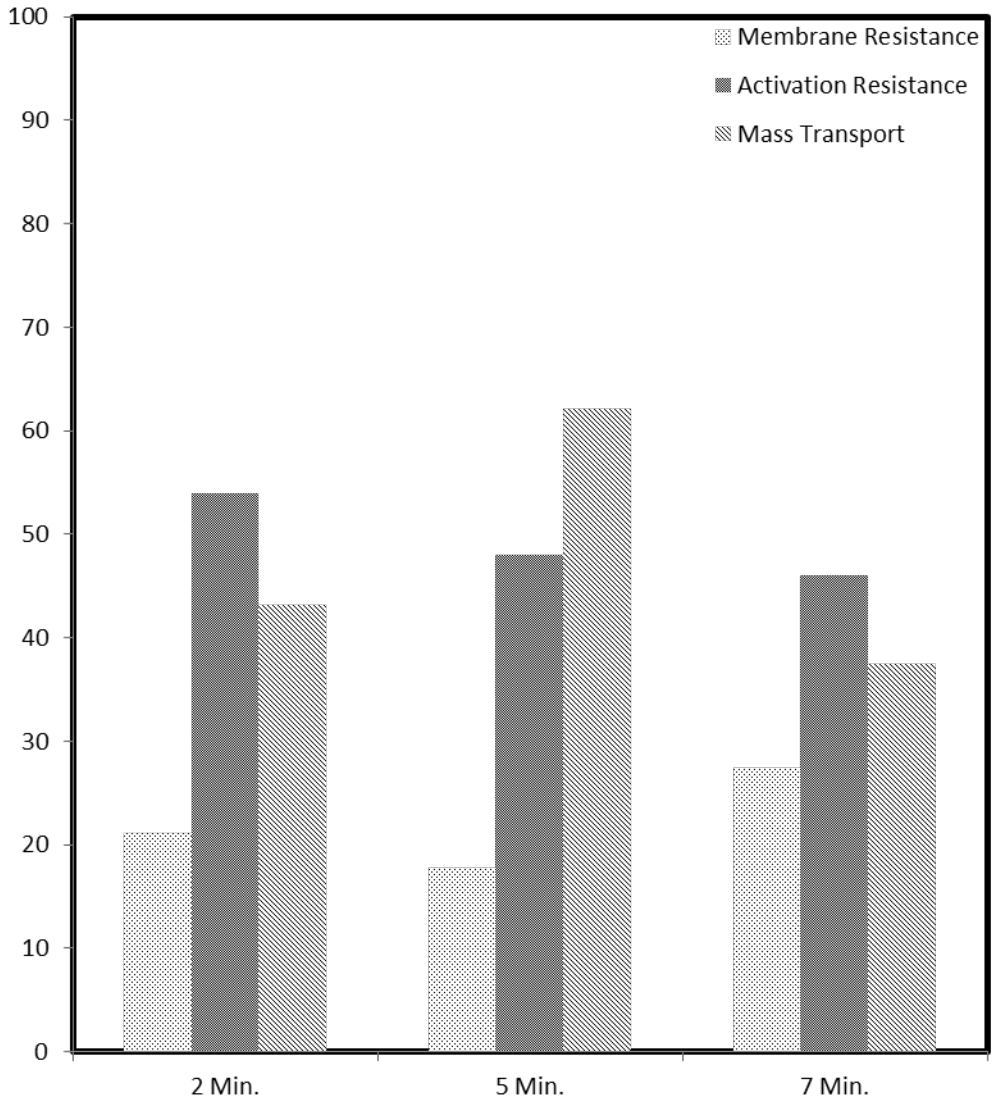

Figure 3.8: Model Values (mΩ) for different hot pressing time.

3.3.3 OPERATING TEMPERATURE

To illustrate the influence of temperature on current density, SO_2 electrolysis was conducted at 50 and 80°C. In Figure 3.9, the polarisation curves for both the 50 and 80°C run experiments are shown. The increased performance of the electrolyser with increasing temperature was expected in view of the increased reaction kinetics and higher ion conductivity of the membrane at elevated temperatures [25].

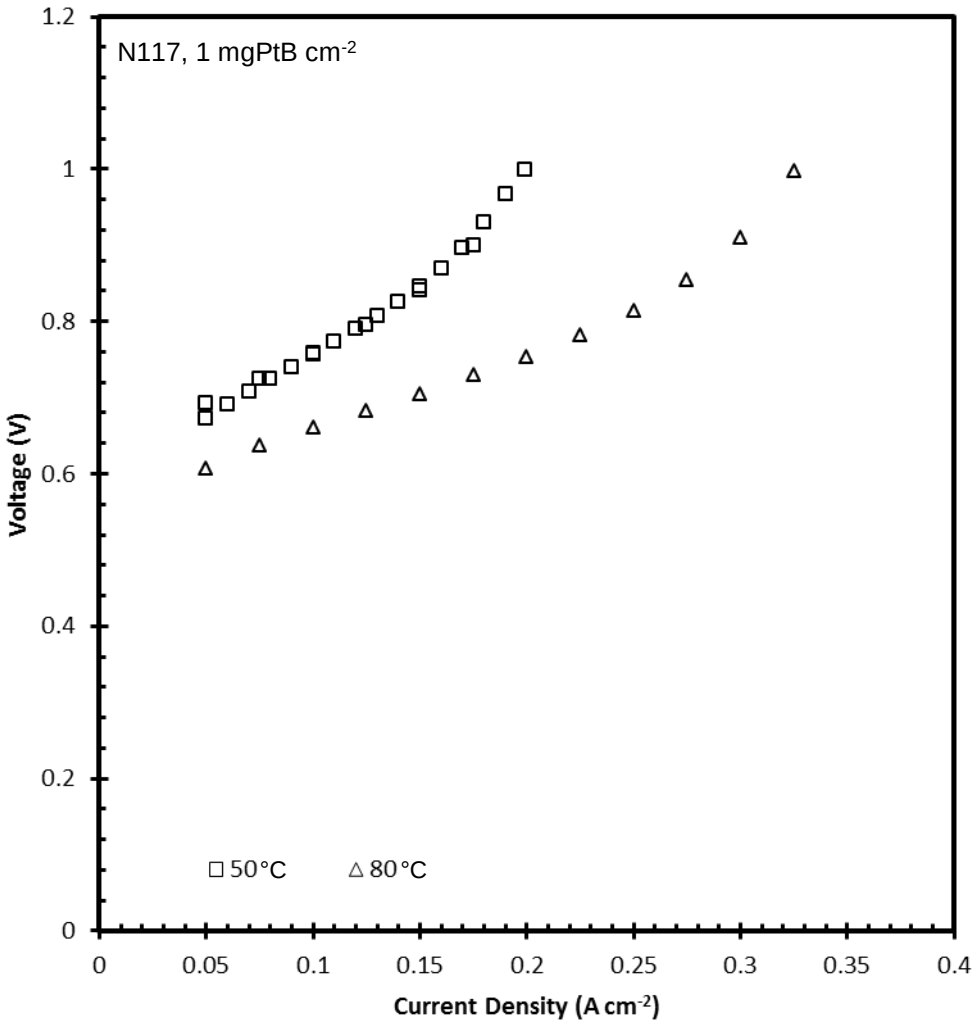

Figure 3.9: Polarisation curve obtained as a function of temperature when using N117, hot pressed at 50kg cm^{-2} for 5 minutes.

While the effect of temperature on the VI curve of Nafion has been previously demonstrated [18], the electrochemical impedance spectroscopy analysis as a function of operating temperature for SO_2 electrolysis has not yet been presented.

Figure 3.10 shows the EIS data of the temperature differences at 0.2 A cm^{-2} for N117 and 1 mgPtB cm^{-2}.

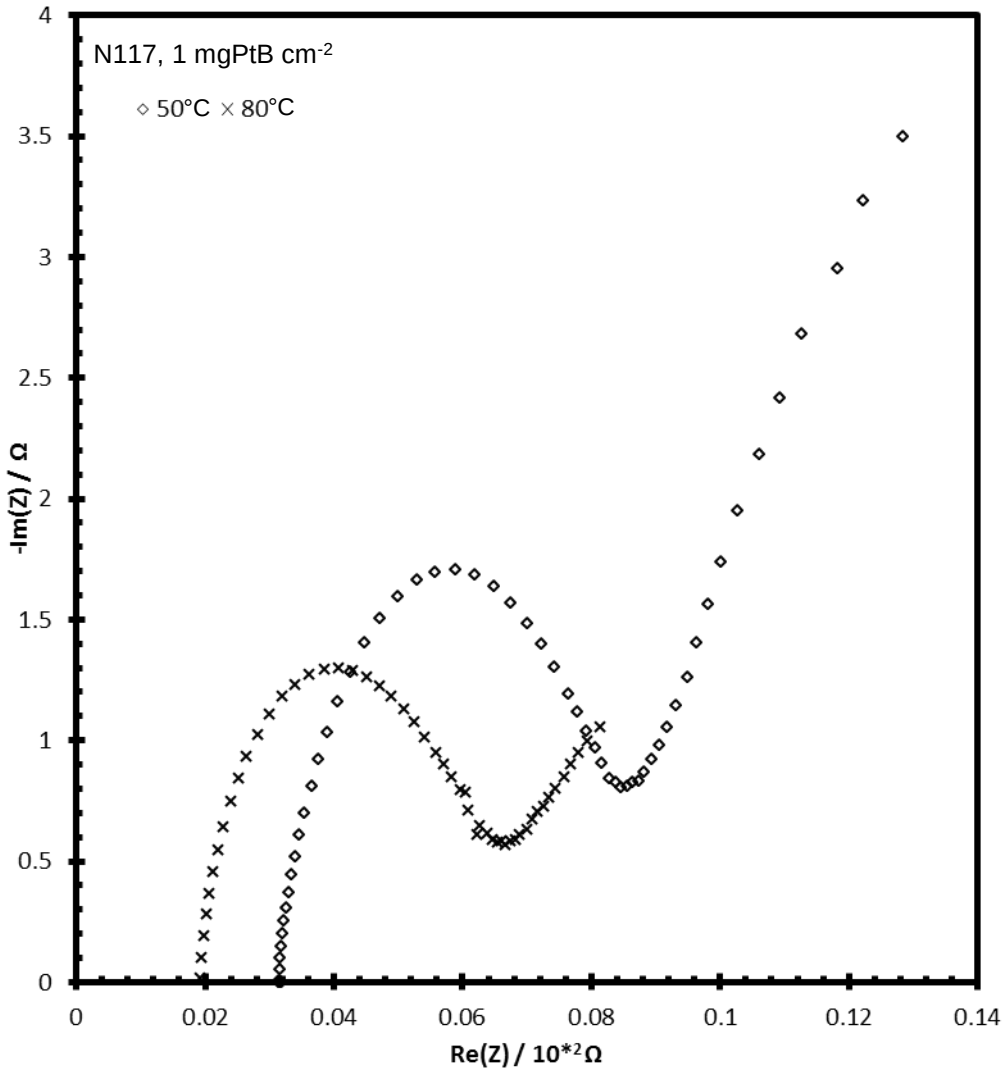

Figure 3.10: EIS data as a function of temperature at 0.2 A cm^{-2}.

The data obtained using the proposed model (fitting not shown) showed a decrease in membrane resistance from 31 to 18 mΩ when increasing the temperature from 50 to 80°C. This reduction is due to an increase in the water content of Nafion® with increasing temperature [26]. Better kinetics was also observed at higher temperatures with an activation resistance of 47 mΩ (80°C) compared to 53 mΩ (50°C). The mass transport however was significantly higher at 50ºC (22.89 compared to 62.03) due to the lower water content of the membrane [8].

3.3.4 MEMBRANE THICKNESS

To compare the effect of membrane thickness on SO_2 electrolysis, a MEA was made from Nafion N1110 (245 µm) and Nafion N117 (171 µm). The V*i* data was obtained at 80°C using 1 mgPt cm^{-2} catalyst. According to Figure 3.11 the membrane thickness had a significant influence on the electrolysis. It is understandable that the reduction in membrane thickness resulted in a reduced cell voltage over the entire current density range resulting in the increased current density observed when using N117.

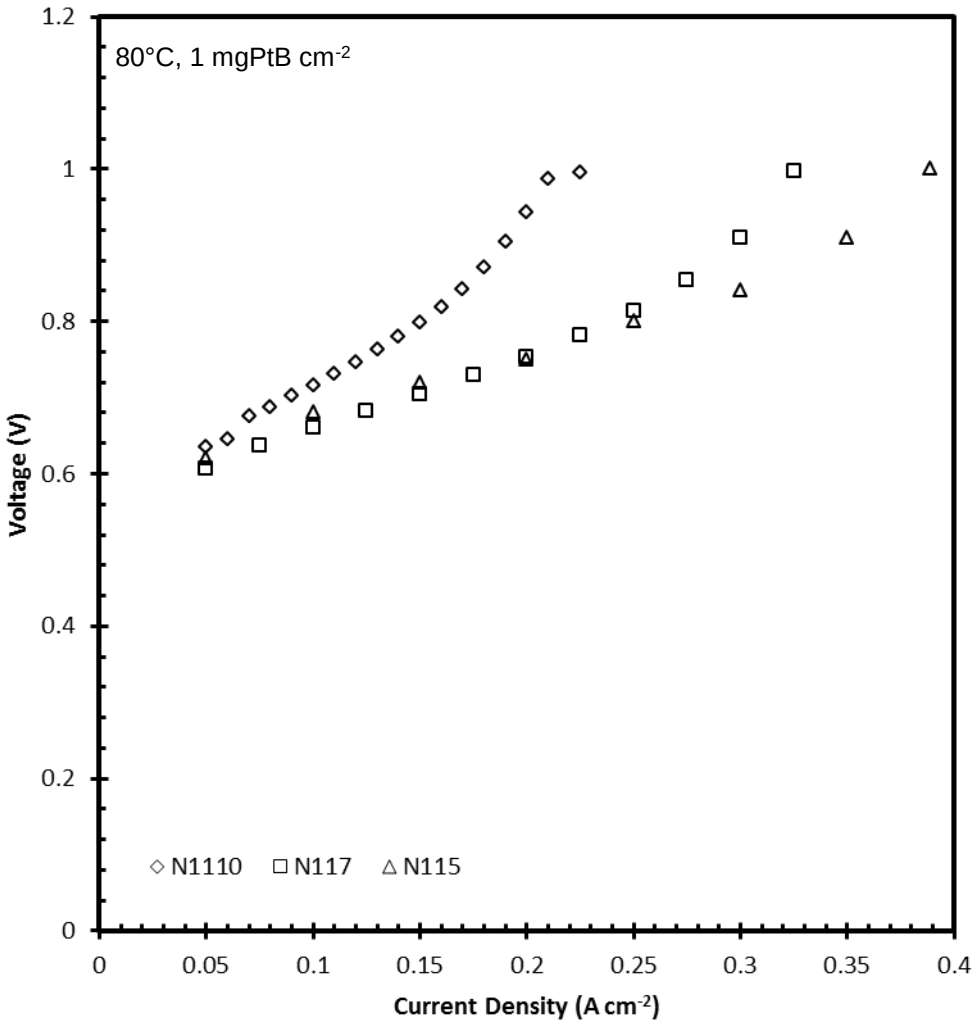

Figure 3.11: Effect of membrane thickness on SO_2 electrolysis.

At the beginning of the electrolysis (0.05 A cm^{-2}), the differences between the membranes were almost negligible (30 mV). However, as the current density was increased, the difference in voltage became significant. This increase can be

attributed to both the water uptake difference between the membranes and their proton conductivity [26].

When considering the EIS analysis presented in Figure 3.12, it is clear that the thickeer membrane had a higher membrane resistance. The values obtained from the model (data not shown) supports this increase in membrane resistance with N1110 having a resistance of 36.3 mΩ and N117 a resistance of 17.8 mΩ. While the activation resistance is comparable (58.47 and 47.92 mΩ for N1110 and N117 respectively), the mass transport was significantly different (62.03 vs 23.76) as can be seen by the extended 45 degree line in Figure 3.12. This implies that the thickness of the membrane had an influence on both the membrane resistance and mass transport effect, while the activation energy comparable.

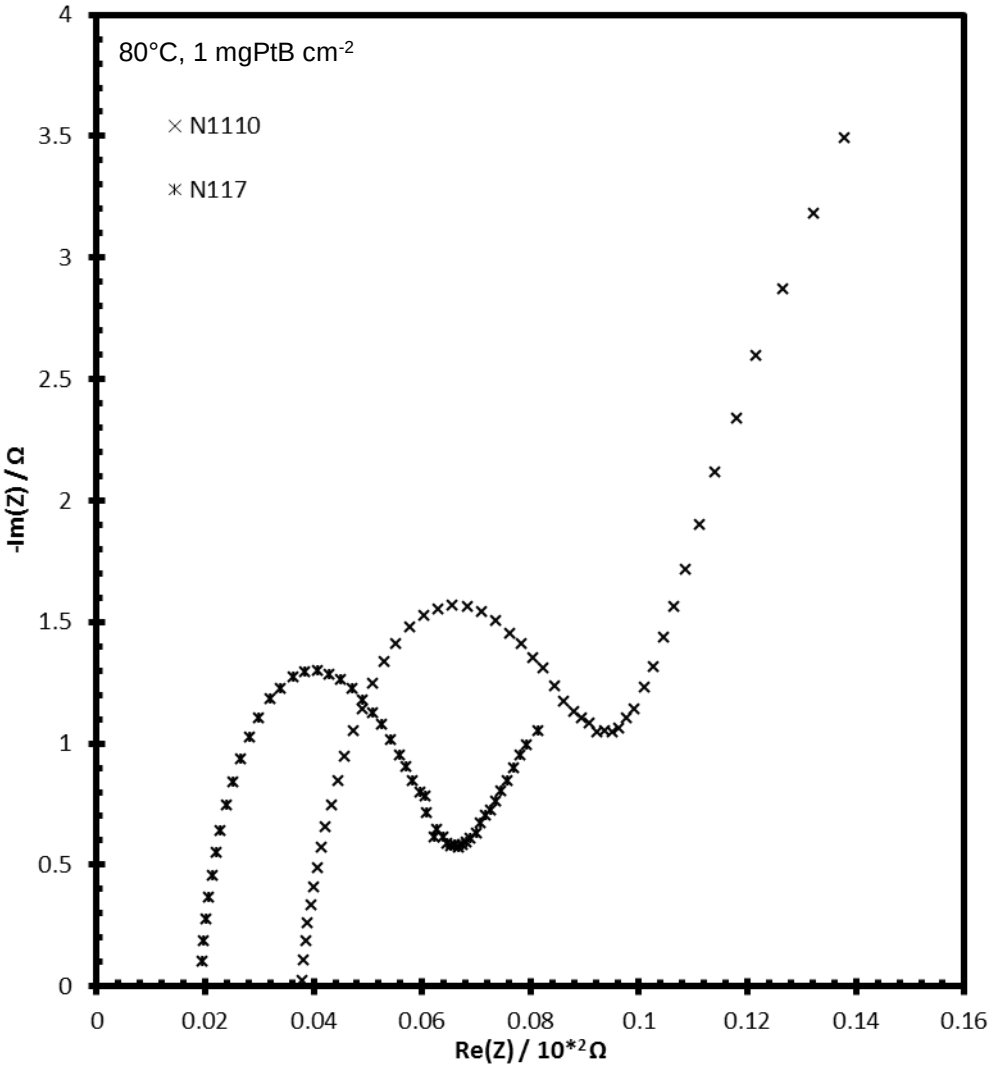

Figure 3.12: EIS analysis as a function of membrane thickness for 0.2 A cm^{-2}.

3.3.5 CATALYST LOADING

Figure 3.13 shows the data as a function of catalyst loading at 80°C when using N117. While, it is clear that higher catalyst loading resulted in an increased performance of the SO_2 electrolyser by 40 mA cm^{-2} when changing from a 1 mgPtB cm^{-2} to a 0.3 mgPtC cm^{-2} catalyst loading, Staser *et al.* [25] observed that no significant effect of catalyst loading on cell performance. However, their data was attained using a pressure differential across the membrane thereby reducing the SO_2 crossover and increasing the water content of the membrane thus reducing the possible effect of catalyst loading.

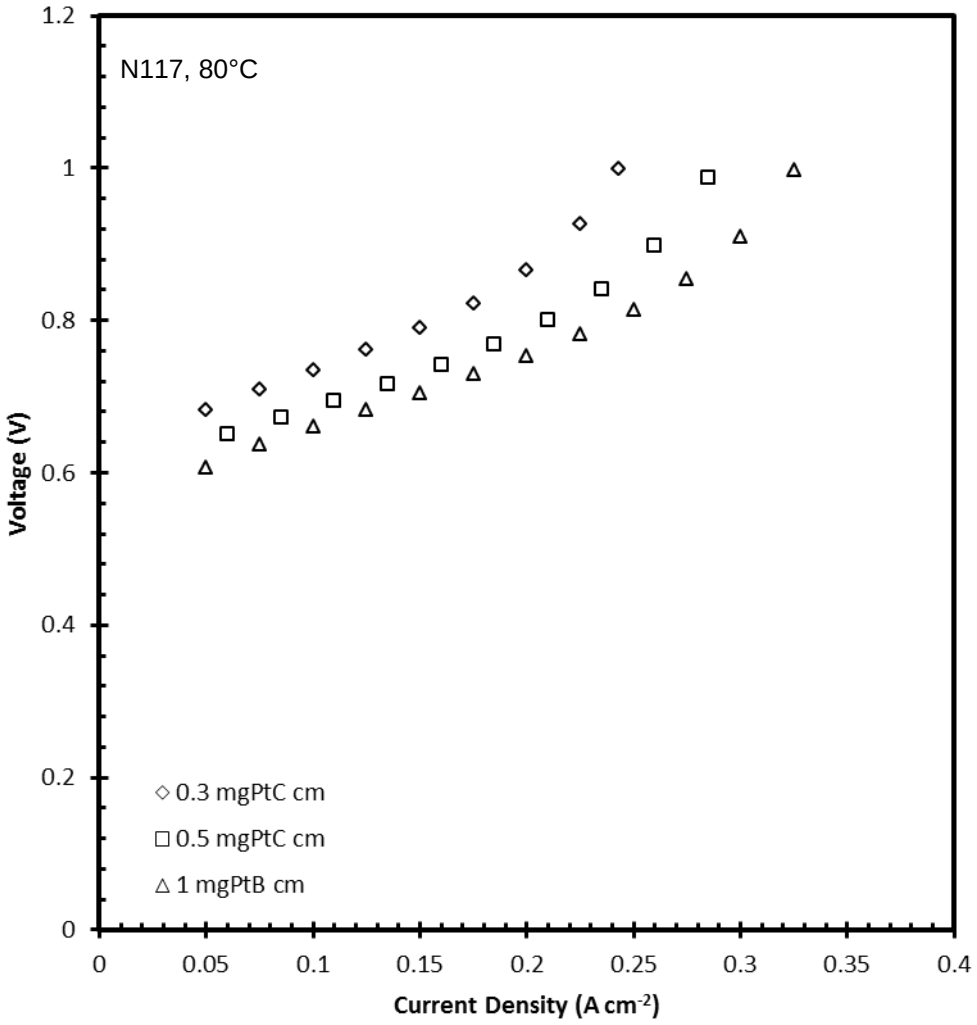

Figure 3.13: Polarisation curve as a function of catalyst loading.

Figure 3.14 shows the EIS data obtained for the different catalyst loadings used. It clearly support the data obtained from the polarisation curve with the 1 mgPtB cm^{-2} having the best performance followed by the 0.5 and 0.3 mgPtC cm^{-2} respectively.

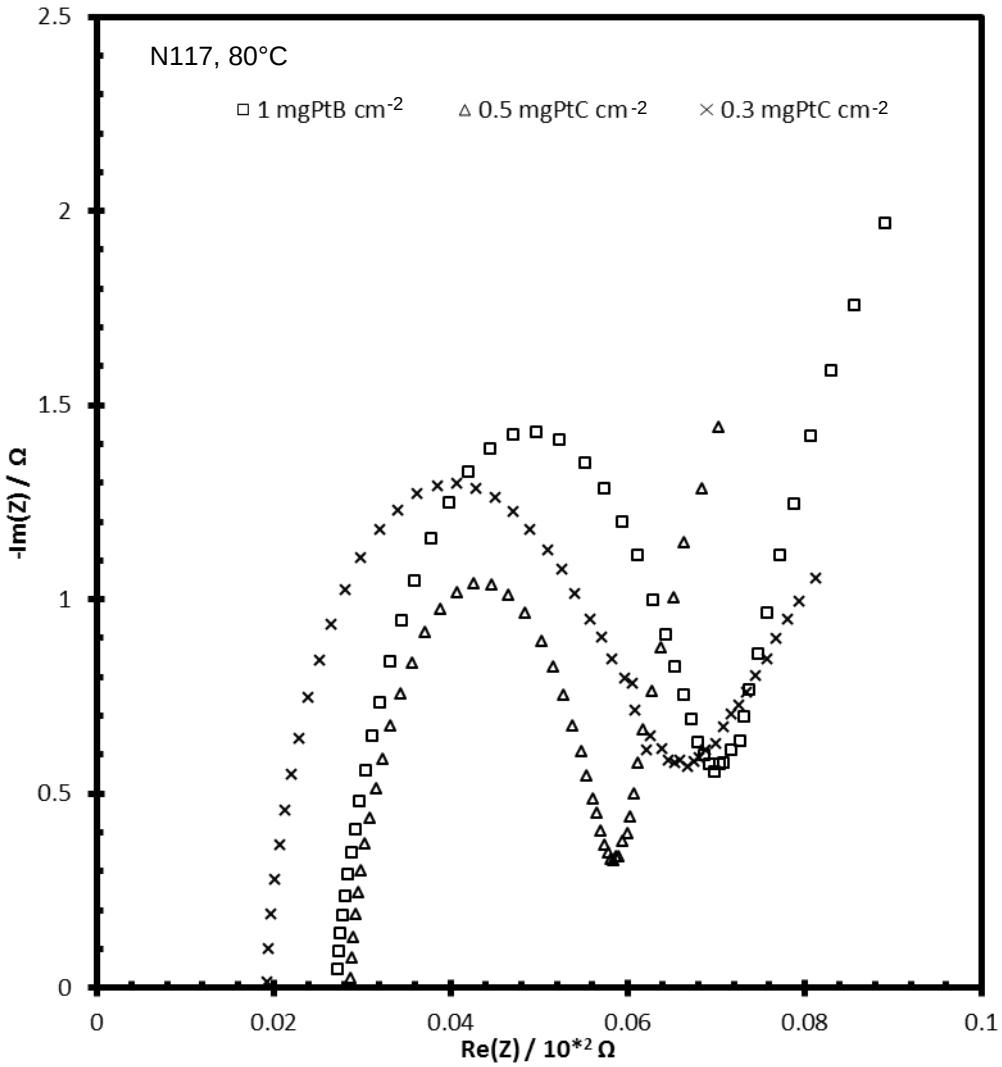

Figure 3.14: EIS analysis as a function of catalyst loading at 0.2 A cm^{-2}.

It should be noted that the catalyst used to manufacture the GDE for both the 0.5 and 0.3 mgPtC cm^{-2} was platinum supported on carbon, while for the GDE containing 1 mgPtB cm^{-2}, platinum black was used. This difference in catalyst configuration is also characterized by a difference in the particle size with the platinum supported on carbon having an average size of 4nm and the platinum black used for the 1 mgPtB cm^{-2} a particle size of 9 µm (according to the supplier). Due to the larger particle sizes of the 1mg PtB loading it is expected that the water transport

through the GDE is higher than 0.3 and 0.5 mg Pt/C as noted from the membrane resistance in Figure 3.15.

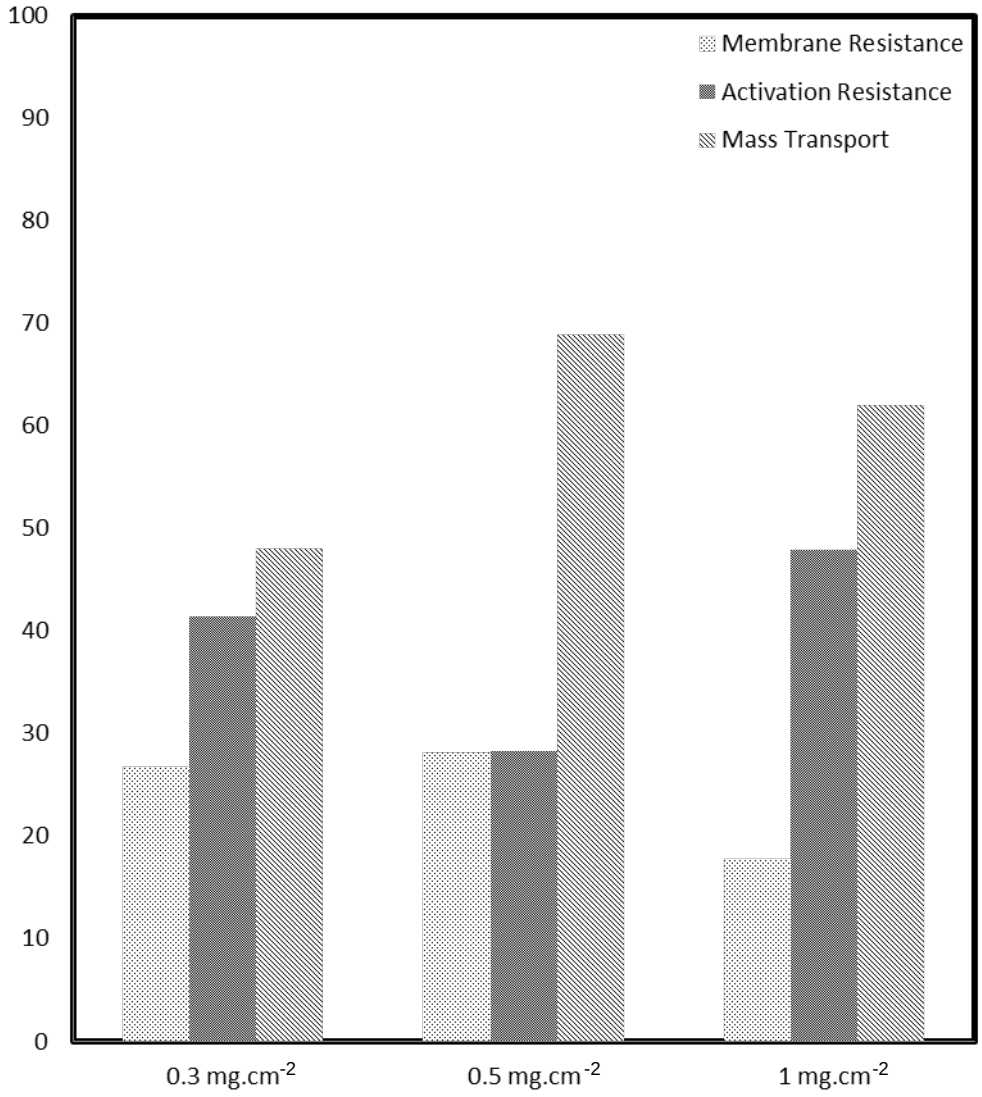

Figure 3.15: EIS data obtained (mΩ) from the model for different catalyst loadings.

As described in Section 2 the ohmic resistance is a combination of the membrane, GDE, catalyst and contact resistances. The difference in ohmic resistance (from Figure 3.15) is therefore attributed to the catalyst resistance (Pt/C vs. PtB) as the contact and membrane resistances should stay the same as the MEA manufacturing process was the same. Comparing the activation energies, it can be concluded that the 0.5 Pt/C mg cm^{-2} yielded the best catalyst utilisation however the catalyst particle size lead to the 1 mgPtB cm^{-2} having a better overall performance. The catalyst loading did not have a significant effect on the mass transport.

3.4 CONCLUSION

The use of polarisation curves and electrochemical impedance spectroscopy (EIS) were used to evaluate both the MEA manufacturing process and operating parameters (cell temperature, membrane thickness and catalyst loading). In all cases the EIS data was suitable in elucidating the tendencies observed with the polarisation curve data, while allowing for the identification of the limiting effects more clearly. Both the hot pressing pressure and hot-pressing time used in the MEA manufacturing process showed an effect on the overall performance. A pressure of 50 kg cm^{-2} for 5 min yielded the best performance. Lower pressures resulted in an inadequate contact between the membrane and GDE as shown by high activation resistances while a higher pressure resulted in over pressuring the GDE material which increased the mass transport effect. It was further shown that an increase in operating temperature decreased both the activation energy and mass transport resistances. Significant mass transport limitations were observed when thicker membranes were used while the activation energies were comparable over the current densities used. Finally it was shown that the catalyst used for the electrolysis in terms of the amount and the particle size differences also had a significant influence both on the activation energy and mass transport resistances.

3.5 REFERENCES

[1] James T. Hinkley, Christopher J. Fell, Sten-Eric Lindquist JAO. Prospects for solar only operation of the hybrid sulphur cycle for hydrogen production. Int J Hydrogen Energy 2011;36:11596–603.

[2] Gorensek MB. Hybrid Sulfur cycle flowsheets for hydrogen production using high-temperature gas-cooled reactors. Int J Hydrogen Energy 2011;36:12725–41.

[3] Gorensek MB, Summers WA. Hybrid Sulfur flowsheets using PEM electrolysis and a bayonet decomposition reactor. Int J Hydrogen Energy 2008;34:1–18.

[4] Brecher LE, Spewock S, Warde CJ. The Westinghouse Sulfur Cycle for the thermochemical decomposition of water. Int J Hydrogen Energy 1977;2:7–15. doi:http://dx.doi.org/10.1016/0360-3199(77)90061-1.

[5] Lokkiluoto A, Taskinen PA, Gasik M, Kojo A V, Peltola H, Barker MH, et al. Novel process concept for the production of H2 and H2SO4 by SO2-depolarized electrolysis. Environ Dev Sustain 2012;15:529–40.

[6] Hocking MB. Handbook of Chemical Technology and Pollution Control. Third Edit. Academic Press Inc., U.S; 2006.

[7] Sivasubramanian P, Ramasamy RP, Freire FJ, Holland CE, Weidner JW. Electrochemical hydrogen production from thermochemical cycles using proton exchange membrane electrolyzer. Int J Hydrogen Energy 2007;32:463–8.

[8] Staser JA, Weidner JW. Effect of Water Transport on the Production of Hydrogen and Sulfuric Acid in a PEM Electrolyzer. J Electrochem Soc 2009;156:B16–21.

[9] Schoeman H, Krieg HM, Kruger AJ, Chromik A, Krajinovic K, Kerres J. H2SO4 stability of PBI-blend membranes for SO2 electrolysis. Int J Hydrogen Energy 2012;37:603–14.

[10] Peach R, Krieg HM, Kruger AJ, Chromik A, Krajinovic K, Kerres J. Comparison of ionically and ionical-covelently cross-linked polyaromatic membranes for SO2 electrolysis. Int J Hydrogen Energy 2014;39:28–40.

[11] Hector R. Colon-Mercado DTH. Catalyst evaluation for sulfur dioxide-depolarized electrolyzer. Electrochem Commun 2007;9:2649–53.

[12] Xue L, Zhang P, Chen S, Wang L. Pt-based bimetallic catalysts for SO2-depolarized electrolysis reaction in the hybrid sulfur process. Int J Hydrogen Energy n.d. doi:http://dx.doi.org/10.1016/j.ijhydene.2014.02.128.

[13] O'Brien JA, Hinkley JT, Donne SW, Lindquist SE. The electrochemical oxidation of aqueous sulfur dioxide: A critical review of work with respect to the

hybrid sulfur cycle. Electrochim Acta 2010;55:573–91. doi:http://dx.doi.org/10.1016/j.electacta.2009.09.067.

[14] Lee S-K, Kim C-H, Cho W-C, Kang K-S, Park C-S, Bae K-K. The effect of Pt loading amount on SO2 oxidation reaction in an SO2-depolarized electrolyzer used in the hybrid sulfur (HyS) process. Int J Hydrogen Energy 2009;34:4701–7.

[15] Van der Merwe J, Uren K, van Schoor G, Bessarabov D. Characterisation tools development for PEM electrolysers. Int J Hydrogen Energy 2014;39:14212–21. doi:http://dx.doi.org/10.1016/j.ijhydene.2014.02.096.

[16] Jayakumar JV, Gulledge A, Staser JA, Kim C-H, Brian C B, Weidner JW. Polybenzimidazole Membranes for hydrogen and sulfuric acid production in the Hybrid Sulfur Electrolyzer. ECS Electrochem Lett 2012;1:F44–8.

[17] Kim CH, Jung SW, Cho WC, Kang KS, Park CS, Bae KK. A study on the sulfur dioxide and water electrolyzer for the production of hydrogen and sulfuric acid. 2012 Int. Conf. Hydrog. Prodcution, Seoul: n.d.

[18] Ting F-P, Lin J-C, Lai C-M, Chyou S-D, Hsueh K-L. Electrochemical Impedance Spectroscopy to Evaluate the Effect of Pressure Exerted in the Hot-Pressing Stage on the Performance of PEMFC. Int J Electrochem Sci 2012;7:7165–78.

[19] Van der Merwe J, Uren K, van Schoor G, Bessarabov D. A study of the loss characteristics of a single cell PEM electrolyser for pure hydrogen production. Ind. Technol. (ICIT), 2013 IEEE Int. Conf., 2013, p. 668–72. doi:10.1109/ICIT.2013.6505751.

[20] Wangner N. Characterization of membrane electrode assemblies in polymer fuel cells using A.C. impedance spectroscopy. J Appl Electrochem 2002;32:859–63.

[21] Staser JA, Gorensek MB, Weidner JW. Quantifying Individual Potential Contributions of the Hybrid Sulfur Electrolyzer. J Electrochem Soc 2010;157:B952–8.

[22] Merwe JH van der, Uren DKR, Schoor PG van, Bessarabov DDG. Characterisation of a proton exchange membrane electrolyser using electrochemical impedance spectroscopy. North-West University, 2012.

[23] Gorensek MB, Staser JA, Stanford TG, Weidner JW. A thermodynamic analysis of the SO2/H2SO4 system in SO2-depolarized electrolysis. Int J Hydrogen Energy 2009;34:6089–95.

[24] Khaldi C, Mathlouthi H, Lamloumi J. Electrochemical impedance spectroscopy study of the metal hydride alloy/electrolyte junction. J Alloys Compd 2009;479:284–9. doi:10.1016/j.jallcom.2008.12.150.

[25] Staser J, Ramasamy RP, Sivasubramanian P, Weidner JW. Effect of Water on the Electrochemical Oxidation of Gas-Phase SO2 in a PEM Electrolyzer for H2 Production . Electrochem Solid-State Lett 2007;10:E17–9.

[26] Majsztrik PW, Satterfield MB, Bocarsly AB, Benziger JB. Water sorption, desorption and transport in Nafion membranes. J Memb Sci 2007;301:93–106. doi:http://dx.doi.org/10.1016/j.memsci.2007.06.022.

CHAPTER 4: EFFECT OF H_2S ON SO_2-DEPOLARISED WATER ELECTROLYSIS*

Chapter Overview

The performance of a PEM SO_2 electrolyser, used for the production of H_2 gas and liquid H_2SO_4, was evaluated when the feed was contaminated with hydrogen sulfide. Transient voltage response at constant current density and polarisation curves showed a decrease in operating efficiency over time for all H_2S concentrations tested. Electrochemical impedance spectroscopy (EIS) was applied to separate and quantify the membrane resistance, charge resistance and mass transport limitations to evaluate the influence of H_2S exposure time. The charge resistance increased by 64.70 mΩ over 40 min when the anode was exposed to 80 ppm H_2S. Cyclic voltammetry (CV) was applied to determine the electrochemical surface area (ECSA, $cm^2.g^{-1}$) by CO stripping as a function of SO_2 and SO_2/H_2S exposure (10, 30, 60 and 80 ppm H_2S). An ECSA of 83.52 cm^2 g^{-1} was obtained for a clean catalyst while exposing the anode to SO_2, at 0.1 A cm^{-2} for 3 minutes, reduced the ECSA to only 9.10 resulting in an 89% reduction in active platinum sites. The reduction in ECSA for a fresh anode, when exposed to 80 ppm H_2S, was calculated as 12.56 cm^2 g^{-1} which is a reduction of 85% in active catalytic sites.

*Krüger AJ, Krieg HM, Bessarabov D. Effect of H_2S on SO_2-depolarised water electrolysis. Int J Hydrogen Energy 2015;40:4442–50. doi:10.1016/j.ijhydene.2015.02.036.

4.1 INTRODUCTION

Hydrogen production through SO_2 assisted water electrolysis, known as SO_2 depolarised electrolysis (SDE), has received increased attention as a possible clean alternative to current industrial processes for the production of hydrogen. The SO_2 electrolyser was initially incorporated in the Hybrid Sulfur (HyS) thermochemical cycle proposed by the Westinghouse Corporation in the 1970's [1]. The cycle incorporates a sulphuric acid decomposition step (into SO_2, H_2O and O_2), oxygen separation step and an electrolysis step (reacting SO_2 and H_2O). Although the overall theoretical efficiency of the HyS cycle was estimated at 41.7% (HHV) [2] using traditional PFSA (such as Nafion®) proton exchange membranes (PEM) and 44.0 – 47.6% (HHV) [3] when using polybenzimidiazole (PBI) proton exchange membranes in the electrolyser, significant research is needed for the entire process to come close to the calculated efficiency. In the electrolyser, which is the focus of this paper, water reacts in the presence of SO_2 over a platinum group metal (PGM) anode, usually platinum supported on carbon, producing concentrated sulphuric acid (equation (4.1)) and hydrogen gas (equation (4.2)) giving an overall reaction shown in equation (4.3).

$$SO_2(g) + 2H_2O(l) \rightarrow H_2SO_4 + 2H^+ + 2e^- \qquad E^o = 0.158V \text{ vs. SHE} \qquad (4.1)$$

$$2H^+ + 2e^- \rightarrow H_2(g) \qquad E^o = 0 \text{ vs. SHE} \qquad (4.2)$$

$$SO_2(g) + H_2O(l) \rightarrow H_2SO_4(l) + H_2(g) \qquad (4.3)$$

Gaseous SO_2 is fed to the anode while pre-heated water is circulated through the cathode (which diffuses to the anode for the reaction). Concentrated sulphuric acid is produced when the SO_2 reacts with water producing protons and electrons. The protons are conducted through the membrane to the cathode which produces hydrogen gas by combining with the electrons.

Other applications of the SO_2 electrolyser can be identified where the entire HyS cycle, acid decomposition and oxygen separation step is not needed. One such application could be in coal firing plants where large amounts of SO_2 are produced as air pollutant [4]. Removal of SO_2 impurities from flue gas, before venting to the atmosphere, can be achieved by several established methods. For example, lime

based sorbents (spray dryer process, wet limestone process or wet lime process) can be used to absorb SO_2 into liquid form and later converted into solid gypsum [5]. The lime sorbents used in these processes can include calcium oxide, calcium carbonate and calcium hydroxide. Although these processes are effective, problems such as scaling and process cost opens the field for the development of other processes for the removal of SO_2.

The SO_2 electrolyser could also be applied for the removal of SO_2 by feeding SO_2 dissolved in sulphuric acid [6], water [7] or in the gas form to the anolyte of the SO_2 electrolyser; producing H_2SO_4 and hydrogen. The main operating difference between the SO_2 electrolyser and normal water electrolyser is that the water electrolyser uses liquid water as the anode reactant compared to the SO_2 used in the SO_2 electrolyser. For water electrolysers the typical contaminates include dissolved metals such as sodium [8], cobalt and silver [9]. While, when the reactant is a gas, typical contaminants include CO_2 [10], CO [11], H_2S [11,12], SO_2 [13] and NH_3 [14] for systems such as the fuel cell or SO_2 electrolyser.

In fuel cells the presence of SO_2 or H_2S is seen as the contaminant which adsorbs on the catalyst surface reducing the active catalyst sites for the oxygen reduction reaction (ORR). The adsorption of H_2S on PGM, specifically on platinum, has been extensively investigated [11,15–19]. In the SO_2 electrolyser system the SO_2 is however one of the reactants while the H_2S is seen as the contaminant.

The advantage of the electrolysis of SO_2 in the presence of water over conventional scrubbing techniques is that both H_2 and H_2SO_4 are produced from one impurity or by-product. Although the SO_2 electrolyser performance has been investigated for a variety of conditions including temperature, pressure, anode/cathode feed stream composition, membrane thickness, catalyst loading and even SO_2 concentration to the anode, these parameters were investigated for applications where pure SO_2 was available. It is acceptable to assume that flue gas consists of SO_2, H_2S, CO, CO_2, NO and NO_2 mixtures [20–22]. If the SO_2 electrolyser is to be applied in the flue gas environment, i.e. in the presence of hydrogen sulfide gas for example, further studies are needed to determine the performance under these specific conditions.

This chapter reports, to the best of our knowledge, for the first time, on the operating performance of the SO_2 electrolyser in the presence of H_2S under conditions typically found in current industrial environments. The focus is given on the influence of various concentrations of hydrogen sulfide on the SO_2 electrolyser performance. Main methods of characterisation include polarisation curves, electrochemical impedance spectroscopy and cyclic voltammetry in this paper.

4.2 EXPERIMENTAL

Evaluation of the effect of hydrogen sulphide (H_2S) on the performance of the SO_2 electrolyser was investigated using a system schematically depicted in Figure 4.1. An additional picture is available in Appendix A, Figure A-1(b). The system used is based on a previous method for SO_2 electrolysis operation [23,24] with the exception of the supply of H_2S to the anode. Pure SO_2 is supplied to the anode using a thermal mass flow controller (SLA5850, Brooks) at a constant 0.15 L min^{-1} while DI water is circulated to the cathode. Membrane electrode assemblies (MEA) were prepared using N115 as PEM and 1 mgPtB cm^{-2} catalyst loading as GDE's. The GDE's were hot-pressed on both sides of the PEM using 50 kg cm^{-2} pressure at 120°C for 5 min. The active area of the cell was 10 cm^{-2}. All membrane samples were pre-treated in 1 M H_2SO_4 for 90 min before hot-pressing [25].

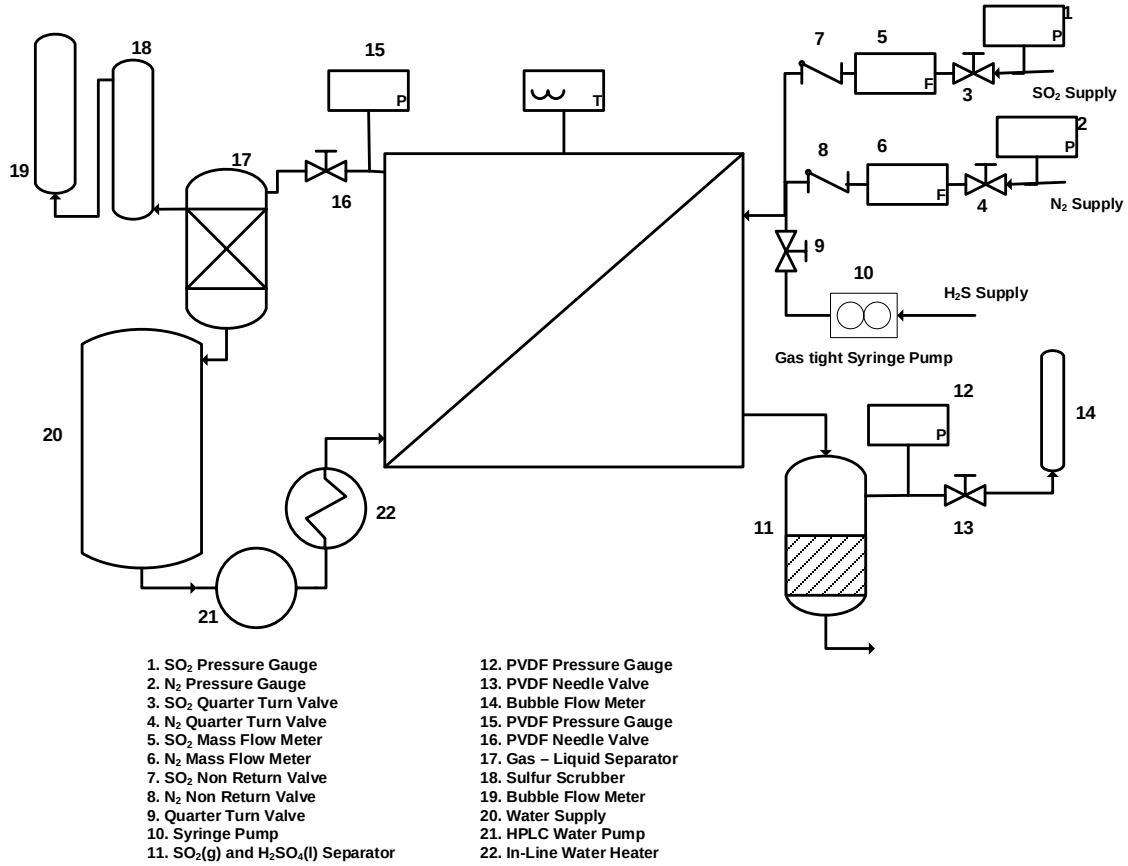

Figure 4.1: Schematic of the experimental system used to evaluate the effect of H_2S on the performance of an SO_2 electrolyser system.

Polarisation curves were obtained using a DC power supply (GenH12.5-60, Accutronics) by increasing the current incrementally every 90 seconds while recording the voltage. Diluted hydrogen sulfide (10% H_2S balanced in N_2, Afrox SA) was introduced to the anode using a syringe pump with a 50 mL gas tight syringe (NE-1000, DLD Scientific). The concentration of the H_2S was first determined using N_2 (instead of SO_2) to dilute the 10% H_2S to the desired ppm level before each experiment. The flow rate of the syringe pump was carefully calibrated over a period of 4 hours (per ppm level) to ensure stable/homogeneous mixing. The mixing of the H_2S and SO_2 was performed using an in-house manufacture “y-piece”. The main line, for the pure SO_2, was made of ¼” tubing while the H_2S line was 1/16” which could be inserted into the ¼” tubing of the SO_2. The gas line downstream of the mixing piece was 10 cm long before connecting to the electrolyser. This ensured that the mixed gasses were uniformly distributed inside the tubing.

Electrochemical impedance spectroscopy (EIS) and cyclic voltammetry (CV) was used to evaluate the effect of H_2S on the SO_2 electrolyser system using a Gamry REF300 potentiostat/galvanostat. Galvanostatic EIS was applied using an AC current of 10% of the DC current over a frequency range of 0.1 – 100 kHz with 10 points per decade [26,27]. The membrane resistance, charge resistance and mass transport limitations were separated using an electrical circuit model as previously described for the SO_2 electrolyser [26]. Figure 4.2 shows the electrical equivalent circuit (EEC) that was used to determine the membrane, charge resistance and the mass transport limitations (Warburg impedance).

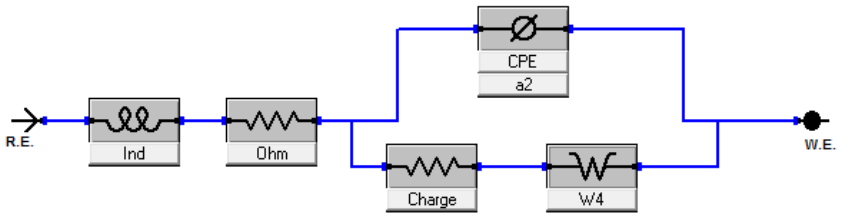

Figure 4.2: Electrical equivalent circuit (EEC) diagram used to fit the experimental data. Ind - Inductance, Ohm - Ohmic resistance, Charge - Charge resistance, CPR - Constant phase element and W - Warburg impedance.

Cyclic voltammetry was used to determine both the electrochemical surface area (ECSA, $cm^2\ g^{-1}$) using CO stripping (using a method based on literature [28,29]) and the effect of H_2S on the catalyst [12,17,18,30]. The voltage was cycled from 20 mV up to 1.1 V before cycling back to 20 mV with a scan rate of 50 mV s^{-1}. The ECSA was determined for a clean catalyst after SO_2 exposure and after exposure to different H_2S concentrations. All calculations of ECSA were baseline corrected to exclude any double layer capacitance present within the system [19].

4.3 RESULTS AND DISCUSSION

4.3.1 HYDROGEN SULFIDE DEACTIVATION

Firstly, the effect of H_2S gas as an impurity on the performance of the SO_2 electrolyser was investigated. Figure 4.3 shows the transient voltage response at a constant 0.1 A cm^{-2} for the exposure of the anode to various H_2S concentrations. A fresh MEA was used for each concentration, although it is shown on the same timeline. It should be mentioned that the exposure time decreased as the H_2S concentration increased due to the use of the syringe pump i.e. a higher flow rate of the 10% H_2S was needed for higher concentrations (only 50 mL of the 10% H_2S was available per experiment due to syringe size). The presence of SO_2 in PEM fuel cells as impurity has been thoroughly investigated and is well-known to decrease the cell performance dramatically [10,13,19,31–33]. SO_2 gas on the fuel cell set-up prevents H_2 oxidation due to catalyst deactivation thereby reducing the active sites available for the reaction of H_2. When SO_2 is used as the only reactant, as in SO_2 electrolysis, the surface coverage of SO_2 on the Pt catalyst is desired. Similarly the effect of H_2S as impurity is clearly visible when SO_2 is the reactant as shown in Figure 4.3. Although the deactivation effect is not as dramatic as in fuel cells, a clear increase in operating voltage is apparent with an increase in the H_2S concentration.

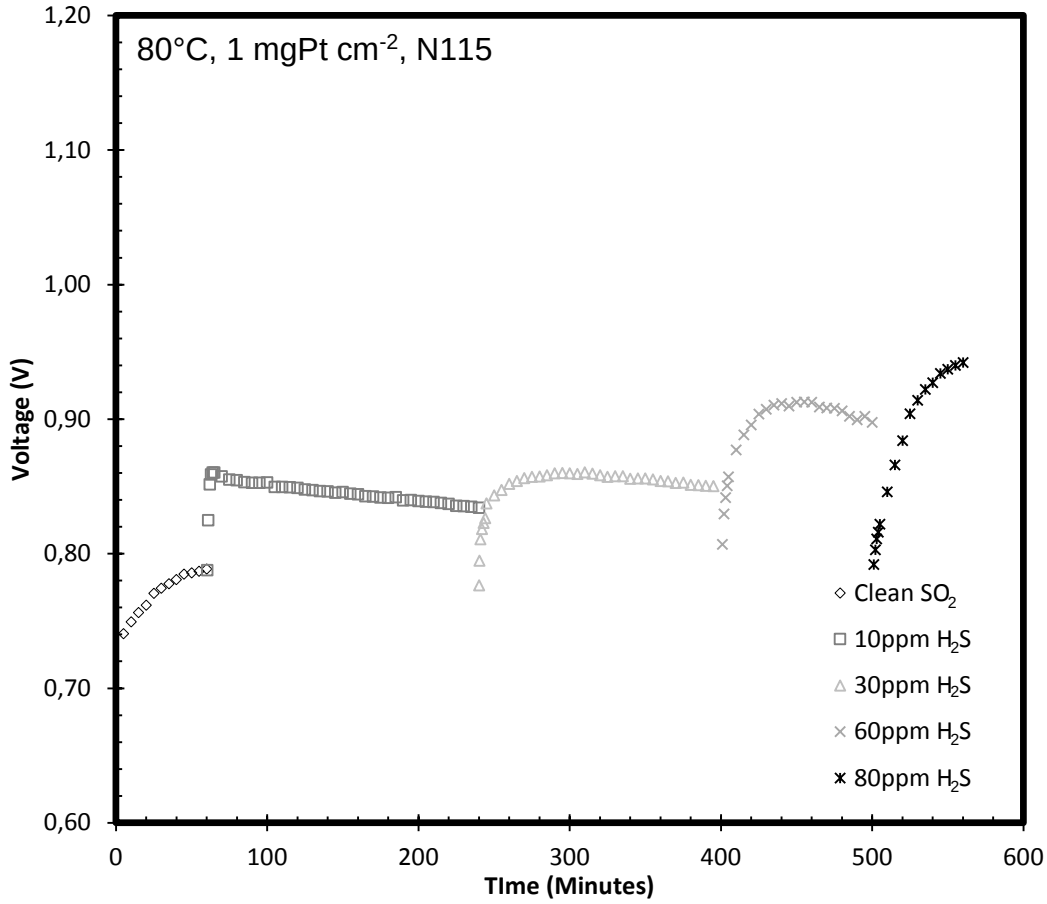

Figure 4.3: Voltage response at 0.1 A cm^{-2} as a function of H_2S concentration at 80°C, N115 and 1 mgPt cm^{-2}.

A voltage increase of 46 mV was observed in the presence of the 10 ppm H_2S while increasing the H_2S concentration to 30 ppm resulted in a further potential increase of 62 mV. A further increase in the H_2S concentration from 60 to 80 ppm resulted in an increase of 110 and 155 mV respectively. According to these results the voltage increased linearly (R^2 = 0.95) by 1.75 mV per ppm H_2S. The rate of voltage increase is clearly not linear as a sharp increase is observed within the first minute of exposure after which a stable operating voltage seems to appear. It has been shown previously that the presence of 25 ppm SO_2 in PEMFC showed a significant reduction of operating current (at constant voltage of 0.7 V) within 60 min [31]. When comparing the 30 ppm H_2S in this study with that of contaminating a PEMFC with 25 ppm SO_2 PEMFC, the effect is not as detrimental for the SO_2 electrolyser when exposed to H_2S at concentrations below 30 ppm [31].

To evaluate the effect of H_2S exposure at different concentrations and operating current densities, polarisation curves were recorded. Figure 4.4 shows the polarisation curves as a function of the H_2S concentration supplied to the anode. As can be expected, compared to the transient data, a clear decrease in the overall performance is observed as the H_2S concentration is increased.

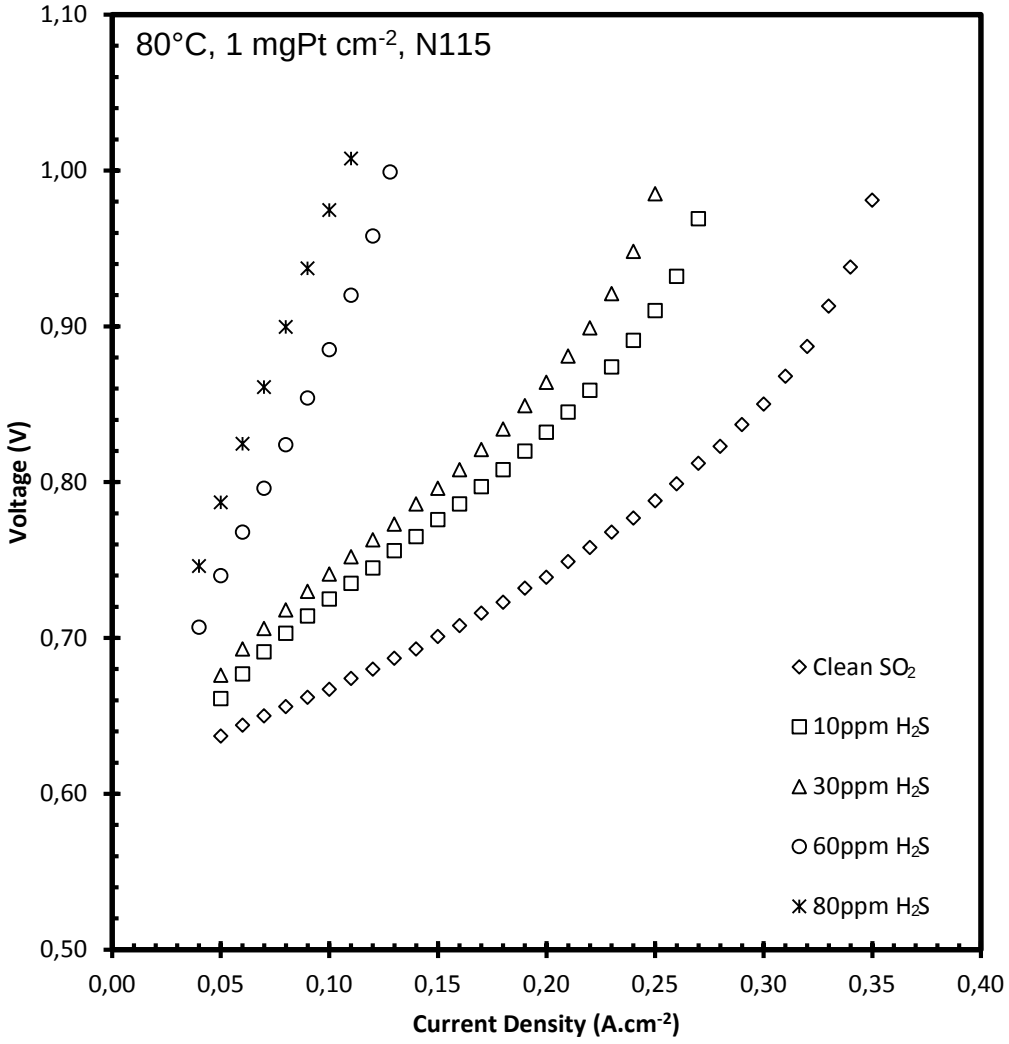

Figure 4.4: Polarisation curves as a function of H_2S concentration at 80°C using N115 and 1 mgPt cm^{-2}.

A clear reduction in the current density achievable is visible when increasing the H_2S concentration from 10 to 80 ppm H_2S. If a linear decrease in current density is assumed ($R^2 = 0.95$), the maximum current density attainable decreases with 3.1 mA cm^{-2} per ppm H_2S. At low current densities (kinetics), a significant voltage increase

is observed with 0.637 vs. 0.787 V for clean SO_2 and 80 ppm H_2S respectively. This could be explained by the reduced ability of SO_2 adsorption as the H_2S present in the feed steam blocks some of the active catalyst sites [34].

Although the general method is to derive the impedance expressions from kinetic aspects of any process [35–38], this paper focuses on the membrane resistance, charge resistance and mass transport limitations as these are the main parameters influencing the operating voltage, a simplified method based on literature is used [26,27]. Electrochemical impedance spectroscopy as a function of time was obtained for each H_2S concentration to determine which component is responsible for the reduction in performance. Figure 4.5 shows the EIS data obtained after 20 min and 60 min exposure times under constant current (0.1 A cm^{-2}) operation. It should be mentioned that the normal practice of using the same scales for both the x and y axis was not used to better illustrate the curvature in the data.

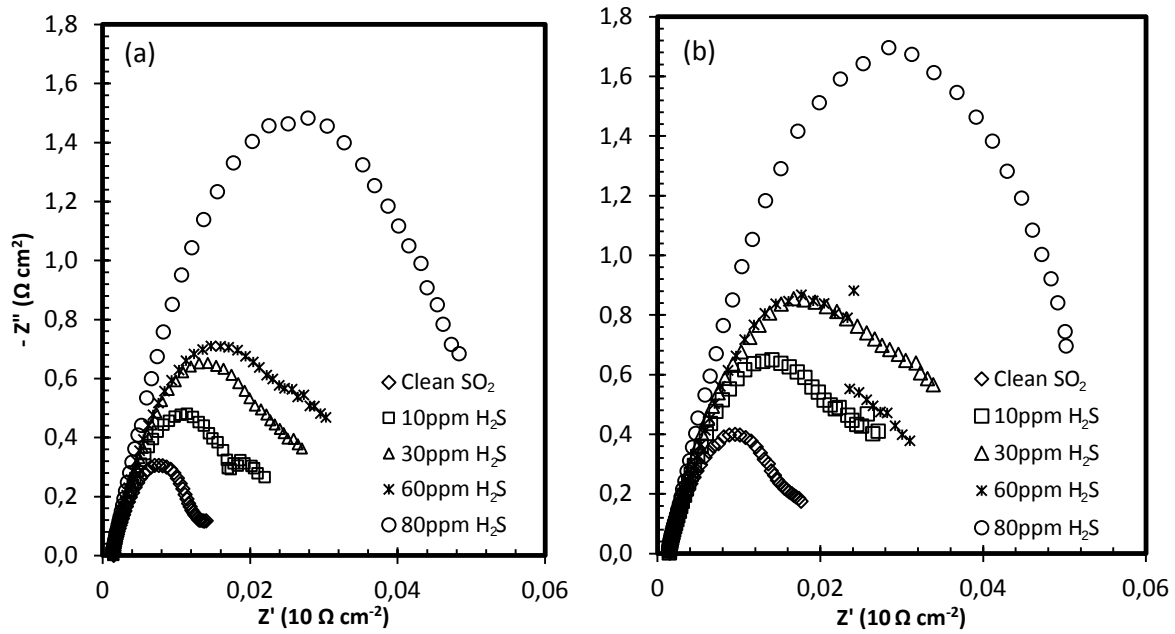

Figure 4.5: EIS data obtained at 0.1 A cm^{-2} as a function of H_2S concentration at (a) 20 min and (b) 60 min.

The interception of the imaginary data with the real axis is used as the membrane resistance (Ohmic), while the charge resistance and mass transport limitations can be determined by applying an electric circuit model to the rest of the data as previous

described for the SO_2 electrolyser system [26]. It is clear that the membrane resistance was not influenced by the presence of the H_2S in the anode feed stream for both 20 and 60 min exposure times. The charge resistance however was influenced and increased with H_2S concentration as can be expected as more H_2S present would occupy more active sites of the catalyst. Mass transport limitations could not clearly be identified (a straight line in the low frequency range) from the EIS data.

To quantify the membrane resistance, charge resistance and mass transport limitations the data was used to fit the electrical equivalent circuit model using the Echem Analyst software from Gamry. Table 4.1 shows the values obtained from the model at 0.1 A cm^{-2} at 20 and 60 min for the H_2S concentrations tested. The inductance (Ind, from the wired connecting to the potentiostat and electrolyser) values are given followed by the membrane resistance (Ohm), charge resistance (Charge), constant phase element (CPE) and the mass transport limitations (W – Warburg).

Table 4.1: Parameter values obtained from fitting the EEC to the experimental data.

Amount of H_2S (ppm)	*Ind (H)*	*Ohm (mΩ cm^{-2})*	*Charge (mΩ cm^{-2})*	*CPE (S s^a)*	*W (-)*
		After 20 min			
0	3.47×10^{-8}	1.33	12.33	0.54	57.20
10	3.43×10^{-8}	1.28	26.41	0.58	61.11
30	2.26×10^{-8}	1.28	28.63	0.54	31.75
60	3.64×10^{-8}	1.23	19.87	0.66	60.25
80	2.81×10^{-14}	1.30	55.11	0.44	67.29
		After 60 min			
0	3.47×10^{-8}	1.34	16.03	0.58	68.97
10	3.42×10^{-8}	1.29	26.23	0.59	46.11
30	2.25×10^{-8}	1.29	34.18	0.56	35.31
60	3.6×10^{-8}	1.26	33.61	0.65	82.60
80	2.53×10^{-13}	1.33	61.58	0.65	97.33

The membrane resistance (Ohm) showed no significant change when varying the H_2S concentration or time. It was shown previously that membrane resistance does not increase significantly in other systems such as PEMFC and water electrolysis over a 60 min period [8,31]. The charge resistance (Charge) was however influenced by the presence of H_2S, reaching 55.11 mΩ cm^{-2} after 20 min when exposed to 80 ppm H_2S indicating that the catalyst efficiency is reduced. The charge resistance is higher for all ppm levels tested after 60 min of exposure with the 80 ppm being the highest at 61.58 mΩ cm^{-2}. Both Figure 4.4 and Figure 4.5 have some deviation when the 60 ppm H_2S data is concerned. The exact cause is however not fully understood requiring further research. Interestingly an improved mass transport is observed for pure SO_2, 30 – 80 ppm H_2S. It is widely accepted that both SO_2 and H_2S adsorbs onto Pt forming an intermediate of Pt-S [12,30,31,39]. It is assumed that the available active catalytic sites, after SO_2 is adsorbed, are covered by H_2S; which could also facilitate the electrolysis of water although a higher potential would be needed.

4.3.2 CYCLIC VOLTAMMETRY

From the EIS data it can be concluded that the charge resistance is the significant parameter influencing the cell voltage and overall performance when the SO_2 electrolyser is exposed to H_2S. Generally cyclic voltammetry can be used to evaluate the catalytic activity of a catalyst towards an electrochemical reaction [40,41]. The conventional method for this technique is to use an electrolyte (such as diluted H_2SO_4) which facilitates transport of the oxidised species in a three electrode setup [42]. Although important information can be deduced from this type of experiment, it is difficult to extrapolate to a MEA and electrolyser/fuel cell system. For this reason cyclic voltammetry was performed within the SO_2 electrolyser cell to measure the electrochemical active surface area (ECSA) using the CO stripping method [19,43].

The ECSA is calculated by dividing the charge area, integrated under the CO peak, Q_{CO} (mC cm^{-2}) with the catalyst loading CL_{Pt} (mg cm^{-2}) and 0.420 mC as shown in Equation 4 [18]. The 0.420 mC is included as the amount of charge needed to remove one monolayer of adsorbed CO. Keeping in mind that the use of this value

is based on the assumption that all the CO adsorbed onto the catalyst is linearly bonded while a bridged bonding could also occur [43].

$$\mathrm{ECSA} = \frac{\mathrm{Q_{CO}}}{0.42 \times \mathrm{CL_{Pt}}} \tag{3.4}$$

The charge area in equation 3.4 was integrated from 0.600 to 0.800 V for all measurements. Figure 4.6 shows the CV's for a clean catalyst, i.e. where the anode was exposed to H_2 and the cathode exposed to N_2. By recording CV's in this operating method, the ECSA for a pure catalyst was determined while also showing that all CO species had been removed from the surface after one cycle. In Figure 4.6, the H_2 (solid line) was obtained before CO exposure on the clean catalyst, while *CO_1* (cycle 1) and *CO_2* (cycle 2) was obtained after CO exposure. It should be mentioned that a third CV was performed (*CO_3*) but the data fell exactly on the H_2 baseline making it not clearly visible. The fact that the third CO CV was almost identical to the H_2 "baseline" CV shows that all CO had been removed from the catalyst.

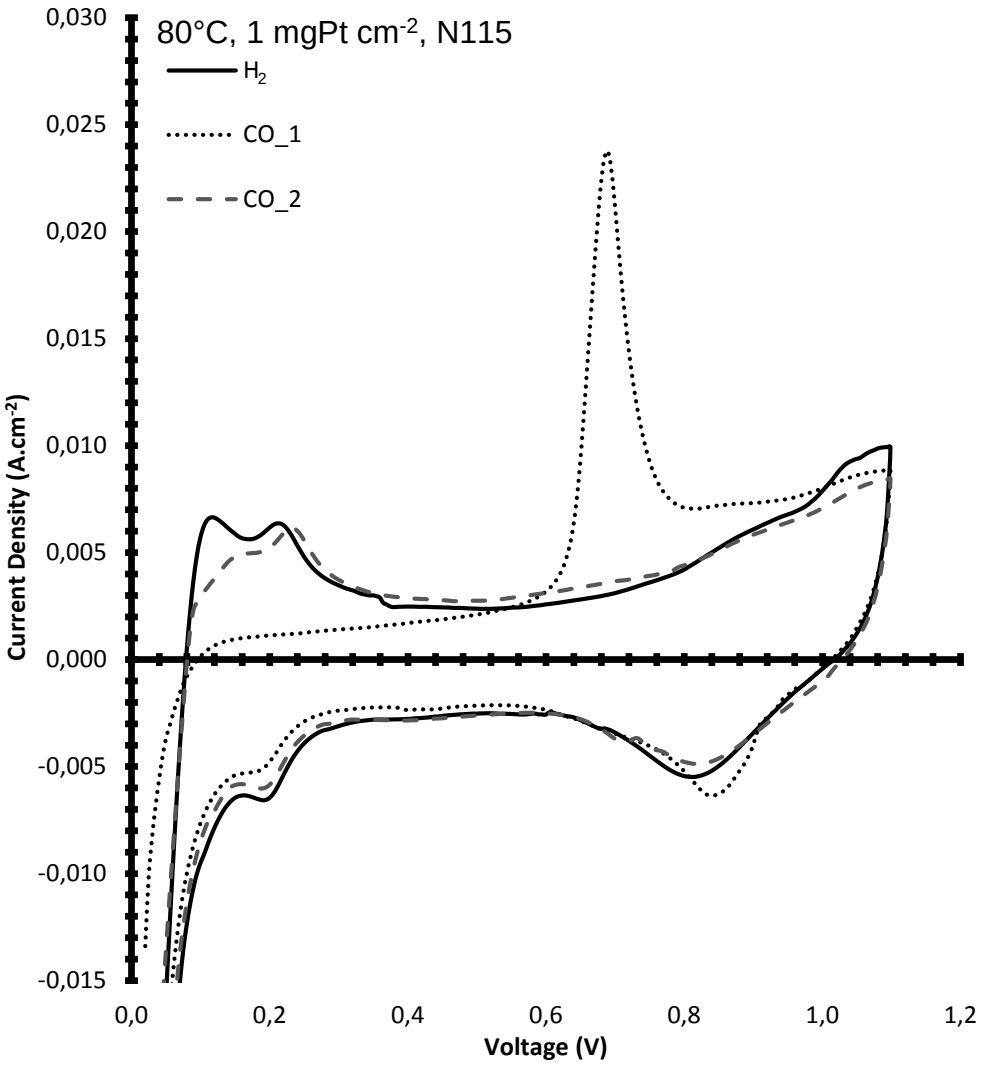

Figure 4.6: CV of CO stripping for a clean catalyst. H_2 baseline generated using N_2 anode and H_2 cathode.

The H_2 adsorption/desorption peaks (0.02 – 0.250 V) are clearly visible on the H_2 CV (Figure 4.6), while they are not visible on the first CO cycle confirming complete coverage of the catalytic active sites with CO [11,18,31]. The hydrogen peak however starts to appear after the first CO cycle changing until it almost reached the identical shape of the H_2 CV. Integration of the first CO peak gave a charge area of 35.08 mC cm^{-2} corresponding to an ECSA of 83.52 cm^2 g^{-1}. This value is almost twice of that obtained for fuel cell applications (40.2 m^2 g^{-1}), although the hydrogen adsorption/desorption peak area was used in the calculation of the ECSA and not the CO stripping method [18].

Figure 4.7 shows the CO CV's obtained after the anode had been exposed to pure SO_2 gas for 3 min at a constant current of 0.1 A.cm^{-2}. The application of the constant current of 0.1 A.cm^{-2} used during the SO_2 exposure was based on the operating method of the electrolyser, i.e. running the SO_2 electrolyser at a constant 0.1 A.cm^{-2} for 20 min to ensure equilibrium of temperature, acid production and water transport to and from the anode [24,26]. The H_2 baseline is also added for comparison of both the H_2 adsorption/desorption peaks (0.02 – 0.250 V) and the CO adsorbed peak (0.600 – 0.800 V).

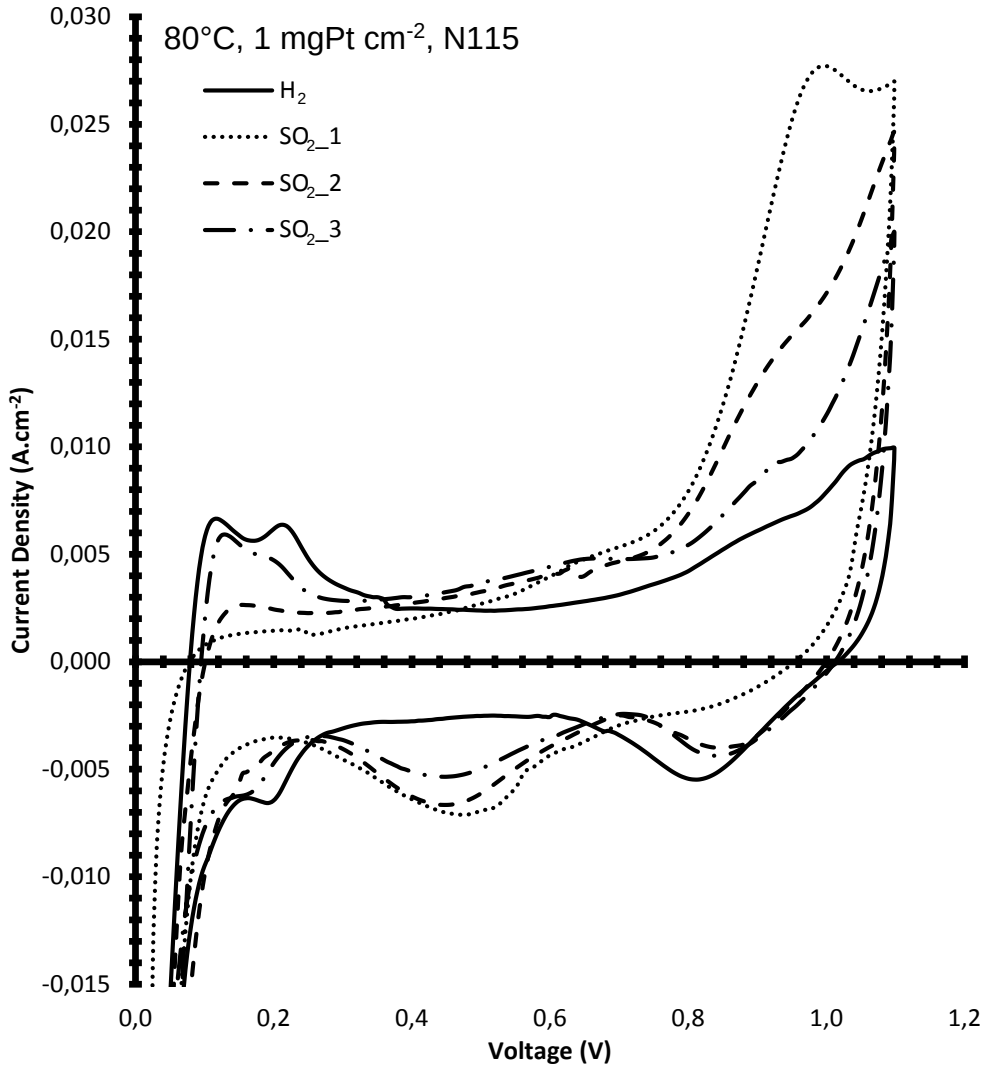

Figure 4.7: CV after SO_2 exposure at 0.1 A cm^{-2} for 3 min.

When comparing the H_2 baseline curve with the first cycle after SO_2 exposure, it is clear that both the H_2 adsorption/desorption and CO peaks disappeared indicating

that all active platinum sites have been covered by the SO_2 [32]. Two further cycles (*SO_2_2 and SO_2_3*) were performed showing the reappearance of the H_2 peaks increasing from *SO_2_2 to SO_2_3*. The increase in the H_2 peaks indicates the removal of sulphur species from the catalyst layer as is further supported by the reduction of the oxide peak present in the broad peak visible in the potential range above 0.700 V [19,31,32] for cycle 2 and 3. Although no clear CO peak was evident, a small charge area of 3.82 mC cm^{-2} was obtained, which corresponds to an ECSA of 9.10 cm^2 g^{-1} and an 89% reduction in active sites available for CO adsorption. It has been previously shown that exposure of a PEM fuel cell platinum cathode to 25 ppm SO_2 results in a reduction in the ECSA from 280 to below 25 cm^2 mg^{-1}, which is a reduction of 91 % of active catalyst sites [31]. The significant reduction in active platinum sites, when exposed to SO_2, is desirable as the maximum amount of active sites should be utilised when running a SO_2 electrolyser.

Figure 4.8 shows the CV curves obtained at different H_2S concentrations using CO stripping. While exposing the anode to the various H_2S concentrations for 3 min in the absence of SO_2 [19], its voltage was kept constant at 0.600 V. The CO curve for the clean catalyst was included as reference. A clear decrease in the CO charge area is visible when H_2S was introduced, irrespective of the H_2S concentrations used. A steady decrease was observed with the exception of 60 ppm H_2S which showed a shift in the onset potential of the CO peak from 0.612 V for the clean catalyst to 0.649 V. Nevertheless, a clean charge area integration was possible and used to compare the different electrochemical surface areas.

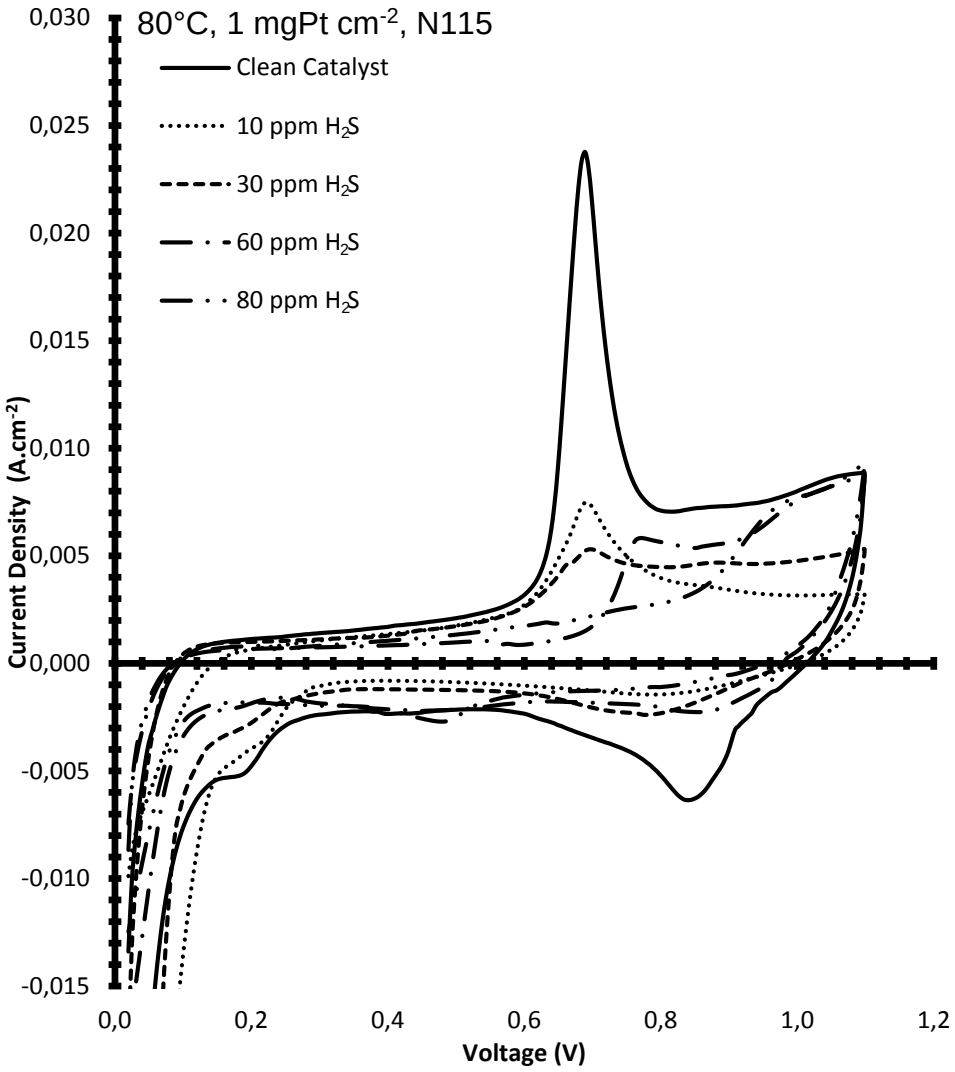

Figure 4.8: CV's as a function of H_2S concentration.

It should be mentioned that Figure 4.8 shows only the first CV after CO adsorption while the second and third curve, for each ppm level tested, showed the H_2 adsorption/desorption peaks and is representative of the H_2 baseline curve shown in both Figure 4.6 and Figure 4.7 indicating a complete removal of H_2S from the catalyst. Levels as low as 8 ppm H_2S have been shown to reduce the available platinum surface by 94% over a period of 1.78 h for PEM fuel cells [17].

Figure 4.9 shows a summary of all the electrochemical surface areas obtained from the CO stripping procedure. It is clear that exposure to the pure SO_2 resulted in the highest ECSA loss of 89% while a decrease is observed with increasing H_2S exposure levels. A decrease in ECSA from 52 to 12.56 $cm^2\ g^{-1}$ was observed when

increasing the H_2S concentration from 10 to 80 ppm which corresponds to a decrease of 85% in active catalyst sites for 80 ppm H_2S.

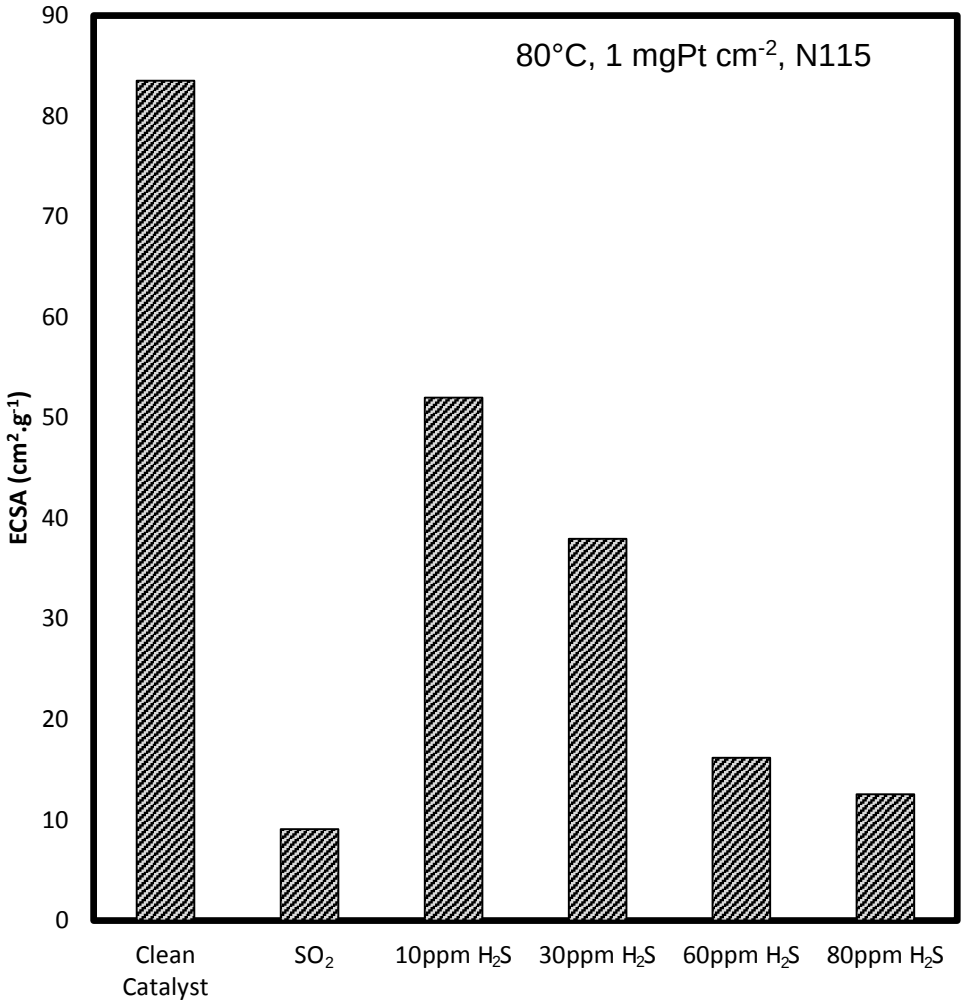

Figure 4.9: ECSA values determined by CO stripping for a clean catalyst and after SO_2, 10 ppm H_2S, 30 ppm H_2S, 60 ppm H_2S and 80 ppm H_2S exposure.

When considering that the exposure of the SO_2 electrolyser anode to 80 ppm H_2S has resulted in a reduction of active catalyst sites by 85%, the current transient performance in Figure 4.3 is actually surprising. From literature it has been shown that platinum supported on carbon catalyst exposed to low levels of H_2S (5 – 30 ppm) for PEM fuel cell application is deactivated to a greater extent than has been observed in this study [11,12,17,19]. For other systems like PEM fuel cells the catalyst activity could be recovered to 97.5% of the initial operation, it is interesting that such a significant decrease in operation was not observed in Figure 4.3. One explanation could be related to the 20 min conditioning step done prior to each

concentration in which the anode was exposed to SO_2 (see Experimental) at a constant current of 0.1 A cm^{-2} for the cell to reach a steady state of operation. This step ensured that the catalyst was properly covered (89% as shown in Figure 4.7 and Figure 4.9) by S species originating from the SO_2 i.e. only 11% was essentially available for H_2S to adsorb.

4.4 CONCLUSION

The effect of various H_2S concentrations on the performance of the SO_2 electrolyser used for H_2 and H_2SO_4 production was investigated. Transient data revealed a reduced performance when H_2S levels were increased from 10 to 80 ppm. The performance loss was less than the performance loss observed in PEM fuel cell operation in the presence of H_2S/SO_2 contamination. Polarisation curves showed that the reduced performance was not affected by the operating current density. The use of electrochemical impedance spectroscopy revealed that the charge resistance was most influenced when compared to the membrane resistance and mass transport limitations. The catalyst activity was further investigated by using cyclic voltammetry and CO stripping to determine the electrochemical surface area of the catalyst as a function of pure SO_2, 10 – 80 ppm H_2S exposures. This technique revealed that the SO_2 conditioning step, used in the determination of the transient, resulted in an almost complete coverage of the catalyst active sites which impaired the deactivation effect of the H_2S. It was also shown that when only H_2S was used in the exposure step in the absence of SO_2, the ECSA was reduced significantly with 80 ppm H_2S resulting in a catalyst coverage of 89%.

4.5 REFRENCES

[1] Brecher LE, Spewock S, Warde CJ. The Westinghouse Sulfur Cycle for the thermochemical decomposition of water. Int J Hydrogen Energy 1977;2:7–15. doi:http://dx.doi.org/10.1016/0360-3199(77)90061-1.

[2] Gorensek MB, Summers WA. Hybrid Sulfur flowsheets using PEM electrolysis and a bayonet decomposition reactor. Int J Hydrogen Energy 2008;34:1–18.

[3] Gorensek MB. Hybrid Sulfur cycle flowsheets for hydrogen production using high-temperature gas-cooled reactors. Int J Hydrogen Energy 2011;36:12725–41.

[4] Kriek RJ, Ravenswaay JP van, Potgieter M, Calitz A, Lates V, Bjorketun ME, et al. SO_2 - an indirect source of energy. J South African Inst Min Metall 2013;113:593–604.

[5] Liu Y, Bisson TM, Yang H, Xu Z. Recent developments in novel sorbents for flue gas clean up. Fuel Process Technol 2010;91:1175–97.

[6] Un UT, Koparal AS, Ogutveren UB. Electrochemical Desulfurization of Waste Gases in a Batch Reactor. J Environ Eng 2007;133:13–9.

[7] Un UT, Koparal AS, Ogutveren UB. Sulfur dioxide removal from flue gases by electrochemical absorption. Sep Purif Technol 2007;53:57–63.

[8] Zhang L, Jie X, Shao Z-G, Wang X, Yi B. The dynamic-state effects of sodium ion contamination on the solid polymer electrolyte water electrolysis. J Power Sources 2013;241:341–8. doi:10.1016/j.jpowsour.2013.04.049.

[9] Carmo M, Fritz DL, Mergel JJ, Stolten D. A Comprehensive review on PEM electrolysis. Int J Hydrogen Energy 2013;38:4901–34. doi:10.1016/j.ijhydene.2013.01.151.

[10] Cheng X, Shi Z, Glass N, Zhang L, Zhang J, Song D, et al. A review of PEM hydrogen fuel cell contamination: Impacts, mechanisms, and mitigation. J Power Sources 2007;165:739–56.

[11] SHI W, YI B, HOU M, SHAO Z. The effect of H_2S and CO mixtures on PEMFC performance. Int J Hydrogen Energy 2007;32:4412–7. doi:10.1016/j.ijhydene.2007.06.029.

[12] Mohtadi R, Lee W-K, Van Zee JW. The effect of temperature on the adsorption rate of hydrogen sulfide on Pt anodes in a PEMFC. Appl Catal B Environ 2005;56:37–42. doi:10.1016/j.apcatb.2004.08.012.

[13] Jayaraj P, Karthika P, Rajalakshmi N, Dhathathreyan KS. Mitigation studies of sulfur contaminated electrodes for PEMFC. Int J Hydrogen Energy 2014;39:12045–51. doi:10.1016/j.ijhydene.2014.06.011.

[14] Postole G, Auroux A. The poisoning level of Pt/C catalysts used in PEM fuel cells by the hydrogen feed gas impurities: The bonding strength. Int J Hydrogen Energy 2011;36:6817–25. doi:10.1016/j.ijhydene.2011.03.018.

[15] Kakati BK, Kucernak ARJ. Gas phase recovery of hydrogen sulfide contaminated polymer electrolyte membrane fuel cells. J Power Sources 2014;252:317–26. doi:10.1016/j.jpowsour.2013.11.077.

[16] Clark P., Dowling N., Huang M, Okemona O, Butlin G., Hou R, et al. Studies on sulfate formation during the conversion of H_2S and SO_2 to sulfur over activated alumina. Appl Catal A Gen 2002;235:61–9. doi:10.1016/S0926-860X(02)00235-1.

[17] Lopes T, Paganin VA, Gonzalez ER. The effects of hydrogen sulfide on the polymer electrolyte membrane fuel cell anode catalyst: H_2S-Pt/C interaction products. J Power Sources2 2011;196:6256–63. doi:10.1016/j.jpowsour.2011.04.017.

[18] Shi W, Yi B, Hou M, Jing F, Ming P. Hydrogen sulfide poisoning and recovery of PEMFC Pt-anodes. J Power Sources 2007;165:814–8. doi:10.1016/j.jpowsour.2006.12.052.

[19] Sethuraman V a., Weidner JW. Analysis of sulfur poisoning on a PEM fuel cell electrode. Electrochim Acta 2010;55:5683–94. doi:10.1016/j.electacta.2010.05.004.

[20] Frins E, Bobrowski N, Osorio M, Casaballe N, Belsterli G, Wagner T, et al. Scanning and mobile multi-axis DOAS measurements of SO_2 and NO_2 emissions from an electric power plant in Montevideo, Uruguay. Atmos Environ 2014;98:347–56. doi:10.1016/j.atmosenv.2014.03.069.

[21] Lupiáñez C, Guedea I, Bolea I, Díez LI, Romeo LM. Experimental study of SO_2 and NO_x emissions in fluidized bed oxy-fuel combustion. Fuel Process Technol 2013;106:587–94. doi:10.1016/j.fuproc.2012.09.030.

[22] Mandi RP, Yaragatti UR. Control of CO_2 emission through enhancing energy efficiency of auxiliary power equipment in thermal power plant. Int J Electr Power Energy Syst 2014;62:744–52. doi:10.1016/j.ijepes.2014.05.039.

[23] Schoeman H, Krieg HM, Kruger AJ, Chromik A, Krajinovic K, Kerres J. H2SO4 stability of PBI-blend membranes for SO_2 electrolysis. Int J Hydrogen Energy 2012;37:603–14.

[24] Peach R, Krieg HM, Krüger AJ, van der Westhuizen D, Bessarabov D, Kerres J. Comparison of ionically and ionical-covalently cross-linked polyaromatic membranes for SO_2 electrolysis. Int J Hydrogen Energy 2014;39:28–40.

[25] Sivasubramanian P, Ramasamy RP, Freire FJ, Holland CE, Weidner JW. Electrochemical hydrogen production from thermochemical cycles using proton exchange membrane electrolyzer. Int J Hydrogen Energy 2007;32:463–8.

[26] Krüger AJ, Krieg HM, van der Merwe J, Bessarabov D. Evaluation of MEA manufacturing parameters using EIS for SO_2 electrolysis. Int J Hydrogen Energy 2014;39:18173–81. doi:10.1016/j.ijhydene.2014.09.012.

[27] Modestov AD, Tarasevich MR, Filimonov VY, Zagudaeva NM. Degradation of high temperature MEA with PBI-H_3PO_4 membrane in a life test. Electrochim Acta 2009;54:7121–7. doi:http://dx.doi.org/10.1016/j.electacta.2009.07.031.

[28] Sethuraman VA, Lakshmanan B, Weidner JW. Quantifying desorption and rearrangement rates of carbon monoxide on a PEM fuel cell electrode. Electrochim Acta 2009;54:5492–9. doi:10.1016/j.electacta.2009.04.049.

[29] Rockward T, Urdampilleta IG, Uribe FA, Brosha EL, Pivovar BS, Garzon FH. The effects of multiple contaminants on polymer electrolyte fuel cells. ECS Trans 2007;11:821–9.

[30] Sethuraman VA, Weidner JW. Analysis of sulfur poisoning on a PEM fuel cell electrode. Electrochim Acta 2010;55:5683–94. doi:10.1016/j.electacta.2010.05.004.

[31] Jie Fu Chao Du, Zhigang Shao, Baolian Yi MH. Potential dependance of sulfur dioxide poisoning and oxidation at the cathode of proton exchange membrane fuel cells. J Power Sources 2009;187:32–8.

[32] Zhai Y, Bender G, Bethune K, Rocheleau R. Influence of cell temperature on sulfur dioxide contamination in proton exchange membrane fuel cells. J Power Sources2 2014;247:40–8.

[33] St-Pierre J, Zhai Y, Angelo M. Quantitative ranking criteria for PEMFC contaminants. Int J Hydrogen Energy 2012;37:6784–9. doi:10.1016/j.ijhydene.2012.01.029.

[34] Yuan X-Z, Li H, Zhang S, Martin J, Wang H. A review of polymer electrolyte membrane fuel cell durability test protocols. J Power Sources 2011;196:9107–16. doi:http://dx.doi.org/10.1016/j.jpowsour.2011.07.082.

[35] Barber J, Morin S, Conway BE. Specificity of the kinetics of H_2 evolution to the structure of single-crystal Pt surfaces, and the relation between opd and upd H. J Electroanal Chem 1998;446:125–38. doi:10.1016/S0022-0728(97)00652-9.

[36] Conway BE, Pierozynski B. A.c. impedance behaviour of processes involving adsorption and reactivity of guanidonium-type cations at Pt(100) surface. J Electroanal Chem 2008;622:10–4. doi:10.1016/j.jelechem.2008.04.025.

[37] Jaouen F, Lindbergh G, Sundholm G. Investigation of Mass-Transport Limitations in the Solid Polymer Fuel Cell Cathode. J Electrochem Soc 2002;149:A437–47.

[38] Ihonen J, Jaouen F, Lindbergh G, Lundblad A, Sundholm G. Investigation of Mass-Transport Limitations in the Solid Polymer Fuel Cell Cathode. J Electrochem Soc 2002;149:A448. doi:10.1149/1.1456917.

[39] Baturina O a., Gould BD, Northrup P a., Swider-Lyons KE. SO_2 adsorption products on Pt nanoparticles as a function of electrode potential and oxidative properties of carrier gas: In situ sulfur K-edge XANES approach. Catal Today 2013;205:106–10. doi:10.1016/j.cattod.2012.08.024.

[40] O'Brien JA, Hinkley JT, Donne SW, Lindquist SE. The electrochemical oxidation of aqueous sulfur dioxide: A critical review of work with respect to the hybrid sulfur cycle. Electrochim Acta 2010;55:573–91. doi:http://dx.doi.org/10.1016/j.electacta.2009.09.067.

[41] Quijada C. Electrochemical behaviour of aqueous SO_2 at polycrystalline gold electrodes in acidic media. A voltammetric and in-situ vibrational study. Part II. Oxidation of SO_2 on bare and sulphur-modified electrodes. Electrochim Acta 2001;46:651–9. doi:10.1016/S0013-4686(00)00642-3.

[42] Hector R. Colon-Mercado DTH. Catalyst evaluation for sulfur dioxide-depolarized electrolyzer. Electrochem Commun 2007;9:2649–53.

[43] Vidaković T, Christov M, Sundmacher K. The use of CO stripping for in situ fuel cell catalyst characterization. Electrochim Acta 2007;52:5606–13. doi:10.1016/j.electacta.2006.12.057.

[44] Krüger AJ, Krieg HM, Bessarabov D. Effect of H2S on SO_2-depolarised water electrolysis. Int J Hydrogen Energy 2015;40:4442–50. doi:10.1016/j.ijhydene.2015.02.036.

CHAPTER 5: CHARACTERISATION OF A POLYAROMATIC PBI BLEND MEMBRANE FOR SO_2 ELECTROLYSIS*

Chapter Overview

The application of a polyaromatic acid-base blend membrane from partially fluorinated and sulfonated aromatic polyether and the polybenzimidazole F_6PBI has been investigated for hydrogen production using SO_2 electrolysis. Several membrane electrode assembly (MEA) pre-doping strategies have been investigated using polarisation curves. Membrane thickness variation, voltage cycling and long term operation at constant current (0.1 A cm^{-2}) was also performed. Scanning electron microscopy (SEM) and TGA-MS was used to evaluate MEA stability before and after long term operation. It was found that doping the MEA after hot pressing performs the best reaching a current density of 0.3 A cm^{-2}. The performance could also be improved by cycling the voltage 16 times to reach 0.33 A cm^{-2}. Long term operation showed stable voltage at 0.1 A cm^{-2} staying below 0.8 V. SEM images showed that no significant sulfur deposition was present while TGA-MA analysis confirmed some degradation after the 140 h of operation.

*Kruger AJ, Cichon P, Kerres J, Bessarabov D, Krieg HM. Characterisation of a polaromatic PBI blend embrane for SO_2 electrolysis. Int J Hydrogen Energy 2015:1–12. doi:http://dx.doi.org/10.1016/j.ijhydene.2014.12.081.

5.1 INTRODUCTION

Hydrogen gas can be viewed as one of the energy carriers of the future especially when used in alternative power systems such as fuel cells. With the fuel cell market on the brink of commercialisation for the automotive industry the demand for hydrogen is expected to increase rapidly [1] resulting in an increased need for alternative methods for the production of low cost hydrogen. The Hybrid Sulfur (HyS) cycle has been proposed as one such possible alternative for the high volume production of hydrogen [2]. This three-step cycle entails the decomposition of sulphuric acid to water, oxygen and sulphur dioxide. After oxygen separation, the sulphur dioxide and water is subsequently electrochemically converted to both hydrogen and sulphuric acid [2,3]. For this step, an electrolyser system is used containing a proton exchange membrane (PEM) coated with a catalyst on both sides of the membrane serving as the anode and the cathode. The produced H_2SO_4 from the electrolyser is fed back to the initial decomposition step completing the cycle. For the HyS cycle to be competitive Gorensek *et al* [4] determined that the electrolyser step should be operated at 0.6 V and 0.5 A cm^{-2} while producing at least a 65 wt% H_2SO_4 product concentration. Similar to fuel cell applications, Nafion® membranes have been initially proposed and tested for the SO_2 electrolyser [5]. The sluggish reaction kinetics of the SO_2 oxidation however requires that higher operating temperatures are needed which is not ideal for Nafion® membranes where water is required for proton transport. The ability of for example polybenzimidiazole (PBI) based membranes to conduct protons when doped with an acid electrolyte is beneficial and could be favoured due to the produced acid in the electrolyser [6].

Previous studies have shown the suitability of these PBI based membranes for this process showing increased performance when compared to the Nafion® based membranes [6–8]. Schoeman *et al.* [6] for example demonstrated the suitability of membranes made from non- and partially fluorinated sulfonated arylene main-chain polymers blended with PBIOO. More recently, both the acid stability and electrolyser suitability of ionically and ionical-covalently cross-linked PBI based membranes was demonstrated with improved cell voltages in the lower current density region [7]. It was shown by Peach *et al.* [7] that of the three cross-linked membranes tested, the MJK 1753 membrane performed better than the MJK 1758 and MJK 1761

membrane. This MJK1753 membrane consists of a blend containing a basic polymer (F_6-PBI – the macromolecular cross-linker), an acidic polymer (sulfonated polymer from decafluorobiphenyl and bisphenol AF) and a crosslinking agent (bisphenol A-di-epoxide). The synthesis procedure for this blend has been described previously [7]. Since the efficiency of the PBI based membranes are highly sensitive to pre-treatment methods due to the influence of the acid content of the membrane on the proton conductivity [9,10], it would be important not only to evaluate the performance of the membrane but also determine the influence of the pre-treatment on the performance of the membrane.

This chapter will report on the optimisation of the MEA doping procedure using the hot pressing procedure determined by comparing polarisation curves. The effect of membrane thickness was also tested while the acid concentration and area specific resistance was used for characterisation. A long term (140 h) constant current procedure was also performed and the MEA characterised (before and after operation) using SEM and TGA-MS.

5.2 EXPERIMENTAL

5.2.1 MEMBRANE SYNTHESIS

The polyaromatic blend membrane used in this study was prepared as previously described [7,11] by preparing solutions of 10 wt% SFS001 and 2 wt% F_6PBI in DMSO (for structure of the blend components see Table 5.1). After neutralising the SFS001 with n-propylamine (if the SFS001 solution would be mixed in the SO_3H form from the PBI, a polyelectrolyte complex would be formed immediately) the F_6PBI was added. The crosslinking agent was then added to the mixture and stirred until a homogeneous solution was made. The solvents were then evaporated by casting the solution onto a glass plate and placing it in a vacuum oven (20 – 200 mbar) at 130°C for 2 h and 150°C for 1h. Post treatment of the membrane were done according to [6]. The acid polymer, base polymer and cross linker used is shown in Table 5.1.

Table 5.1: Chemical structure of the acid, base polymer and cross linker used in the synthesis of the MJK 1753 polyaromatic blend membrane.

Description	Chemical Structure
Acid polymer (3 gram)	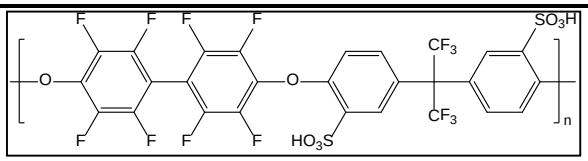
Basic Polymer (0.398 gram)	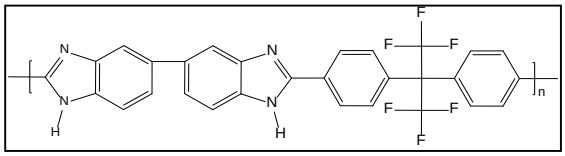
Cross-linker (0.12 gram)	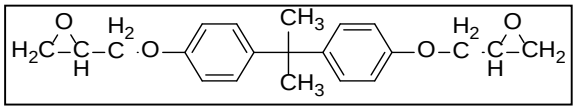

5.2.2 MEA MANUFACTURING

Since PBI based membranes use acid for proton conduction, doping is required. The question arose whether and how the MEA manufacturing process and specifically the hot-pressing (as this might result in the loss of the doped acid) influences the doping of the membrane.

After membrane synthesis, membrane samples were pre-treated using basically a four step process: i) washing the membrane with water at 80°C for 24 h, ii) drying at 80°C for 12 h, iii) hot pressing of the GDE onto the membrane and iv) acid doping in 1 M H_2SO_4 at 80°C for 24 h. During hot-pressing two GDE's (Fuel Cells Etc, USA) with a catalyst loading of 1 mgPt.cm^{-2} were pressed on either side of the membranes at 120°C for 5 min using a pressure of 125 kg cm^{-2}. Of these four steps, the MEA manufacturing and the doping not only have the most important influence on the overall efficiency of the electrolyser, but also on each other as the hot pressing could result in the loss of doped acid.

Hence, to determine the interaction of these two parameters, the following combinations of washing, doping and hot pressing were investigated:

i) H_2SO_4 /Hot pressing (Acid/MEA)
   Doping the membrane in 1 M H_2SO_4 at 80°C for 24 h before the hot-pressing step.

ii) H_2O/Hot pressing(H_2O/MEA)
   Washing the membrane sample in DI water at 80°C for 24 h before the hot-pressing step (no doping).

iii) H_2O/Hot pressing/H_2SO_4(H_2O/MEA/Acid)
   Washing with H_2O as in ii) before hot pressing followed by doping the MEA in 1 M H_2SO_4 at 80°C for 24 hrs.

iv) Air/Hot pressing (Air/MEA)
   Heating the membrane to 80°C using a hot-air oven for 24 h before the hot pressing step (no-doping).

5.2.3 SO_2 ELECTROLYSIS

The electrolysis system that was used for the evaluation of the various pre-treated PBI based membranes was based on the setup described previously [6,7]. In view of the varying pre-treatments of the membranes, all MEA's were heated in the electrolysis cell for 1 h at 80°C with no supply of reactant. Subsequently the anode and cathode were supplied with 150 mL min^{-1} SO_2 gas and 45 mL min^{-1} DI water respectively. A constant current of 0.1 A cm^{-2} was then applied for 20 min after which a polarisation curve was obtained by incrementally increasing the current while recording the voltage. This step is based on previous work for PFSA-based membranes. Both area specific resistance (ASR, Ω cm^2) and acid concentration produced were recorded for all MEA doping variations.

The MEA's performances, based on the polarisation curves, were used to select the best MEA doping procedure. With the best doping procedure identified, the influence of the membrane thickness (20, 80 & 90 µm) was evaluated. Although literature does supply specific break-in procedures for PBI based fuel cells, this information is not available for electrolysis, especially for the SDE.

Cyclic voltammetry was applied to the MEA's, using 16 cycles and a cycle range of 0 – 1 V using a 50 mV s^{-1} ramp rate, to determine the stability of the MEA's (membrane and catalyst) [12].

To determine the stability of the membrane during SO_2 electrolysis, a long term operation of the SO_2 electrolyser was done for 140 h at a current density of 0.1 A cm^{-2} and 80°C while the voltage was recorded every 5 min. For this procedure a 35 µm thick membrane was used. The MEA from the long term operation test was characterised using SEM, FTIR and TGA-MS. A FEI Quanta 250 FEG scanning electron microscope was used to evaluate the MEA structure before and after the long term operation. The ATR-FTIR spectra was obtained using a Bruker Alpha-P spectrometer with a resolution of 4 cm^{-2}, while a TGA system coupled with MS [7] (TA Instruments, SDT model Q60 with mks Cirrus Mass Spectrometer) was used to measure both the weight loss and mass fractions coming of at specific temperatures. The data obtained from the MS system was further analysed by assuming that all signals lower than 2 mbar can be neglected. Moreover, TGA-FTIR coupling investigation was done for the 1753 membrane and its polymer components SFS001 and F_6PBI to elucidate their thermal degradation characteristics as a supplement to the TGA-MS coupling experiments. The used TGA was a Netzsch machine (STA449C) which was coupled with a Nicolet Nexus FTIR (Vectra interferometer) vie a heated transfer line. The TGA was operated under 65 – 70% O_2 atmosphere, and the heating speed was 20 K min^{-1}. For correlation of the TGA and FTIR running time and temperature, CO_2 gas injection for marking of the FTIR spectra was used.

5.3 RESULTS AND DISCUSSION

5.3.1 EFFECT OF MEA PRE-TREATMENT

When PBI based materials are used in fuel cells, the MEA treatment procedures, i.e. the order as well as the method of the doping and the MEA manufacture, needs to be considered as the amount of acid within these membrane types (proton carrier) is important for the proton transfer and hence the overall membrane resistance [13,14]. To our knowledge this step has however not been investigated thus far when using PBI based membranes for SO_2 electrolysis. It is assumed, for this study, that the acid produced through the reaction keeps the membrane doped to an acceptable

level. To investigate the effect of the type of doping and the order of doping vs MEA manufacture four different pre-treatments were chosen as described above. After pre-treatment all four membranes were run in the SO_2 electrolysis cell under identical conditions. In Figure 5.1 the polarisation curve of the membranes with the 4 MEA different doping procedures are presented.

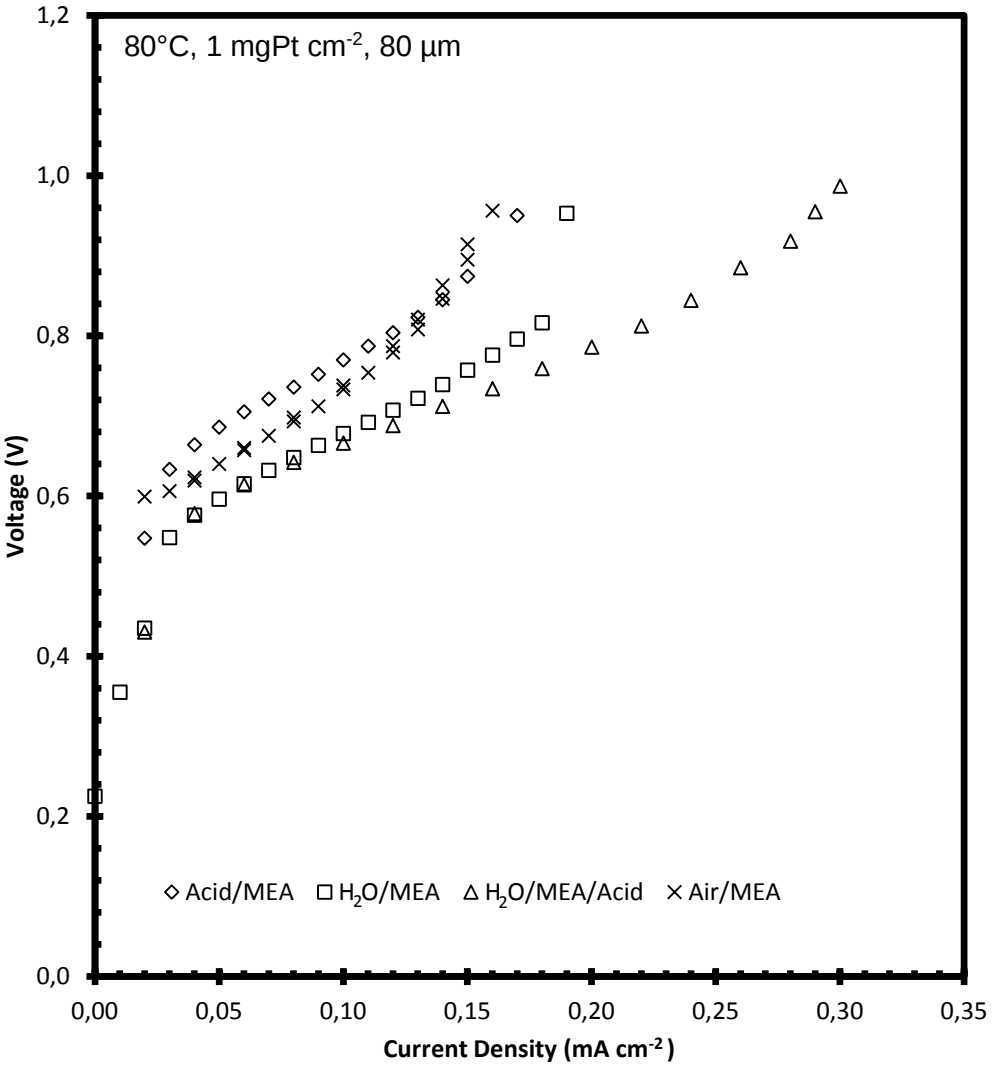

Figure 5.1: Voltage response curves for SO_2 electrolysis as a function of current density for various MEA doping techniques.

It is clear that the SO_2 efficiency is influenced significantly by the MEA doping procedure. The method of acid doping the MEA after hot-pressing (H_2O/MEA/Acid) showed the best performance reaching 0.3 A cm^{-2} compared to the 0.19 A cm^{-2} for the non-doped H_2O/MEA procedure. It is interesting to note that the non-doped MEA

that bad been only treated with air (Air/MEA), i.e. heated to 80°C for 24 h, performed slightly better at current densities below 0.14 A cm^{-2} than the Acid/MEA combination. This could be due to two reasons. Firstly, the acid (Acid/MEA) could have been pressed from the membrane during the hot-pressing step resulting in a low acid content within the MEA. Secondly, the relatively high temperature (120°C) in combination with the applied pressure (125 kg cm^{-2}) of the hot-pressing in the presence of acid could have damaged the polymer structure resulting in the observed lower performance. When comparing H_2O/MEA and H_2O/MEA/Acid, it is clear that although the H_2O/MEA treated membrane attained similar voltages than the H_2O/MEA/Acid at low current densities, the performance of the H_2O/MEA/Acid improved significantly at higher current densities. This is understandable as the water present in the non-acid doped membrane (H_2O/MEA) must first be replaced during the SO_2 electrolysis by the produced acid. Although electrolysis could be performed with only water in the membrane, H_2SO_4 is preferred when higher temperatures are to be used in the future. It is clear that the performance is a function of the water/acid ratios within the membrane. It appears that a low acid concentration should be present within the membrane as can be seen in the low current density region. Higher acid concentration within the membrane (high current density) shows a significant decrease in performance and can be attributed to a lower conductivity for more concentrated acid. It is well-known that the concentration of the acid used and the time period of membrane doping determines the acid doping level of the membrane. In this study the membrane was assumed to have been doped with the acid produced in the 20 min break-in period at 0.1 A cm^{-2}. Although it is not clear if the 20 min was sufficient for the break-in of the H_2O/MEA treated membrane, it was observed that the voltage dropped continuously over the 20 min time frame. However, to facilitate the comparison of the differently pre-treated membranes, the 20 min break-in period was kept constant for all pre-treated membranes. Generally, the results show that acid doping after hot-pressing does improve the performance most specifically at higher current densities.

During the SO_2 electrolysis, the acid concentration produced at the anode was recorded for each doping method. Table 5.2 summarises the acid concentration produced for each MEA doping method as a function of current density. The blank spaces are indicative of MEA's that could not reach adequate current densities for acid production.

Table 5.2: Acid concentration produced as a function of the MEA doping methods at different current densities.

Current Density ($A\ cm^{-2}$)	Acid/MEA	H_2O/MEA	H_2O/MEA/Acid	Air/MEA
		$[H_2SO_4]$ ($mol\ L^{-1}$)		
0.10	6.56	6.56	6.25	6.88
0.15	7.17	7.81	7.50	7.19
0.25	-	-	8.44	-
0.28	-	-	8.13	-

The acid concentrations produced for all the MEA doping procedures were similar at the various current densities. Apart from the applied current density, the acid concentration produced in the SO_2 electrolyser is mainly dependent on the water transport properties of the membrane and the membrane thickness [15- 17]. Since all membranes had similar initial thicknesses, it can be assumed that the doping procedures had little to no influence on the membrane thickness, which has been confirmed in a previous study on the stability of these membrane types in H_2SO_4 [7].

It is well known that the membrane resistance is one of the main contributors to the total cell resistance [18] of which the anode and cathode resistance make up the other two contributing resistances. To evaluate the membrane resistance a high frequency AC milliohm meter (HP, 4328A) was used. Table 5.3 shows a summary of the area specific resistance ($\Omega\ cm^2$) obtained with the MEA's manufactured by the various doping procedures as a function of the operating current density. The empty spaces again indicate that the MEA's could not achieve the current density.

Table 5.3: Area specific resistance as a function of the current density for the 4 different pre-treated membranes.

Current Density ($A\ cm^{-2}$)	Acid/MEA	H_2O/MEA	H_2O/MEA/Acid	Air/MEA
	Area specific resistance ($\Omega\ cm^2$)			
OCV	0.40	0.30	0.25	0.40
0.10	0.28	0.24	0.18	0.40
0.13	0.28	0.22	0.18	0.32
0.15	0.28	0.22	0.19	-
0.17	0.28	0.22	0.18	-
0.22	-	0.22	0.20	-
0.28	-	-	0.20	-
0.30	-	-	0.22	-

The membrane resistance was also recorded at OCV (open circuit voltage – when no current is applied), which is an indication of the natural voltage of the system, i.e. maximum resistance of the cell. It is clear that the area specific resistance is a function of the doping method used and is dependent on the acid doping level and hence the conductivity of the membrane. It can be assumed (see discussion of Figure 5.1) that no acid was present in the Acid/MEA and Air/MEA, prior to the application of current and thus under OCV conditions, resulting in a higher resistance than what had been observed for the H_2O/MEA and H_2O/MEA/Acid doping methods. The relationship between the OCV and the acid level within the membrane is visible when a current is applied (membrane being doped with acid produced) showing a decrease in the area specific resistance (ASR). It was shown that the ASR is a function of the current density (acid concentration produced) i.e. increasing with current density for PFSA-based membranes [18]. This is however not clearly visible in the current density range that was tested in this study. This effect is best seen for the H_2O/MEA/Acid doping method. The stable ASR values observed for the other doping methods could indicate that the membranes are still being doped by the acid produced.

Since the H_2O/MEA/Acid pre-treatment method resulted in the best results, it was used for the experimental work shown further.

5.3.2 EFFECT OF MEMBRANE THICKNESS

It is known that membrane thickness directly influences the performance of both fuel cells and electrolysers [19,20] mainly due to its influence on the ohmic resistance of the system. To determine this effect of the PBI blend membranes on SO_2 electrolysis, 20, 80 µm and 90 µm thick membranes were evaluated that had been pre-treated using the H_2O/MEA/Acid procedure containing 1 mgPt cm^{-2}. In Figure 5.2 the effect of the membrane thickness on the performance of the SO_2 electrolysis is shown. In a previous study it was shown that reducing the membrane thickness resulted in an increased electrolysis efficiency [16]. Although in that case a pressure was applied on the cathode side to increase the water flux to the anode and reduce the SO_2 transport to the cathode. From the data shown in Figure 5.2 it can be seen that the 80 µm thickness showed the best results reaching a current density of 0.3 A cm^{-2} followed by the 90 µm, reaching 0.22 A cm^{-2}. The 20 µm membrane showed the worst performance reaching only 0.12 A cm^{-2}. The performance of all the membrane thicknesses tested showed comparable performance at low current density (low acid concentration produced) while the difference in performance increased significantly with increasing current density. The poor performance of the 20 µm membrane can be attributed to a high SO_2 crossover [21,22], [23] from the anode to the cathode which could increase the catalyst resistance and thus decrease the overall performance of the MEA. The poorer performance of the 90 µm compared to the 80 µm membrane could be explained as follows. The cell voltage is, amongst others, a function of the acid produced at the anode, which in turn is a function of the water transport from the cathode. Due to the thicker path length less water is present at the anode for the electrolytic reaction when using the 90 µm membrane contributing to the lower performance compared with the 80 µm membrane.

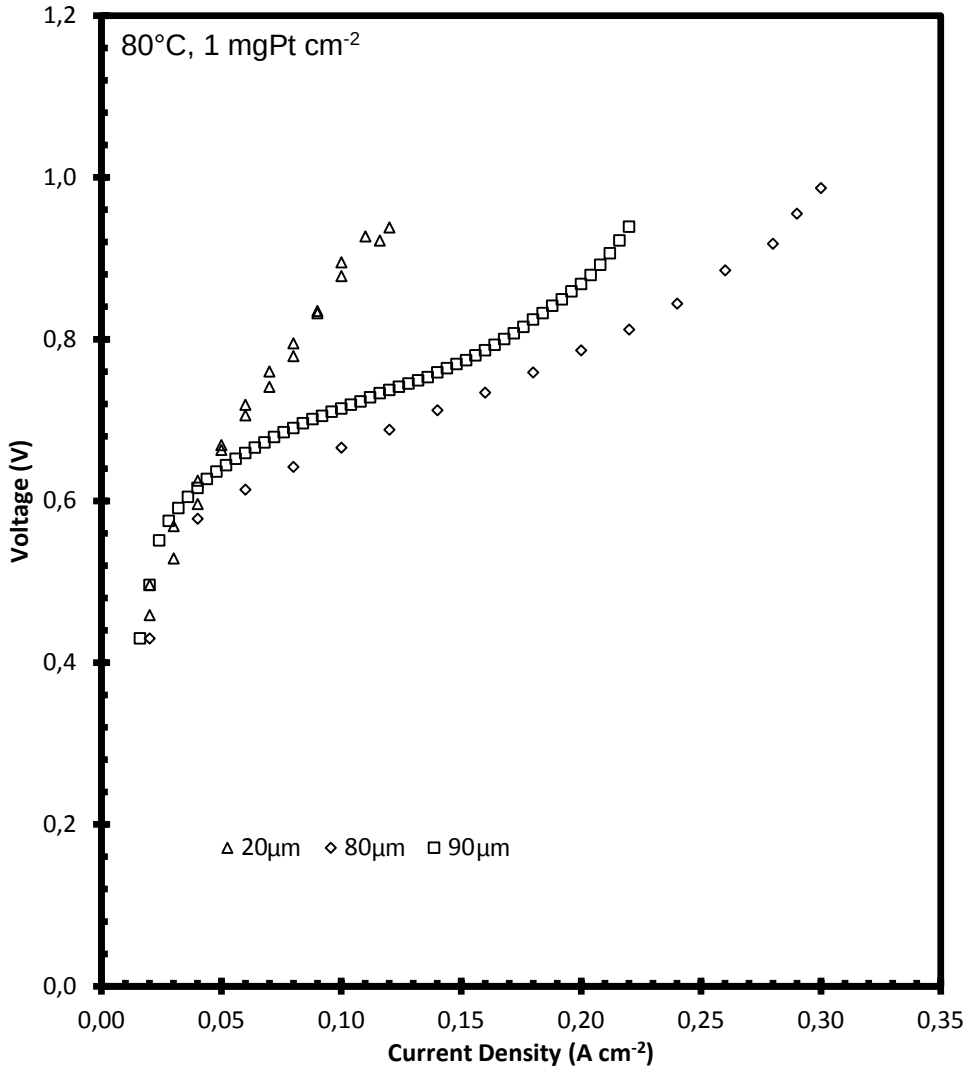

Figure 5.2: Effect of membrane thickness on the SO_2 electrolyser performance.

In view of the influence of membrane thickness on water transport, it is expected that the membrane thickness will also influence the acid concentration. Table 5.4 shows the acid concentration as a function of the membrane thicknesses tested in this study at various current densities. It is clear that the thinnest membrane produced the most dilute acid due to the highest H_2O crossover, while the thickest membrane produced the highest acid concentration. It is however interesting to note that the acid concentration for the 90 µm membrane only increased 0.25 mol L^{-1} when the current density is doubled from 0.1 to 0.2 A cm^{-2}.

Table 5.4 Acid concentrations produced as a function of membrane thickness.

Current Density (A cm^{-2})	20 µm	80 µm	90 µm
	Acid Concentration (mol L^{-1})		
0.1	5.625	6.25	6.31
0.2	-	6.35	6.56
0.28	-	8.44	-

The highest acid concentration achieved was 8.44 mol L^{-1} correlating to about 57 wt% H_2SO_4, which is still below the recommended 65 wt% H_2SO_4 for the HyS cycle. However, it is an improvement over the data published for a PFSA-based membrane (N115®) [15], which had a thickness of 122 µm when considering that with the MJK1753 membrane 8.44 mol L^{-1} was reached at 0.28 A cm^{-2} compared to the 3.5 mol L^{-1} reached at 0.3 A cm^{-2} when using the N115® membrane. It should be mentioned that for the study of the N115 a pressure was applied on the cathode which would result in a higher cross-over of and hence dilution by H_2O [15].

5.3.3 VOLTAGE CYCLING

The activation and break-in procedures of PBI based MEA's have been investigated for high temperature fuel cells (HTFC) [10], where it has been shown that this step is crucial in ensuring that the best performance is achieved from the membrane materials. Different break-in procedures have been proposed ranging from operation of the HTFC at constant voltage for 50 h [10], while other methods include operating the fuel cell at a constant voltage while recording the polarisation curves. The activation of the PBI based membrane used in this study for application in the SO_2 electrolyser have been tested by cycling the voltage (50 mV s^{-1}) from 0 – 1 V. Figure 5.3 shows the forward voltage – current cycles for 16 cycles. It is clear that the cell efficiency actually improved with time, especially at higher current densities, during the cycling of the applied voltage.

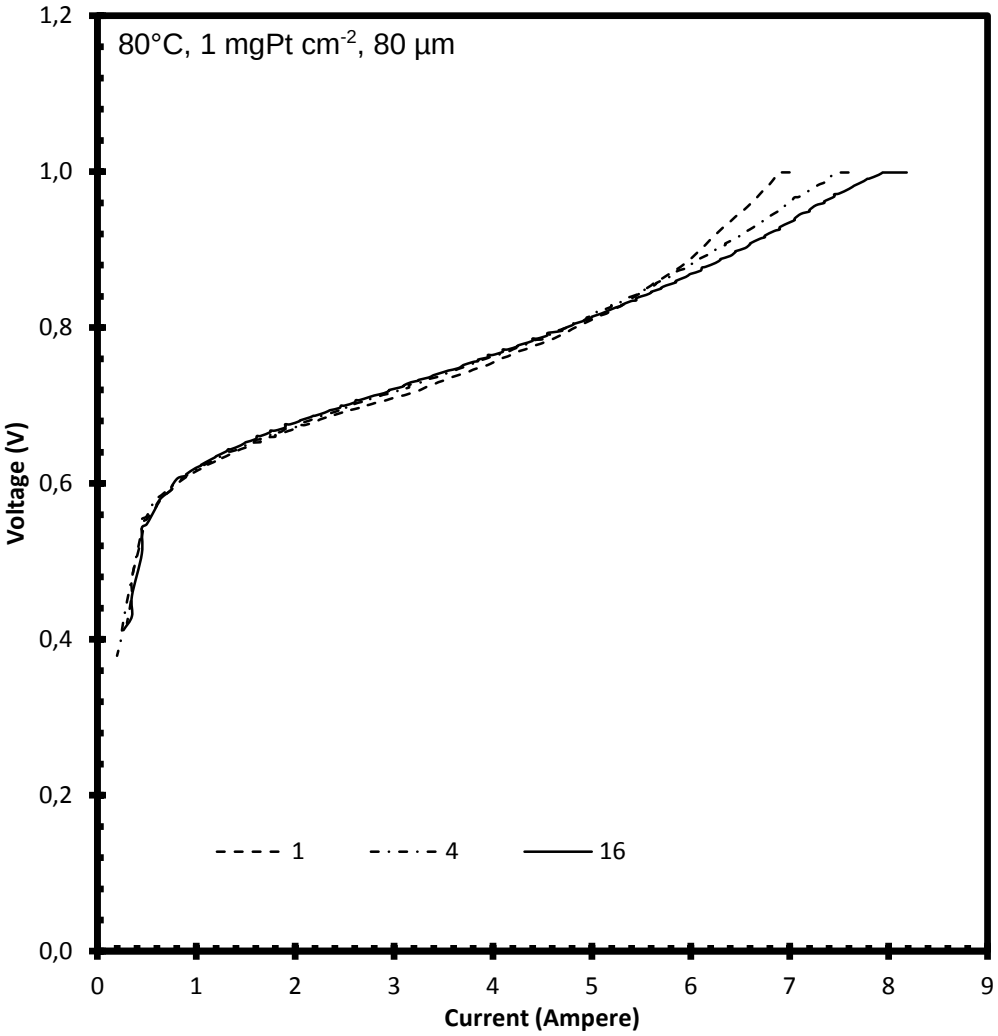

Figure 5.3: Effect of voltage cycling as a break-in procedure on the MEA performance.

The results however do not show whether the current values obtained in Figure 5.3 are stable as the scan rate may be fast enough not to allow the reaction to reach a steady state. For this reason a second series was conducted including the polarisation curves before and after the voltage cycling. Figure 5.4 shows the polarisation curves obtained. Since the current was kept constant for 90 s, it can be assumed that the voltage had reached a steady state operation.

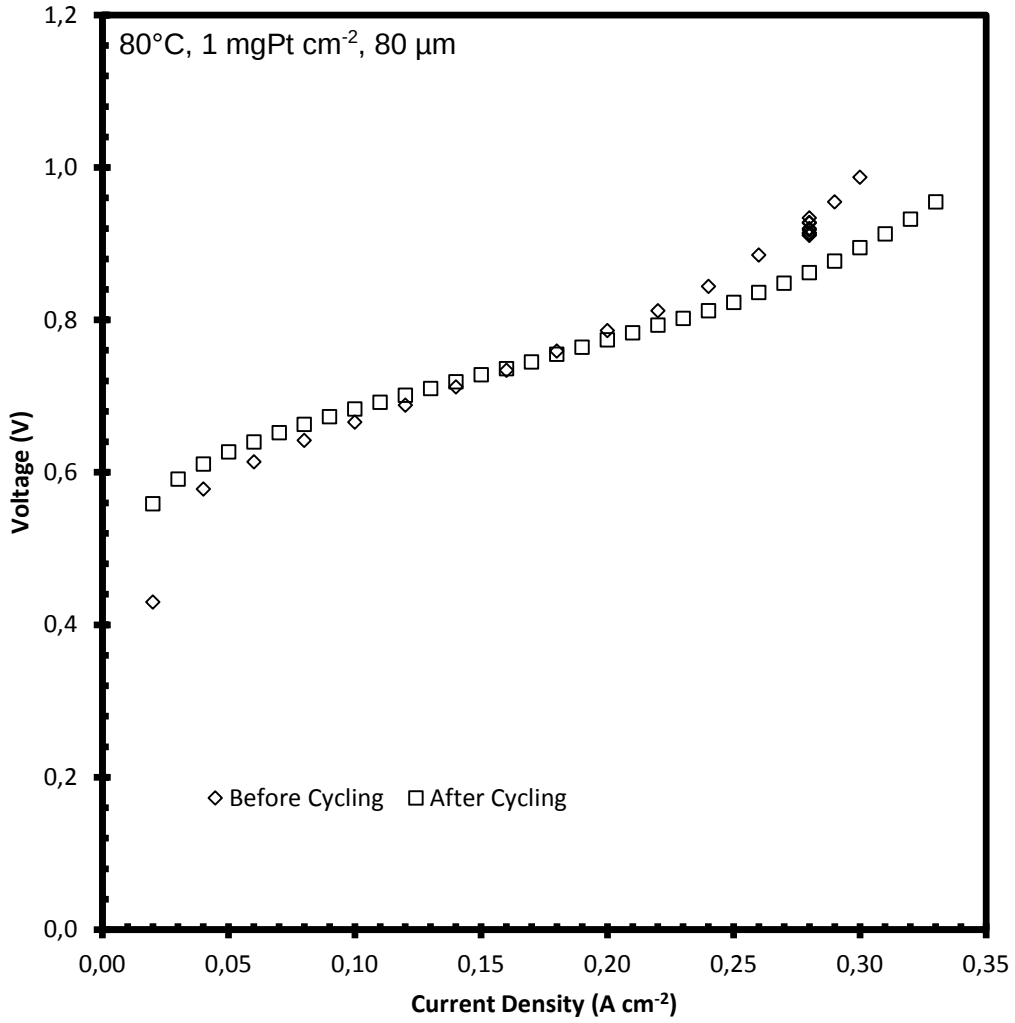

Figure 5.4: Polarisation curves before and after voltage cycling break-in procedure.

From the performance of the cell it is clear that the performance of the membrane improved after voltage cycling in view of both the lower voltages (at higher current densities) and the higher overall current density attained after cycling. The voltage stability was also tested (results not shown) at 0.32 A cm^{-2} after cycling and was found to remain stable at ±0.008 mV when tested for 5 min. This step was also performed on the MEA before voltage cycling at 0.28 A cm^{-2} and it was observed that the voltage increased by 23 mV over the same 5 min time period.

It is evident from the experimental data obtained using voltage cycling that the same applies to electrolysis operation what has been observed for HTFC i.e. when using PBI based membranes, an activation/break-in step is necessary for best performance.

5.3.4 LONG TERM OPERATION

While the characterisation of various MEA combinations by polarisation curves are important for material improvement and system control it is also essential to evaluate its long term operation (24 – 30 hrs [7]). To show the stability of the MJK1753 PBI membrane (80µm, 1 mgPt cm^{-2}), a long term test was recorded at 80°C and a constant current of 0.1 A cm^{-2} while recording the voltage every 5 min for 140 h. The results are shown in Figure 5.5.

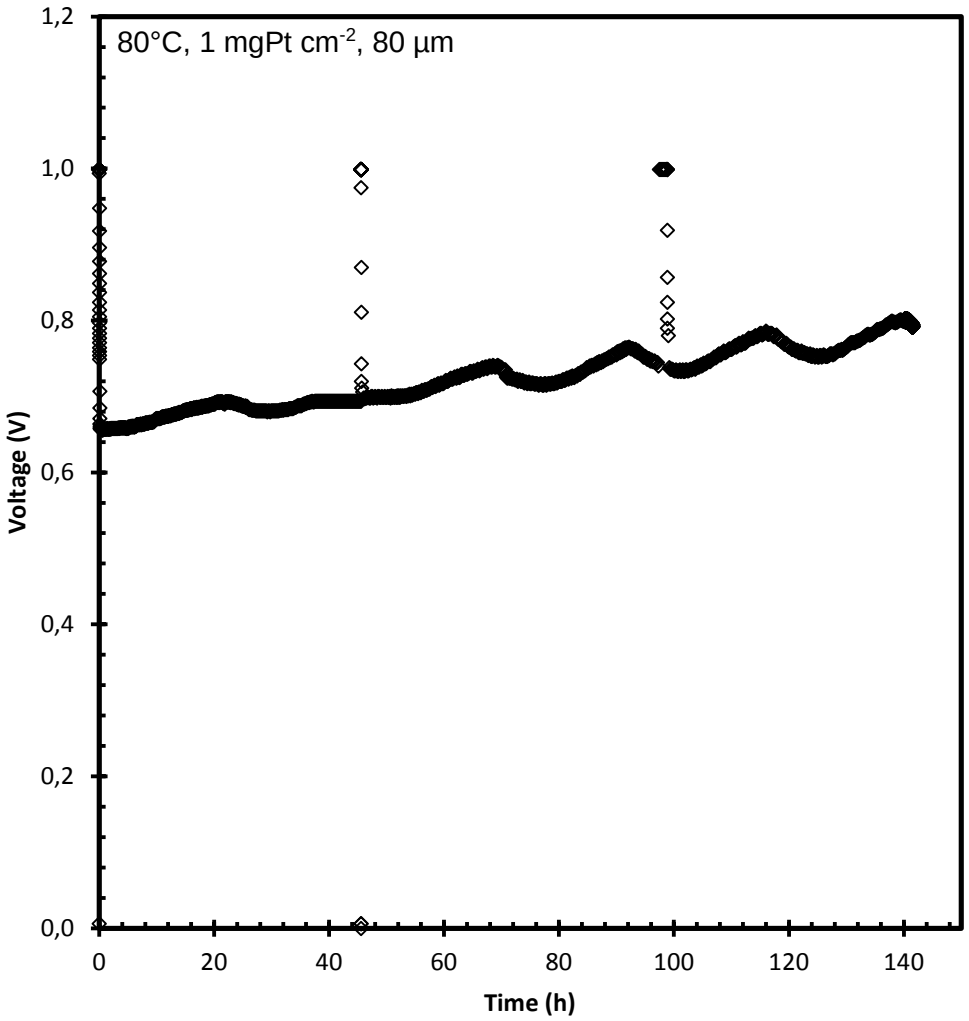

Figure 5.5: Long term SO_2 electrolysis at a constant 0.1 A cm^{-2} and 80°C.

The two discrete increases in voltage at 46 and 98 h were due to a change in the water feed to ensure that clean DI water is continually supplied to the electrolyser. Although the voltage increase over time is most likely due to a combined degradation

of the membrane and the catalyst, the focus of this paper is on the degradation of the membrane. While the voltage remained below 0.800 V, there was a gradual increase from 0.664 to 0.799 V which could be due to sulfur deposition at the cathode as a result of SO_2 crossover.

In order to further elucidate whether membrane internal changes might have contributed to the slight increase in voltage or the patterns observed in the long time test, the MEA before electrolysis and the MEA after the long term operation were characterised using SEM, FTIR, TGA and MS.

5.3.4.1 SCANNING ELECTRON MICROSCOPY

SEM micrographs were taken from the MEA before and after the long term operation to evaluate both the cross section and the top-view of the MEA to determine whether any visible structural changes or sulphur deposition had occurred. The top view is not shown as no significant changes were visible. Figure 5.6 shows the cross section view of the membrane before (Figure 5.6(a)) and after (Figure 5.6(b)) the long term tests with the cathode facing upwards.

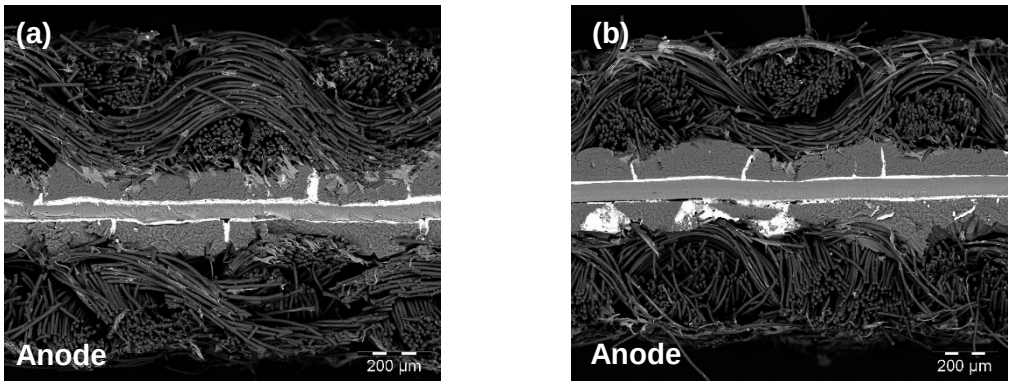

Figure 5.6: Cross sectional scanning electron microscopy images of (a) before and (b) after SO_2 electrolysis.

In both Figure 5.6(a) and (b) the platinum catalyst is clearly visible as the white band followed by the micro porous layer onto which it had been deposited and finally the carbon cloth as the gas diffusion media. Sulfur would appear as small grey granules (as the MEA's were dried at 80°C for 24 h before SEM analysis) either between the catalyst and membrane or within the anode/cathode GDL media. Since no

significant sulphur deposition is visible on the cathode GDL, it is clear that limited SO_2 crossover occurred confirming the suitability of these PBI blended membranes in terms of their SO_2 barrier properties.

5.3.4.2 TGA – MS ANALYSIS

To further characterise the possible degradation of the PBI based membrane, TGA analysis was performed to determine its thermal stability (which is an indication of the membrane stability). Figure 5.7 shows the temperature stability of the membrane only, as well as the MEA before (with GDE's) and the MEA after (with GDE's) SO_2 electrolysis up to 600°C. It is assumed that changes observed for the MEA where mainly due to changes in the membranes, as the GDE is known to be stable within the same operating period, although for high temperature PEM fuel cell applications [24]. No significant difference between the MEA before and after SO_2 electrolysis is observed. The lower peak values for the MEA are assigned to the larges weight fraction of the GDE, resulting in a lower resolution, i.e. a small weight change for the MEA with increasing temperature when compared to the total sample weight.

It is clear that the membrane is stable up to 300°C losing only 6% weight. Some weight loss is observed above 200°C before significant degradation occurs at temperatures above 550°C. The weight loss in the 0 – 160°C region is commonly attributed to water loss due to evaporation [25]. The MJK 1753 membrane showed improved membrane stability when compared to previously PBI based membranes tested for the application in the SO_2 electrolyser [6] which contained ionically cross-linked sFS (partially fluorinated – sulfonated arylene main chain ionomer), sPSU (non-fluorinated – sulfonated arylene main chain ionomer), sPSU-PBI (blended polymer between sPSU and PBIOO) and pure PBIOO membranes [6]. From the previous study on the PBI-based membranes [6], the sPSU-PBIOO blended membrane showed the best performance and will be compared in terms of the TGA results.

The same water evaporation stage is observed for the sPSU-PBIOO in the 0 – 160°C range while the weight change with increased temperature is comparable to the MJK1753 polymer presented here.

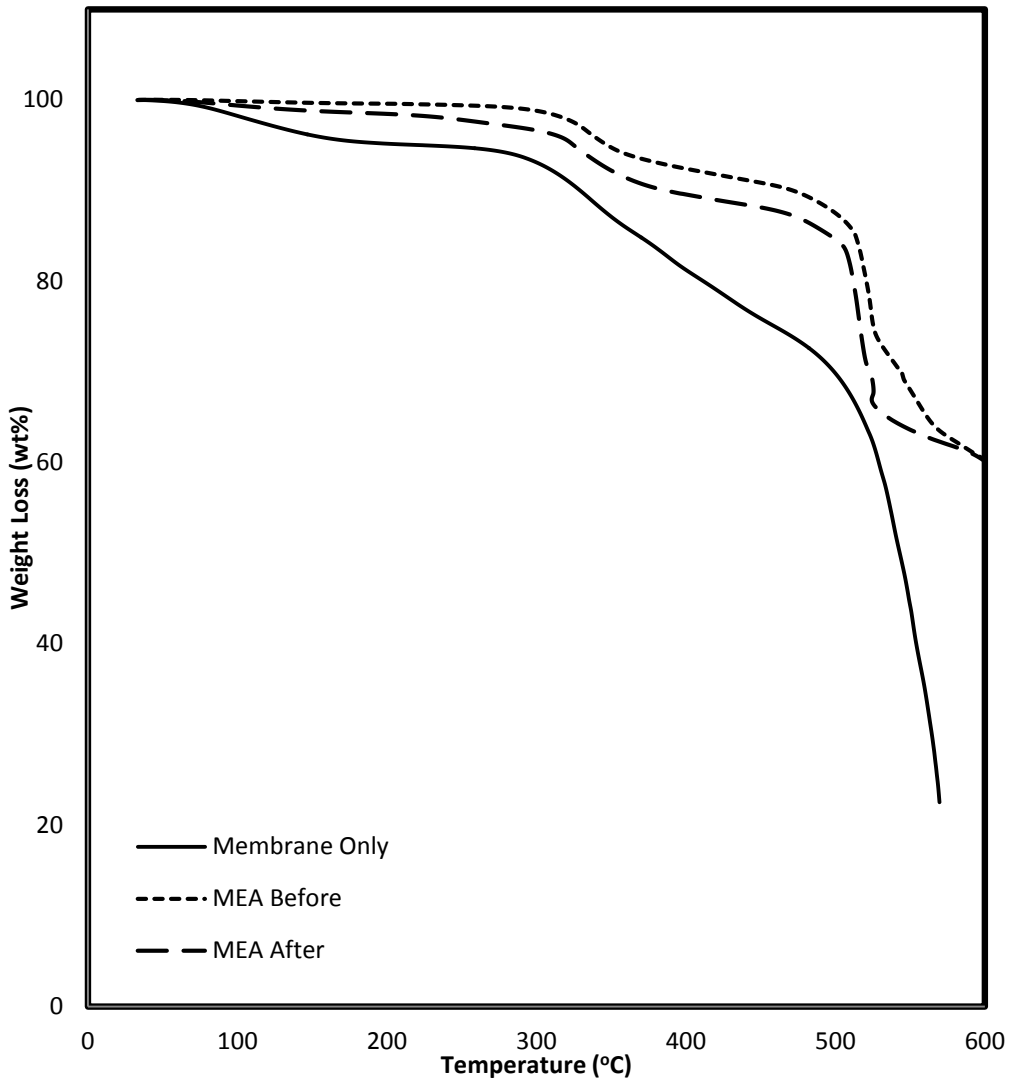

Figure 5.7: Weight loss of the membrane, MEA before and MEA after long term operation as a function of temperature.

The temperature ranges in which the membrane showed maximum weight loss was determined by taking the first derivative between the weight and temperature and is shown in Figure 5.8. Accordingly three temperature ranges were selected at 50 – 120°C, 300 – 350°C and > 450°C.

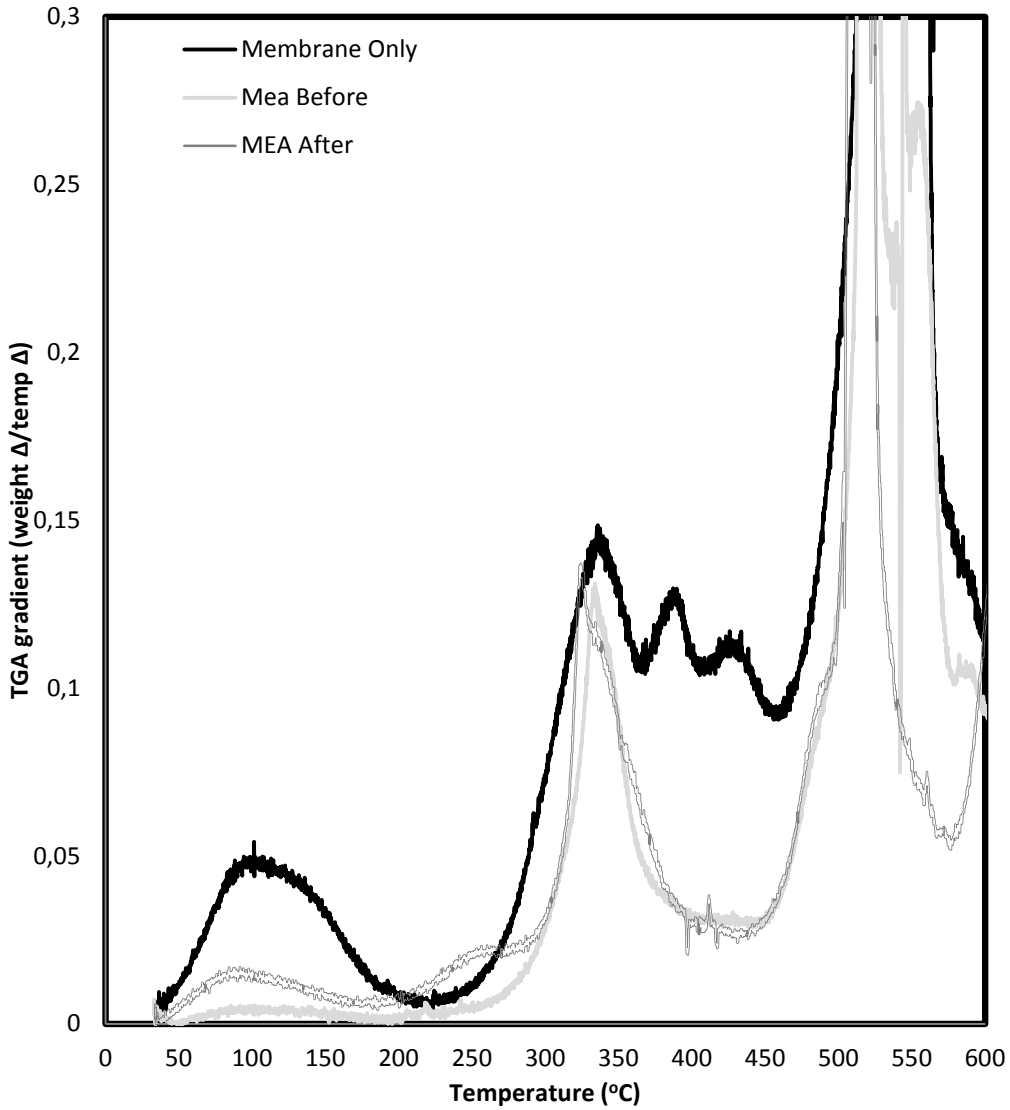

Figure 5.8: Differential TGA for membrane only, MEA Before, MEA After long term operation.

Using the TGA coupled with MS as described previously [7], the mass fraction as a function of the degradation temperatures could be obtained and compared to the temperature region of maximum weight loss as determined from the TGA data, thereby allowing the identification of the species evaporated for each temperature. The MS data for these specific temperature ranges were used to compare the signal of the membrane only, MEA before and the MEA after the long term operation. Table 5.5 shows a summary of the mass fractions selected with their possible molecular structure identified for evaluation.

Table 5.5: Mass fraction (m/z) with their possible molecular identity.

Mass fraction (m/z)	Assigned Identity	Mass fraction (m/z)	Assigned Identity	Mass fraction (m/z)	Assigned Identity
14	N / CH_2	19	F	48	SO
16	O	27	CH_2-CH	64	SO_2
17	OH	32	S	81	SO_3H
18	H_2O	44	CO_2		

Figure 5.9 shows the fragments identified for the 50 – 120°C temperature range. During the membrane synthesis NMP was used as solvent to dissolve the polymeric blend components. The NMP solvent can be identified in the N/CH_2 fragment seen in all three temperature ranges tested. Water evaporation (O, OH and H_2O) can also be expected in all three temperature ranges tested and is shown to increase with temperature showing that some water is trapped inside the membrane structure. It can also be argued that the presence of the GDE materials could also increase the temperature at which water would evaporate as it needs to permeate through the catalyst layer and then the carbon cloth materials. All the intensities of the species shown here were bigger for the MEA after compared to the MEA before as one would expect. It is however not as significant for the species with molecular weights above 44.

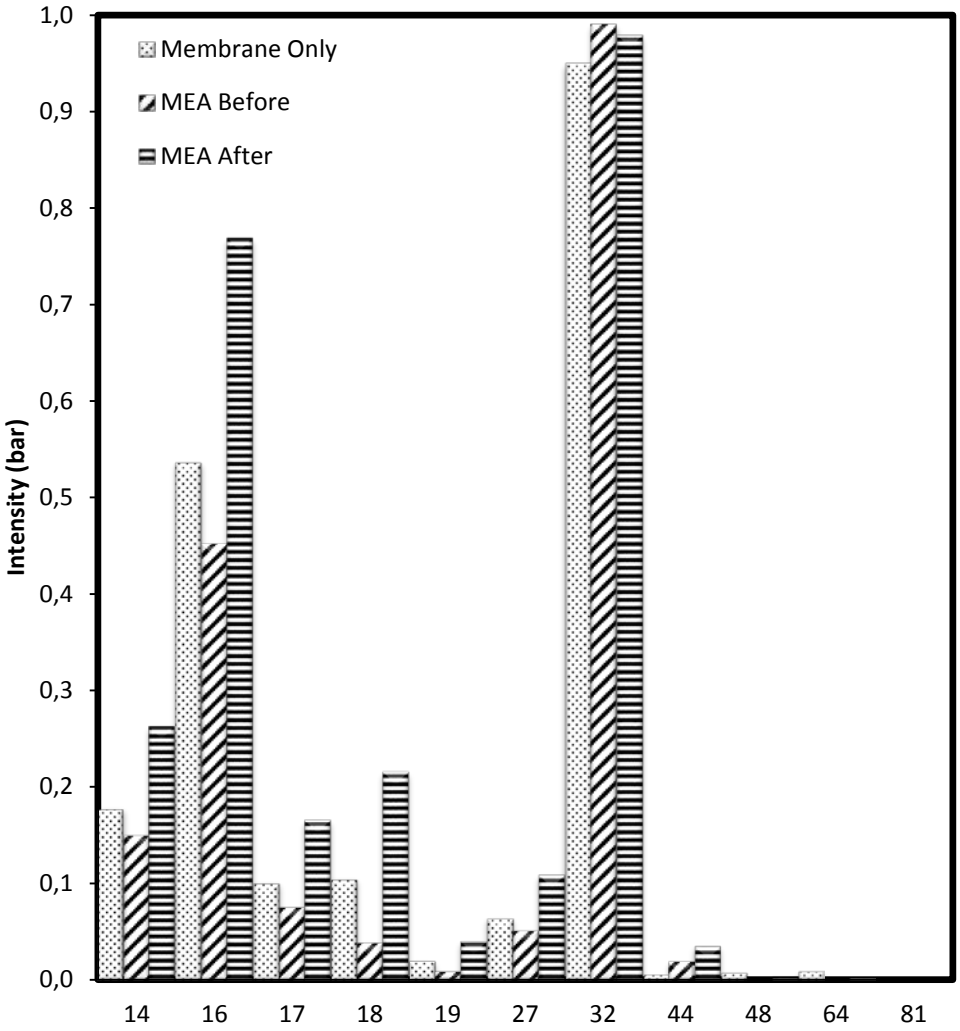

Figure 5.9: MS data for selected temperature range 50 – 120°C for the membrane only, the MEA before and MEA after long term operation.

When considering the intermediate temperature range (300 – 350°C) shown in Figure 5.10, the heavier elements such as F (19), CH_2-CH (27) and CO_2 (44) became more prominent while H_2O (18) and S (32) remained present in high quantities. In this temperature range the components of the blended membrane are known to start to decompose [6,7]. The increase of the F component, coupled with membrane degradation, is especially visible for the MEA after electrolysis which can be an indication of the degradation of SFS001 and F_6-PBI [25].

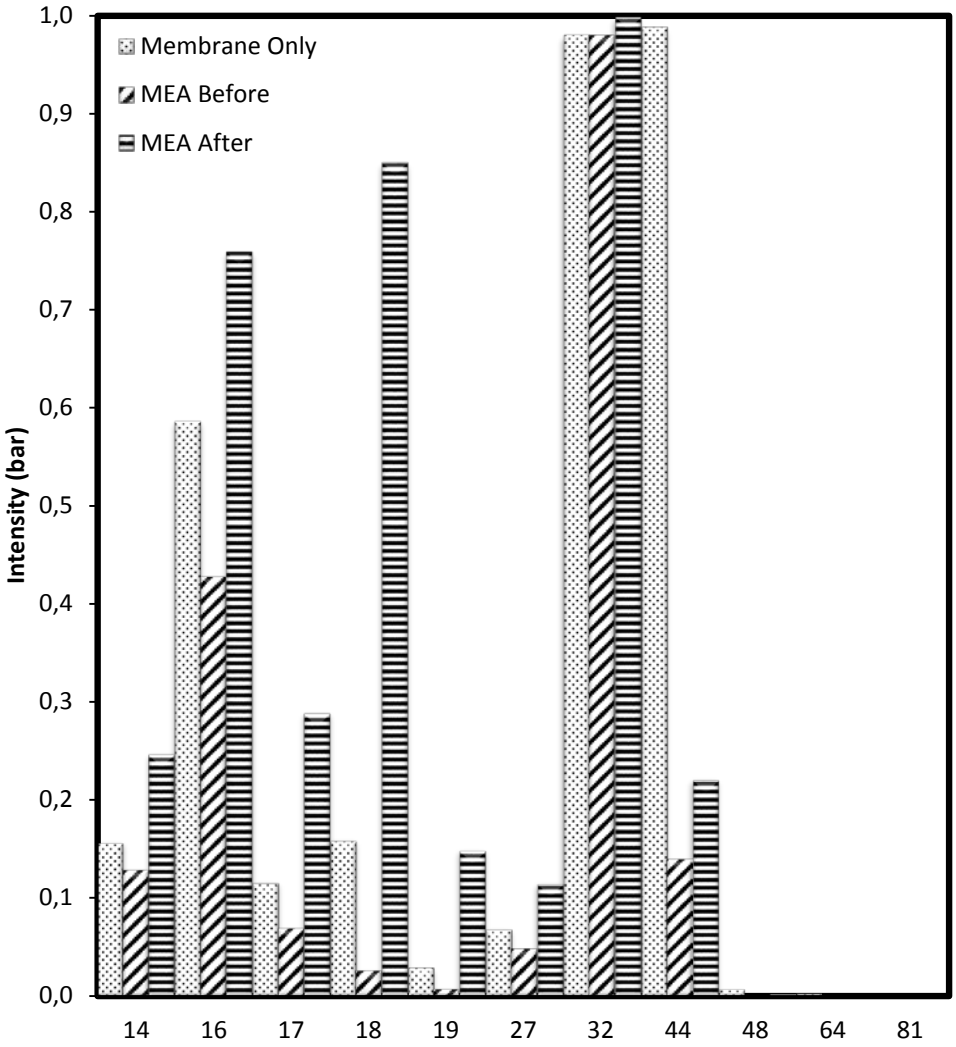

Figure 5.10: MS data for 300 – 350°C temperature range for the membrane only, the MEA before and the MEA after long term operation.

It is clear from Figure 5.10 that the membrane showed some degradation due to SO_2 electrolysis as shown by the MEA after data having bigger peaks for all elements. The presence of the O (16), OH (17) and H_2O (18) can still be associated with water evaporation while the appearance of the more prominent CO_2 (44) peaks are a clear indication of membrane degradation.

Figure 5.11 shows the MS data for the temperature range above 450°C. The degradation pattern is similar to that of the first two temperature ranges although the intensities are higher for all the elements indicating that the polymer has started to decompose completely. The increased CO_2 peak shows this degradation clearly. It

is however interesting to note that no SO (48) or SO_2 (64) peaks were observed for any of the temperature ranges tested here. A possible explanation for this finding is that SO_2 decomposes into S and O under the specific conditions of the MS experiment. In TGA-MS coupling experiments the thermal splitting-off characteristics of the SO_3OH groups could be mentioned (see below).

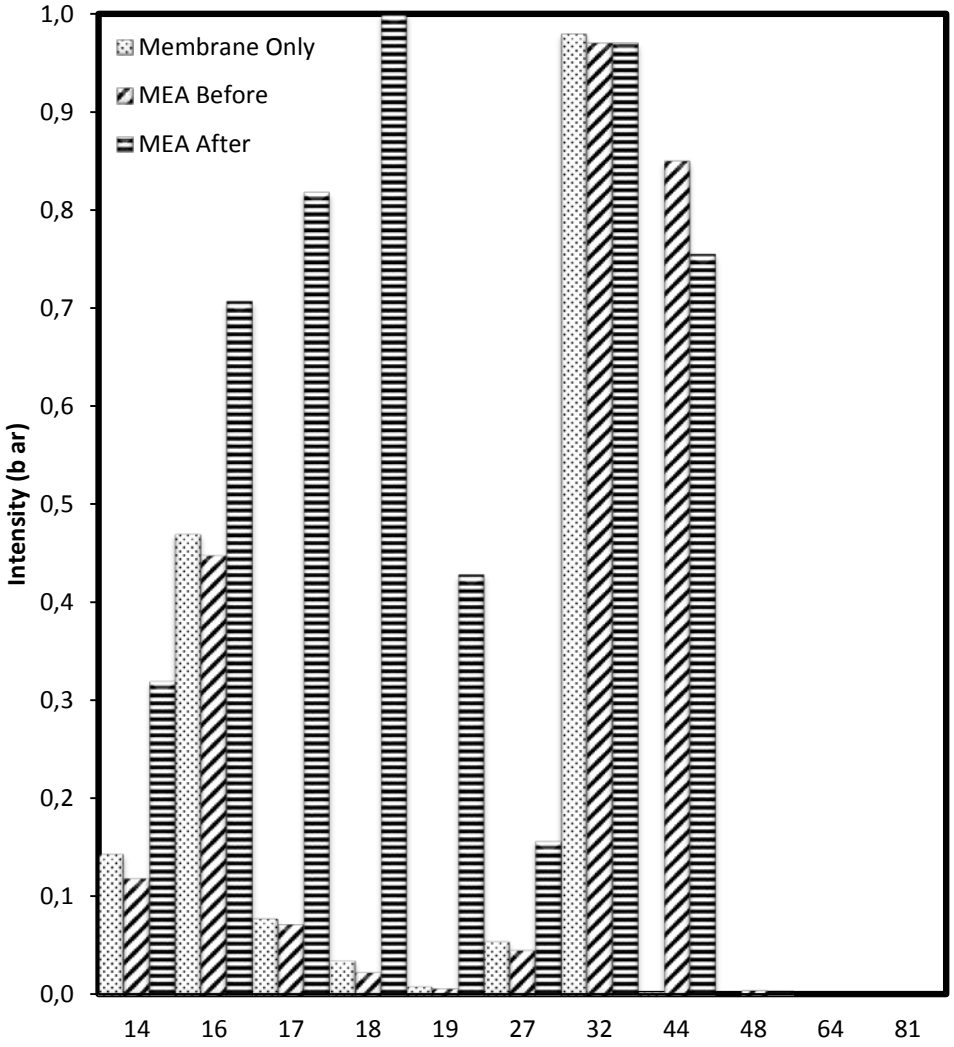

Figure 5.11: MS data shown for temperature range > 450°C for Membrane Only, MEA Before and MEA After the long term operation.

5.3.4.3 TGA – FTIR ANALYSIS

The assistance of the group of Dr. Jochen Kerres must be acknowledged for supplying the TGA-FTIR data discussed in this section. Via TGA-FTIR coupling the thermal degradation characteristics of 1753 and the blend components SFS001 and F_6PBI were investigated. The SO_3H splitting-off characteristics were investigated by monitoring the appearance of SO_2 bands (between 1340 and 1370 cm^{-1}) in the TGA decomposition gases, and the polymer degradation characteristics by monitoring the appearance of CO bands (between 2241 and 1991 cm^{-1}). In Figure 5.12, the FTIR spectra series obtained from TGA-FTIR coupling experiment of the acidic blend membrane component SFS001 is depicted.

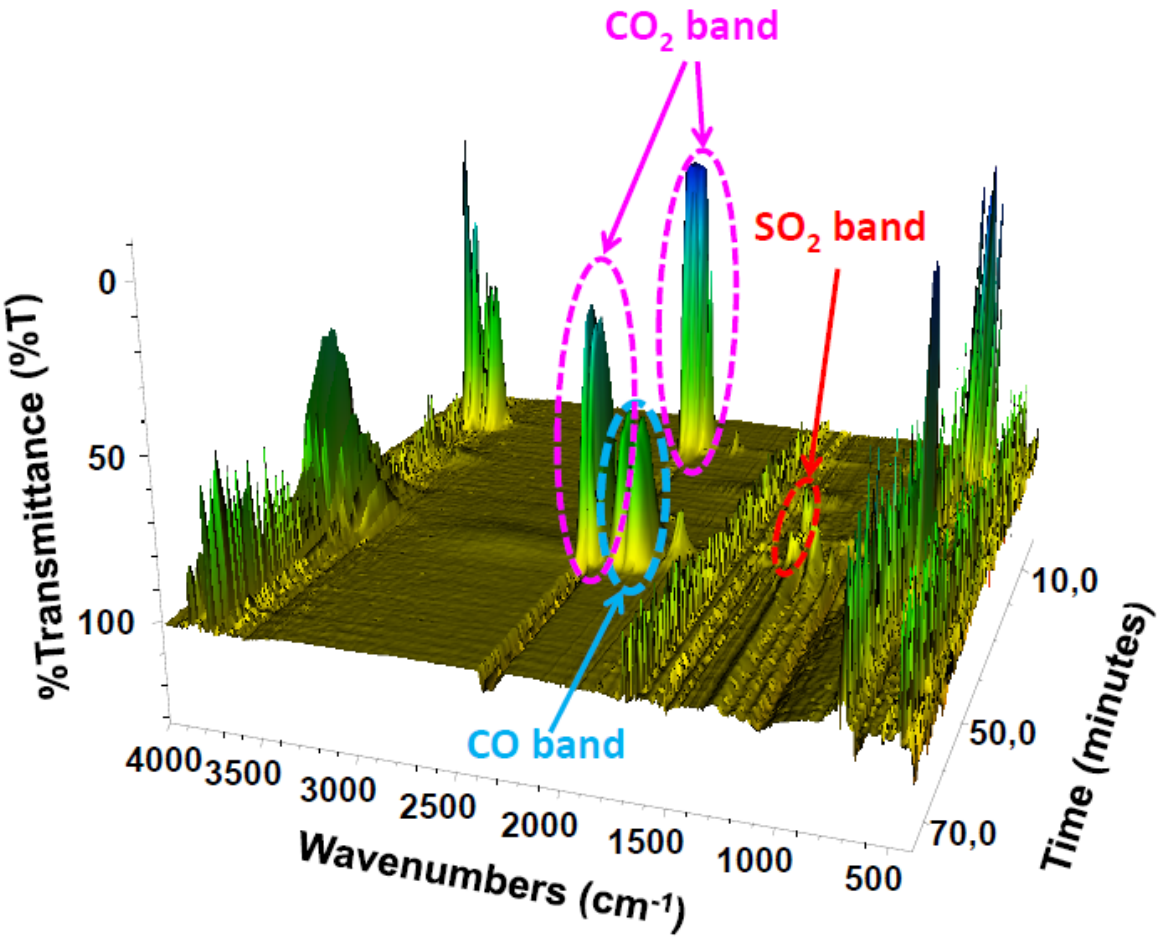

Figure 5.12: FTIR spectra series from TGA-FTIR coupling experiment of SFS001.

Those IR bands relevant for the coupling experiment (CO_2 band →marking signal for assignment of the respective TGA temperature to FTIR bands, SO_2 band →

indication for splitting-off of SO_3H groups, and CO band → indication for degradation of polymer backbone) are marked within the spectra series representation. In Figure 5.13, the Chemigrams of SO_2 band (red: 1: start of SO_2 evolution; 2: maximum of SO_2 evolution), CO band (green: 1: start of CO evolution; 2: maximum of CO evolution) and Gram-Schmidt trace (blue: 1: arrival time of CO_2 in FTIR cuvette) evolution of SFS001 (a), F_6PBI (b) and MJK1753 membrane (c) during TGA-FTIR coupling experiment are represented. From the chemigrams, both the starting temperature of the respective degradation process and the maximum of the respective degradation process can be read.

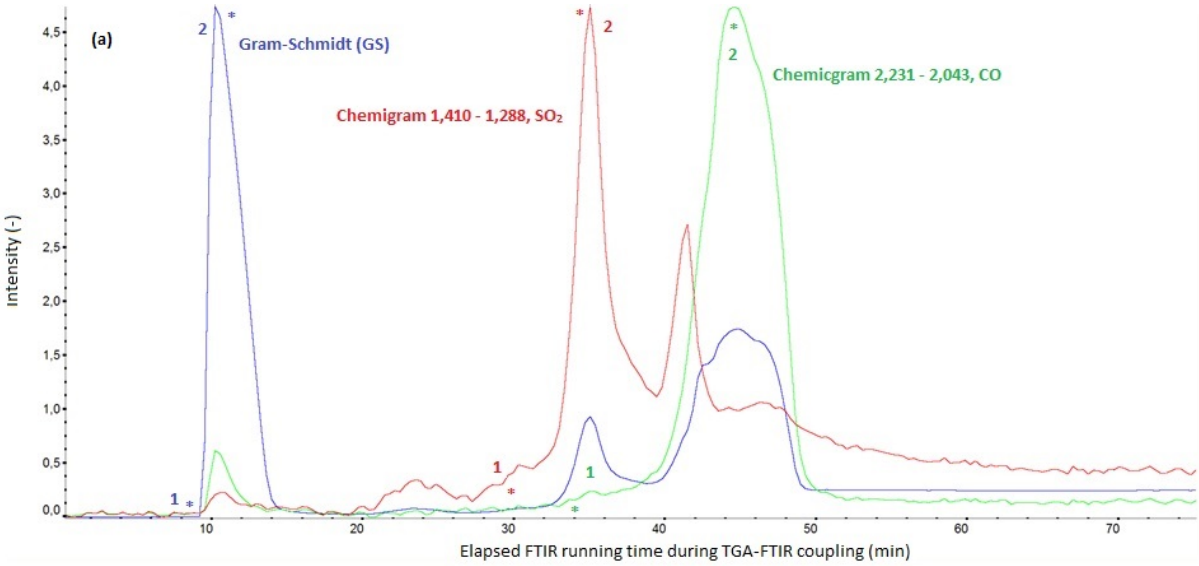

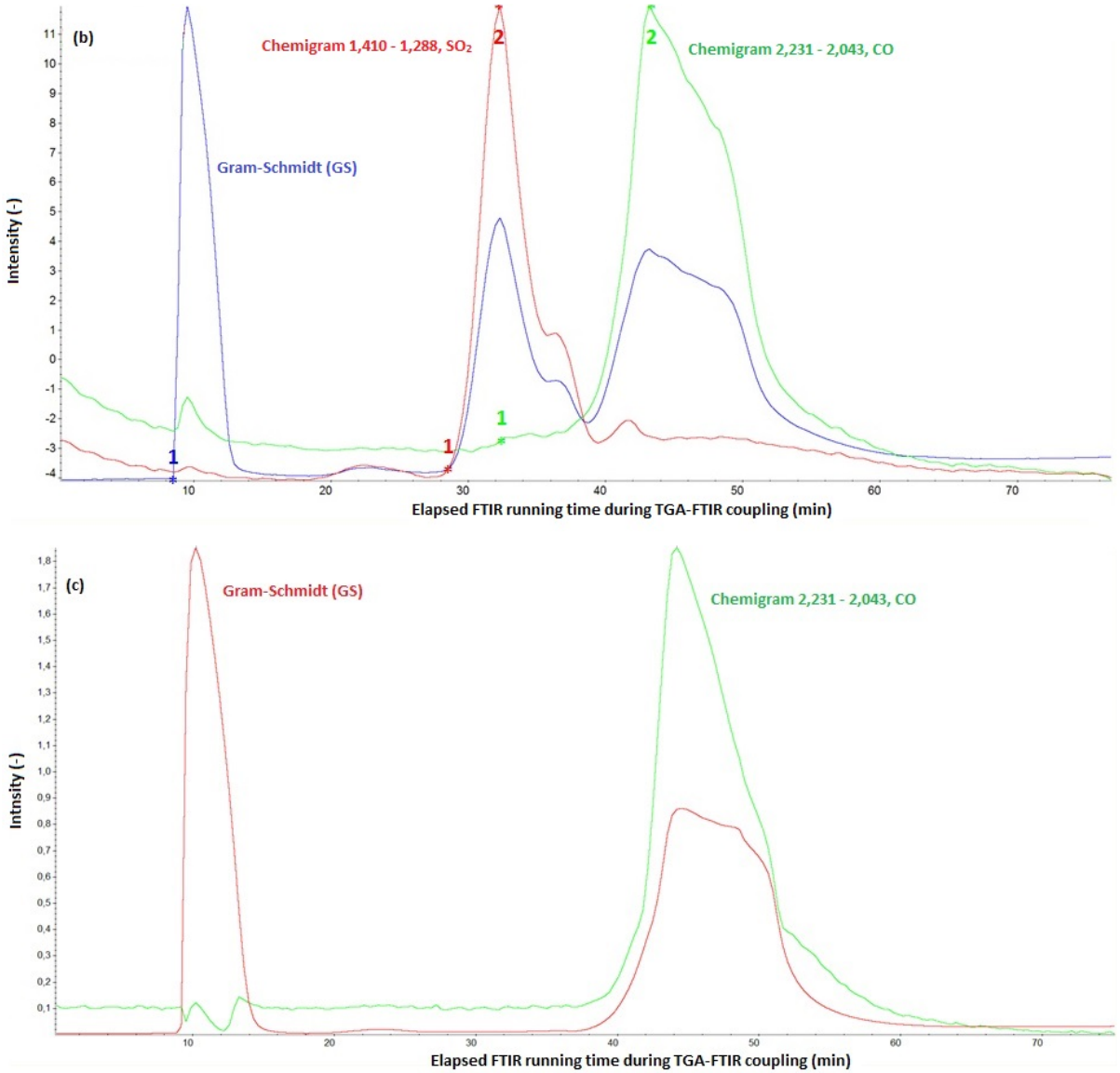

Figure 5.13: Chemigrams of SO_2 band (red: 1: start of SO_2 evolution; 2: maximum of SO_2 evolution), CO band (green: 1: start of CO evolution; 2: maximum of CO evolution) and Gram-Schmidt trace (blue: 1: arrival time of CO_2 in FTIR cuvette) evolution of SFS001 (a), MJK1753 (b) and F_6PBI (c) during TGA-FTIR coupling experiment.

In Figure 5.14, the TGA traces of the sulfonated blend component (a), the blend membrane MJK1753 (b), and the basic blend component F_6PBI (c) are shown along with the characteristic temperatures of degradation processes (SO_3H splitting-off, and start of backbone degradation via CO development).

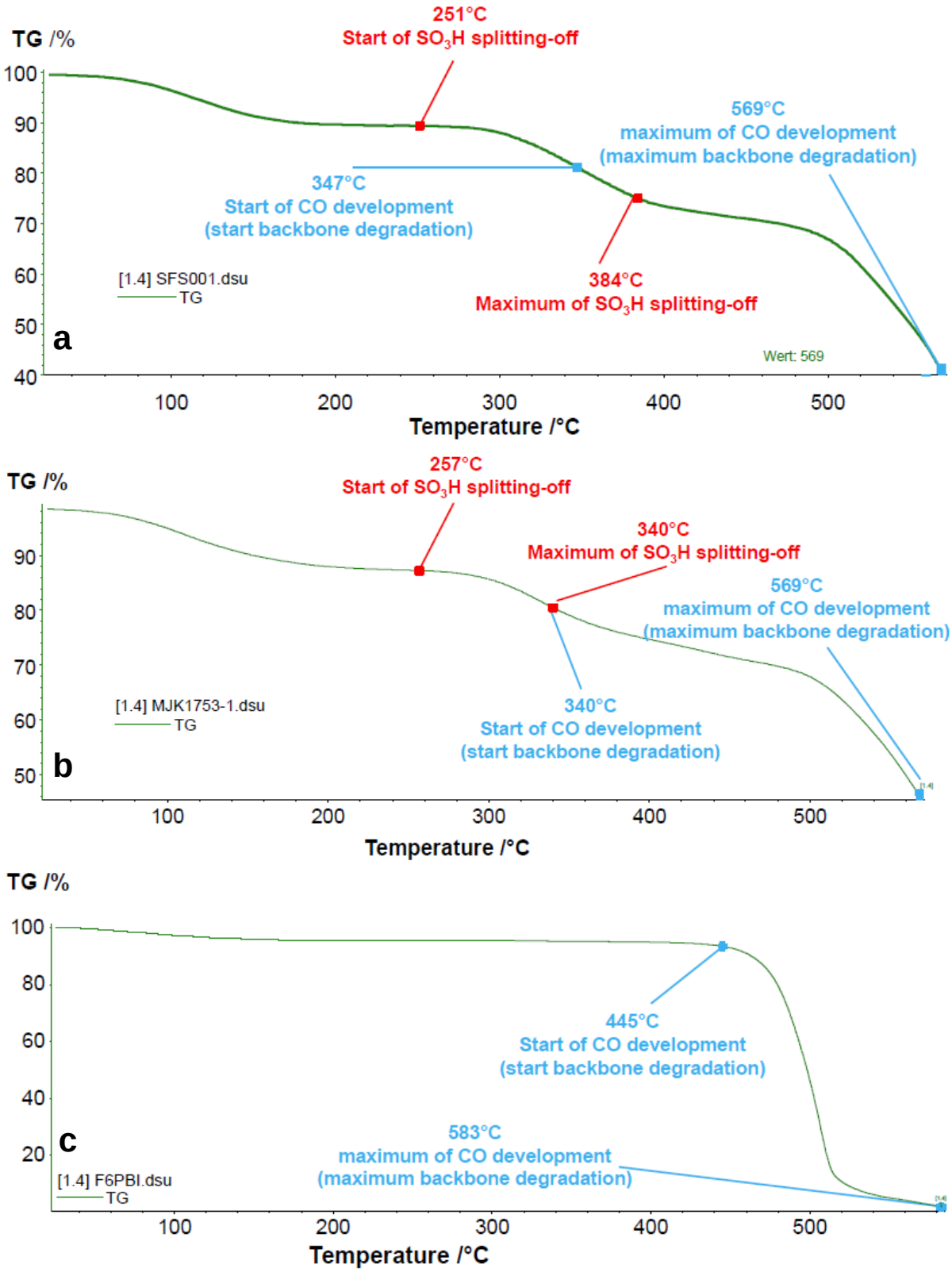

Figure 5.14: TGA of SFS001 (a), MJK1753 (b) and F_6PBI (c) including specific degradation temperatures (from coupled FTIR).

It is clearly seen from the TGA traces that the SO_3H splitting-off start temperature of the pure sulfonated polymer and the blend membrane are nearly equal and lie at 250°C, which is far beyond the operation temperature of SO_2 electrolysis. Moreover, the start temperature of thermal backbone degradation is roughly 100°C higher than the SO_3H splitting-off starting temperature. From these results an excellent thermal stability of the blend membrane can be concluded.

5.4 CONCLUSION

In this study the pre-treatment and stability of a PBI based blended proton exchange membrane in an SO_2 electrolyser was investigated. The results showed that the MEA manufacturing procedure had a significant influence on the overall cell performance, where the best performance was attained when the doping was done after the hot pressing of the MEA. It was also shown that the MEA conditioning (voltage cycling) improved the overall cell performance. Long term operation (140 h) confirmed that the voltage remained below 0.8 V for the duration of the test. Following the long term testing, the MEA was characterised using SEM, FTIR and TGA-MS. The SEM images showed minimal sulfur deposition while the FTIR indicated that no significant chemical change occurred during SO_2 operation. The TGA coupled with MS data for the membrane only showed that the membrane is stable when exposed to H_2SO_4 while degradation was seen when operated in the SO_2 electrolyser. Improvement on the cell performance can be achieved by operating at temperatures higher than 100°C and will form part of future work.

5.5 REFERENCES

[1] Brey JJ, Brey R, Contreras I, Carazo AF. Roll-out of hydrogen fueling stations in Spain through a procedure based on data envelopment analysis. Int J Hydrogen Energy 2014;39:4116–22. doi:http://dx.doi.org/10.1016/j.ijhydene.2013.09.141.

[2] Brecher LE, Spewock S, Warde CJ. The Westinghouse Sulfur Cycle for the thermochemical decomposition of water. Int J Hydrogen Energy 1977;2:7–15. doi:http://dx.doi.org/10.1016/0360-3199(77)90061-1.

[3] Gorensek MB, Staser JA, Stanford TG, Weidner JW. A thermodynamic analysis of the SO_2/H_2SO_4 system in SO_2-depolarized electrolysis. Int J Hydrogen Energy 2009;34:6089–95.

[4] Gorensek MB. Hybrid Sulfur cycle flowsheets for hydrogen production using high-temperature gas-cooled reactors. Int J Hydrogen Energy 2011;36:12725–41.

[5] Sivasubramanian P, Ramasamy RP, Freire FJ, Holland CE, Weidner JW. Electrochemical hydrogen production from thermochemical cycles using proton exchange membrane electrolyzer. Int J Hydrogen Energy 2007;32:463–8.

[6] Schoeman H, Krieg HM, Kruger AJ, Chromik A, Krajinovic K, Kerres J. H2SO4 stability of PBI-blend membranes for SO_2 electrolysis. Int J Hydrogen Energy 2012;37:603–14.

[7] Peach R, Krieg HM, Krüger AJ, van der Westhuizen D, Bessarabov D, Kerres J. Comparison of ionically and ionical-covalently cross-linked polyaromatic membranes for SO2 electrolysis. Int J Hydrogen Energy 2014;39:28–40.

[8] Jayakumar JV, Gulledge A, Staser JA, Kim C-H, Brian C B, Weidner JW. Polybenzimidazole Membranes for hydrogen and sulfuric acid production in the Hybrid Sulfur Electrolyzer. ECS Electrochem Lett 2012;1:F44–8.

[9] Tingelöf T, Ihonen JK. A rapid break-in procedure for PBI fuel cells. Int J Hydrogen Energy 2009;34:6452–6. doi:http://dx.doi.org/10.1016/j.ijhydene.2009.05.003.

[10] Boaventura M, Mendes A. Activation procedures characterization of MEA based on phosphoric acid doped PBI membranes. Int J Hydrogen Energy 2010;35:11649–60. doi:http://dx.doi.org/10.1016/j.ijhydene.2010.03.137.

[11] Wang S, Zhang G, Han M, Li H, Zhang Y, Ni J, et al. Novel epoxy-based cross-linked polybenzimidazole for high temperature proton exchange membrane fuel cells. Int J Hydrogen Energy 2011;36:8412–21. doi:10.1016/j.ijhydene.2011.03.147.

[12] Xue L, Zhang P, Chen S, Wang L, Wang J. Sensitivity study of process parameters in membrane electrode assembly preparation and SO_2 depolarized

electrolysis. Int J Hydrogen Energy 2013;38:11017–22. doi:http://dx.doi.org/10.1016/j.ijhydene.2012.12.120.

[13] Ferng YM, Su A, Hou J. Parametric investigation to enhance the performance of a PBI-based high-temperature PEMFC. Energy Convers Manag 2014;78:431–7. doi:http://dx.doi.org/10.1016/j.enconman.2013.10.069.

[14] Kondratenko MS, Gallyamov MO, Khokhlov AR. Performance of high temperature fuel cells with different types of PBI membranes as analysed by impedance spectroscopy. Int J Hydrogen Energy 2012;37:2596–602. doi:http://dx.doi.org/10.1016/j.ijhydene.2011.10.087.

[15] Staser J, Ramasamy RP, Sivasubramanian P, Weidner JW. Effect of Water on the Electrochemical Oxidation of Gas-Phase SO_2 in a PEM Electrolyzer for H_2 Production . Electrochem Solid-State Lett 2007;10:E17–9.

[16] Staser JA, Weidner JW. Effect of Water Transport on the Production of Hydrogen and Sulfuric Acid in a PEM Electrolyzer. J Electrochem Soc 2009;156:B16–21.

[17] Lokkiluoto A, Gasik MM. Modeling and experimental assessment of Nafion membrane properties used in SO_2 depolarized water electrolysis for hydrogen production. Int J Hydrogen Energy 2013;38:10–9. doi:http://dx.doi.org/10.1016/j.ijhydene.2012.09.168.

[18] Staser JA, Gorensek MB, Weidner JW. Quantifying Individual Potential Contributions of the Hybrid Sulfur Electrolyzer. J Electrochem Soc 2010;157:B952–8.

[19] Prasanna M, Cho EA, Lim TH, Oh IH. Effects of MEA fabrication method on durability of polymer electrolyte membrane fuel cells. Electrochim Acta 2008;53:5434–41. doi:http://dx.doi.org/10.1016/j.electacta.2008.02.068.

[20] Carmo M, Fritz DL, Mergel JJ, Stolten D. A Comprehensive review on PEM electrolysis. Int J Hydrogen Energy 2013;38:4901–34. doi:10.1016/j.ijhydene.2013.01.151.

[21] Opperman H, Kerres J, Krieg H. SO_2 crossover flux of Nafion and sFS-PBI membrane using a chronocoulometric (CC) monitoring technique. J Memb Sci 2012;415 - 416:842–9.

[22] John A. Staser Cy H. Fujimoto, Micheal A. Hickner, John W. Weidner KN. Transport Properties and Performance of Polymer Electrolyte Membranes for the Hybrid Sulfur Electrolyzer. J Electrochem Soc 2009;156:B842–7.

[23] Nayoung Kim DK. SO_2 permeability and proton conductivity of sPEEK membranes for SO_2-depolarized electrolyzer. Int J Hydrogen Energy 2009;34:7919–26.

[24] Liu G, Zhang H, Hu J, Zhai Y, Xu D, Shao Z. Studies of performance degradation of a high temperature PEMFC based on H_3PO_4-doped PBI. J Power Sources 2006;162:547–52. doi:http://dx.doi.org/10.1016/j.jpowsour.2006.07.008.

[25] Atanasov V, Gudat D, Ruffmann B, Kerres J. Highly phosphonated polypentafluorostyrene: Characterization and blends with polybenzimidazole. Eur Polym J 2013;49:3977–85. doi:http://dx.doi.org/10.1016/j.eurpolymj.2013.09.002.

[26] Kruger AJ, Cichon P, Kerres J, Bessarabov D, Krieg HM. Characterisation of a polaromatic PBI blend membrane for SO_2 electrolysis. Int J Hydrogen Energy 2015:1–12. doi:http://dx.doi.org/10.1016/j.ijhydene.2014.12.081.

CHAPTER 6: EVALUATION OF COVALENTLY AND IONICALLY CROSS-LINKED PBI-EXCESS BLENDS FOR APPLICATION IN SO_2 ELECTROLYSIS*

Chapter Overview

Proton exchange membranes (PEM) containing various combinations of PPOBr (poly(2,6-dimethylbromide-1,4-phenylene) oxide, covalently cross-linked) or PWN (poly(tetrafluorostyrene-4-phosphonic acid), ionically cross-linked) were evaluated for their suitability in an SO_2 electrolyser environment. Since H_2SO_4 is produced during the oxidation of SO_2 in the presence of water, the membranes used in the electrolyser must be both chemically and electrochemically stable. Acid stability tests showed that the blend membranes were stable in 80 wt% acidic media at 80°C for 120 h. The electrochemical characterisation included polarisation curves, voltage stepping and long-term operation. Using polarisation curves two blend combinations were selected for the voltage stepping. Both types of blended membranes showed high stability up to 110 cycles while the F_6PBI/PPOBr blend membrane had comparable (to N115®) long term operating voltage, while the F_6PBI/PWN blend membrane showed improved voltage, attaining 0.781 V compared to the 0.812 V obtained when using N115 at 0.1 A cm^{-2}.

* Krüger AJ, Kerres J, Bessarabov D, Krieg HM. Evaluation of covalently and ionically cross-linked PBI-excess blends for application in SO_2 electrolysis. Int J Hydrogen Energy 2015;40:8788-96. Doi:10.1016/j.ijhydene.2015.05.063.

6.1 INTRODUCTION

When considering the amount of applications for hydrogen it makes sense to focus on a clean and efficient method of producing hydrogen without using carbon-based fuels. An alternative method of producing environmentally clean hydrogen is through the electrolysis of pure water which produces both hydrogen and oxygen. Theoretically a voltage of 1.23 V would be needed to split the water into its separate gaseous molecules. The reaction however takes place at higher voltages due to contact resistances within the electrolyser hardware (among others) and an operating voltage in the order of 1.5 – 2 V is more reasonable [1].

The Westinghouse Corporation suggested the sulphur-based thermochemical cycles to further reduce the theoretical voltage input for the electrochemical oxidation of water [2]. The traditional Hybrid Sulfur (HyS) cycle uses the thermal energy produced by gas cooled nuclear reactors to decompose concentrated sulphuric acid into SO_2, O_2 and H_2O [3,4]. After separating the O_2 the SO_2 and water is electrolysed in an electrolyser, where a similar hardware design can be used as in fuel cells, to form H_2 and H_2SO_4. The produced acid is then concentrated and returned to the decomposition step. During the electrolysis step SO_2 dissolved in sulphuric acid is reacted at the anode, producing sulphuric acid, while the hydrogen is formed at the cathode. Sivasubramanian *et al*. showed that the electrolyser could also be operated by supplying the anode with dry SO_2 gas and liquid water to the cathode [5]. In this setup the water diffuses through the polyperfluorinated sulfonic acid (PFSA) membrane, due to a concentration gradient and/or pressure differential, to the anode to react with the SO_2. Although this modification has proven to increase the operating current density of the electrolyser significantly it has the limitation of not producing enough sulphuric acid required for the decomposition step. Various methods can be employed to increase the acid concentration produced, such as increasing membrane thickness (which decreases the cell efficiency) or operating the electrolyser at higher temperatures (which will decrease the water content of the PFSA membrane and also reduce cell efficiency).

In the initial design it was shown that temperatures above 100°C in the electrolyser would be required for a feasible HyS cycle [4]. However, above 100°C Nafion would

not be suitable. An alternative membrane materials that have shown their suitability at these temperatures are polybenzimidazole PBI-based membranes [6]. These types of membrane require the presence of an acid to facilitate the conduction of protons across the membrane [7]. The sulfonation of a partially fluorinated (sFS) arylene, blended with commercial PBI, has been shown to produce a thermal and chemical stable proton exchange membrane for use in the SO_2 electrolyser environment.

The aim of this chapter is to evaluate both covalently and ionically cross-linked PBI blend membranes for use in low temperature (<100°C) SO_2 electrolysis. Firstly both types of membranes were tested for acid stability [7,8] simulating the acidic environment of the electrolyser. Weight change, swelling and FTIR analysis were used to characterise the effect of the acidic medium on the membranes. Characterisation of the membranes in an operating electrolyser was performed by polarisation curves, voltage stepping and long term operation (> 200 h).

6.2 EXPERIMENTAL

As sulphuric acid is produced in the SO_2 electrolyser, the acid stability of any membrane to be used in the electrolyser has to be tested. After determining the acid stability, MEAs were made from the selected membranes before evaluating these membranes in an electrolyser. Polarisation curves were used for the evaluation of the membranes' performances after which the MEA stability, for long term operation, was determined. This section will describe i) how the membranes were synthesised, ii) how the acid stability was determined and iii) how the selected membranes were evaluated in the SO_2 electrolyser.

6.2.1 MEMBRANE SYNTHESIS

Two series of membranes were synthesised for testing in the SO_2 electrolyser. The first series (abbreviated as series A, see Table 6.1) comprised blends of F_6PBI and PBIOO with a phosphonated PBI entitled PWN, which is ionically cross-linked between the phoshonated polymer and the F_6PBI by proton transfer from the phosphonic acid group to the basic N of F_6PBI. The second series (abbreviated as series B, see

Table 6.2) consisted of covalently cross-linked blend membranes between F_6PBI and the CH_2Br group of bromomethylated PPO. The cross-linking reaction is shown in Figure 6.1.

The main differences between Series A and series B were the blending polymers used and the type of cross-linking. The same F_6PBI polymer was used for both series, but the second polymer was either PWN (Series A) or PPOBr (Series B). One of these series A membranes (MJK-1898) contained PBIOO instead of F_6PBI, while the subscript used for PWN relates to the phosphonic groups carried by the pentafuorostyrene, *i.e.* 1 indicates a phosphonic group per pentafluorostyrene unit and 0.4 indicates that 4 pentafluorostyrene carries a phosphonic group for every 10 repeating units. Different mass or molar proportion of the blend components (as indicated in both Table 6.1and/or Table 6.2 b is used. The PBI membranes used in this chapter were supplied by the Institute of Chemical Process Engineering, University of Stuttgart, Germany.

Table 6.1: Summary of membranes tested under Series A

Membrane Name	Description	Mass or molar relation between PWM and F_6PBI	Basic polymer	Cross-linking polymer or acidic polymer
MVA175	Ionically cross-linked blend with phosphonated polymer as ionical cross-linker	PWN_1/F_6PBI 20/80 w/w Blend (Base-excess, HT)	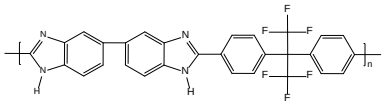	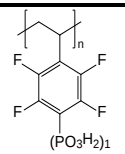
MVA176	Ionically cross-linked blend with phosphonated polymer as ionical cross-linker	PWN_1/F_6PBI 1eq/1eq Blend (equimolar, HT)	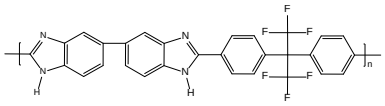	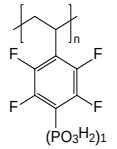
MJK-1895	Ionically cross-linked blend with phosphonated polymer as ionical cross-linker	PWN_1/F_6PBI 10/90 w/w Blend (Base-excess, HT)	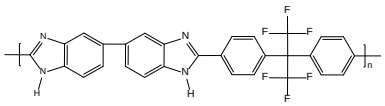	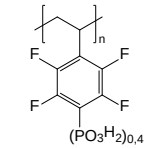
MJK-1896	Ionically cross-linked blend with phosphonated polymer as ionical cross-linker	$PWN_{0.4}/F_6PBI$ 20/80 w/w Blend (Base-excess, HT)	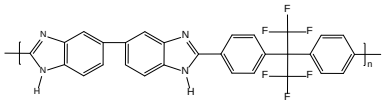	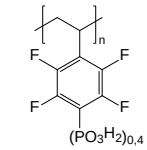
MJK-1898	Ionically cross-linked blend with phosphonated polymer as ionical cross-linker	$PWN_{0.4}$/PBIOO 20/80 w/w Blend (Base-excess, HT)	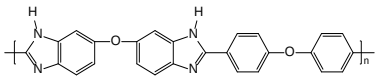	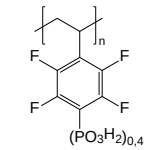

Table 6.2: Membranes tested under Series B.

Number of Sample	Description	Mass or molar relation between polymer 1 and polymer 2	Basic polymer	Cross-linking polymer or acidic polymer
MAK30b	Covalently cross-linked PBI blend	F_6PBI/PPOBr 90/10 w/w Blend (Base-excess, HT)	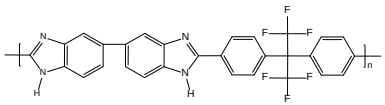	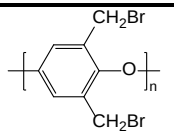
MAK31b	Covalently cross-linked PBI blend	F_6PBI/PPOBr 80/20 w/w Blend (Base-excess, HT)	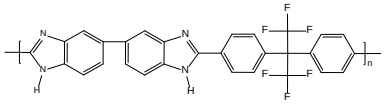	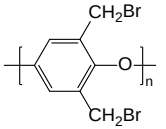
MAK32b	Covalently cross-linked PBI blend	F_6PBI/PPOBr 70/30 w/w Blend (Base-excess, HT)	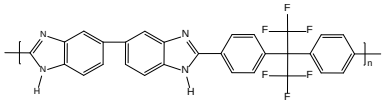	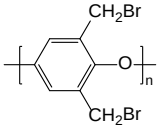
MAK33b	Covalently cross-linked PBI blend*	F_6PBI/PPOBr 60/40 w/w Blend (Base-excess, HT)	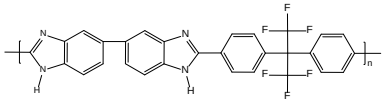	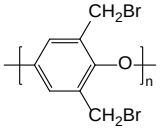

*See Figure 6.1:

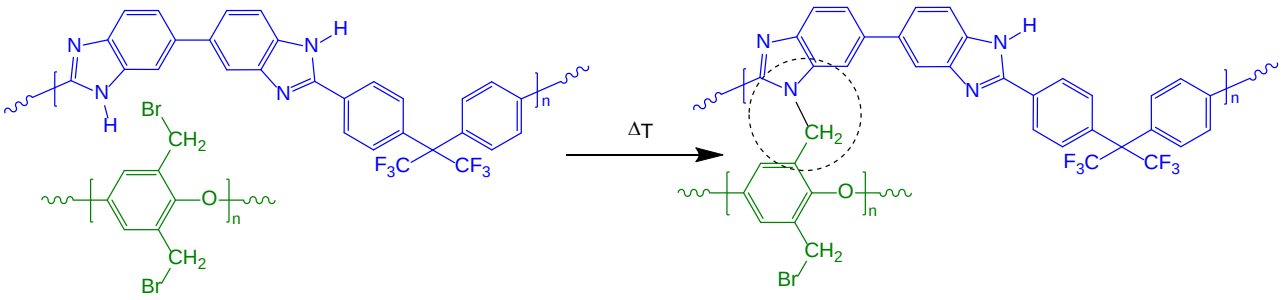

Figure 6.1: Cross-linking reaction between F_6PBI and the CH_2Br group of bromomethylated PPO.

6.2.2 ACID TREATMENT

All membrane samples were tested using an acid treatment step adopted from literature [8], which included membrane drying, acid treatment and again drying while the thickness and weight changes of each sample were recorded for each step. The membranes were placed in 80 wt% H_2SO_4 at 80°C for 120 h before drying the treated membranes in air at 80°C for 12 h.

6.2.2.1 MEMBRANE WEIGHT CHANGE AND SWELLING

Both the weight change (wt%) and membrane swelling (%) were recorded before and after acid treatment. Excess acid, from the acid treatment step, was removed by pressing the membrane sample between two paper cloths. This was repeated until no liquid was soaked up by the paper. The samples were then weighed using an Adams balance (PW Analytical grade, 0.0001 g). The starting membrane thickness was determined after the first drying step using a Mitutoyo digital micrometer (293 MDC-MX). The change in thickness was determined after the weighing step. All thickness measurements reported were the averages of at least 5 measurements across the entire membrane surface to ensure a true representation of the change in thickness.

6.2.2.2 FTIR

The ATR-FTIR spectra used in this study were obtained on a Bruker Alpha – P spectrometer with a resolution of 4 cm^2 [8]. FTIR was used to evaluate if the chemical structures of the membranes were affected by the presence of H_2SO_4.

6.3 SO_2 ELECTROLYSIS

6.3.1 GENERAL PROCEDURE

All membranes were pre-treated in 1M H_2SO_4 solution at 80°C for 90 min. to remove any solutions that might still be present within the membrane after synthesis. Membrane electrode assemblies (MEA) with an active area of 10 cm^2 were manufactured by hot-pressing two gas diffusion electrodes (GDEs) on either side of the membrane using a pressure of 50 kg cm^{-2} for 5 min at 120°C. The electrolysis for all membranes was evaluated using a system described previously [9]. Before electrolysis was performed the MEA had been doped using the same acid concentration used for the acid stability testing at 80°C for 24 h before cell assembly. All MEAs were kept at 80°C for 1 h. (within the electrolyser) before a beak-in step had been initiated at 0.1 A cm^{-2} for 20 min. Polarisation curves were obtained by increasing the current density by 0.01 A cm^{-2} every 90 s while recording the voltage. After the polarisation curve, the MEAs were kept at 0.1 A cm^{-2} for 24 h, after which another polarisation curve was taken. This operating procedure was controlled electronically using a Labview® based program which included the necessary safety checks such as shutdown when the voltage reached 1.05 V.

6.3.2 MEA DURABILITY

The term MEA durability can be interpreted in various ways. In this study the term MEA durability will focus on the membrane degradation aspect of MEA durability and not on the catalyst and gas diffusion durability. Two methods, used for both water electrolysers and fuel cells, were adapted from literature to determine the MEA durability (also known as accelerated stress tests – AST) of the best performing membrane, based on the general SO_2 electrolysis procedure described previously. Voltage stepping and steady state operation at constant current are well-known methods used in fuel cell systems for the evaluation of MEA stability [10–13]. It is known that both voltage stepping and constant current operation do influence the

catalyst's ability to facilitate the reaction but it will be shown that the effect of the catalyst degradation is not as significant, in this case, when compared to the membrane degradation.

6.3.2.1 VOLTAGE STEPPING

The voltage stepping method was done at 80°C for the three best performing membranes i.e. N115, MVA175 and MAK30b. The voltage was kept constant for 2 min while alternating between 0.9 and 0.3 V. The voltage was stepped between the higher 0.9 V limit to the lower 0.3 V limit 250 times while the current density was recorded every second. A schematic of the sequence is shown in Figure 6.2.

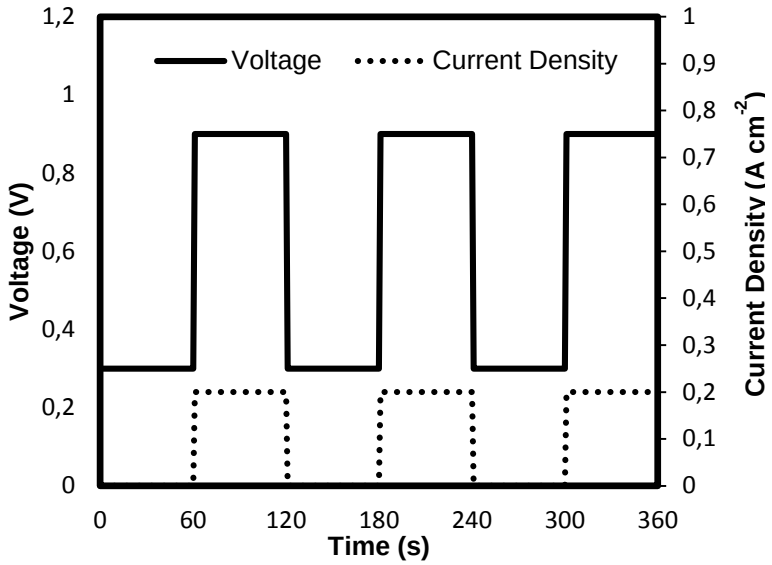

Figure 6.2: Voltage stepping sequence used in the membrane degradation test, current density shown on secondary axis.

6.3.2.2 STEADY STATE OPERATION

The best performing membranes (N115, MVA175 and MAK30b) were further evaluated using a steady state operation. The electrolyser was operated under a constant current of 0.1 A cm^{-2} at 80°C for 237 h while the voltage was recorded every 5 min.

6.4 RESULTS AND DISCUSSION

6.4.1 ACID TREATMENT

With the production of concentrated sulphuric acid within the SO_2 electrolyser it is necessary to evaluate the membrane stability of the proton exchange membranes in such environments before evaluating these membranes in the SO_2 electrolyser. The membrane weight and swelling were measured when exposed to concentrated H_2SO_4. FTIR was performed to determine if any chemical change had occurred during the acid exposure.

6.4.2.1 MEMBRANE WEIGHT AND SWELLING

It has previously been shown that pure PBIOO (Fuma-Tech) dissolved in high acidic environments (≈90 wt% H_2SO_4) while the stability could be improved when blending with a sulfonated ionomer, for example a sFS (partially fluorinated sulfonated arylene main-chain ionomer) co-polymer [7]. The chemical stability of the polyaromatic blend membrane from sFS with PBIOO has also been investigated and shown to be stable in the same acid environment used in this study i.e. 80 wt% H_2SO_4. By using TEM analysis [8] it was, however, shown that the blend membrane showed some sulfonation. When F_6PBI was used instead of PBIOO, no sulfonation of the F_6PBI blend component could take place, which was due to electron deficiency in this polybenzimidazole.

Figure 6.3 shows both the weight change and swelling percentages due to exposure to concentrated sulphuric acid for the various membranes tested.

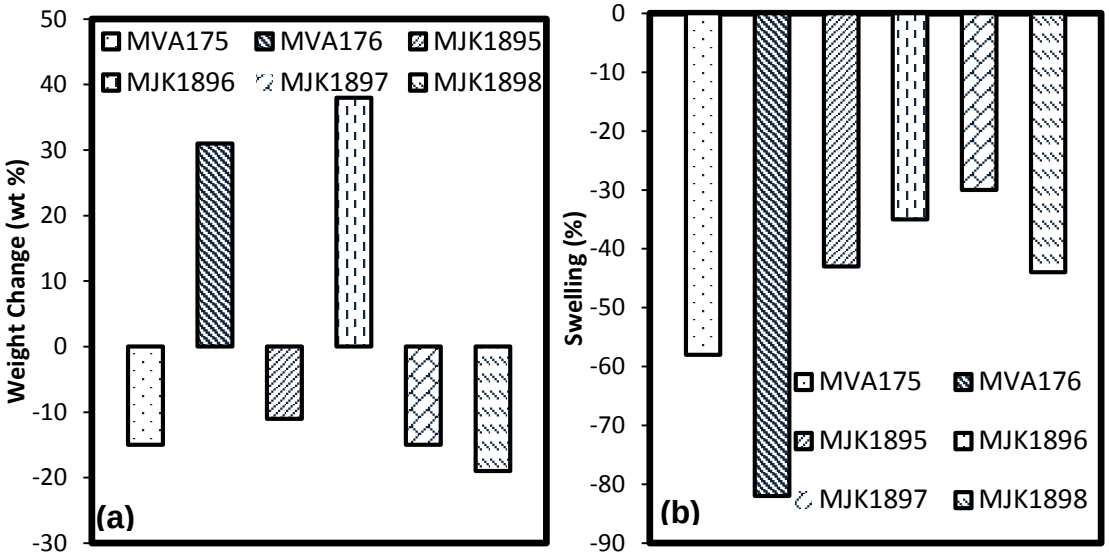

Figure 6.3: Membrane weight change (a) and swelling (b) due to acid treatment for series A.

The only difference between the MVA175, MVA176 and MJK1895 is the weight ratio between the two polymers used (PWN and F_6PBI or PBIOO– see Table 6.1). The weight increase of the MVA175 and MJK1985 can be due to formation of HSO_3^- salts of the PBI component by transfer of one proton of H_2SO_4 to the imidazole-N. The sulfonation of hydrogen sulphate salts of PBI-based polymers is known to occur during H_2SO_4 exposure [7]. Further weight loss can be due to the loss of short chain oligomers of the polymeric phosphonic acid component of the blend due to their (partial) water solubility, which is also present in other PBI-based ionically cross-linked blend membranes [7].

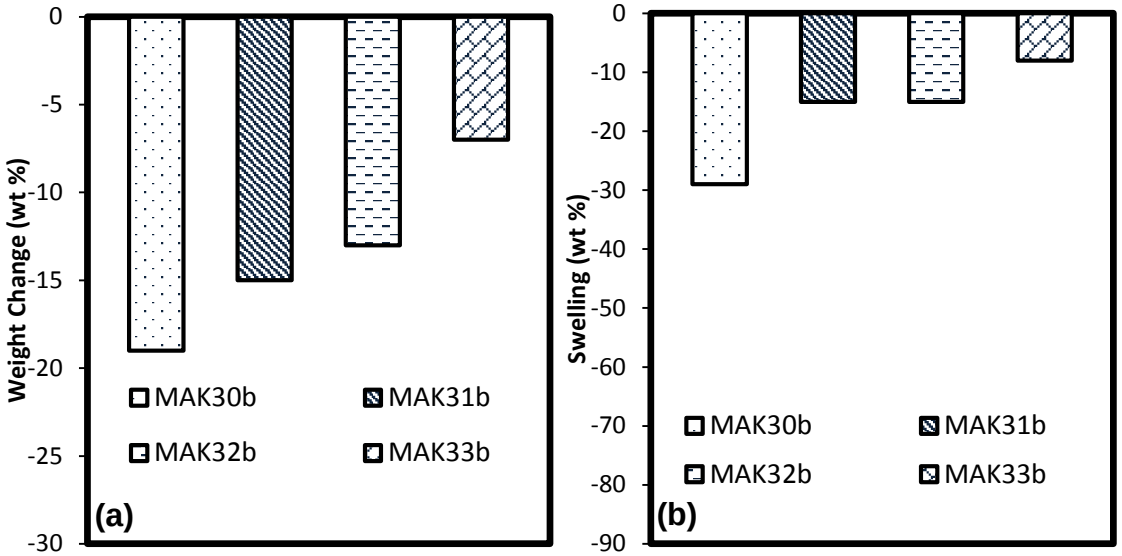

Figure 6.4: Membrane weight change (a) and swelling (b) due to acid treatment for series B.

Figure 6.4 shows the weight and swelling stability of the series B membranes in the presence of concentrated sulphuric acid. Although all the variation (Table 6.2) showed a decrease in weight it is however comparable with other PBI-blend membranes previously investigated. In the case of the Series B membranes it is highly probable that the partial sulfonation of the PPOBr blend component takes place (since PPO is an electron-rich aromatic polymer which can be easily sulfonated), which leads to partial dissolution of those PPOBr chains which are not included into the covalent network within the blend membrane. It turns out that the 32b membrane shows the optimal balance between cross-lining density and PPO content since these membranes report the lowest weight loss among all Series B membranes. As can be seen in Figure 6.4b, the swelling is reduced upon increase of cross-linking density.

6.4.2.2 FTIR

FTIR was performed of all the membrane samples to detect any chemical change due to the exposure to the concentrated sulphuric acid. As an example Figure 6.5 shows the spectra obtained before (MVA175_B & MAK30b_B) and after (MVA175_A & MAK30b_A) acid exposure.

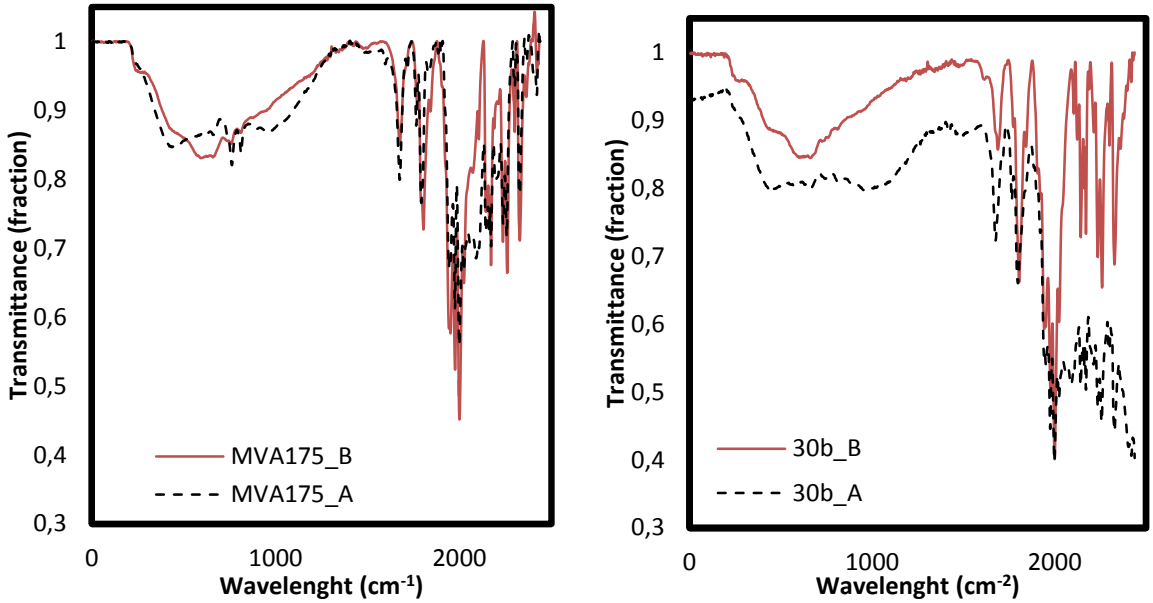

Figure 6.5: FTIR spectra obtained for MVA175 and MAK30b before and after exposure to concentrated H_2SO_4.

Although no significant difference in spectra is observed in the high wavelength region a small change is observed for the lower range. This range (640 – 1270 cm^{-1}) is indicative of the presence of H_2SO_4 within the membrane [14], which could still be present from the acid treatment, implying that it has not been washed out completely. The FTIR data for MJK1898 (not shown) shows a clear increase in the lower range (700 – 1300 cm^{-1}) which can be either H_2SO_4 (still present from the acid treatment) or HSO_3^- salts indicating a degree of sulfonation and which further supports the weight and swelling data presented in Figure 6.3(a) and (b). Series B FTIR data (not shown) show similar spectra i.e. increase in sulfonation component indicating that the electron rich polymers are sulfonated under these conditions.

6.4.2 SO_2 ELECTROLYSIS

6.4.2.1 MEA SCREENING

While acid treatment of the polymer membranes gives an indication of its chemical stability, it is not possible to predict its performance in the SO_2 electrolyser. To determine their performance, membrane electrode assemblies (MEAs) were made from all the polymer membranes tested for acid stability.

To determine the best MEAs, a combination of tests was conducted. The first test was to operate the electrolyser at a constant current of 0.1 A cm^{-2} for 20 min before starting a polarisation curve [9,15]. After the polarisation curve had been recorded, the MEA was kept at the 0.1 A cm^{-2} again for 24 h after which another polarisation curve was determined.

The first set of polarisation curves is shown in Figure 6.6. It should be mentioned that for Series A the MVA176 and MJK1986 did not survive the hot pressing and post MEA doping step. Both became brittle when stored before use, causing them to crack when sandwiched between the two graphite flow fields of the electrolyser. For the B series, membranes MAK32b and MAK33b did survive the hot pressing and MEA post-doping but could not maintain the 0.1 A cm^{-2} at a voltage below 0.999 V which is part of the break-in procedure and the rest of the testing protocol could not be followed.

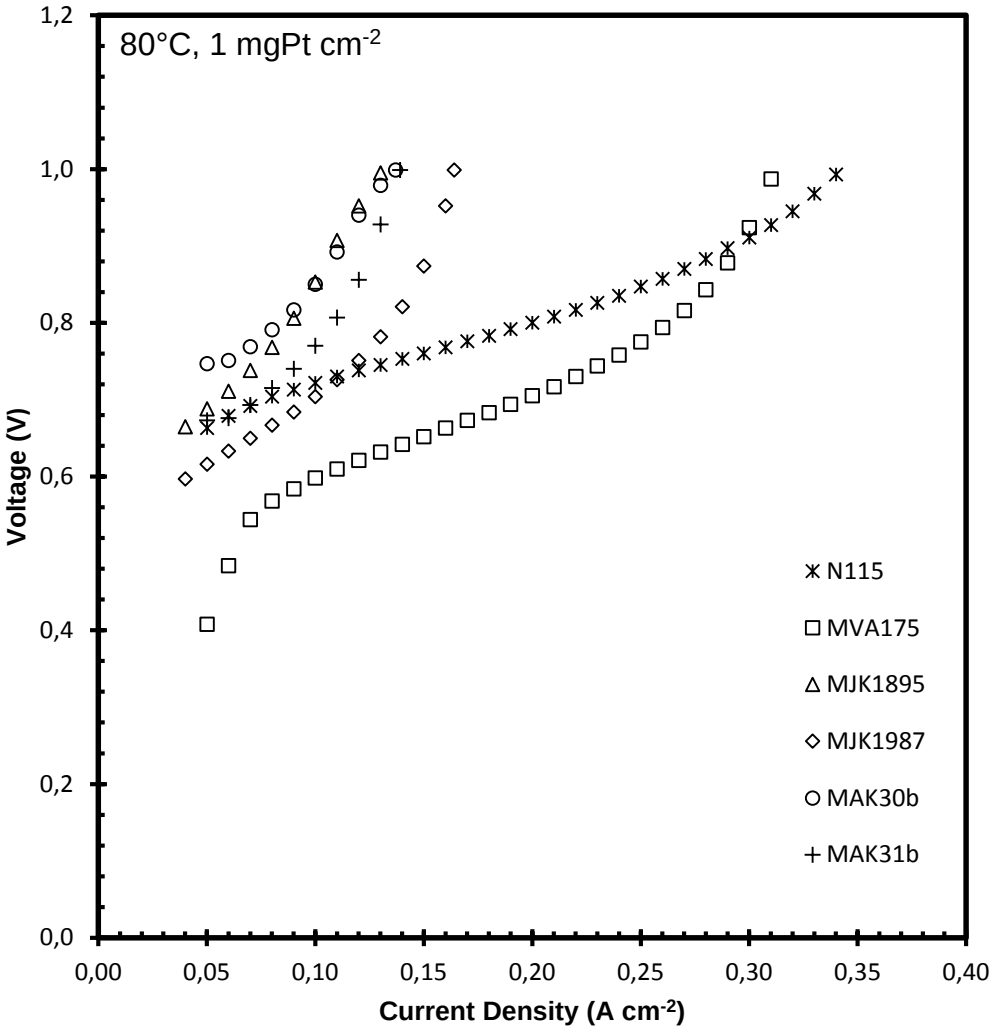

Figure 6.6: Polarisation curves for both Series A and B.

From Figure 6.6 it is clear that the MVA175 performed better than the N115 below a current density of 0.28 A cm^{-2} while the MJK1987 performed better below 0.1 A cm^{-2}. None of the B series membrane showed an improved performance over the commercial N115. Although an improvement could be achieved for MVA175 and MJK1987 over the N115, the operating voltage stability should also be investigated. The voltage stability at 0.1 A cm^{-2} was recorded over a 24 h period and is shown in Figure 6.7.

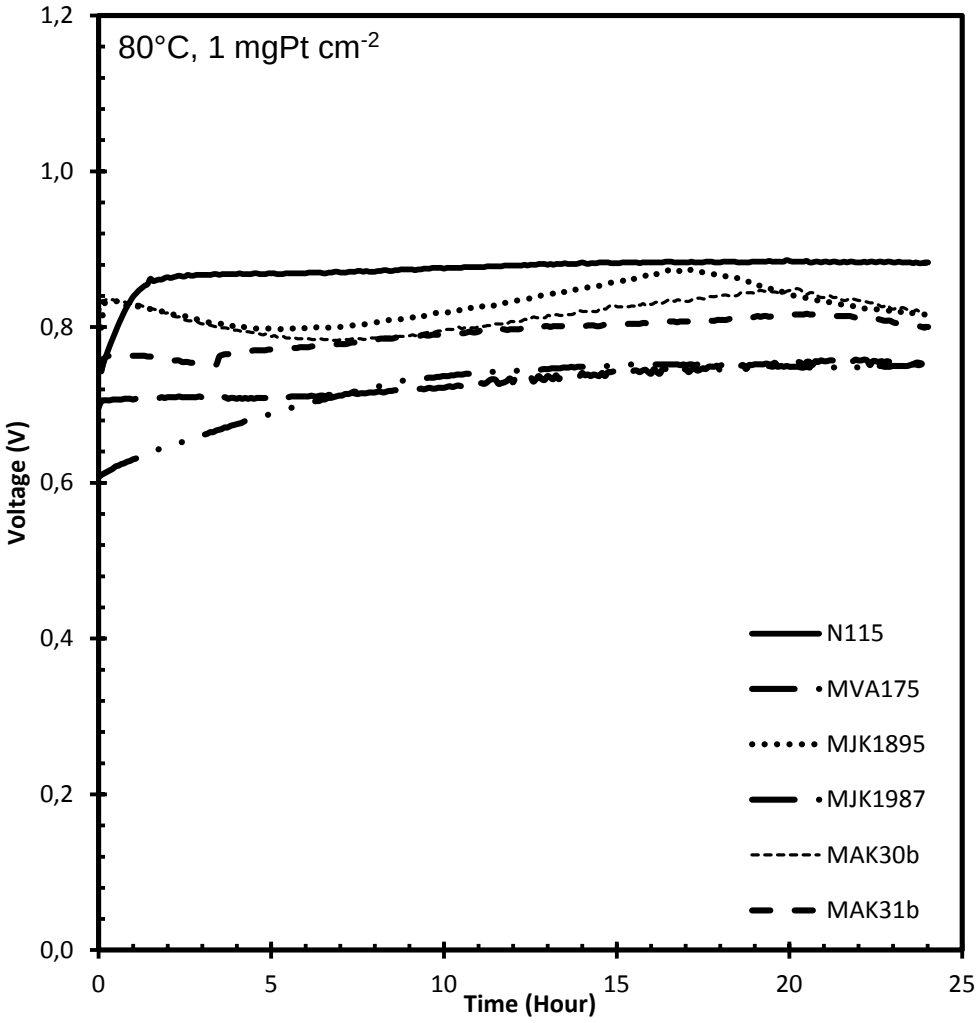

Figure 6.7: 24 h voltage stability at 0.1 A cm^{-2} for all membrane tested.

It can be seen that the operating voltage for the N115 is stable over the 24 h testing period. The voltage is noticeably lower for the PBI blend membranes tested, although the voltage seems to drift, e.g. for MJK1895 the voltage starts at a fairly high 0.836 V but drops to 0.784 V after 6.5 h and then increases again to 0.873 V over the next 10 h. It is noticeable that the voltage is lower for the PBI blend membranes for the constant current method although a higher voltage is recorded in the polarisation curve (Figure 6.6). One explanation for this could be that the membranes were conditioned after operation at a high current density (above 0.1 A cm^{-2}). A second polarisation curve was taken of all the membranes after the 24 h steady state operation, as shown in Figure 6.8. The first noticeable point is the poor polarisation performance of N115 after the 24 h period. The performance of the N115 returned to near exactly the same as the first polarisation curve (before the 24 h steady state operation) when a second polarisation curve was recorded. This

phenomenon could be explained by the dehydration of the PFSA membrane during the 24 h period, which could increase the membrane resistance. This is however not seen for the PBI-based materials.

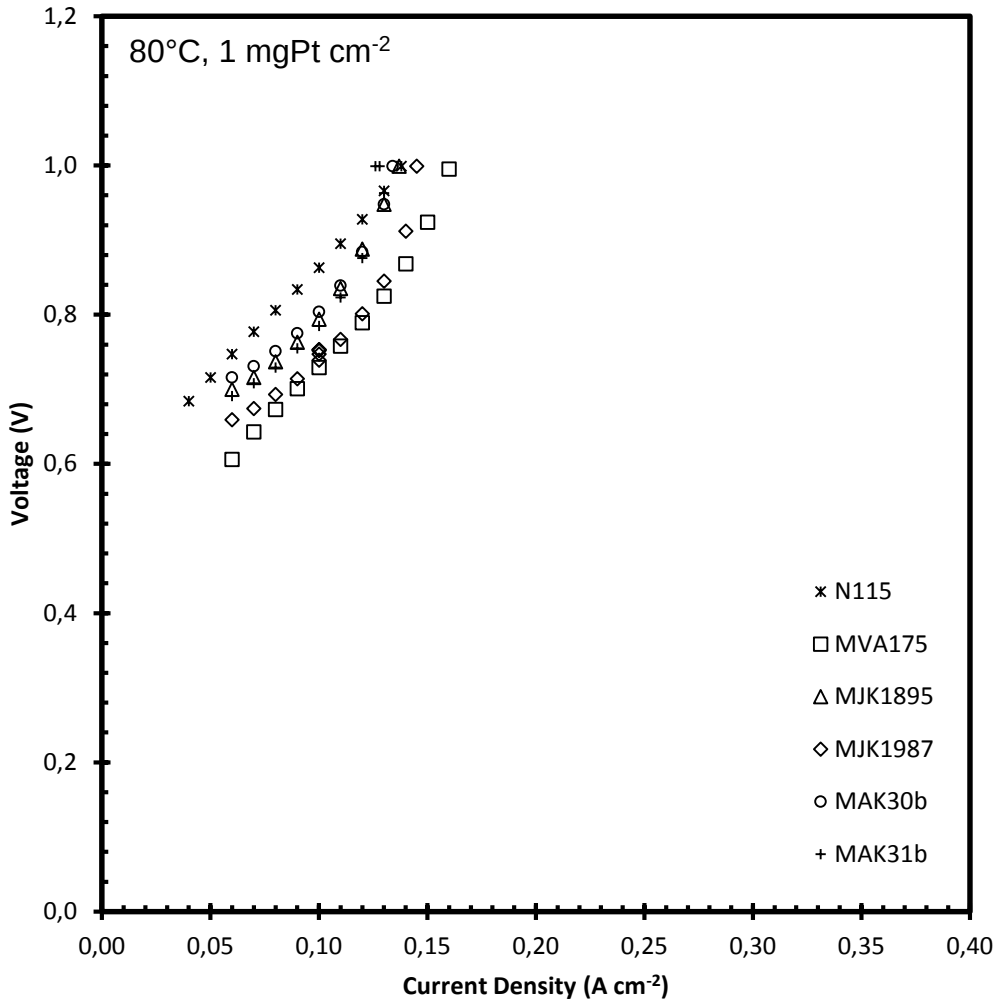

Figure 6.8: Polarisation curves for the membranes tested after the 24 h steady state operation at 0.1 A cm^{-2}.

For the series A membranes tested the MVA175 showed the worst second polarisation curve (reduction of 52% of the current density in the first polarisation curve) while the series B membranes seemed stable with a reduction of only 10% for MAK31b.

6.4.2.2 VOLTAGE STEPPING

After the polarisation curve and constant current of all the membranes had been achieved, a membrane degradation study, known as voltage stepping, was done. This method is different from the well-known cyclic voltammetry (usually performed for catalyst evaluation by increasing the voltage per second, mV s^{-1}) by holding the cell voltage at two pre-selected points and times, usually a low and high value. This increases the stress under which the MEA operates and promotes degradation. For this study the two voltage points used were 0.3 and 0.9 V for 2 min. Three membranes (best of series A, B and N115 as standard) were selected, based on their polarisation curves for this test i.e. N115, MVA175 and MAK30b. A cycle consisted of keeping the MEA at 0.3 for 2 min and then at 0.9 V for another 2 min. All MEAs tested were subjected to 250 cycles to determine the membrane stability under increased stress conditions. Figure 6.9 shows the current density achieved as a function of voltage cycles.

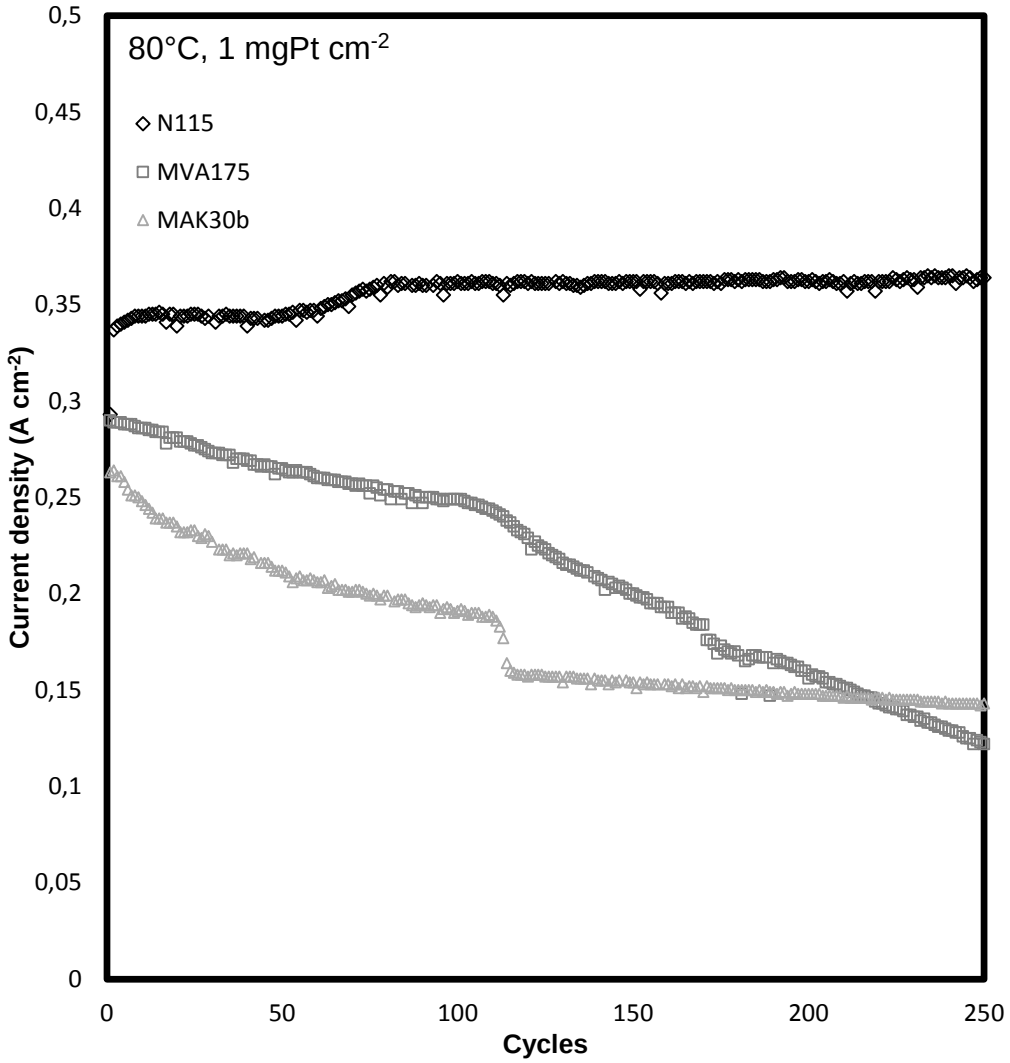

Figure 6.9: Current density (A cm^{-2}) as a function of the voltage cycling.

The assumption that the reduced current density is due to the membrane degradation rather than catalyst degradation is supported (at least for the number of cycles used in this study) by the N115 data. If the catalyst would degrade the N115 data would also show signs of reduced current density. The fact that the current density is constant for the 250 cycles shows that the catalyst is also stable for this number of cycles.

Since the degradation of the current density is due to the membrane it is clear that the Nafion® has sufficient stability while the PBI blend membranes show degradation. A clear reduced performance can be identified for both MVA175 and MAK30b at 110 cycles. A steady decrease in current density is observed for

MVA175 while MAK30b shows a sharp decrease in performance from cycle 107 to 115, after which a near steady operation is observed. This shows that voltage stepping can be used in not only determining membrane stability but also in membrane selection.

Polarisation curves were recorded before and after the voltage stepping as shown in Figure 6.10. A reduced performance for the PBI-blend membrane is clear and expected in view of the results presented in Figure 6.9. It is interesting to note that the current density reached for the polarisation curve of N115 is higher than before the voltage stepping, suggesting that the membrane performance is improved rather than degraded over the 250 cycles tested.

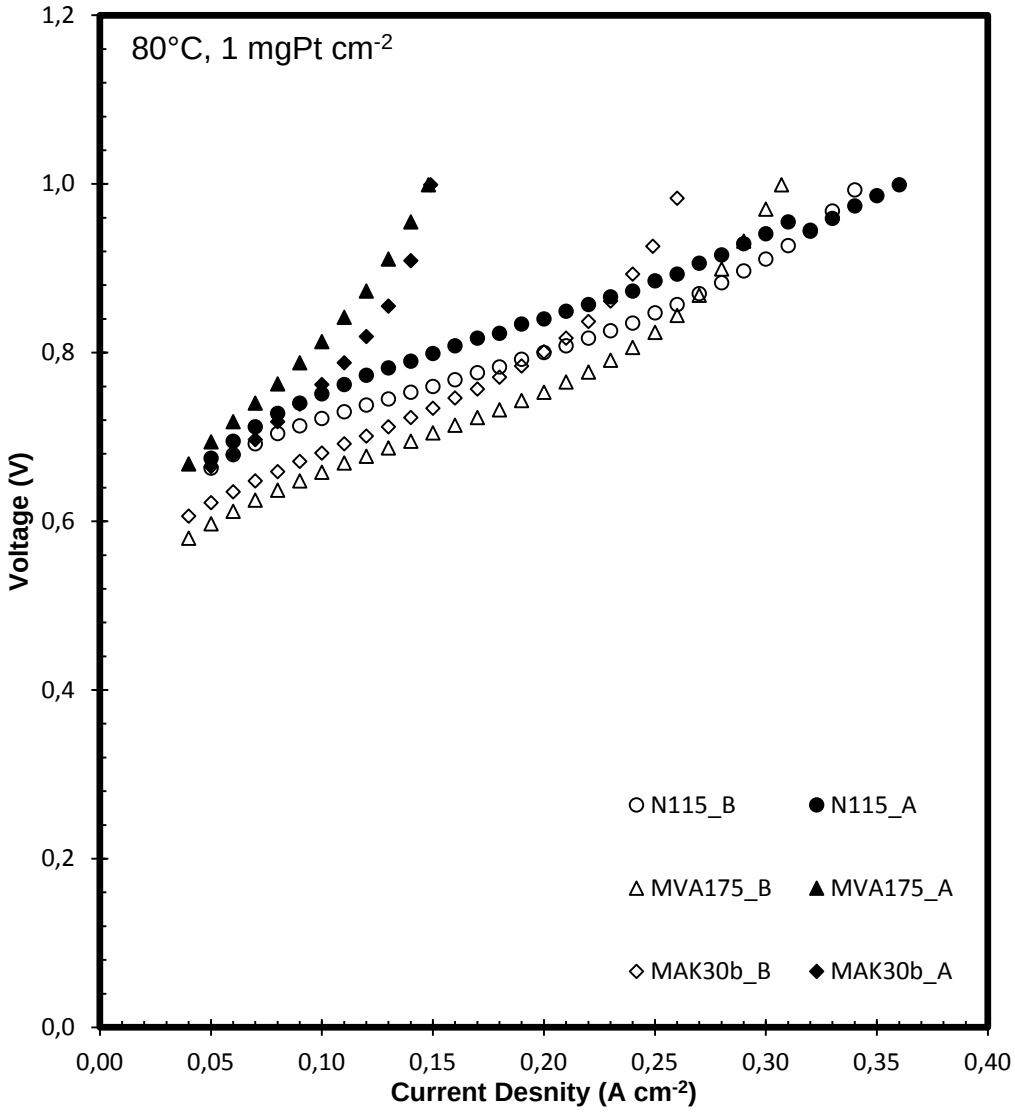

Figure 6.10: Polarisation curves before (B) and after (A) voltage stepping.

Although the PBI blend membranes showed degradation using the voltage stepping method, it is however difficult to extrapolate to the duration for which the membrane can be operated at a fixed current density before an unacceptable voltage would be reached (20% increase in voltage for example).

6.4.2.3 OPERATING STABILITY

Another method of testing proton conductive membranes is to operate the electrolyser at a constant reaction rate (current density) while recording the voltage as a function of time. Figure 6.10 shows the voltage response of the three membranes tested in the voltage stepping section for 70, 158 and 238 h for N115, MAK30b and MVA175, respectively. Due to the non-linearity of the voltage increase it is difficult to report a voltage decrease as a function of time, as is customary for this type of test. It can however be said that the MVA175 membrane showed a better voltage response than both the N115 and MAK30b up to 70 h, reaching a maximum voltage of 0.782 V compared to 0.841 V and 0.817 V for N115 and MAK30b, respectively. The voltage increased drastically for MAK30b after the 70 h period reaching 0.856 V after 155 h. The operating voltage for the MVA175 membrane seemed to stabilise after 130 h. The wavelike variation of the voltage over time has previously been reported for other membranes as well, and could therefore be characteristic of this type of SO_2 electrolyser.

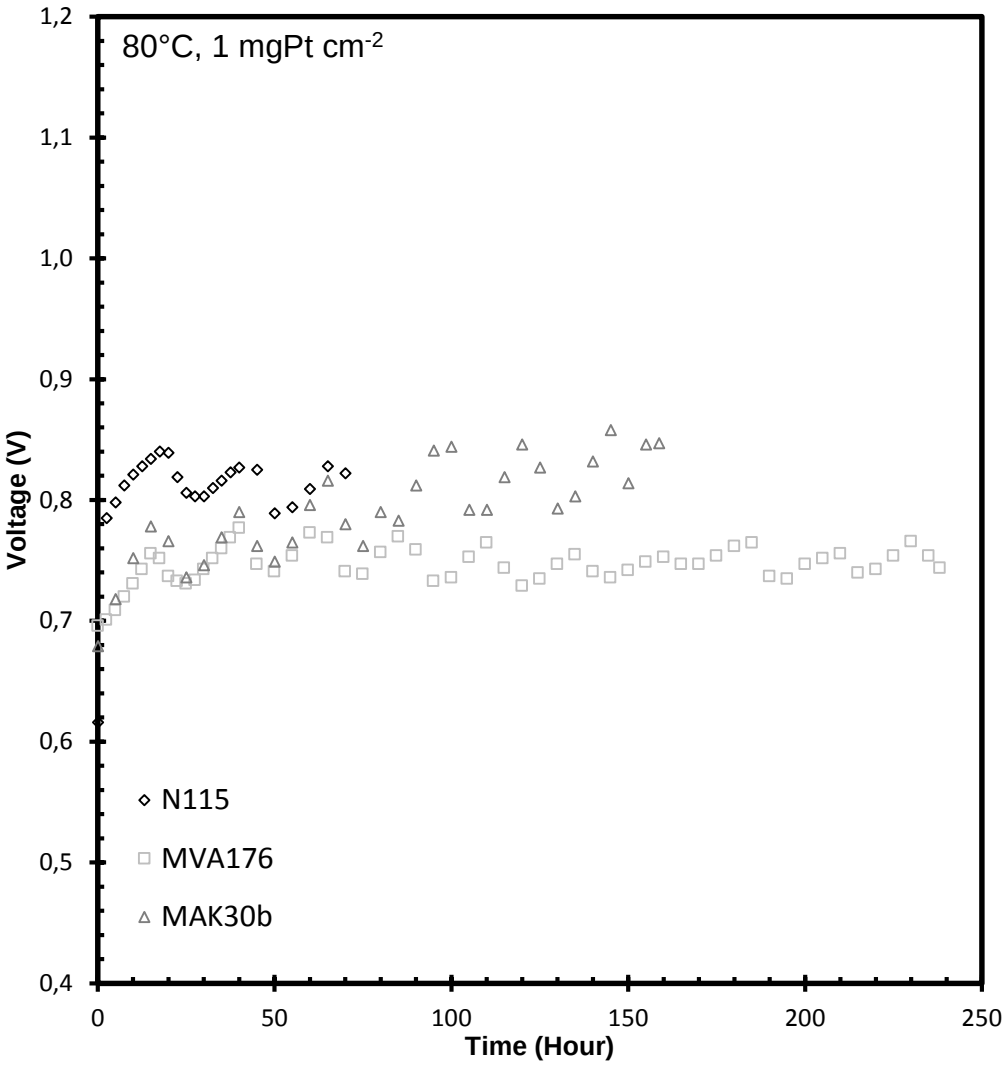

Figure 6.11: Voltage stability of N115, MVA175 and MAK30b at 0.1 A cm^{-2}.

Although it has been shown that various parameters influence the operating voltage, such as temperature, differential pressure, catalyst loading and membrane thickness when PFSA membranes are used, other parameters need further investigation when using PBI-based membranes, such as acid doping, acid content in the membrane and high operating temperature (>100°C), to name a few. For this method of operating the electrolyser, i.e. using a liquid cathode, it is possible that the acid within the membrane is removed by the water and must be replaced with the acid produced by the reaction. Although the membrane degradation is not as apparent in the long term operation as in the voltage stepping technique, it is still a valuable test to identify possible membranes to be used in the SO_2 electrolyser. Further studies would be required to be able to evaluate the PBI based membrane in a low liquid

water environment. Two modes of operation would be available, i.e. either by operating the electrolyser, with a PBI membrane, using SO_2 dissolved in sulphuric acid, or using humidified SO_2 as anode feed at high temperatures.

6.5 CONCLUSION

The characterisation of various PBI-blend polyaromatic membranes was shown for the application in a SO_2 depolarised electrolyser system. Weight and membrane swelling showed that chemical stability of the blend membranes were reasonable when treated in concentrated sulphuric acid. Polarisation curves showed that most of the synthesised membranes were able to operate in the acidic environment. Stable voltage values were obtained, in the membrane selection step over a 24 h period. The selected membranes were subjected to voltage stepping, which showed that both PBI membranes showed a gradual decline up to 100 cycles. A strong decrease was observed after the 100 cycles for the next 10 cycles, after which another steady decline was observed. The N115 showed a slight improvement over the 250 cycles tested. Long term operation at 0.1 A cm^{-2} showed an overall higher voltage for N115 (for the 0 – 70 h time region) while the MAK30b membranes' voltage increased significantly after 7 h of operation. Further studies would be required to further increase the advantage of the PBI membranes over PFSA, such as either operating the electrolyser using SO_2 dissolved in H_2SO_4 as anode feed, or increasing the operating temperature (>100°C) using humidified SO_2 gas as anode feed.

6.6 REFERENCE

[1] Carmo M, Fritz DL, Mergel JJ, Stolten D. A Comprehensive review on PEM electrolysis. Int J Hydrogen Energy 2013;38:4901–34. doi:10.1016/j.ijhydene.2013.01.151.

[2] Brecher LE, Spewock S, Warde CJ. The Westinghouse Sulfur Cycle for the thermochemical decomposition of water. Int J Hydrogen Energy 1977;2:7–15. doi:http://dx.doi.org/10.1016/0360-3199(77)90061-1.

[3] Gorensek MB, Summers WA. Hybrid Sulfur flowsheets using PEM electrolysis and a bayonet decomposition reactor. Int J Hydrogen Energy 2008;34:1–18.

[4] Gorensek MB. Hybrid Sulfur cycle flowsheets for hydrogen production using high-temperature gas-cooled reactors. Int J Hydrogen Energy 2011;36:12725–41.

[5] Sivasubramanian P, Ramasamy RP, Freire FJ, Holland CE, Weidner JW. Electrochemical hydrogen production from thermochemical cycles using proton exchange membrane electrolyzer. Int J Hydrogen Energy 2007;32:463–8.

[6] Li Q, Jensen JO, Savinell RF, Bjerrum NJ. High temperature proton exchange membranes based on polybenzimidazoles for fuel cells. Prog Polym Sci 2009;34:449–77.

[7] Schoeman H, Krieg HM, Kruger AJ, Chromik A, Krajinovic K, Kerres J. H2SO4 stability of PBI-blend membranes for SO_2 electrolysis. Int J Hydrogen Energy 2012;37:603–14.

[8] Peach R, Krieg HM, Krüger AJ, van der Westhuizen D, Bessarabov D, Kerres J. Comparison of ionically and ionical-covalently cross-linked polyaromatic membranes for SO_2 electrolysis. Int J Hydrogen Energy 2014;39:28–40.

[9] Peach R, Krieg HM, Kruger AJ, Chromik A, Krajinovic K, Kerres J. Comparison of ionically and ionical-covelently cross-linked polyaromatic membranes for SO_2 electrolysis. Int J Hydrogen Energy 2014;39:28–40.

[10] Zhang S, Yuan X, Wang H, Mérida W, Zhu H, Shen J, et al. A review of accelerated stress tests of MEA durability in PEM fuel cells. Int J Hydrogen Energy 2009;34:388–404. doi:http://dx.doi.org/10.1016/j.ijhydene.2008.10.012.

[11] Yuan X-Z, Li H, Zhang S, Martin J, Wang H. A review of polymer electrolyte membrane fuel cell durability test protocols. J Power Sources 2011;196:9107–16. doi:http://dx.doi.org/10.1016/j.jpowsour.2011.07.082.

[12] Yuan X-Z, Zhang S, Sun JC, Wang H. A review of accelerated conditioning for a polymer electrolyte membrane fuel cell. J Power Sources 2011;196:9097–106. doi:http://dx.doi.org/10.1016/j.jpowsour.2011.06.098.

[13] Grigoriev SA, Dzhus KA, Bessarabov DG, Millet P. Failure of PEM water electrolysis cells: Case study involving anode dissolution and membrane thinning. Int J Hydrogen Energy 2014. doi:10.1016/j.ijhydene.2014.05.043.

[14] Elvington MC, Colon-Mercado H, McCatty S, Stone SG, Hobbs DT. Evaluation of proton-conducting membranes for use in a sulfur dioxide depolarized electrolyzer. J Power Sources 2010;195:2823–9.

[15] Krüger AJ, Krieg HM, van der Merwe J, Bessarabov D. Evaluation of MEA manufacturing parameters using EIS for SO_2 electrolysis. Int J Hydrogen Energy 2014. doi:10.1016/j.ijhydene.2014.09.012.

CHAPTER 7: EVALUATION AND RECOMMENDATIONS

7.1 INTRODUCTION

As presented in Chapter 1, the aim of this study was twofold: i) to determine the influence of specific variables (operating conditions, MEA manufacturing and H_2S contamination) on the performance of the SO_2 electrolyser using Nafion® as benchmark and ii) to investigate the suitability of PBI-based membranes for SO_2 electrolysis. While a conclusion was presented within each experimental chapter, it is the purpose of this chapter to summarize and evaluate the key findings obtained during the study, followed by recommendations for possible further studies.

7.2 NAFION AS BENCHMARK – CHAPTERS 2 - 4

As mentioned in *Chapter 1*, the objective of building an automated SO_2 electrolyser system to facilitate the safe operation was completed as described in Appendix A. The automation of the system contributed to improved operational safety and efficiency, as well as data processing. The automated sequences, as described in Appendix A, allowed for the system to be operated from start to end of an experiment entirely without supervision.

Chapter 2 investigated the influence of various operating parameters on the SO_2 electrolyser (using a 25 cm^2 active area cell), such as hot pressing pressure, cell temperature, membrane thickness, catalyst loading, membrane type and SO_2 feed concentration (diluted with N_2). An additional operating method was also investigated which used SO_2-saturated H_2SO_4 (as anode supply) and clean H_2SO_4 (as cathode supply) [1]. The effect of cell temperature, membrane thickness and acid concentration was investigated for this operating method. Of these parameters tested, the factors which had the most influence were cell temperature, membrane thickness and SO_2 concentration. A temperature above 80°C was preferred. In addition it was shown that PFSA was ideally operated under water saturated conditions, a high catalyst loading (around 1 mgPtB cm^{-2}) using thin membranes (N115 vs. N1110) [2]. High cell resistance was observed when using SO_2-containing H_2SO_4 as anode supply, which was ascribed to the restricted mass transport of SO_2 through the viscous acid.

A detailed investigation (*Chapter 3*) comprising the separation of the charge transfer resistance, ohmic resistance and mass transport limitations using EIS analysis, revealed that the activation resistance was a function of cell temperature (which was expected), catalyst type (Pt/C vs. PtB), catalyst particle size and hot pressing pressure. The ohmic resistance, which relates to the membrane resistance and thus to its conductivity, was mostly influenced by the cell temperature and membrane thickness, while the mass transport limitations were affected by the cell temperature and hot pressing pressure used in the MEA manufacturing step. According to these results the operating point where the electrolyser can be operated at its highest efficiency would be at high cell temperatures (>100°C) with the optimised MEA manufacturing procedure (as determined in Chapter 2) preferably by using thin membranes.

The voltage degradation, i.e. voltage increase during electrolysis, observed in *Chapter 4*, due to a low level (ppm) H_2S contamination, when the anode was conditioned with SO_2 before exposing it to H_2S, was not as detrimental to the SO_2 electrolysis as has been reported in the PEMFC literature, when Pt/C was used as catalyst [3]. It is clear from this that it is important to operate the SO_2 electrolyser using "clean" SO_2 before exposing the anode to any level of H_2S. Although an increase of, for example 63 mΩ (charge transfer resistance), which was observed after operating at 0.1 A cm^{-2} for 60 min, is significant it could be reduced by operating the electrolyser at further optimised conditions, which according to Chapters 2 and 3, could be by increasing the operating cell temperature or by using alternative catalysts.

7.3 PBI-BASED MEMBRANES - CHAPTERS 5 AND 6

The results in *Chapters 5 and 6* have confirmed that PBI-based membranes were stable in an H_2SO_4 environment, as well as being suitable for SO_2 electrolysis. Although various parameters were tested, the results reported in these chapters show that the most influential factors for the overall SO_2 electrolysis performance included the MEA doping procedures, MEA activation sequence, membrane thickness and blending ratios of the different polymers involved.

The MEA doping procedure was evaluated in *Chapter 5* for a specific PBI-blended membrane (MJK 1753), which formed the basis for *Chapter 6*. The data obtained for different membrane thicknesses did not show similar tendencies (where thinner membranes had improved performance) as when using PFSA-based materials i.e. thinner membranes having improved performance. An optimal thickness is however possible where a balance between SO_2 crossover and membranes resistance needs to be established to provide the desired cell efficiency and voltage stability [4]. An additional activation step (voltage cycling) showed improved cell performance, increasing the current density obtainable (at 80°C) by almost 10%.

The influence of blending the PBI-based membrane with various fluorinated polymers was investigated in *Chapter 6*. By varying the two blending polymers, poly(2,6-dimethylbromide-1,4-phenylene oxide) (PPOBr) and poly(tetrafluorostyrene-4-phosphonic acid) (PWN), with the PBI component (F_6PBI) it was shown that using 20/80 wt% PWN/F_6PBI and 10/90 wt% F6PBI/PPOBr combinations, the highest stability, as well as SO_2 electrolysis performance was obtained.

7.4 NAFION vs. PBI MEMBRANES

With the focus on Nafion in Chapters 2 - 4 and PBI in Chapters 5 & 6, respectively the question of the comparison of the performances of the Nafion® and PBI-based membranes arose. From the results obtained it is clear that the Nafion was chemically more stable than the PBI-based membranes, while PBI-based membranes showed similar to better performance than Nafion in the SO_2 electrolyser. However, Nafion® would be the preferred choice when operating at temperatures below 100°C due to its commercial availability.

While all PBI-based membranes used in this study were prepared for scientific purposes and are not yet commercially available, various institutions worldwide (Sandia National Laboratory (SNL), Case Western Reserve University and Clemson University) are focussing on the development and production of PBI-based membranes. In addition the number of possibilities is in essence endless when considering the numerous possible blending polymers and ratios that can be varied. It is however clear that the most important advantage, and hence reason, for including PBI-based membranes in this study is their suitability at higher

temperatures [5]. While this study demonstrated comparable results when using Nafion and PBI-based membranes ≤80°C, it is clear that above 100°C, as would be optimal for SO_2 electrolysis [5], Nafion will not be stable. While it was not the purpose of this study to investigate high temperature SO_2 electrolysis, a recent study in our group (unpublished) clearly shows the influence when comparing a Nafion 115 to the most recently developed PBI-based membrane provided by the group of Dr Kerres (University of Stuttgart). According to Figure 7.1, this optimised membrane outperformed the Nafion, especially at high current densities, both at 80°C and at 95°C, showing the substantial potential of these membrane materials.

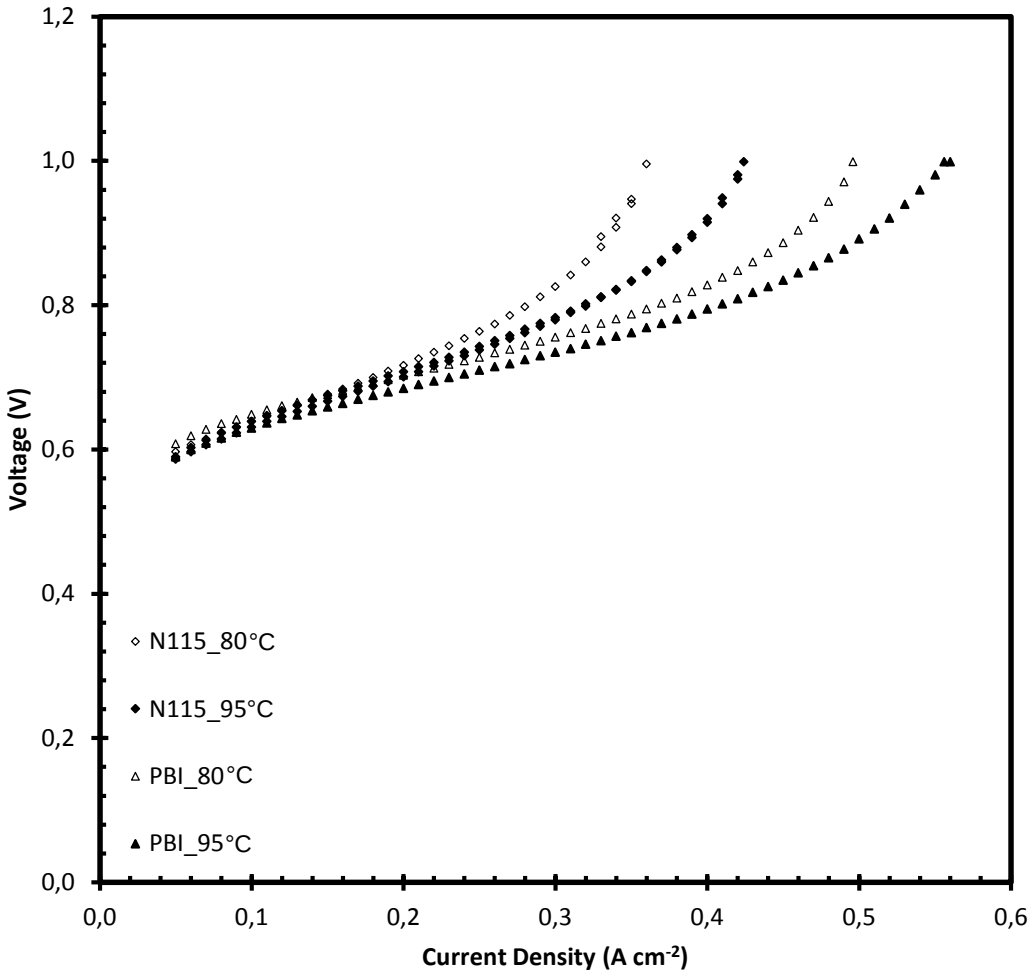

Figure 7.1: Comparison between SO_2 electrolysis polarisation curves for N115 and a novel PBI membrane blend at 80 and 95°C.

7.5 RECOMMONDATIONS

While the aim and objectives of this study have been attained, various opportunities for further research on SO_2 electrolysis became apparent during this study.

- While according to literature current densities as high as 1 A cm^{-2} have been attained when operating the SO_2 electrolyser using a pressure differential, lower acid concentrations were however attained. The acid concentration can possibly be increased at 1 A cm^{-2} and acceptable operating voltages by increasing the cell temperature, which would decrease the charge transfer resistance.

- For elevated pressure differentials, re-enforced PFSA-based membranes, which are currently emerging from industry for the application in electrochemical hydrogen compression, might be suitable.

- An aspect that has not received significant attention both in this study and in literature is the further development of catalysts with faster SO_2 oxidation kinetics and long term stability, possibly including non-PGM metals which would reduce the overall costs of this process.

- When the SO_2 supply to the electrolyser is contaminated with other gases such as H_2S, alternative catalyst materials could be developed that are more prone to withstand poisoning such as platinum-ruthenium combinations. However, the challenge would be to find catalysts that do not reduce sulfur adsorption.

- High temperature SO_2 electrolysis (> 100°C) must be developed to reduce the kinetic and ohmic resistances of the electrolyser.

- For the high temperature application, PBI-based membranes can be used. However, for the extreme conditions within the electrolyser at higher temperatures (120 – 160°C), the suitability of the membranes has to be established. Simultaneously, alternative MEA manufacturing techniques

would be required to replace the Nafion that is currently used as binder during MEA manufacturing.

- Membrane acid treatment, currently being done at 80°C, must be performed at temperatures of at least 120°C to evaluate chemical stability.

- Apart from the variables evaluated in this study, further MEA parameters should be optimised to ensure the lowest overall MEA resistance. These could include i) the optimisation of membrane blend combinations (PBI / sulfonated polymer ratios), ii) selecting the use of CCMs (catalyst coated membranes) over GDEs, iii) binder selection for the catalyst ink preparation (must be stable in acidic environment while being able to conduct protons at elevated temperatures) and v) determine the optimal SO_2 / water vapour ratio needed to produce the highest acid concentration possible while operating at acceptable voltage and current densities.

7.6 References

[1] Lee S-K, Kim C-H, Cho W-C, Kang K-S, Park C-S, Bae K-K. The effect of Pt loading amount on SO_2 oxidation reaction in an SO_2-depolarized electrolyzer used in the hybrid sulfur (HyS) process. Int J Hydrogen Energy 2009;34:4701–7.

[2] Staser JA, Weidner JW. Effect of Water Transport on the Production of Hydrogen and Sulfuric Acid in a PEM Electrolyzer. J Electrochem Soc 2009;156:B16–21.

[3] Mohtadi R, Lee W-K, Van Zee JW. The effect of temperature on the adsorption rate of hydrogen sulfide on Pt anodes in a PEMFC. Appl Catal B Environ 2005;56:37–42. doi:10.1016/j.apcatb.2004.08.012.

[4] Kruger AJ, Cichon P, Kerres J, Bessarabov D, Krieg HM. Characterisation of a polaromatic PBI blend membrane for SO2 electrolysis. Int J Hydrogen Energy 2015:1–12. doi:http://dx.doi.org/10.1016/j.ijhydene.2014.12.081.

[5] Jayakumar JV, Gulledge A, Staser JA, Kim C-H, Brian C B, Weidner JW. Polybenzimidazole Membranes for hydrogen and sulfuric acid production in the Hybrid Sulfur Electrolyzer. ECS Electrochem Lett 2012;1:F44–8.

APPENDIX A: SYSTEM AUTOMATION

A – 1 INTRODUCTION

In this appendix the automation process needed to accurately and safely operate the SO_2 electrolyser system used in this study is discussed. Firstly, the electronically controlled hardware is discussed (A - 2) followed by the Labview® (manufactured by National Instruments) interface and the general coding used to execute operation (A - 3).

A – 2 ELECTRONICALLY CONTROLLED HARDWARE

The list of electronically controlled hardware presented in Table A - 1 is based on the general setup used in this study (see Figure 2.1 Chapter 2, page 21). The hardware used for automation in the setup was carefully selected to only use a 4 – 20 mA signal input/output. When considering the thermal mass flow meters for example, which were used to control the flow of the gases, the set point of the meter was given by a current between 4 – 20 mA with 4 mA being the lowest flow rate, i.e. 0 nL min^1 and 20 mA corresponding to the flow controllers' highest flow rate, i.e. 2 nL min^{-1}. As the relationship between the current and the calibrated flow rate is linear, it is easy to calculate the required current for any flow rate. This concept is also applicable to the liquid pump.

Table A - 1: Electronically controlled hardware used in the SO_2 electrolyser that was automated using Labview®.

Item	Description	Communication Method	Input (mA)	Output (mA)	Operating Range	Power Required
PS	Power Supply	RS-232	VISA*	VISA	12.5V – 60A	12 Vdc
MFC1/2/3	Thermal Mass Flow Controller	Analog	4 – 20	4 – 20	0 – 1 nL/min^{+}	24 Vdc
P4/5	Pressure Transducer	Analog	N/A	4 – 20	0 – 20 Barg$^{\#}$	12 Vdc
T	Thermocouple	Anaolog	N/A	0 – 20	0 – 700 °C	N/A
Liquid Pump	High rpm piston pump	Analog	4 – 20	4 – 20	0 – 2 L/min	240 VAC
NI-9174	Compaq Daq	Housing for modules	N/A	N/A	N/A	240 VAC
NI-9207	4 – 20 mA Input	Analog	0 – 20	N/A	N/A	N/A
NI-9265	4 – 20mA Output	Analog	0 – 20	N/A	N/A	N/A
NI-9211	Thermocouple module	Analog	0 – 100 Ω	N/A	N/A	N/A
NI-9481	Temperature Control	Digital	ON/OFF	ON/OFF	ON/OFF	N/A

*VISA – Visual Instrument Software Architecture

$^{+}$nL/min – Flow controller is calibrated at normalised (n) conditions which is 0 °C and 1 atm (atmospheric pressure)

$^{\#}$Barg – Indicates that the pressure is not normalised to atmospheric pressure

A – 3 PROGRAMMING

The Labview® program used in this study has two main features: the front panel (where the user operates) and the block diagram (where the program is written). Figure A - 1 shows a representation of the front panel design used in this study. It was designed is such a way that the most important information was always visible. The black highlighted section of Figure A - 1 mainly includes the operating voltage (V), current (A), current density ($A.cm^{-2}$), cell temperature (°C), SO_2 flow ($L\ min^{-1}$), heater ON/OFF, anode/cathode pressure (Barg) and the amount of points logged.

Both the red and yellow highlighted sections are part of the first tab (Controls – see white highlighted section). The red highlighted section provides general information regarding the current experiment provided by the user i.e. membrane type, electrodes used, cell temperature (°C), catalyst loading ($mgPt\ cm^{-2}$), as well as the suppliers of the membranes and the MEA parts used. The yellow highlighted section is divided in two sections, one for the power supply and pump inputs, such as the current set point (A), voltage limit (V), active area being used (cm^2), power supply ON/OFF, pump flow rate ($mL\ min^{-1}$) and the pump flow set point ($mL\ min^{-1}$), while the second part deals with the inputs for the cell temperature (°C) and SO_2 flow rate set point ($L\ min^{-1}$).

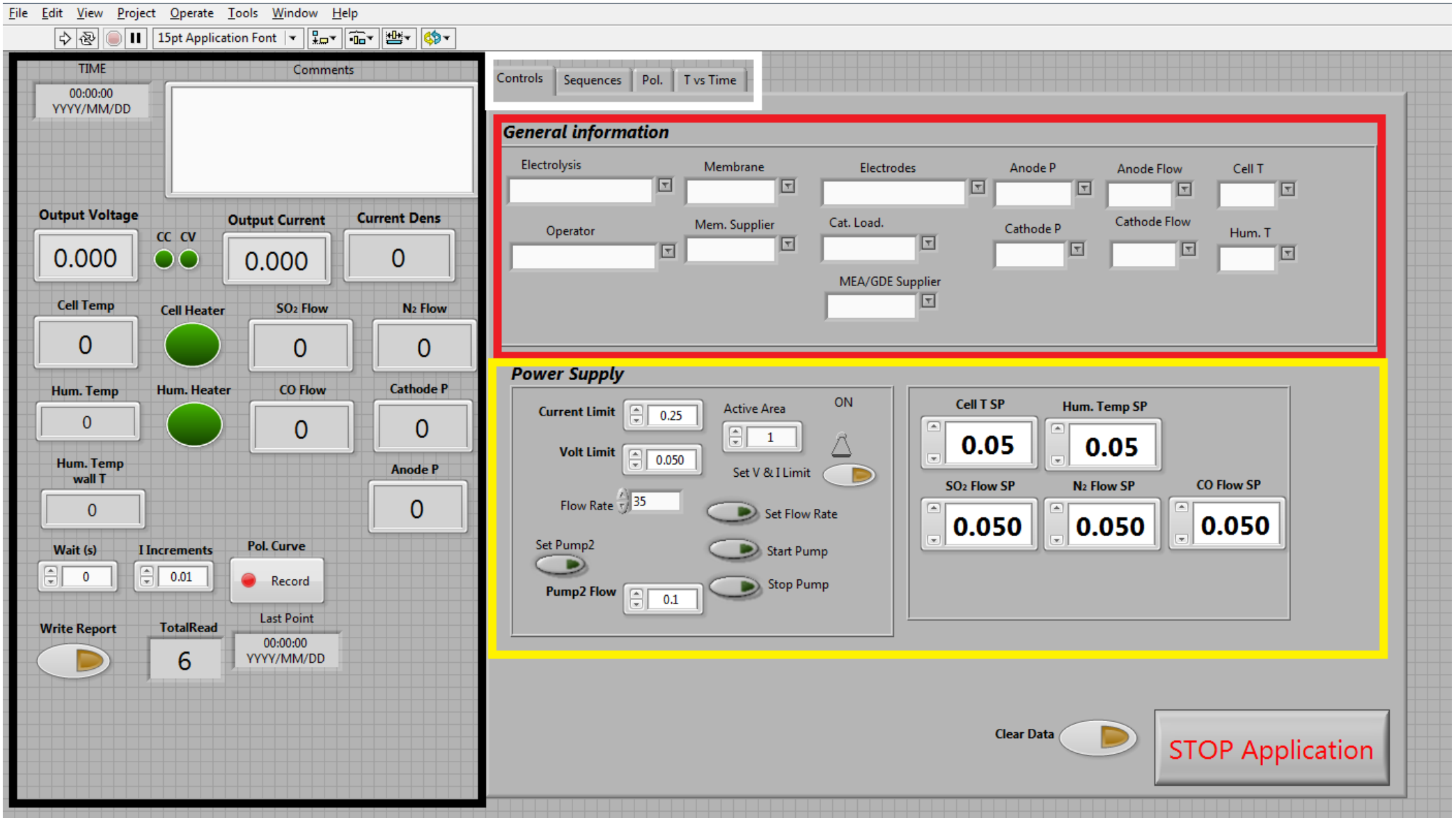

Figure A - 1: Representation of the Front Panel design used.

Additional functionality was obtained by selecting a different tab (white highlighted section), which was used to house all the sequences planned for this study: Sequence 1: Polarisation curves, Sequence 2: Polarisation curves – constant current for a pre-determined time – polarisation curve, Sequence 3: Cyclic voltammetry, Sequence 4: Voltage stepping and Sequence 5: Long term operation. Figure A - 2 shows the information for the additional tabs from the white highlighted section (Sequences, Pol. and T vs. Time) used to visually show the polarisation curves and temperature vs. time data.

When considering EIS using a 10 cm^2 active area Sequence 1, which is the bases for the other sequences, consisted of the following:

- Idling – Setting of all parameters, such as temperature, SO_2 flow rate and water flow rate.
- MEA hydration – when PFSA membranes are used the membrane must be properly hydrated to ensure optimal operation. This step supplies the heaters with 240 VAC power using the relay module controlled by the temperature set point while the cathode feed is being circulated. A safety interlock is in place to monitor the cell temperature (if the cell temperature increases above 90°C the system will stop). A point is logged every minute and after the required 180 min (3 hrs.) the program proceeds to the next step.
- CC (Constant Current) @ 0.1 A cm^{-2} – this step is the pre-conditioning step for 20 min and ensures that the anode and cathode reactant flow and cell temperature have stabilised. The anode supply (SO_2) is applied 1 min before the power supply is switched on. The program automatically converts the current density to the required current using the active area supplied by the user. The voltage is logged every 30 s for the 20 min period. The program will again stop the system if the voltage reaches 1 V, indicating that the membrane does not perform sufficiently. If the voltage is less than 1 V the system will go to the next step.
- Polarisation Curve – This step will produce the polarisation curve by increasing the current density (according to the information supplied by the supplier) every 90 s while recording each point before increasing the current. This process will be done until the voltage reaches 1 V after which the current

density will be reduced every 90 s until the current (not current density) reaches 0.3 amp. When this happens the next step is initiated. Report Writing – This step writes all the logged information to an Excel template file which already includes the formatting and graphs typically used, such as the polarisation curve, voltage as a function of time and temperature.

As mentioned above, sequence 1 formed the basis of sequence 2. The only difference is the additional steps of running the electrolyser at a constant current (0.1 A cm^{-2}) followed by a secondary polarisation curve. Figure A-3 shows a typical voltage vs. time graph for Sequence 1 and 2.

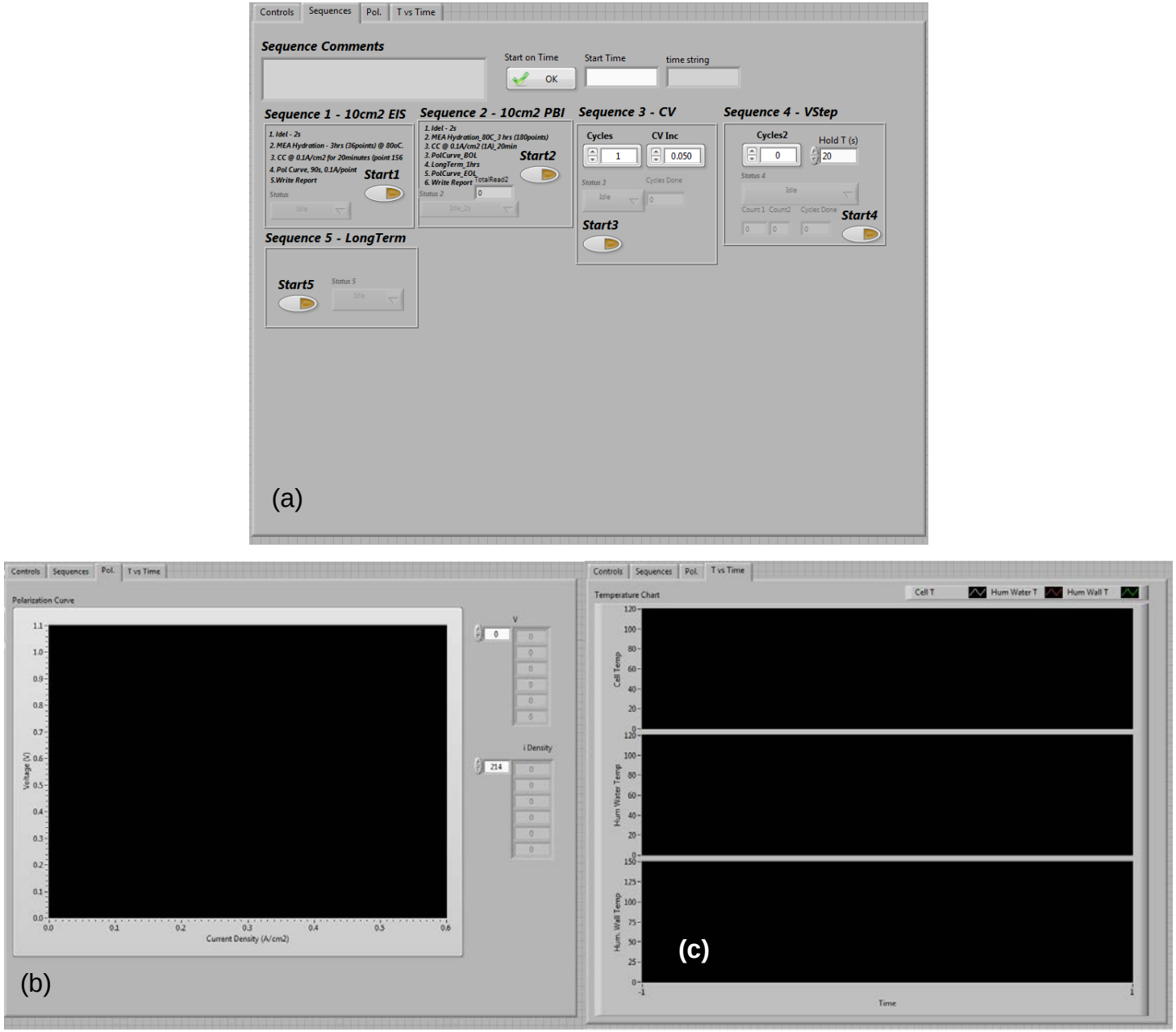

Figure A - 2: Tabs used for (a) sequence selection, (b) polarisation curve figure, (C) temperature vs. time.

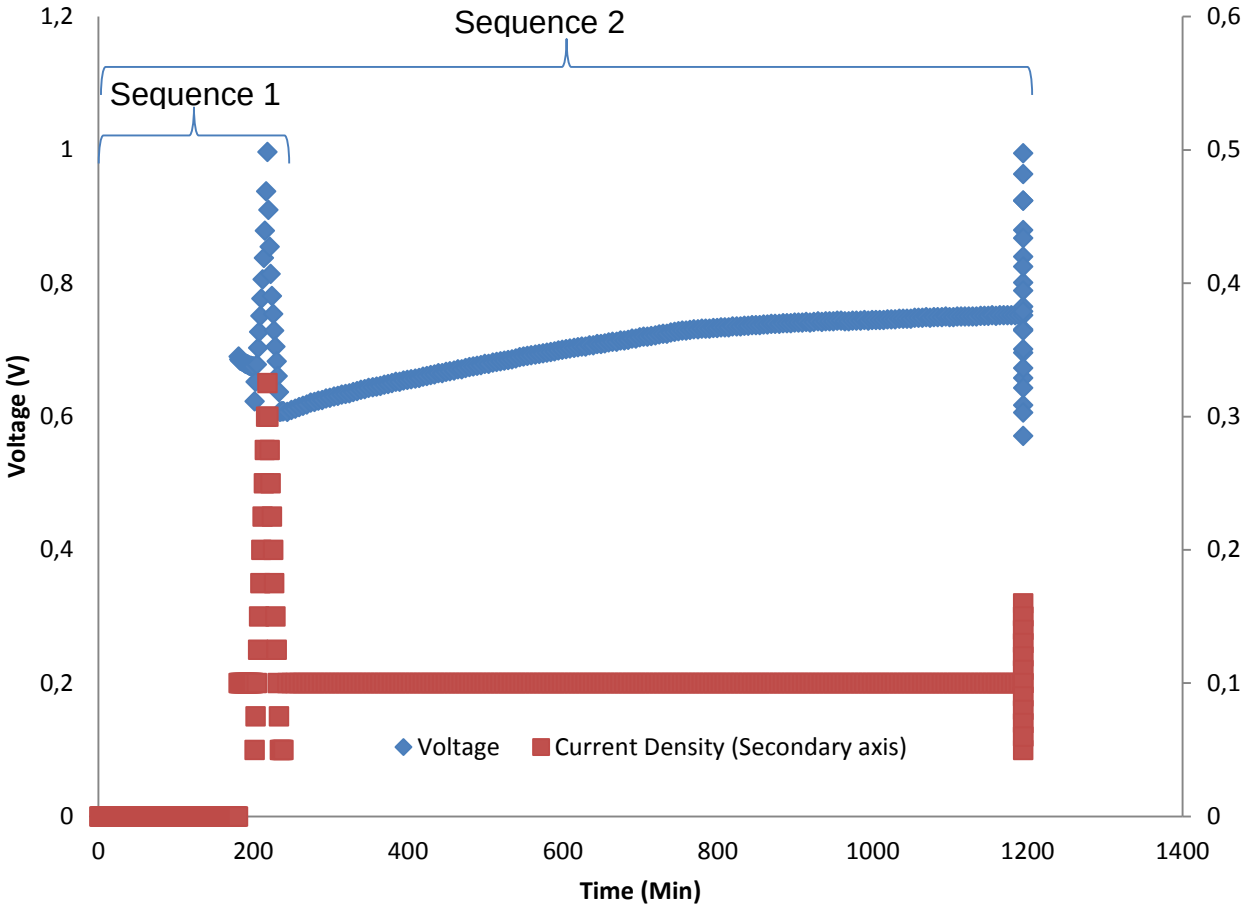

Figure A - 3: Voltage and current density as a function of time for both Sequence 1 and 2.

Apart from the front panel that is used to select the operating parameters, the block diagram mentioned above, is used for the actual programming which controls the system. For simplicity, Figure A - 4 only shows a typical block diagram containing the coding needed for the actual read/write of the compact Daq. After each component, which needs to be controlled electronically, has been connected to the appropriate module (See Table A - 1) the coding can be started. In Figure A - 4 (black highlighted area) it can be seen that the specific module and channel must be selected corresponding to where the part was connected. For example, the CO mass flow controller analog input, for selecting the setpoint of the meter, was connected to module 2 (which has several channels) and on channel ai0. The other SO_2 thermal mass flow controller, for example, was connected to the same module but on channel ai1.

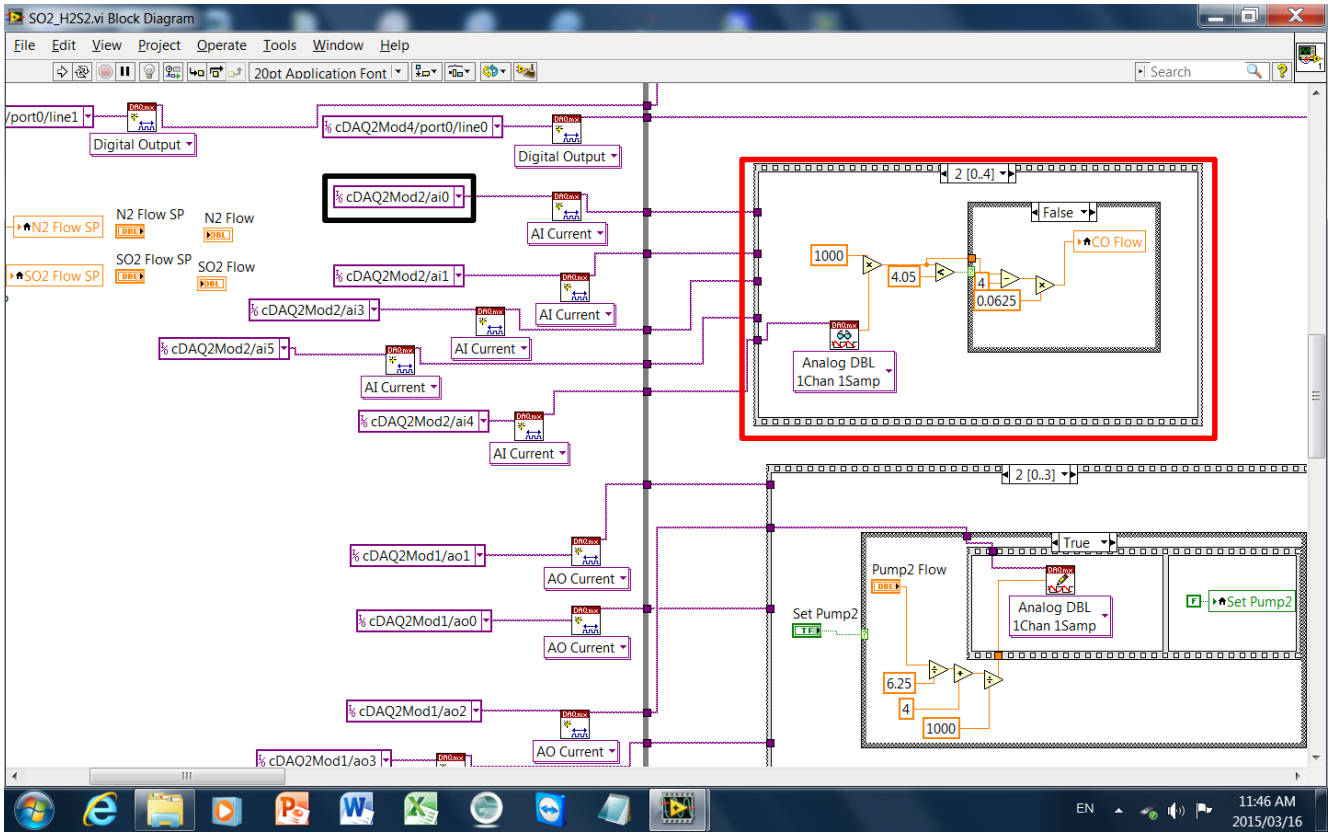

Figure A - 4: Example of the coding needed to read/write to the compact daq.

The red highlighted section in Figure A - 4 shows the scaling procedure used as the actual input to the thermal mass flow controller is 4 – 20 mA and the user selects a flow set point in nL/min. The program will then force the appropriate current (4 – 20 mA) across two pins on the thermal mass flow controller which controls the valve resulting in the desired flow rate through the meter. It should be clear that the description of controlling each and every item/part will be rudimentary as the same principle applied to the greater part of the system.

APPENDIX B: ARTICLES PUBLISHED FROM THIS STUDY

Energy Science & Engineering

Open Access

RESEARCH ARTICLE

Various operating methods and parameters for SO_2 electrolysis

Andries J. Krüger[1,2], Henning M. Krieg[2], Sergey A. Grigoriev[3,4] & Dmitri Bessarabov[1]

[1]DST HySA Infrastructure Centre of Competence, Faculty of Engineering, North-West University, Potchefstroom, South Africa
[2]Faculty of Natural Science, Chemical Resource Beneficiation, North-West University, Potchefstroom, South Africa
[3]National Research University "Moscow Power Engineering Institute" Krasnokazarmennaya, 14, 111250 Moscow, Russia
[4]National Research Center "Kurchatov Institute" Kurchatov Sq. 1, 123182 Moscow, Russia

Keywords
Electrochemical impedance spectroscopy, hydrogen, proton exchange membrane, SO_2 electrolyzer, thermochemical

Correspondence
Andries J. Krüger, DST HySA Infrastructure Centre of Competence, Faculty of Engineering, North-West University, Potchefstroom, South Africa.
Tel: +27 (18) 285 2461; Fax: 086 549 6670;
E-mail: andries.kruger@nwu.ac.za

Funding Information
The authors thank the DST (Department of Science and Technology, South Africa) for their financial support through HySA Infrastructure CoC under project KP5 – IO3, L. Tiedt for the support in attaining the SEM images, and H. Dannhauser and H. van der Merwe who helped with some of the electrolysis work. The support from the Ministry of Education and Science of the Russian Federation is also acknowledged.

Received: 10 December 2014; Revised: 26 June 2015; Accepted: 29 June 2015

Abstract

The application of PFSA-based proton exchange membranes was investigated for the production of hydrogen and sulfuric acid using a SO_2-depolarized electrolyzer system. Parameters investigated included hot pressing pressure for the membrane electrode assembly (MEA) manufacturing, cell temperature, membrane thickness, catalyst loading, membrane type, and SO_2 anode feed concentration. The effect of cell temperature, membrane thickness, and acid concentrations was also investigated when using a second method, where clean sulfuric acid as cathode and SO_2 saturated sulfuric acid as anode were used. Electrochemical impedance spectroscopy showed that the pressure exerted in the MEA manufacturing step had a significant influence with 125 kg cm^{-2} yielding the highest current density. High temperatures (>80°C) and thin membranes (≈120 μm) showed the best performance while thicker membranes produced higher acid concentration when using the first system. The SO_2 concentration in the anode had a significant influence with the over potential increasing with decreasing SO_2 concentration. When using the second method, it was found that the SO_2 solubility in sulfuric acid is important as the mass transport of the SO_2 limits the overall reaction rate. From the two systems tested, the first method, that is, dry SO_2 anode and liquid water cathode showed the best operational effectiveness reaching a maximum of 0.32 A cm^{-2} at 80°C using N115 coated with 1 mgPt cm^{-2} while the second system under the same conditions achieved a current density of 0.18 A cm^{-2} when using N117.

doi: 10.1002/ese3.80

Introduction

It is well known that the electrolysis of water is regarded as an alternative to the conventional methods for the production of hydrogen. With the development of proton exchange membranes (PEM), the interest in the electrochemical production of oxygen and hydrogen from water has significantly increased as PEM-based water electrolysis is an efficient and environmental friendly method that can be used for the production of hydrogen when zero-carbon power sources, such as renewable or nuclear, are used [1]. Also, the theoretical energy input for water electrolysis is 1.229 V with the practical operating voltage in the 1.7–2 V range. Attempts to increase the overall electrolysis efficiency have been made, for example, in the development of high temperature steam electrolysis [2]. More intricate systems have also been nominated as possible improvements on normal electrolysis including the

INTERNATIONAL JOURNAL OF HYDROGEN ENERGY 39 (2014) 18173–18181

Available online at www.sciencedirect.com

ScienceDirect

journal homepage: www.elsevier.com/locate/he

Evaluation of MEA manufacturing parameters using EIS for SO_2 electrolysis

Andries J. Krüger [a,b,*], *Henning M. Krieg* [b], *Jan van der Merwe* [a], *Dmitri Bessarabov* [a]

[a] DST HySA Infrastructure Centre of Competence, Faculty of Engineering, North-West University, Potchefstroom, South Africa

[b] Chemical Resource Beneficiation, North-West University, Potchefstroom, South Africa

ARTICLE INFO

Article history:
Received 4 June 2014
Received in revised form
26 August 2014
Accepted 1 September 2014
Available online 24 September 2014

Keywords:
Electrochemical impedance spectroscopy
SO_2 electrolyser
Proton exchange membrane
Hydrogen production

ABSTRACT

Membrane electrode assembly (MEA) manufacturing parameters such as hot pressing pressure and pressing time were investigated for the use in a SO_2 electrolyser. The SO_2 electrolysis was optimised in terms of cell temperature, membrane thickness and catalyst loading. The electrolysis efficiency was evaluated using polarisation curves while electrochemical impedance spectroscopy (EIS) was used to determine the membrane resistance, activation energy and mass transport limitations. An electrical circuit, which included inductance, ohmic resistance, charge transfer, constant phase and Warburg elements, was used to fit the experimental data. The optimum hot pressing conditions were 50 kg cm^{-2} for 5 min at 120 °C. Increased cell temperature (80 °C) resulted in a reduction of mass transport, while thicker membranes resulted in an increased mass transport due to lower water transport through the membrane. Increased catalyst loading (from 0.3 to 1 mgPtC.cm^{-2}) improved the cell performance due to improved kinetics confirmed by the EIS data.

Introduction

The production of hydrogen as an energy carrier in the energy sector has received increased interest in both the research and commercial community [1,2]. Since many current methods of hydrogen production, for example from coal result in the production of pollutants, it is necessary to evaluate alternative methods. The Westinghouse Corporation in the 70's proposed such an alternative method known as the Hybrid Sulphur (HyS) cycle which forms part of the so-called thermo-chemical cycles [3]. The HyS process aims at producing high quantities of hydrogen and sulphuric acid from both water and SO_2 gas in an electrolysis step which is incorporated into the three step HyS cycle [4]. Although it was initially suggested to couple this process with a nuclear heat source, recent papers have shown that other heat sources could also be used, for example, the coupling of the SO_2 electrolysis step with a pyrometallurgical plant of nickel and copper concentrate [5]. According to Lokkiluoto et al., this process would not be closed as had been initially proposed for the HyS cycle, but would use the SO_2, which is a by-product produced from current industrial processes like flash smelting of metal sulfides, for the production of H_2 and H_2SO_4. Commercially H_2SO_4 is generally produced by a contact process whereby sulphur solids are oxidised in the presence of oxygen to produce SO_2 gas. The SO_2 is then further

* Corresponding author. Tel.: +27 18 285 2641 (office).
E-mail addresses: 13061631@nwu.ac.za, kruger.andries@gmail.com (A.J. Krüger).
http://dx.doi.org/10.1016/j.ijhydene.2014.09.012

INTERNATIONAL JOURNAL OF HYDROGEN ENERGY 40 (2015) 4442–4450

Available online at www.sciencedirect.com

ScienceDirect

journal homepage: www.elsevier.com/locate/he

Effect of H_2S on SO_2-depolarised water electrolysis

Andries J. Krüger [a,b,*], Henning M. Krieg [b], Dmitri Bessarabov [a,*]

[a] DST HySA Infrastructure Centre of Competence, Faculty of Engineering, North-West University, Potchefstroom, South Africa

[b] Faculty of Natural Science, Chemical Resource Beneficiation, North-West University, Potchefstroom, South Africa

ARTICLE INFO

Article history:
Received 27 November 2014
Received in revised form
3 February 2015
Accepted 6 February 2015
Available online 4 March 2015

Keywords:
SO_2 electrolysis
Hydrogen sulphide deactivation
Electrochemical impedance spectroscopy
Cyclic voltammetry
CO stripping
Electrochemical surface area

ABSTRACT

The performance of a PEM SO_2 electrolyser, used for the production of H_2 gas and liquid H_2SO_4, was evaluated when the feed was contaminated with hydrogen sulfide. Transient voltage response at constant current density and polarisation curves showed a decrease in operating efficiency over time for all H_2S concentrations tested. Electrochemical impedance spectroscopy (EIS) was applied to separate and quantify the membrane resistance, charge resistance and mass transport limitations to evaluate the influence of H_2S exposure time. The charge resistance increased by 64.70 mΩ over 40 min when the anode was exposed to 80 ppm H_2S. Cyclic voltammetry (CV) was applied to determine the electrochemical surface area (ECSA, $cm^2\ g^{-1}$) by CO stripping as a function of SO_2 and SO_2/H_2S exposure (10, 30, 60 and 80 ppm H_2S). An ECSA of 83.52 $cm^2\ g^{-1}$ was obtained for a clean catalyst while exposing the anode to SO_2, at 0.1 A cm^{-2} for 3 min, reduced the ECSA to only 9.10 resulting in an 89% reduction in active platinum sites. The reduction in ECSA for a fresh anode, when exposed to 80 ppm H_2S, was calculated as 12.56 $cm^2\ g^{-1}$ which is a reduction of 85% in active catalytic sites.

Introduction

Hydrogen production through SO_2 assisted water electrolysis, known as SO_2 depolarised electrolysis (SDE), has received increased attention as a possible clean alternative to current industrial processes for the production of hydrogen. The SO_2 electrolyser was initially incorporated in the Hybrid Sulfur (HyS) thermochemical cycle proposed by the Westinghouse Corporation in the 1970's [1]. The cycle incorporates a sulfuric acid decomposition step (into SO_2, H_2O and O_2), oxygen separation step and an electrolysis step (reacting SO_2 and H_2O). Although the overall theoretical efficiency of the HyS cycle was estimated at 41.7% (HHV) [2] using traditional PFSA (such as Nafion®) proton exchange membranes (PEM) and 44.0–47.6% (HHV) [3] when using polybenzimidiazole (PBI) proton exchange membranes in the electrolyser, significant research is needed for the entire process to come close to the calculated efficiency. In the electrolyser, which is the focus of this paper, water reacts in the presence of SO_2 over a platinum group metal (PGM) anode, usually platinum supported on carbon, producing concentrated sulfuric acid (equation (1)) and hydrogen gas (equation (2)) giving an overall reaction shown in equation (3).

* *Corresponding authors.* DST HySA Infrastructure Center of Competence, Faculty of Engineering, North-West University, Potchefstroom, South Africa. Tel.: +27 (18) 285 2461; fax: +27 (18) 299 2350.
E-mail addresses: andries.kruger@nwu.ac.za (A.J. Krüger), dmitri.bessarabov@nwu.ac.za (D. Bessarabov).
http://dx.doi.org/10.1016/j.ijhydene.2015.02.036

INTERNATIONAL JOURNAL OF HYDROGEN ENERGY 40 (2015) 3122–3133

Available online at www.sciencedirect.com

ScienceDirect

journal homepage: www.elsevier.com/locate/he

Characterisation of a polyaromatic PBI blend membrane for SO_2 electrolysis

Andries J. Krüger [a,b,*], Patrizia Cichon [c], Jochen Kerres [b,c], Dmitri Bessarabov [a], Henning M. Krieg [b]

[a] DST HySA Infrastructure Centre of Competence, Faculty of Engineering, South Africa
[b] Focus Area, Chemical Resource Beneficaition, Faculty of Natural Science, North-West University, Potchefstroom, South Africa
[c] Institute of Chemical Process Engineering, University of Stuttgart, D-70199, Stuttgart, Germany

ARTICLE INFO

Article history:
Received 17 November 2014
Received in revised form
12 December 2014
Accepted 19 December 2014
Available online 29 January 2015

Keywords:
SO_2 electrolysis
Polyaromatic PBI blend membranes
TGA-MS
MEA doping

ABSTRACT

The application of a polyaromatic acid–base blend membrane from partially fluorinated and sulfonated aromatic polyether and the polybenzimidazole F_6PBI has been investigated for hydrogen production using SO_2 electrolysis. Several membrane electrode assembly (MEA) pre-doping strategies have been investigated using polarisation curves. Membrane thickness variation, voltage cycling and long term operation at constant current (0.1 A cm^{-2}) was also performed. Scanning electron microscopy (SEM) and TGA-MS was used to evaluate MEA stability before and after long term operation. It was found that doping the MEA after hot pressing performs the best reaching a current density of 0.3 A cm^{-2}. The performance could also be improved by cycling the voltage 16 times to reach 0.33 A cm^{-2}. Long term operation showed stable voltage at 0.1 A cm^{-2} staying below 0.8 V. SEM images showed that no significant sulfur deposition was present while TGA-MA analysis confirmed some degradation after the 140 h of operation.

Introduction

Hydrogen gas can be viewed as one of the energy carriers of the future especially when used in alternative power systems such as fuel cells. With the fuel cell market on the brink of commercialisation for the automotive industry the demand for hydrogen is expected to increase rapidly [1] resulting in an increased need for alternative methods for the production of low cost hydrogen. The Hybrid Sulfur (HyS) cycle has been proposed as one such possible alternative for the high volume production of hydrogen [2]. This three-step cycle entails the decomposition of sulphuric acid to water, oxygen and sulphur dioxide. After oxygen separation, the sulphur dioxide and water is subsequently electrochemically converted to both hydrogen and sulphuric acid [2,3]. For this step, an electrolyser system is used containing a proton exchange membrane (PEM) coated with a catalyst on both sides of the membrane serving as the anode and the cathode. The produced H_2SO_4 from the electrolyser is fed back to the initial decomposition step completing the cycle. For the HyS cycle to be competitive Gorensek et al. [4] determined that the electrolyser step

* Corresponding author. DST HySA Infrastructure Centre of Competence, Faculty of Engineering, North-West University, Potchefstroom, South Africa. Tel.: +27 18 285 2641; fax: +27 18 299 1667.
E-mail address: andries.kruger@nwu.ac.za (A.J. Krüger).
http://dx.doi.org/10.1016/j.ijhydene.2014.12.081

INTERNATIONAL JOURNAL OF HYDROGEN ENERGY 40 (2015) 8788–8796

Available online at www.sciencedirect.com

ScienceDirect

journal homepage: www.elsevier.com/locate/he

Evaluation of covalently and ionically cross-linked PBI-excess blends for application in SO_2 electrolysis

Andries J. Krüger [a,*], *Jochen Kerres* [b,c], *Dmitri Bessarabov* [a], *Henning M. Krieg* [b]

[a] DST HySA Infrastructure Centre of Competence, Faculty of Engineering, North-West University, Potchefstroom, South Africa

[b] Focus Area: Chemical Resource Beneficiation, Faculty of Natural Science, North-West University, Potchefstroom, South Africa

[c] Institute of Chemical Process Engineering, University of Stuttgart, D-70199, Stuttgart, Germany

ARTICLE INFO

Article history:
Received 25 March 2015
Received in revised form
5 May 2015
Accepted 11 May 2015
Available online 6 June 2015

Keywords:
SO_2 electrolysis
F_6PBI blend proton exchange membranes
Covalently cross-linked
Ionically cross-linked
Voltage stepping
Long term operation

ABSTRACT

Proton exchange membranes (PEM) containing various combinations of PPOBr (pol(2,6-dimethylbromide-1,4-phenylene oxide, covalently cross-linked) or PWN (poly(tetrafluorostyrene-4-phosphonic acid), ionically cross-linked) were evaluated for their suitability in an SO_2 electrolyser environment. Since H_2SO_4 is produced during the oxidation of SO_2 in the presence of water, the membranes used in the electrolyser must be both chemically and electrochemically stable. Acid stability tests showed that the blend membranes are stable in 80 wt % acidic media at 80 °C for 120 h. The electrochemical characterisation included polarisation curves, voltage stepping and long term operation. Using polarisation curves two blend combinations were selected for the voltage stepping. Both types of blend membranes showed high stability up to 110 cycles while the F_6PBI/PPOBr blend membrane had comparable (to N115®) long term operating voltage, while the F_6PBI/PWN blend membrane showed improved voltage, attaining 0.781 V compared to the 0.812 V obtained when using N115 at 0.1 A cm^{-2}.

Introduction

When considering the amount of applications for hydrogen it makes sense to focus on a clean and efficient method of producing hydrogen without using carbon based fuels. An alternative method of producing environmentally clean hydrogen is through the electrolysis of pure water which produces both hydrogen and oxygen. Theoretically a voltage of 1.23 V would be needed to split the water into its separate gaseous molecules. The reaction however takes place at higher voltages due to contact resistances within the electrolyser hardware (among other) and an operating voltage in the order of 1.5–2 V is more reasonable [1].

* Corresponding author. Tel.: +27 18 285 2461; fax: +27 18 299 2350.
E-mail address: andries.kruger@nwu.ac.za (A.J. Krüger).

http://dx.doi.org/10.1016/j.ijhydene.2015.05.063